Saving the Joint

Biological Strategies to Preserve Cartilage

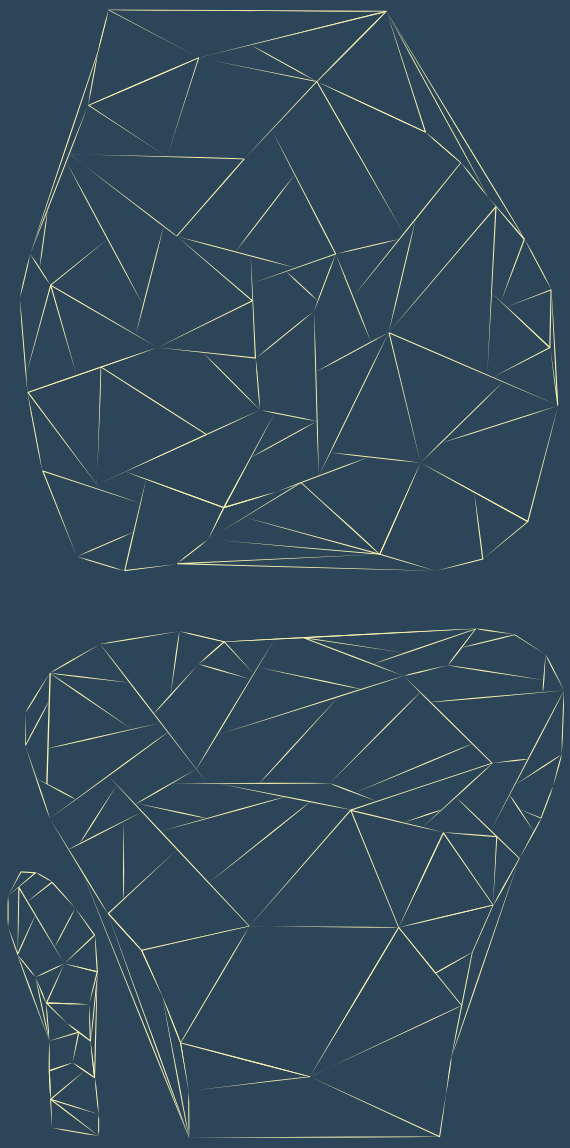

Margot Rikkers

Saving the Joint

Biological Strategies to Preserve Cartilage

Margot Rikkers

ISBN: 978-90-393-7473-3
Author: Margot Rikkers
Cover design and layout: Margot Rikkers
Printing: ProefschriftMaken || www.proefschriftmaken.nl

The printing of this thesis is financially supported by: the Dutch Society for Matrix Biology (NVMB), Anna Fonds|NOREF, Stichting ETB-BISLIFE, and the Netherlands Society for Biomaterials and Tissue Engineering (NBTE).

Saving the Joint

Biological Strategies to Preserve Cartilage

Het Gewricht Redden

Biologische Strategieën om Kraakbeen te Behouden

(met een samenvatting in het Nederlands)

Proefschrift

ter verkrijging van de graad van doctor aan de
Universiteit Utrecht
op gezag van de
rector magnificus, prof.dr. H.R.B.M. Kummeling,
ingevolge het besluit van het college voor promoties
in het openbaar te verdedigen op

woensdag 8 juni 2022 des ochtends te 10.15 uur

door

Margot Rikkers

geboren op 1 februari 1994
te Doetinchem

Promotor:
Prof. dr. ir. J. Malda

Copromotoren:
Dr. L.A. Vonk
Dr. R. Levato

This thesis forms part of 'Regenerative Medicine Crossing Borders' (RegMed XB), a virtual institute that uses regenerative medicine strategies to cure common chronic diseases and comprises an intensive Flemish-Dutch public-private partnership between governments, health foundations, doctors, scientists, and specialized companies.

TABLE OF CONTENTS

Chapter 1

General Introduction

GENERAL INTRODUCTION

The personal and societal burden of cartilage injury

Suffering from limitations in functional movement and physical activities because of cartilage injury is a major societal and healthcare challenge[1], in particular when this starts at an early age. Focal injuries of the articular cartilage typically occur during sports, sudden movements, or other trauma and provoke pain and limit the functionality of the joint. More than half of the patients with symptomatic complaints undergoing knee arthroscopy suffer from cartilage defects[2,3]. If left untreated, the patient is likely to develop post-traumatic osteoarthritis (OA) at an early age[4–7]. Besides the burden on the individual patient[8], the incidence and societal burden of cartilage degeneration worldwide is growing due increasing age of the population[9]. Replacement of the joint in young patients is associated with lower implant survival[10] and goes hand in hand with the disadvantages of revision surgery, like perioperative complications and longer hospital stay[11]. This further emphasises the importance of early treatment to restore the articular surface in order to delay the need for joint replacement.

Articular cartilage

Articular cartilage is the glossy, white layer of hyaline cartilage covering the ends of the long bones when they meet in synovial joints. The tissue is perfectly equipped to absorb shocks and distribute loading, and facilitate frictionless motion during joint movement. The composition of articular cartilage is to a large extent made up of type II collagen, while other types of collagen, like I, III, VI, IX, and X, are less abundant[12]. The second major component of cartilage are its proteoglycans, large protein-polysaccharide complexes containing negative charges, attracting water into the tissue[13]. Lastly, only a small percentage, 1.7%, of cartilage

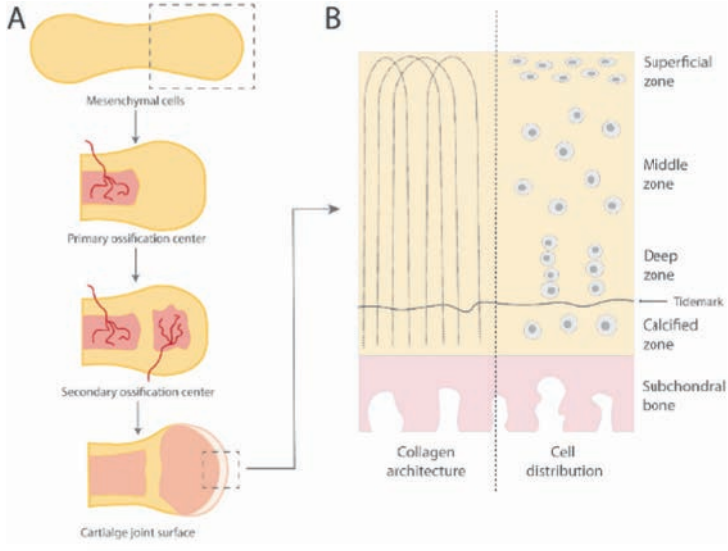

Figure 1. A) Fetal development of articular cartilage in a synovial joint. B) Structural architecture and cell distribution within the layers of articular cartilage.

is made up of its endogenous cell, the chondrocyte[14]. Recent studies have investigated the presence of a subset of cells in articular cartilage that possesses progenitor-like features, generally referred to as articular cartilage-derived progenitor cells (ACPC)[15,16]. In healthy conditions, chondrocytes reside in a resting state and maintain the turnover of mainly proteoglycans[17] while type II collagen is hardly replaced and has a half-life of over one hundred years[18].

During fetal development, cartilage emerges from the mesenchyme through mesenchymal cell condensation and subsequent differentiation of chondroprogenitor cells. As the long bones form, a secondary ossification center forms at either end, separating articular cartilage from growth plate cartilage (Figure 1A)[12]. Articular cartilage is characterized by its typical layered structure, in which the superficial layer consists of elongated cells distinguished by expression of lubricin, a splice form of proteoglycan 4 (PRG4)[19], facilitating the lubrication of the articular joint. The extracellular matrix (ECM) in the superficial layer is characterized by a low concentration of type II collagen and more type I collagen [20,21]. The middle zone contains a lower cell density with rounded cells, and the deep zone consists of round cells usually stacked into a columnar arrange. The cartilage is separated from the underlying bone by the tidemark, a dense layer of matrix clearly visible on histological stains, where calcified cartilage covers the subchondral bone (Figure 1B). Healthy articular cartilage is also hallmarked by the complete absence of innervation and vascularization, suppressing intrinsic healing upon acute damage. Within the cartilage's ECM, the chondrocyte is directly surrounded by its pericellular matrix, connecting the chondrocyte to the territorial and interterritorial matrix[22]. The pericellular matrix consists mainly of type VI collagen and plays an important role in mechanosensing[23,24]. A chondrocyte surrounded by its pericellular matrix is called a chondron[25].

The unique function of articular cartilage is a direct result of the inherent structure of the tissue. Collagen fibers stretch from the subchondral bone and calcified cartilage towards the superficial layer and back, forming the arcade structure typical for the tissue[26]. The interplay of these strong fibers with the water-retaining proteoglycans, results in its exceptional mechanical stability. It is this mechanical strength that enables us to carry the weight of our body throughout the day and absorb great forces during physical exercise.

Pathologies of articular cartilage

Diseases of articular cartilage are common, as prevalence is estimated to be between 15 and 30% in the adult population[27,28]. Damage of the tissue brings forward a major problem due to the lack of intrinsic regeneration. Pathologies of articular cartilage are divers and their fundamental causes vary. Focal defects can affect the chondral layer as a result of an acute injury. Osteochondral defects extend into the subchondral bone, which can either be a result of acute damage or an underlying disorder of the bone, osteochondritis dissecans (OCD), which typically occurs in patients between the ages of ten and twenty[29]. While OA is the most prevalent disease affecting the complete joint[28], other inflammatory rheumatic diseases, like

rheumatoid arthritis, gout, and juvenile idiopathic arthritis can also severely damage cartilage tissue[30].

Focal chondral defects

Damage to articular cartilage predominantly occurs in the knee joint, but the hip, elbow, wrist, ankle, and shoulder can also be affected. Sports injuries are the leading cause of traumatic injury to the cartilage, generally resulting in a focal chondral defect. Here, only the cartilage layer is affected, as opposed to an osteochondral defect, where also the underlying bone is damaged. Chondral damage can be classified into several grades, depending on the depth of the defect and tissue quality (ICRS grading)[31]. Defects in the chondral layer do not heal spontaneously and require surgical intervention in order to restore the cartilage surface and decrease clinical symptoms.

Osteoarthritis

Post-traumatic injury, obesity, or limb malalignment can result in OA at an early age and can present itself in any synovial joint. It can also emerge as a result of precedent damage to the other tissues in the joint, like the menisci[32,33], or prior damage or rupture of the anterior cruciate ligament (ACL)[34,35]. Limb malalignment causes asymmetric distribution of forces on either the lateral or medial side of the knee joint and is therefore associated with an increased risk of developing (unilateral) OA[36]. In OA aetiology, multiple factors play a role in the development and progression of the disease. It is hallmarked by an imbalance in cartilage homeostasis and inflammation in the cartilage, bone, and synovium. During OA, chondrocytes enter a proliferative state in an attempt to synthesize matrix proteins and repair the initial damage. However, this goes hand in hand with an increase in production of matrix degrading enzymes and inflammatory mediators, counteracting repair and progression of OA. This leads to an imbalance in matrix build-up and breakdown, inflammation, and mechanical stress[37]. The progressive loss of articular cartilage, remodelling and sclerosis of subchondral bone, formation of bone cysts and/or osteophytes, and inflammation of the synovium are all features of the degenerative joint disease[13,38].

CURRENT TREATMENTS

The cartilage's capacity for self-restoration is limited, as a consequence of its avascularity and its absence of neural innervation[39]. When conservative, non-surgical treatments like physical therapy or pain medication are insufficient, several surgical options can be considered, depending on the specific pathology[40]. During the last few decades, many treatments for both cartilage defects and OA have been investigated and developed with varying degrees of success.

Cell-based treatments for focal chondral defects

Early treatment of cartilage defects is key to prevent accelerated degeneration and development of OA. Treatment of focal cartilage defects with cell transplantation started in

the 1990s with the use of culture-expanded autologous chondrocytes. This technique consists of two surgical procedures, one in which a small biopsy is taken from a non-weight bearing area in the cartilage, and a next in which isolated and culture-expanded chondrocytes are transplanted into the debrided defect. The procedure has known several generations, starting with injection of the cells under a periost flap[41] that covers the defect or in a collagen membrane[42] (first- and second-generation autologous chondrocyte implantation; ACI), followed by newer generations of matrix-assisted and matrix-associated ACI[43–46].

Alternatively, chondral defects smaller than 2 cm^2 can be treated with microfracture, in which small holes are drilled in the subchondral bone, enabling marrow to flow into the defect and stimulate regeneration[47]. For defects proceeding entirely into the subchondral bone, chondral treatment is insufficient. These patients can be treated using osteochondral autograft transplantation (OATs), in which the defect is filled with multiple small cylindrical osteochondral plugs from a non-weight bearing area of the joint[48,49].

Treatments for osteoarthritis

As OA is a more complex, multi-factorial disease, treatments vary from intra-articular injections until total joint replacement. For early-stage OA, patients can be treated with non-invasive treatments like injection with a corticosteroid, hyaluronic acid (HA), or platelet-rich plasma (PRP)[50,51]. Preclinical and clinical studies are investigating the effectiveness of bone marrow concentrate (BMC)[52–54], stromal vascular fraction (SVF)[52,54,55], and culture-expanded mesenchymal stromal cells (MSCs)[56] to treat OA. Although these therapies were found to be safe, high-quality randomized controlled trials (RCTs) have to confirm effectiveness. Finally, for end-stage OA in the knee joint, the only treatment option is to replace the joint by a total knee arthroplasty (TKA). Replacing the joint has proven to be very effective in pain relief and regain of function[57]. However, the life span of a prosthesis is its biggest drawback. Prostheses last for about ten to fifteen years after which a revision surgery is necessary, generally resulting in decreased patient satisfaction[58].

Cartilage-preserving therapies

Several therapies have been developed to preserve cartilage in an earlier stage to reverse (some of the) damage. Knee joint distraction is utilized for a beginning stage of OA, aimed at delaying the need for a TKA[59]. During joint distraction, an external frame is fixed with bone pins on the femur and tibia, in order to increase the joint space width for six to nine weeks. As a result, joint homeostasis is altered and signs of cartilage restoration are observed at one and two years after distraction[60,61].

Secondly, unicompartmental OA can be treated by limb realignment through an osteotomy surgery[62,63]. Finally, damages to tissues other than cartilage are correlated with an increased risk of OA development. As mentioned earlier, ACL rupture and damage to the menisci contribute to OA over time, and repair procedures are often performed simultaneously with cartilage repair procedures. Therefore, repair of all tissues in the knee is essential to minimize

the risk of OA development.

MOVING TOWARDS BETTER TREATMENTS

Despite the fact that through the years many therapies have become available to treat cartilage pathologies, several challenges are still to overcome. To date, it has proven difficult, if not impossible, to mimic the structural mechanical integrity of articular cartilage accurately, which is generally thought to be the holy grail in successful and durable cartilage regeneration[64]. Research generally approaches the problem from two distinct angles: 1) to grow or regenerate a piece of articular cartilage, mimicking native cartilage as close as possible. Outcome measures here are collagen fiber orientation, cell density and arrangement, ECM production and composition, and mechanical stability. 2) to improve patient outcome after treatment.

While cell transplantation is widely used as a treatment option for cartilage defects, research is continuously moving in order to improve outcomes and reduce failure rate[65]. One of the challenges in transplantation of autologous chondrocytes is that the cells lose their phenotype over culture-expansion, limiting their capacity to produce cartilage matrix[66,67]. Finding ways to improving cell performance would address this issue. Furthermore, developing single-step procedures would improve cost-effectiveness of the intervention[68], and at the same time improve patient comfort as a single intervention allows for shortened rehabilitation.

Enhancing cell performance

Complementing chondrocytes with a second cell type, like MSCs, leads to enhanced cartilage regeneration. Coculture of these two cell types improves matrix formation through chondroinduction rather than differentiation of MSCs into chondrocytes[69–71]. Besides MSCs, cocultures with adipose-derived stem cells (ASC)[71,72], embryonic stem cells (ESCs)[73,74], and induced pluripotent stem cells (iPSCs)[75] were shown to improve chondrogenesis. Although the exact mechanisms of action of MSCs in chondroinduction are yet to be elucidated, further research is based on the findings. Uncovering the stimulus or a cocktail of factors that triggers cartilage ECM production would increase applicability, logistics, decrease costs, and possibly facilitate an off-the-shelf product not requiring any specific in-house laboratories of qualifications. MSC-derived extracellular vesicles (EVs) play a role in intercellular communication and EVs were shown to exert immunomodulatory and regenerative properties *in vitro*[76]. EVs contain important cargo, like proteins, RNA, and inflammatory mediators, and can potentially target specific cells[77]. Application of MSC-derived EVs to improve chondrogenesis facilitates an off-the-shelf product.

Likewise, chondroinductive growth factors, like fibroblast growth factor (FGF), transforming growth factor beta (TGF-β), and insulin-like growth factor (IGF), can be used to stimulate either proliferation, chondrogenesis, or both[78]. Alternatively, increasing interest has emerged for use of PRP and platelet lysate (PL). Both products can be prepared from autologous blood

and consist of a concentrated cocktail of growth factors and inflammatory mediators[79]. Although PRP and PL seem to stimulate cartilage ECM formation in chondrocytes, study outcomes vary greatly and no consensus exists on this matter[80–82].

Besides external stimulation of chondrocytes, performance of the cells might also be increased by pre-selection of cells for populations that are capable of stable hyaline cartilage formation *in vivo*. Several molecular markers have been identified as predictive of the chondrogenic capacity of the cells and improve structural repair[66,83].

Alternative cell types

Similar approaches are looking into the use of cell types other than chondrocytes to facilitate and ease procedures or provide for an off-the-shelf product. MSCs seem to be an ideal candidate cell population, as the cells are readily accessible in various tissues (e.g. bone marrow, adipose tissue, synovial tissue, and the umbilical cord) and allow for extensive culture expansion to obtain a substantial number of cells. However, the tendency of bone marrow-derived MSCs to differentiate into a hypertrophic chondrocyte phenotype limits its popularity. In addition, tissue engineered (TE) cartilage by human bone marrow-derived MSCs differs in epigenetic landscape and transcription profile compared to native cartilage[84] and neonatal or adult chondrocyte-derived TE cartilage[85].

Looking further into other tissues in the synovial joint, multipotent progenitor cells have been isolated and characterized from meniscus[86,87], periost[88], synovium[89], and the articular cartilage itself[15,90]. Especially ACPCs are of interest, as this subpopulation of cells has been extensively investigated. ACPCs are isolated from the total pool of chondrocytes by differential adhesion to fibronectin[15]. The cells were shown to have similar characteristics as MSCs and can be extensively culture-expanded without loss of chondrogenic potential[90,91]. Furthermore, ACPCs are successful in regenerating articular cartilage *in vitro* and *in vivo*[90,92,93], and have limited expression of markers hinting at terminal differentiation into hypertrophic chondrocytes[92,94,95].

Alternative to culture-expanded bone marrow-derived MSCs, BMC provides for a cell product that can be applied autologous and with minimal manipulation. As a concentrated bone marrow product, BMC contains a cocktail of growth factors similar to PRP, but also a small portion of progenitor cells[96]. Besides the use of BMC to treat chondral defects[53], BMC could also be of interest for bone repair, as improvement of bone union in animal models through BMC is seen[97].

Finally, pluripotent stem cells, like iPSCs and ESCs, are attractive cells for tissue regeneration because of their ability to differentiate into cell types of all three germ layers and indefinite self-renewal capacity. Implementation of these cells into treatments has proven to be difficult because of ethical and safety concerns[98,99]. Nevertheless, TE cartilage derived from iPSCs has been successful and resembled TE cartilage derived from primary human chondrocytes better

than bone marrow-MSC-TE cartilage[100]. Although safety studies are of particular importance[101,102], initial preclinical studies have shown no signs of tumorigenicity of iPSC-derived cartilage[103]. With clinical studies currently ongoing, pluripotent cell types might provide interesting treatment options for the future.

Providing structural support

Biological cues such as cells and growth factors alone are sometimes not sufficient to optimize tissue growth in the defect. A biocompatible, three-dimensional (3D) support can be provided to retain cells in their desired location, promote cell performance and/or tissue regeneration, and provide mechanical and structural integrity. Addition of various acellular biomaterials after microfracture was shown to significantly improve cartilage repair on a histological level[104].

The use of a 3D product facilitates the possibility to mould, cut, or print the construct into a desired shape or combine multiple materials or structures depending on the specific needs. Additionally, (chemical) composition or concentrations can be adjusted in order to obtain structures with mechanical stability similar to that of native tissue, providing strength and restore the progressing imbalance in the joint[105,106]. Loading of a scaffold with bioactive cues can stimulate simultaneously seeded cells or recruit endogenous cells, like chondrocytes or synovial cells, to induce regeneration of the tissue. Besides providing support for tissue regeneration, a material can be designed to degrade in a controlled fashion, while at the same time tissue remodelling takes place[107].

AIM AND THESIS OUTLINE

Main aim

The overall aim of this thesis is to advance cartilage regeneration in order to treat patients with focal chondral defects. To address this matter, the problem is approached from different angles, but all are based on biological modes of action, divided into two sections:

Part I: Cell-based cartilage regeneration
Part II: Orthobiologics for cartilage repair and joint preservation

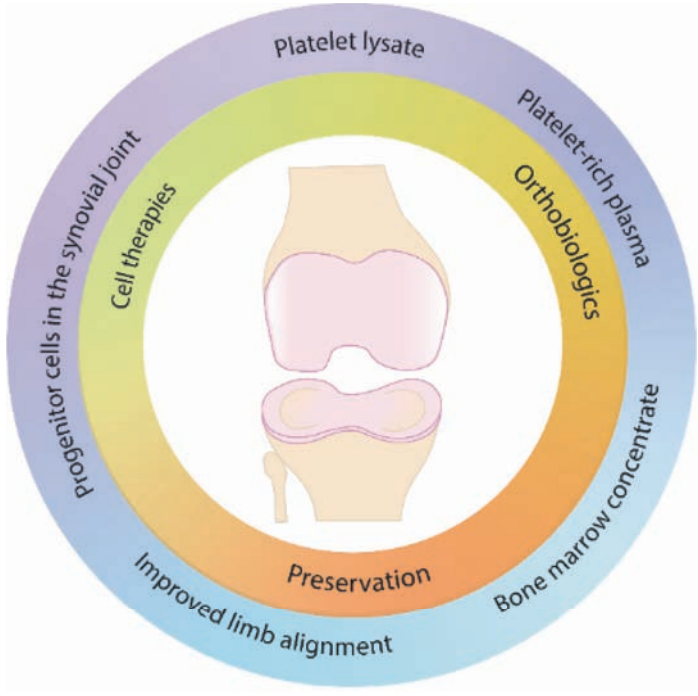

Figure 2. Thesis topics (outer circle) and their relevance in cartilage regeneration and joint preservation (inner circle).

The aim of **Part I** of this thesis is to investigate cell-based neo-cartilage formation *in vitro* and to investigate communication between cells. **Chapter 2** evaluates the current literature on human ACPCs and the potential of this cell type to be used in cell-based therapies. The systematic review aims to systematically summarize and align outcomes of published research. **Chapter 3** then provides a direct comparison of ACPCs derived from healthy and OA human knee cartilage. The potential of these cell populations to be extensively culture-expanded, as well as their chondrogenic differentiation potential is examined. In line with Chapter 3, **Chapter**

4 investigates the presence and performance of a progenitor cell population derived from another intra-articular tissue, the meniscus. As meniscus is closely related to articular cartilage, the progenitor cells residing in this tissue could also be of interest for regenerative cartilage therapies. To finalize the first part of this thesis, **Chapter 5** describes an in-depth investigation into cocultures of chondrocytes and MSCs. As communication between cells by the exchange of intracellular components might be responsible for increased cartilage matrix formation, transport of mitochondria was specifically studied.

The aim of **Part II** of this thesis is to enhance cartilage regeneration (or prevent its degeneration) by use of orthobiologics. Chapter 6 and 7 investigate two widely used blood-derived products, PL and PRP. In **Chapter 6**, PL is used as a supplement in culture medium, attempting to enhance chondrocyte yield in culture-expansion and at the same time preserve their chondrogenic potential. **Chapter 7** describes the effects of PRP on chondrocytes that are stimulated towards inflammation and investigates its potential to be used as a biomaterial to provide chondrocytes with a regenerative 3D environment. The final chapter, **Chapter 8**, combines a multidisciplinary approach to advance open-wedge osteotomy procedures by using MSCs and BMC in combination with a novel ceramic biomaterial fabricated into a patient-specific implant. The chapter concludes with a proof-of-concept surgical procedure of the wedge implantation. Finally, **Chapter 9** summarizes the findings of this thesis and integrates the work into the currently available literature.

Part I

Cell-based cartilage regeneration

Chapter 2

The clinical potential of articular cartilage-derived progenitor cells–a systematic review

Margot Rikkers
Jasmijn V. Korpershoek
Riccardo Levato
Jos Malda
Lucienne A. Vonk

NPJ Regenerative Medicine (2022)

ABSTRACT

Over the last two decades, evidence has emerged for the existence of a distinct population of endogenous progenitor cells in adult articular cartilage, predominantly referred to as articular cartilage-derived progenitor cells (ACPCs). This progenitor population can be isolated from articular cartilage of a broad range of species, including human, equine, and bovine cartilage. *In vitro*, ACPCs possess mesenchymal stromal cell (MSC)-like characteristics, such as colony forming potential, extensive proliferation, and multilineage potential. Contrary to bone marrow-derived MSCs, ACPCs exhibit no signs of hypertrophic differentiation and therefore hold potential for cartilage repair. As no unique cell marker or marker set has been established to specifically identify ACPCs, isolation and characterization protocols vary greatly. This systematic review summarizes the state-of-the-art research on this promising cell type for use in cartilage repair therapies. It provides an overview of the available literature on endogenous progenitor cells in adult articular cartilage and specifically compares identification of these cell populations in healthy and osteoarthritic (OA) cartilage, isolation procedures, *in vitro* characterization, and advantages over other cell types used for cartilage repair. The methods for the systematic review were prospectively registered in PROSPERO (CRD42020184775).

INTRODUCTION

Hyaline cartilage facilitates smooth movement of articular joints and transmission of mechanical forces. The mechanical strength of cartilage tissue is provided by the combination of highly organized collagen arcades and negatively charged proteoglycans that draw water into the tissue[108]. Persisting damage to this structural organization leads to a change in distribution of forces and loss in mechanical strength[109]. Cartilage injury can be post-traumatic, where defects are generally isolated, or it can occur during progression of osteoarthritis (OA) where defects can emerge simultaneously. Both focal defects and OA impair quality of life leading to pain, reduced mobility, and disability[8,9]. As healthy articular cartilage is an avascular tissue, its endogenous healing capacity is limited.

Adult chondrocytes, the cells residing in articular cartilage, are used to treat cartilage defects in autologous chondrocyte implantation (ACI)[41]. Due to the low cell density in cartilage, chondrocytes are culture-expanded to obtain a sufficient number of cells for treatment. Expansion of chondrocytes is limited in population doublings[110], as they tend to acquire a fibroblastic appearance and lose their chondrogenic phenotype[111,112], before becoming senescent. Alternatively, the use of mesenchymal stromal cells (MSCs) for cartilage repair has been evaluated extensively in clinical studies[113]. Despite their capacity to generate a cartilaginous tissue, MSCs have a tendency for differentiation into hypertrophic chondrocytes and subsequent endochondral ossification[114]. In contrast, MSCs are suggested to have chondro-inductive effects when combined with autologous chondrons for treatment of focal cartilage defects[115].

A distinct population of endogenous progenitor cells that resides in articular cartilage, named articular cartilage-derived progenitor cells (ACPCs), has been described in the last two decades[16,92,93,116]. The key *in vitro* characteristics of ACPCs include stem cell-like properties such as clonal expansion, extensive proliferation, and differentiation potential into multiple mesenchymal lineages, including the chondrogenic lineage. ACPCs were first identified in bovine cartilage[15], and later also in different species, including equine[111,116] and human cartilage[90,117]. Interestingly, ACPCs were shown not to upregulate type X collagen gene expression *in vitro*, a marker for hypertrophic differentiation during redifferentiation, contrary to MSCs[111,116]. The use of an endogenous cartilage progenitor cell population for treatment of cartilage defects and tissue engineering purposes therefore seems favourable over the use of other cell types[92,95,118]. Yet, isolation protocols and specific characterization for these cells differ greatly amongst researchers. In addition, a wide range of terms is being used to name the cells, like chondrogenic progenitor cells (CPCs), cartilage stem cells (CSCs), mesenchymal progenitor cells (MPCs), or cartilage-derived stem/progenitor cells (CSPCs). For clarity, this review refers to ACPCs to address all endogenous progenitor populations identified in adult hyaline cartilage and characterized *in vitro*.

The purpose of this review is to systematically evaluate the available literature on ACPCs derived from healthy and diseased adult articular cartilage. We summarize the state-of-the-art research and discuss its potential for clinical use in cartilage repair therapies.

METHODS

Literature search

A systematic search of literature was conducted according to the Preferred Reporting Items for Systematic Reviews and Meta-Analyses (PRISMA) guidelines on adult endogenous ACPCs. The review protocol was prospectively registered with PROSPERO (registration number CRD42020184775). The electronic databases of EMBASE and PubMed were searched using the following search terms: (cartilage AND (articular OR hyaline OR knee OR hip OR ankle)) AND (progenitor OR progenitor cell OR multipotent cell OR chondroprogenitor OR multipotent cell OR cartilage-derived OR articular cartilage-derived OR (stem cell OR MSC OR mesenchymal stem cell OR mesenchymal stromal cell AND (cartilage-derived OR cartilage resident))). A final search was performed on 17 February 2021. Two authors (M.R. and J.V.K.) independently screened all selected studies for eligibility, first by title and abstract followed by full-text screening. After duplicate removal, inconsistencies between the researchers were discussed in a consensus meeting.

Inclusion and exclusion criteria

Inclusion criteria that were used during title, abstract, and full-text screening for eligible studies included: adult endogenous cartilage stem/progenitor cells; knee, hip, or ankle cartilage; *in vitro* and/or *in vivo* and/or in man studies; English language. Reviews, case reports, conference papers, studies of which the full texts were not retrievable, studies investigating cell line chondroprogenitors, cells other than endogenous cartilage-derived progenitors, and lineage-tracing studies were excluded. Extracted data from the selected studies included species, anatomical location of cartilage, isolation procedure, cell characterization, and application of the cells. Quality of a study was considered inferior if methods or results are poorly reported on. Study limitations/inconsistencies are discussed at the end of a paragraph in the results.

RESULTS

The literature search yielded 1017 studies in EMBASE and 662 studies in PubMed. After duplicate removal, 1064 studies were identified. After title and abstract screening, the full text of 180 studies was screened. A total of 84 studies were then found eligible based on the inclusion and exclusion criteria (Figure 1).

Markers to identify ACPCs in vivo

The presence of ACPCs was first described by Dowthwaite *et al.* in 2004[15]. Enhanced expression of fibronectin and one of its key receptors, integrin-$\alpha 5\beta 1$, was found in the superficial zone of bovine articular cartilage. Isolation of this fraction resulted in a population with high clonogenicity. As a unique marker or marker set is lacking, MSC or chondrocyte markers are mostly used for identification (Table 1). Classical MSC markers CD105[119–121], CD166[122], CD146[123], VCAM[124], or combinations including these markers[125,126] have been used

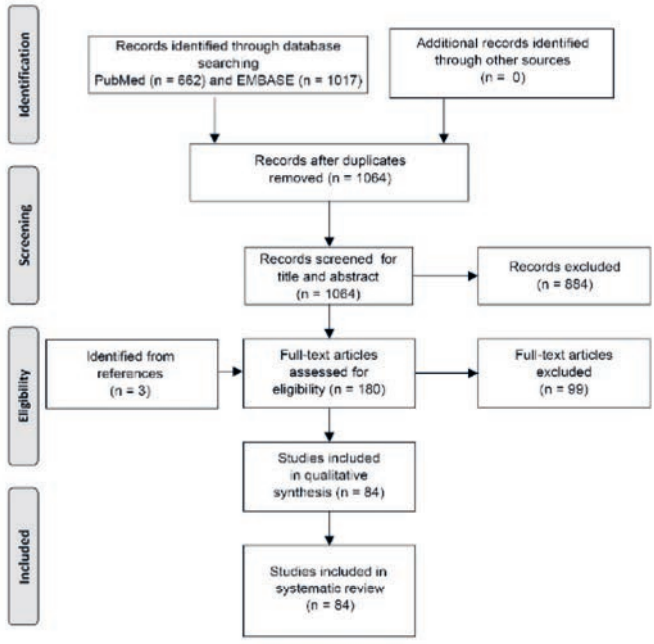

Figure 1. Preferred Reporting Items for Systematic Reviews and Meta-Analyses (PRISMA) workflow showing systematic selection process for studies.

by others. In essence, this results in identification of an MSC-like population in articular cartilage. Additional markers have been described to identify ACPCs in the tissue more specifically. Proteins involved in the Notch signalling pathway, like Notch-1, Notch-2, Delta, and Jagged[124,127], or integrin-$\alpha5\beta1$[119], proteoglycan 4 (PRG4, or lubricin)[128], and laminin[129] are used. Alternative approaches to identify ACPCs in cartilage tissue have focussed on visual distinction by an elongated cell morphology of ACPCs in cartilage tissue samples[129,130], cell clustering of ACPCs[131], proliferation marker Ki-67[131,132] and migration of ACPCs upon stimulation of the cartilage[133].

Methods for isolation of ACPCs from cartilage

Differential adhesion to fibronectin

A protocol for selective isolation of ACPC by differential adhesion to fibronectin (DAF) was established[15,90,127], taking advantage of the enriched expression of the fibronectin receptor[15] and the finding that isolation based on integrins resulted in selection for stem cells rather than transit amplifying cells[134]. In two-thirds of the studies using DAF, this protocol is followed by isolation of colonies, that are subsequently formed by the cells that adhere (generally) in 20 minutes[90,91,139–141,92,116,120,127,135–138]. Six out of nineteen studies did not perform colony isolation and the complete pool of cells that adhered to fibronectin was isolated[132,142–146].

Cell sorting based on marker expression

Alternatively, ACPCs are sorted from the total cell population either via immunomagnetic separation or fluorescence-activated cell sorting (FACS). ACPCs were isolated by FACS based on co-expression of CD105 and CD166[16], a marker combination which defines a subset of bone marrow-derived MSCs[147] and was proposed to select for ACPCs. Another marker set used for cell sorting that resulted in an ACPC population is $CD9^+/CD90^+/CD166^+$[148].

Isolation of ACPCs by ex vivo migration from cartilage

Finally, cells migrating out of cartilage explants, whether or not the cartilage is stimulated in any way, hold progenitor characteristics such as multilineage differentiation potential and colony forming efficiency (CFE)[95,126,130,149–151]. These migratory cells were distinctly different from chondrocytes and osteoblasts[152]. To stimulate migration of cells, explants were stimulated by nerve growth factor (NGF)[150], platelet lysate[95], or migrating cells were isolated after partial digestion of the tissue by collagenase[126]. Cell migration could also be triggered by induction of injury[130,151]. Cells with progenitor characteristics migrated towards the site of cartilage injury and a role in repair of adult cartilage upon damage was suggested by the authors[130].

Nine studies did not report on any distinct method to isolate a population from the total cell population[111,128,153–159]. Five others performed an isolation step after one or two passages in culture[122,123,160–162]. It can therefore be questioned whether these are investigating a population that is different from what are generally referred to as chondrocytes, as most of the studies were also lacking a chondrocyte control group.

In vitro characterization of ACPCs after isolation

Isolated ACPCs are characterized based on their proliferative potential, CFE, differentiation potential, and expression of markers that are also used for their isolation (Table 2). ACPCs could be maintained in culture for up to 30 – 60 population doublings[90,91,135,136,141] and early-passage cells were able to form colonies in culture[15,91,164,95,111,126,130,141,144,150,163]. Moreover, human ACPCs were found to maintain telomere length and telomerase activity up to at least 20 population doublings[135,141]. However, ACPCs derived from OA cartilage contained a sub-population of cells that have reduced proliferative potential and undergo early senescence when cultured *in vitro*[141].

ACPCs could be differentiated into the chondrogenic, osteogenic, and adipogenic lineage, a feature that MSCs also possess[165]. There is one report of reduced osteogenic differentiation potential of ACPCs[139], while 20% of the studies looking into multilineage potential found indications for reduced osteogenesis[93,95,116,118,148,166].

Surface marker expression of ACPCs was in general similar to MSCs, with ACPCs being positive for CD90, CD105, CD73, and CD166, while negative for hematopoietic markers, highlighting the challenge to distinguish the two cell types[95,116,161,126,128,137–139,149,150,154]. Of note, about half of the studies mentioned here examine immunophenotype of cells in

culture[95,116,149,154,159,164,167,120,126,128,132,137,139,142,145], while cells tend to change their phenotype during *in vitro* expansion[168,169]. Moreover, investigating marker expression by gene expression or flow cytometry on the bulk populations makes it problematic to define whether these markers are co-expressed or not.

In vitro comparison of ACPCs to other cell types with regard to surface marker expression

Cell surface marker expression and *in vitro* performance of ACPCs were directly compared to MSCs from various sources, like bone marrow[16,92,162,116,128,130,132,137,149,153,157], adipose tissue[123,128,137], and infrapatellar fat pad[144,157,158]. Other cell types compared are chondrocytes[90,95,144,146,151,163,164,170,120,123,127,130,132,135,138,139] and other intra-articular cells, like synoviocytes[151,157,158], synovial fluid cells[151], and periosteal cells[157,158,162] (Table 2).

A clear distinction between MSCs and ACPCs based on expression of markers was only reported once, when equine ACPCs were compared to bone marrow-derived MSCs, an increase in gene expression for CD44 was found[116]. One-third of the studies directly compares ACPCs to chondrocytes, as these also reside in adult hyaline cartilage and distinction of these cell types is crucial for isolation and application. Proliferation of ACPCs was faster than chondrocytes in one study[95], but slower in a different report[139]. In addition, ACPCs were found to form more colonies compared to chondrocytes[130]. A distinction was made between chondrocytes and ACPCs based on high expression of CD90[90,123,132], CD44[132], CD105[144], CD166[144], Notch-1[90], and HLA-ABC[123] in ACPCs while culture-expanded chondrocytes showed little to no expression of these markers. Co-expression of CD44 and CD90 was found to distinguish between rat chondrocytes and ACPCs[132,143]. When ACPCs were sorted from the total pool of chondrocytes by CD49e-expression, a difference was found in expression of CD29 in chondrocytes (50%) versus ACPCs (100%)[164]. When ACPCs were treated with platelet lysate, an increased expression of CD166 and decreased expression of CD106 compared to chondrocytes was found[95].

Differences between species

Identification of similarities and differences in ACPCs between species is challenging, due to the diversity of isolation procedures and variety of study objectives. Colony formation was identified in several human studies, as well as in the first report on bovine ACPCs. CFE in bovine cartilage cells was reported to be 0.6%[15], while all other literature on non-human cells lacked this analysis. In human cells, consistency is found to some extent. CFE in healthy cartilage cells on fibronectin-coated dishes was 1.47%[91], while this was almost double (2.8%) in OA cells in the same study. Others reported on CFEs of <0.1%[141] and 0.66%[164] of OA cells on fibronectin-coated dishes. When OA cells were seeded on uncoated culture plastic, a CFE of <0.01% was found[155–157]. The percentage of colony forming cells increased when cells were culture expanded. Passage one OA cells (isolation method not specified) had 18% CFE[128] and the same passage cells that migrated from OA tissue in response to platelet lysate had 7.8% CFE[95]. Cells that migrated from OA tissue with NGF and were expanded for four passages

had increased their CFE to 38.6%[150]. When $CD105^{+}/CD166^{+}$-sorted cells were quantified, CFEs of 3.5% (healthy) and 8% (OA) were found in one study[16] and 15% (healthy) and 17% (OA) were found in another[122]. Of note, the latter used cells that were culture expanded for one passage. Overall, when comparing human ACPC studies, it seems that OA tissue contains more colony forming cells than healthy cartilage. Also, CFE increases after culture-expansion, possibly as a consequence of culture-related changes in immunophenotype[169].

Differences between ACPCs from healthy and osteoarthritic cartilage

ACPCs have been identified in hyaline cartilage from different pathological states. Identification and characterization can contribute to our understanding of their role in homeostasis and disease, as well as their accessibility for clinical use.

In healthy articular cartilage, ACPCs most likely reside in the superficial zone, as Notch-1 expressing cells are found here[15] and possess progenitor cell characteristics[90,124,127]. In addition, enhanced expression of fibronectin and one of its receptors, integrin-α5 and -β1, was found in the superficial zone[15]. As a direct consequence, most of the cells isolated via DAF originated from the superficial zone. The same group also showed that the CFE of surface zone cells is higher compared to deep zone cells[15].

Upon damage of cartilage, ACPCs seem to migrate towards the site of injury[171]. Cells that migrated into the site of injury were found to possess progenitor-like characteristics[130]. An increase of CD271-expression was seen in ACPCs from increased OA severity[126]. Classical MSC markers CD105[119,120], VCAM[124], or combinations including these markers[125,126] were all enhanced in OA cartilage or upon trauma. A shift of expression of PRG4[128] from the superficial layer to deeper zones was seen in OA, whereas CD271- and CD105-positive cells shifted towards the superficial zone in OA[126]. In OA cartilage, cell clusters were observed which express ACPC-associated markers like Notch-1, Stro-1[125], VCAM, FGF-2, and Ki-67[124,131]. These cells proliferated faster and produced more cartilaginous nodules *in vitro* compared to cells isolated from macroscopically healthy cartilage[131]. Contradictory, others found that ACPCs derived from healthy cartilage proliferated faster than OA-derived ACPCs[161]. Lastly, a high number of CD105/CD166-positive[16] and CD146-positive cells[123] was found in OA cartilage and these cells had multilineage potential. OA-derived cells also formed more colonies compared to cells from normal human cartilage[91] and this increased with OA severity[126].

In vitro culture of ACPCs

Effects of culture conditions on ACPC behaviour

Three studies made an attempt to optimize growth kinetics examining factors like seeding density, culture systems, and serum concentrations[172–174]. The authors reported on optimal expansion conditions when the medium was supplemented with fetal bovine serum (FBS) and TGF-β1 at 40% and 1 ng/mL, respectively[172]. However, more recent studies have not used FBS concentrations that were as high as 40%. A passage length of five days was optimal for cell yield and the authors reported on reduced costs of expansion by 60%[174]. Furthermore, a

method for expansion on microcarriers eliminated the need for a harvesting step and was thus suggested to prevent dedifferentiation[173]. A direct comparison of fibronectin versus laminin, another important cell adhesion molecule, for differential adhesion of ACPCs resulted in higher population doubling, increased gene expression of type II collagen, and increased osteogenic and adipogenic differentiation potential of laminin-selected ACPCs[167]. Likewise, expansion with platelet lysate compared to FBS showed more population doublings and increased expression of chondrogenic genes aggrecan and type II collagen, but at the same time expression of type X collagen was also increased[175]. Others found increased gene expression of aggrecan, type II collagen and Sox9, as well as proteoglycan and type II collagen production of ACPCs by application of intermittent hydrostatic pressure[144] or mechanical stimulation in a bioreactor system[176], and inhibition of CFE by high glucose levels during growth culture[158]. Moreover, normoxic versus hypoxic conditions revealed greater production of glycosaminoglycans, low alkaline phosphatase expression, and weaker type I collagen staining in both conditions compared to MSCs[118]. In line, consistently low levels of type X collagen were expressed by ACPCs when normoxia and hypoxia were compared[166]. A reduction of oxygen tension during culture is also known to delay chondrocyte aging and improve their chondrogenic potential[177,178].

In brief, optimization of culture conditions for ACPCs have been investigated extensively. There are no uniform protocols for expansion and optimal differentiation for cartilage formation. Consensus on these matters would aid in comparing outcomes of studies in the future.

In vitro response of ACPCs to injury

Upon *ex vivo* injury of bovine cartilage, migratory cells with progenitor-characteristics were found[130,133]. Additional research showed that the phagocytic capacity of these ACPCs was higher compared to chondrocytes and comparable to synoviocytes and macrophages, suggesting a macrophage-like role for ACPCs in cartilage injury[179]. After treating ACPCs with supernatant from injured explants, proliferation, migration, and expression of immunomodulatory mediators were enhanced, while chondrogenic capacity was impaired[125].

In vitro response of ACPCs to compounds

Stimulation of chondrogenesis in ACPCs was successful by inhibition of the NF-κB pathway, the major signalling pathway involved in OA[180]. Inhibition of this pathway was achieved by an inhibiting peptide[132] and magnoflorine[143], both resulting in increased chondrogenesis. IL-1β and TNF-α, inflammatory factors involved in OA, were reported to inhibit migration of ACPCs[149]. Similarly, β-Catenin and NGF are elevated in OA[181,182]. Inhibition of the Wnt/β-Catenin pathway promoted proliferation and differentiation[160], while NGF failed to stimulate chondrogenesis in ACPCs[150]. The specific role of these compounds in OA remains to be investigated.

Alternatively, chondrogenesis could be triggered by direct activation of chondrogenic pathways. Combined mechanical stimulation and shear stress induced chondrogenesis

through an increase in endogenously produced TGF-β1, while overexpression of BMP2 reduced chondrogenesis[176]. Also, BMP9 was a potent stimulator of chondrogenesis[183]. Direct treatment of ACPCs with extracellular matrix components Link protein N-terminal peptide (LLP)[142] or nidogen-2[129] increased expression of chondrogenic genes. Proliferation of ACPCs was promoted by kartogenin[184], a small molecule that induces chondrogenic differentiation of MSCs. Finally, sex hormones estrogen and testosterone influenced human ACPC performance[185].

To summarize, initial results indicate that ACPCs respond to injury and chondrogenesis can be induced *in vitro,* which could make the cells interesting as therapeutic targets. These findings could be used to provoke neo-cartilage formation or inhibit inflammation in OA.

Application and translation of progenitors

ACPCs used for tissue engineering and biofabrication approaches

The potential of ACPCs for tissue engineering, biofabrication, and clinical application has been investigated widely. Biofabrication allows for production of constructs consisting of (bio)materials, bioactive cues, and/or cells, with a detailed predefined architecture[186]. The extensive proliferative potential of ACPCs combined with their chondrogenic capacity make these cells good candidates to use in tissue engineering and biofabrication approaches to repair or regenerate articular cartilage.

Under the influence of intermittent hydrostatic pressure, performance of rabbit ACPCs embedded in alginate was enhanced significantly. These cultures were pre-treated for one week with TGF-β3-containing medium but did not receive any exogenous growth factors thereafter. After two and four weeks, glycosaminoglycan, collagen, and DNA content were significantly higher than groups not treated with intermittent hydrostatic pressure[144]. Two studies investigating equine ACPC-performance in hydrogels both reported on good outcomes. When the cells were embedded in gelatin methacrolyl (gelMA) hydrogel cultured in chondrogenic medium, mainly a difference was found in the expression of zonal markers compared to bone marrow-derived MSCs. Expression of PRG4 was increased in ACPC-loaded gels, while type X collagen expression was decreased compared to MSCs[116]. Furthermore, when equine ACPCs were embedded in gelMA/gellan and gelMA/gellan/HAMA hydrogels and cultured in chondrogenic medium, these produced more glycosaminoglycans and type II collagen than chondrocytes, whereas performance of MSCs in the same gels was comparable to ACPCs[187]. Similar to hydrogels, printed scaffolds have also been successfully seeded with ACPCs. Human ACPCs seeded on fibrin-polyurethane composite scaffolds were responsive to mechanical stimulation. The cells produced more glycosaminoglycans and aggrecan gene expression was increased without addition of exogenous growth factors[176]. Furthermore, human ACPCs could also be seeded onto polycaprolactone/polylactic electrospun nanofibrous scaffolds where the cells attached and spread over the fibers. Further research has to shed light on chondrogenic performance of the cells in this specific setting[137].

Besides tissue engineering, ACPCs were successfully used in several biofabrication

techniques. It was shown that equine ACPCs have the potential to be bioprinted and while exact mechanisms remain to be elucidated, an interplay between MSCs, ACPCs, and chondrocytes was found to be important for neo-cartilage synthesis[116]. The same cells were also successfully used for encapsulation in various hydrogels[188–191] in combination with biofabrication techniques like extrusion-based bioprinting[116,187], digital light processing[192], and volumetric bioprinting[193], while maintaining cell viability. While these are only first indications to use ACPCs with various techniques, additional research is necessary to assess chondrogenic performance of the cells in these settings. Nevertheless, initial results are promising to move forward with this cell population.

In vivo and preclinical applications

Several attempts were made to take the next steps in application of ACPCs for *in vivo* cartilage formation and repair. These are important to translate *in vitro* findings and define the potential of ACPCs for the clinic.

When DAF-selected ACPCs were applied in a caprine model for cartilage defect filling using a cell-seeded type I/III collagen membrane (Chondro-Gide®), ACPC-seeded scaffolds showed good lateral integration with the surrounding tissue and type II collagen-positive repair tissue. However, no difference was found between chondrocyte- or ACPC-treated defects[90]. In the same study, engraftment into the growth plate of developing chick hind limbs of isolated and culture-expanded ACPCs was shown. Contradictory, DAF-selected bovine ACPCs that were injected intramuscularly in immune-deficient mice failed to produce cartilage matrix[136]. In an equine model, DAF-selected ACPCs were applied in a layered biofabricated osteochondral plug and showed good integration with the native cartilage, but the repair tissue contained mainly type I collagen[189]. When autologous and allogeneic ACPCs were directly compared in an equine cartilage defect model, an advantage of autologous over allogeneic cells was seen in histological outcomes[194].

When human ACPCs were used in immune-deficient mice, the cells were successful in production of cartilage matrix, whereas MSCs produced mainly bone[153]. The cells in this study were not isolated using any distinct method for ACPC isolation, but were 2D expanded in low density with low glucose. Furthermore, migratory human ACPCs expanded using platelet lysate outperformed chondrocytes in an *in vivo* ectopic chondrogenesis assay in athymic mice[95].

Finally, an attempt was made to proceed to human application, by using ACPCs to replace chondrocytes for matrix-assisted autologous chondrocyte transplantation (MACT), similar to the caprine study mentioned earlier. The pilot study with 15 patients[93] reported on repair tissue rich in type II collagen and proteoglycans and without types I and X collagen. Furthermore, IKDC and Lysholm questionnaire scores improved significantly. However, there was no direct comparison between ACPCs and expanded chondrocytes in this study.

While the discussed studies provide initial evidence of *in vivo* chondrogenic potential of these cells, further investigation is essential to ascertain promise cartilage repair and clinical translatability.

DISCUSSION

With this review, we aimed to systemically evaluate the available literature on adult ACPCs and their use for cartilage tissue engineering and repair therapies. We are the first to provide a thorough overview of research from the last two decades that demonstrates the presence of a progenitor cell population residing in adult hyaline cartilage (Figure 2). Although great effort was made to study the identity and applications of ACPCs, many uncertainties remain. As a result of differences in isolation protocols, characterization, and culture expansion, most cell populations discussed in literature are likely to be heterogeneous populations and difficult to compare between laboratories. This stresses the need for this systematic review to expose certain inconsistencies and arriving at a shared definition of ACPCs.

The reviewed literature employs a wide variety of procedures for isolation and characterization of ACPCs. Broadly speaking, three main methods for ACPC isolation are described. The method using differential adhesion to fibronectin, used in 42% of the investigated studies, is based on enriched expression of integrin-$\alpha 5\beta 1$, as first described by Dowthwaite et al[15]. The other two main methods are based on expression of (a combination of) cell surface markers (19%)[16,148] or migratory capacity (6%)[149]. Most populations isolated through these methods employed multilineage potential, responded to acute injury or mobilized during OA, and were able to produce hyaline cartilage extracellular matrix *in vitro* or *in vivo*.

The heterogeneity in isolation and characterization creates discrepancies between donors and laboratories. Direct comparisons of ACPC populations isolated through different procedures are lacking and would aid to improve our understanding of the populations. The identification of a unique cell marker would facilitate extensive and coordinated research into the cell type. This could pave the way towards clinical application or cell targeting to promote cartilage regeneration in OA. Recently, Gdf5-expressing cells in developing joints were identified to contribute to joint cell lineages[195]. Co-expression of Lgr5 and Col22a1 was identified as an important lineage marker towards juvenile articular chondrocytes in the developing mouse joint[196]. Additionally, single-cell RNA sequencing has revealed several novel markers that are potentially specific for ACPCs in human OA cartilage[197].

The available literature suggests that ACPCs resemble MSCs[165] *in vitro* based on surface marker expression and multilineage potential. The comparison to MSCs is often made due to the fact that MSCs (derived from various tissues) are a useful cell type for clinical application and are currently applied[113]. As the general view on the origin and role of MSCs is changing[198], characterization of ACPCs based on MSC-features might not be the way to go and other routes should be investigated. More recent work has shed light on the cellular basis of bone and cartilage formation by identifying skeletal stem cells in mice and humans[199,200], a cell type that might be closer related to (the origin of) ACPCs in adult hyaline cartilage. Although the comparison to clinically used chondrocytes is relevant, research into similarities between ACPCs and skeletal stem cells or more downstream progenitor cells is lacking and finding resembling features would contribute to knowledge about the origin and identity of ACPCs.

Establishing the role of ACPCs in cartilage development and homeostasis, as well as their response upon injury or in OA would provide additional insights into their physiological function in mature cartilage. Regeneration in the early stages of OA could be stimulated or progression of the disease halted. Several studies discussed here suggested that ACPCs have a possible role in immunomodulation, based on their capacity to migrate upon injury[130,133], excretion of inflammatory mediators[125] and phagocytic capacities[179]. Others found a higher prevalence of these cells upon cartilage damage and OA[119,120,124–126,128,130–133]. Of note, these are all *in vitro* indications for which *in vivo* validation is essential. During OA, cell density and clustering in cartilage increases[201], for which ACPCs might partly be responsible. On the other hand, there is contradicting evidence that Prg4-expressing cells from the synovium migrate into sites of acute cartilage injury and contribute to cartilage repair[195]. In order to expand the application of ACPCs to OA besides repair of chondral defects alone, immunomodulatory properties should be demonstrated *in vivo* as is known for MSCs[202].

The described ACPC populations generally surpassed other cell types in proliferative potential and producing cartilage extracellular matrix *in vitro*[95,118,123,139,144]. In addition, most studies implanting animal-derived ACPCs *in vivo* confirmed their chondrogenic potential[90,136,189], and even two studies using human cells reported on successful neo-cartilage formation[95,153]. As isolation methods do not seem to be associated with *in vivo* outcomes of cell performance and tissue formation, the challenge remains to compare findings between studies. Furthermore, differences between species and pathological states could influence cell performance. Donor age might play an important role, although none of the studies investigated this specifically. Nevertheless, the cells' potency of prolonged *in vitro* expansion[90,95,135] combined with limited tendency towards hypertrophic differentiation[92,95,116,166] and their ability to form neo-cartilage can make ACPCs an appropriate cell type for repair of focal chondral defects.

Despite the great deal of research that has been done on ACPCs, certain actions need to take place in order to close the gaps and reach consensus between researchers and laboratories. As noted before, isolation based on a unique marker is crucial to ascertain similarity in cell population between laboratories. Comparison of culture media and additives for ACPCs in a recent systematic review[203] highlights the importance of consistency to align research. As ACPCs currently have no discrete set of cell surface markers that can be used to isolate the cells from tissue, the question remains if ACPCs are a distinct cell type or it refers to a heterogeneous mix of many cell types. Establishment of a cell marker and consistency in isolation and culture protocols ascertain comparability between populations. Another limitation might be availability of tissue for cell isolation. Cartilage from OA patients is generally more accessible than healthy cartilage, as it is redundant after knee replacement surgery. A direct comparison of ACPC populations of healthy and OA cartilage would shed light on differences in performance. In the same view, investigation of allogeneic use of ACPCs is valuable, as this would greatly improve the potential of application by availability, reduction of costs, and preselection of chondrogenic cells.

Limitations of the current review

The current systematic review is limited by the restriction to cell populations that are isolated from adult hyaline cartilage. The comparison and relation to cell types in the developing joint is lacking and would contribute to our further understanding of the origin of the populations discussed here and their role in joint development and homeostasis. However, the current review and discussed literature is predominantly directed at clinical translation as opposed to etiology or the role of a cartilage progenitor cell in development.

Guidelines and/or recommendations for minimal criteria of ACPC populations

Arriving at a shared definition of a homogenous cell population that can be isolated and characterized in a comparable manner is crucial. This work could be used as a basis for research groups and clinicians to harmonize study protocols and characterization. First, studies should report on origin of the cell in terms of species, anatomical location of the hyaline cartilage, and disease state. Second, method of isolation should be described in detail and preferably identical to one of the established protocols. Finally, phenotype of the isolated populations should be examined directly following isolation and culture media (and additives) as well as expansion time and/or passage number should be reported and synchronized.

Conclusions and future implications

To conclude, the available literature indicates that a cell population with progenitor-like characteristics resides in adult hyaline cartilage, which has extensive chondrogenic and proliferative potential. These features highlight the suitability of ACPCs as a cell source for focal chondral repair. In addition, it is crucial to investigate the role of ACPCs in development and disease, in order to determine their potential to slow down or reverse OA. If the current challenges can be overcome and consensus can be reached on this population, ACPCs hold great potential as a cell type for tissue engineering and for repair of cartilage damage in both focal cartilage injury and OA.

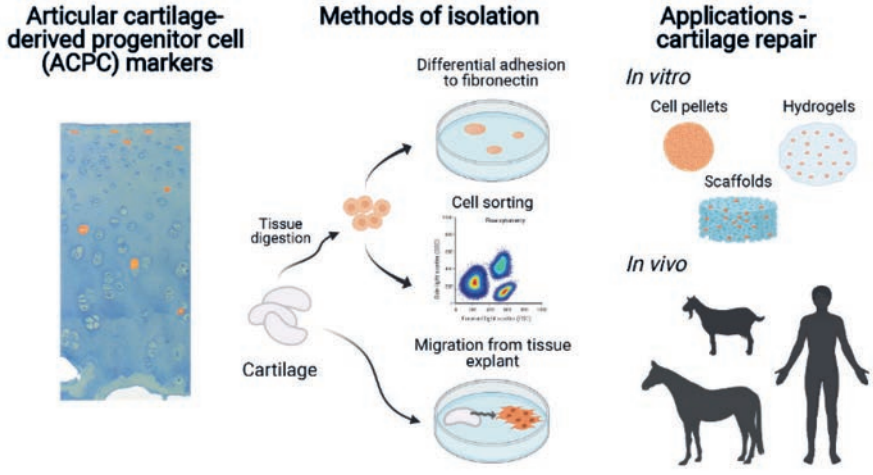

Figure 2. Schematic overview of the identification of articular cartilage-derived progenitor cells (ACPCs) in cartilage, isolation methods, and applications of ACPCs. Created with BioRender.com

Table 1. Identifying an ACPC population in articular cartilage

	Species	Anatomical location of cartilage	Disease model/state	Method of progenitor identification in tissue	Outcomes
Tao et al., 2018[120]	Murine	Knee	Unknown	$CD105^+$ in superficial layer	$CD105^+$ cells in superficial layer increased after induced OA and FN treatment. $CD105^+/CD166^+$ cells increased consistently
Tong et al., 2015[132]	Rat	Knee	Unknown	Ki-67/BrdU labeling	Prevalence of ACPCs increases in OA. Highest frequency in superficial layer. Inhibition of NF-κB pathway increased ACPCs in OA progression and lowered OARSI scores
Zhang et al., 2016[119]	Rat	Hip	Unknown	$CD105^+$/integrin-$\alpha5\beta1^+$ co-expression	$CD105^+$/integrin-$\alpha5\beta1^+$ cells are activated by partial-thickness cartilage defects
Cai et al., 2020[143]	Rat	Knee	ACLT-induced OA	$CD44E^+/CD90^+$ co-expression	Recovery of $CD44E^+/CD90^+$ cells in cartilage after ACLT and treatment with HA and magnoflorine
Walsh et al., 2020[121]	Porcine	Knee	Unknown	Mechanical loading of immature, adolescent, and mature cartilage followed by surface marker expression, gene expression, and histology.	Increased expression of CD105 and CD29 in immature cartilage; decreased expression of ACAN, Col-X and SOX9 in immature cartilage, increased expression of Col-I, Col-II in immature cartilage
Dowthwaite et al., 2004[15]	Bovine	Articular cartilage (surface, middle, and deep zone)	Unknown	Expression of integrin-α5, integrin-β1, fibronectin, and Notch-1	All markers are mainly expressed in the superficial zone
Jang et al., 2014[133]	Bovine	Stifle (tibial plateau)	Unknown	Calcein-AM/Ethidium homodimer staining of cells migrated into fibrin in partial- and full-thickness defects, treated with low-intensity pulsed ultrasound	More cells migrated in low-intensity pulsed treated defects. FAK activation increased in treated samples

Seol et al., 2012[130]	Bovine and human	Stifle (bovine) and talus (human)	Healthy	Morphology	Increased number of elongated cells in impacted cartilage explants of both species
Ustunel et al., 2008[127]	Human	Knee (intercondylar notch)	Healthy	Expression of Notch-1, Notch-2, Notch-3, Notch-4, Delta, Jagged-1, and Jagged-2	Notch-1 and Delta were abundantly expressed in the superficial zone
Grogan et al., 2009[124]	Human	Knee	Healthy and OA	Expression of Notch-1, VCAM, and Stro-1	All markers show expression throughout all cartilage layers; expression in superficial zone is increased
Pretzel et al., 2011[122]	Human	Knee	Healthy and OA	Expression of CD166	High percentage (22%) of $CD166^+$ cells. Highest prevalence in superficial and middle zone
Su et al., 2015[123]	Human	Knee (femoral condyles)	OA	Expression of CD146	$CD146^+$ cells observed in OA cartilage and are smaller size than $CD146^-$ cells
Hoshiyama et al., 2015[131]	Human	Knee (femoral condyles)	OA	Cell clustering; expression of Stro-1, FGF-2, Ki-67	More cell clustering and higher expression of all markers in cells adjacent to cartilage damage
Schminke et al., 2016[129]	Human	Knee (lateral femoral condyles)	Healthy and OA	Morphology; expression of laminin-α1 and laminin-α5 in the pericellular matrix.	More laminins expressed in the pericellular matrix of cells with an elongated morphology
De Luca et al., 2019[128]	Human	Hip (femoral head and neck)	Healthy and OA	Expression of PRG-4	Expression of PRG-4 shifts from the superficial layer (healthy cartilage) to deeper zones (OA cartilage)
Wang, Y et al., 2020[126]	Human	Knee (tibial plateau)	OA	$CD271^+$ and $CD105^+$ cell distribution in WORMS grade 1 - 2 versus 3 - 4 cartilage	Enhanced expression of CD105 and CD271 in the superficial zone of grade 3 - 4 cartilage.

ACLT anterior cruciate ligament transection, *FAK* focal adhesion kinase, *FN* fibronectin, *HA* hyaluronic acid, *OA* osteoarthritis, *PRG-4* proteoglycan 4, *VCAM* vascular cell adhesion molecule

Table 2. Isolation and characterization of ACPCs

Study	Species	Anatomical location of cartilage	Disease state	Isolation procedure of cells	Cell characterization		Compared to (cell type)
				Differential adhesion to fibronectin		*Marker expression*	
Tao et al., 2018[120]	Murine	Knee	Unknown	DAF followed by colony isolation	Proliferation; migration; chondrogenic differentiation	CD34, CD45, CD105, CD166	Chondrocytes
Tong et al., 2015[132]	Rat	Hip and knee	Unknown	DAF	Chondrogenic, osteogenic, and adipogenic differentiation	CD90, CD44, CD45, CD31, CD34	Chondrocytes; BM-MSCs
He et al., 2018[142]	Rat	Knee	Unknown	DAF	Osteogenic and adipogenic differentiation	CD90, CD73, CD105, CD34, HLA-DR (after one passage)	-
Cai et al., 2020[143]	Rat	Knee	OA (ACLT-induced)	DAF	Chondrogenic differentiation	CD44E/CD90 coexpression	-
Li et al., 2016[144]	Rabbit	Knee (surface zone cartilage)	Healthy	DAF	CFE; chondrogenic, osteogenic and adipogenic differentiation in alginate beads	-	Chondrocytes; IFP-stem cells
Dowthwaite et al., 2004[15]	Bovine	Articular cartilage (surface, middle, and deep zone)	Unknown	DAF	Adhesion to FN; CFE	α5 and β1 integrin (immunolocalization)	-
Khan et al., 2009[135]	Bovine	Juvenile metacarpophalangeal joint	Healthy	DAF followed by colony isolation	Population doublings; telomerase activity; telomere length; gene expression; chondrogenic differentiation	Sox-9; Notch-1; PCNA (all immunolocalization)	Full-depth and superficial zone chondrocytes

Marcus et al., 2014[136]	Bovine	Metacarpo phalangeal joint	Healthy	DAF followed by colony isolation	Population doublings	-	-
McCarthy et al., 2012[92]	Equine	Metacarpal joint	Unknown	DAF followed by colony isolation	Chondrogenic, osteogenic, and adipogenic differentiation	Notch-1; Stro-1; CD90; CD166 (all immunolocalization)	BM-MSCs
Levato et al., 2017[116]	Equine	Metacarpo phalangeal joint	Healthy	DAF followed by colony isolation	Chondrogenic, osteogenic, and adipogenic differentiation	CD13; CD29; CD31; CD44; CD45; CD49d; CD73; CD90; CD105; CD106; CD146; CD166 (all gene expression)	BM-MSCs
Ustunel et al., 2008[127]	Human	Knee (intercondylar notch)	Healthy (ACLT repair)	DAF followed by colony isolation	-	Notch-1; Notch-2; Notch-3; Notch-4; Delta; Jagged-1; Jagged-2 (all immunolocalization in colonies)	Chondrocytes
Williams et al., 2010[90]	Human	Knee	Healthy	DAF followed by colony isolation	Population doublings; chondrogenic, osteogenic, and adipogenic differentiation; karyotyping; telomere length analysis; cell engraftment *in ovo*	Notch-1; CD90; Stro-1; Jagged-1; Delta-1 (all immunolocalization)	Full-depth chondrocytes
Nelson et al., 2014[141]	Human	Knee (tibial plateau)	OA	DAF followed by colony isolation	CFE on FN; growth kinetics; chondrogenic, osteogenic, and adipogenic differentiation;	STRO-1	-
Fellows et al., 2017[91]	Human	Knee (tibial plateau)	Healthy and OA	DAF followed by colony isolation	CFE on FN; growth kinetics; chondrogenic, osteogenic, and adipogenic differentiation; telomere length analysis	-	-

Shafiee et al., 2016[137]	Human	Articular cartilage (not specified)	Unknown	DAF followed by colony isolation	Cell cycle analysis; karyotyping; proliferation; chondrogenic differentiation	CD166; CD133; CD106; CD105; CD90; CD73; CD 45; CD34; HLA-DR	Nasal septum-progenitors; BM-MSCs; AD-MSCs
Vinod et al., 2019b[138]	Human	Knee (superficial layer)	Healthy	DAF followed by colony isolation	Chondrogenic, osteogenic, and adipogenic differentiation	CD105; CD73; CD90; CD34; CD45; CD29; CD49e; CD151; CD166	Chondrocytes
Zhang et al., 2019[145]	Murine and human	Knee	Healthy and OA	DAF	Chondrogenic, osteogenic, and adipogenic differentiation; proliferation; high-throughput RNA sequencing	PRDM16; NCAM-1; N-cadherin; CPNE-1; CTGF (protein expression). CD29; CD44; CD90; CD45; CD34	-
Kachroo et al., 2020a[146]	Human	Knee	OA	DAF	Gene expression	-	Non-DAF cells; fresh cartilage cells
Vinod et al., 2020a[139]	Human	Knee	Healthy and OA	DAF followed by colony isolation	Population doublings; chondrogenic, osteogenic, and adipogenic differentiation; gene expression	CD105, CD73, CD90, CD34, CD45, CD14, CD54, CD44, CD9, CD106, CD29, CD151, CD49e, CD166; CD146	Chondrocytes
Vinod et al., 2020b[140]	Human	Knee	Healthy and OA	DAF followed by colony isolation	Expression of immunogenic markers HLA-A2; HLA-B7; HLA-DR; CD80; CD86; CD14	-	Chondrocytes
				Cell sorting			
Karlsson et al., 2008[163]	Bovine	Knee (femoral condyle)	Healthy	FACS for Notch-1 or cell size	CFE (in agarose); chondrogenic, osteogenic, and adipogenic differentiation	-	Notch-1$^-$ cells and larger/smalls cells
Alsalameh et al., 2004[16]	Human	Knee (femoral condyle	Healthy and OA	Immunomagnetic cell separation for CD105$^+$/CD166$^+$	Chondrogenic, osteogenic, and adipogenic differentiation	CD105; CD166 (immunolocalization)	BM-MSCs

		and tibial plateau)					
Fickert et al., 2004[148]	Human	Knee	OA	FACS for $CD9^+/CD90^+/CD166^+$	Chondrogenic, osteogenic, adipogenic differentiation	-	-
Pretzel et al., 2011[122]	Human	Knee	OA	Immunomagnetic cell separation for CD166 (after one passage)	Chondrogenic, osteogenic, adipogenic differentiation	CD105; CD166 (immunolocalization)	-
Peng et al., 2014[160]	Human	Hip (femoral head)	Healthy and OA	Immunomagnetic cell separation for $CD105^+/CD166^+$ (after one passage)	Chondrogenic differentiation	-	-
Su et al., 2015[123]	Human	Knee (femoral condyles)	OA	FACS for CD146 (after one passage)	Chondrogenic, osteogenic, and adipogenic differentiation; gene expression; CFE (after three passages)	CD29; CD31; CD45; CD133; CD44; CD34; CD73; CD90; CD146; CD105; CD166; HLA-ABC; HLA-DR	Unsorted chondrocytes; AD-MSCs
Unguryte et al., 2016[204]	Human	Knee	OA	FACS for ALDH activity	Gene expression	CD29; CD49a; CD49c; CD105; CD349; Notch1; CD54; CD55; CD56; CD63; CD47; CD140b; CD146; CD166	$ALDH^-$ and ALDH-diminished-expressing cells
Xia et al., 2016[161]	Human	Knee (femoral condyles)	OA	FACS for $CD105^+/CD166^+$ (after two passages)	Cell proliferation; gene and miRNA expression; chondrogenic, osteogenic, and adipogenic differentiation	CD29; CD44; CD73; CD90; CD105; CD166; CD19; CD34; CD45; HLA-DR	-
Kachroo et al., 2020b[164]	Human	Knee	OA	FACS for $CD49e^+$	CFE	CD49e; CD29	Fresh chondrocytes; $CD49e^-$ cells

				Migration from tissue			
Joos et al., 2013[149]	Human	Knee	OA	Outgrowth from cartilage tissue	Chondrogenic, osteogenic, and adipogenic differentiation; cell migration; chemotaxis	CD9; CD54; CD146; CD14; CD73; CD166; CD29; CD88; CD184; CD34; CD90; MSCA-1; CD44; CD105; Stro-1 (and quadruplicate combinations of these markers)	BM-MSCs
Jiang et al., 2015[150]	Human	Knee (femoral condyles)	OA	Cell migration through a membrane stimulated by NGF	CFE; chondrogenic, osteogenic, and adipogenic differentiation	CD90; CD73; CD105; CD166; CD44; CD29; CD34; CD45	-
Carluccio et al., 2020[95]	Human	Hip	OA	Outgrowth from cartilage tissue using platelet lysate	Growth kinetics; CFE; chondrogenic, osteogenic, and adipogenic differentiation; migration; chemotaxis; secretory profile; gene expression	Cyclin D1; α-tubulin (protein expression); CD44; CD166; HLA-ABC; HLA-DR; CD90; CD105; CD73; CD146; CD106; CD45; CD34; CD29	Chondrocytes
				Enzymatic			
Seol et al., 2012[130]	Bovine	Stifle (tibial plateau)	Healthy	Trypsin treatment after injury	Migration; chemotaxis; chondrogenic, osteogenic, and adipogenic differentiation; RNA microarray; CFE	-	BM-MSCs; chondrocytes
Zhou et al., 2014[151]	Bovine	Stifle (tibial plateau)	Healthy	Trypsin treatment after injury	Gene expression; chondrogenic differentiation	-	Chondrocytes; synoviocytes; synovial fluid cells
Wang, Y et al., 2020[126]	Human	Knee (tibial plateau)	OA	Collagenase treatment followed by outgrowth	Growth kinetics; CFE; chondrogenic, osteogenic, and adipogenic differentiation	CD29; CD31; CD44; CD45; CD73; CD90; CD105; CD166; CD271	-

				Other isolation procedures			
Hattori et al., 2007[205]	Bovine	Stifle	Healthy	Hoechst 33342$^-$	Chondrogenic differentiation	-	Hoechst 33342$^+$ population
Yu et al., 2014[170]	Bovine	Stifle (femoral condyle)	Healthy	Colony formation of single live cells	Chondrogenic, osteogenic, and adipogenic differentiation; gene expression; migration	-	Chondrocytes
Thornemo et al., 2005[162]	Human	Knee	Healthy	Cluster growth in agarose (after one passage)	Chondrogenic, osteogenic, and adipogenic differentiation	-	Periosteal cells; BM-MSCs; fibroblasts
Grogan et al., 2009[124]	Human	Knee	Healthy and OA	Hoechst 33342$^-$	Chondrogenic, osteogenic, and adipogenic differentiation	-	Hoechst 33342$^+$ population
				No isolation procedure described			
Barbero et al., 2003[111]	Human	Knee (femoral condyle)	Healthy	-	CFE; proliferation rate; chondrogenic, osteogenic, and adipogenic differentiation	-	-
Tallheden et al., 2003[153]	Human	Knee	Healthy	-	Chondrogenic, osteogenic, and adipogenic differentiation	-	BM-MSCs
Bernstein et al., 2013[154]	Human	Knee	OA	-	Chondrogenic, osteogenic, and adipogenic differentiation	CD9; CD166; CD90; CD54; CD44; CD45; CD105; CD73; CD54 (quadruple combinations)	-

Salamon et al., 2013[159]	Human	Knee	OA	-	Growth kinetics; adipogenic and osteogenic differentiation	CD29; CD44; CD105; CD166	AD-MSCs
Mantripragada et al., 2018a[156]	Human	Knee (femoral condyle)	OA	-	CFE; chondrogenic differentiation	-	-
Mantripragada et al., 2018b[155]	Human	Knee (femoral condyle)	OA	-	CFE; chondrogenic differentiation	-	-
De Luca et al., 2019[128]	Human	Hip (femoral head and neck)	OA	-	CFE; chondrogenic, osteogenic, and adipogenic differentiation; immunomodulatory properties	CD14; CD34; CD44; CD45; CD71; CD105; CD166; CD90; CD73; CD151	BM-MSCs; AD-MSCs
Mantripragada et al., 2019[157]	Human	Knee (femoral condyle)	OA	-	CFE; chondrogenic differentiation	-	BM-MSCs; IFP-cells; synovium-derived cells; periosteal cells
Mantripragada et al., 2020[158]	Human	Knee (femoral condyle)	OA	-	CFE; chondrogenic differentiation	-	IFP-cells; synovium-derived cells; periosteal cells

ACLT anterior cruciate ligament transection, *AD* adipose tissue-derived, *ALDH* aldehyde dehydrogenase, *CFE* colony-forming efficiency, *DAF* differential adhesion to fibronectin, *FN* fibronectin, *IFP* infrapatellar fat pad, *NGF* nerve growth factor, *OA* osteoarthritis

Table 3. Application and translation of ACPCs

Study	Species	Anatomical location of cartilage	Disease state	Isolation procedure of cells	Other cell types compared	Application(s)	Outcomes
In vitro studies							
He et al., 2018[142]	Rat	Knee	Unknown	DAF	-	Effect of LLP on cytotoxicity, chondrogenesis, proliferation, migration, chemotaxis, gene, and protein expression	No difference in cytotoxicity, proliferation; migration, chemotaxis and chondrogenesis were increased by LLP; Sox9, Col-II, and Acan gene expression increased with LLP
Melero-Martin et al. 2005[172]	Bovine	Juvenile metatarsophalangeal joint (superficial zone)	Healthy	DAF	-	Effect of cryopreservation on proliferation, viability, and chondrogenesis. Comparison between media and FBS, TGF-β1, and FGF concentrations	Cell density increased 53-fold with optimized FBS concentration up to 40% and feeding rate above 10 uL/cm^2/h. Cell density increased 33-fold when media was supplemented with 1 ng/mL TGF-β1 and 40% FBS. Chondrogenic differentiation potential was maintained
Melero-Martin et al., 2006a[174]	Bovine	Juvenile metatarsophalangeal joint (superficial zone)	Healthy	DAF	-	Effect of seeding density, passage number, and feeding strategy on cell density	Optimal growth kinetics at 10^4 cells/cm^2 seeding density and 73h passage length. However, looking at costs of expansion, a longer culture time was preferred
Melero-Martin et al., 2006b[173]	Bovine	Juvenile metatarsophalangeal joint (superficial zone)	Healthy	DAF	-	Growth kinetics 2D vs 3D microcarriers and differentiation potential afterwards	Expansion slower than in 2D, but upscaling possible and chondrogenic differentiation potential maintained; bead-to-bead migration possible (subcultivation without harvesting)
Seol et al., 2012[130]	Bovine	Stifle (tibial plateau)	Healthy	Enzymatic: Trypsin treatment after injury	BM-MSCs; chondrocytes	Migration of GFP-labelled grafted ACPCs into an impacted area on osteochondral explant	The number of labelled cells in the impact site increased drastically from 2 to 12 days (no quantification)

Jang et al., 2014[133]	Bovine	Stifle (tibial plateau)	Unknown	Enzymatic: Trypsin treatment after injury	-	Cell migration under influence of low intensity pulsed ultrasound	Low intensity pulsed ultrasound stimulated migration of isolated ACPCs into scratch
Zhou et al., 2016[179]	Bovine	Stifle (tibial plateau)	Healthy	Enzymatic: Trypsin treatment after injury	Chondrocytes; synoviocytes	Phagocytic capacity	ACPCs internalized more cell-debris than chondrocytes; similar to synoviocytes and (murine cell-line) macrophages; ACPCs overexpressed markers associated with phagocytosis and internalized more FN fragments than chondrocytes
Morgan et al., 2020[183]	Bovine	Immature metacarpophalangeal joint	Healthy	DAF followed by colony isolation	-	Determination of optimal potent chondrogenic factors	BMP9 increased aggrecan and Col-II gene expression, low Col-X expression, more anisotropic collagen fibril deposition
Koelling et al., 2010[185]	Human	Knee	OA	Outgrowth from cartilage tissue	-	Effect of sex hormones on regenerative potential	Sex hormones influence regenerative potential of progenitor cells
Joos et al., 2013[149]	Human	Knee	OA	Outgrowth from cartilage tissue	-	Cell migration under the influence of IL-1B and TNF-α	Cell migration was inhibited by both IL-1B and TNF-α
Peng et al., 2014[160]	Human	Hip (femoral head)	Healthy and OA	Immunomagnetic cell separation for $CD105^+/CD166^+$ (after one passage)	-	Effect of Wnt-signaling on chondrogenic differentiation	Inhibition of Wnt/β-catenin promoted proliferation and differentiation
Jiang et al., 2015[150]	Human	Knee (femoral condyles)	OA	Cell migration through Transwell stimulated by NGF	-	Influence of NGF on chondrogenesis	Chondrogenesis was not stimulated by NGF

Schminke et al., 2016[129]	Human	Knee (lateral femoral condyles)	OA	Outgrowth from cartilage tissue	-	Effect of laminin or nidogen-2 on gene expression; Nidogen-2 siRNA applied	SOX9 and ACAN increased by nidogen-2. COL2A1 increased and COL1A1 decreased by laminin. ACPCs expressed more Nidogen-2 compared to both chondrocyte types. siRNA knockdown of nidogen-2 caused increased RUNX2 and decreased SOX9 protein expression
Anderson et al., 2016[166]	Human	Knee (femoral condyles)	Healthy	DAF followed by colony isolation	-	Response to normoxia and hypoxia in pellets	Variation in intrinsic chondrogenicity between clones. ACPCs demonstrate a consistently low COLX gene and protein expression in physoxia
Nguyen et al., 2017[206]	Human	Hip and knee	OA	-	-	Expansion with FBS vs PL	PL induces re-entry of cell cycle, stimulates proliferation; PL-expanded cells better at producing cartilage; PL induces cell outgrowth from cartilage pieces
Anderson et al., 2018[94]	Human	Knee (femoral condyles)	Healthy	DAF followed by colony isolation	-	Tissue self-assembly on membranes	Oriented cartilaginous tissue self-assembly by ACPCs on FN membranes. Higher GAG and collagen when compared to chondrocytes; surface lubricin was lower in ACPCs
Riegger et al., 2018[125]	Human	Knee (femoral condyles)	OA	Outgrowth from cartilage tissue	-	Treatment of cells with explant supernatants (impacted or treated with compounds); chondrogenic capacities; gene expression for pro- and anti-inflammatory factors	Enhanced proliferation, migration and expression of immunomodulatory mediators. Chondrogenic capacity was impaired
Vinod et al., 2019a[207]	Human	Knee (superficial layer)	Healthy	DAF followed by colony isolation	-	Micron-sized super paramagnetic iron oxide (M-SPIO) particle uptake and function thereafter	Viability, cell-markers, and chondrogenesis reduced with increasing concentration M-SPIO; osteogenic and adipogenic differentiation were unchanged

Vinod et al., 2019b[138]	Human	Knee (superficial layer)	Healthy	DAF followed by colony isolation	Chondrocytes	Cocultures of ACPCs and chondrocytes in different ratios	No difference in surface marker expression, gene expression, or growth kinetics
Vinod et al., 2019c[208]	Human	Knee (superficial layer)	OA	DAF followed by colony isolation	-	Trilineage differentiation and viability of ACPCs in PRP clots	Maintained differentiation potential and viability in PRP clots
Kachroo et al., 2020[175]	Human	Knee	OA	DAF followed by colony isolation	-	Expansion of ACPCs with 10% FBS vs 10% hPL	hPL-expanded ACPCs had more population doublings, higher expression of CD146, and increased gene expression of COL2A1, ACAN, COL1A1, COL10A1
Mantripragada et al., 2020[158]	Human	Knee (femoral condyle)	OA	-		Growth of ACPCs in high glucose (25mM) and low glucose (5mM)	CFE was inhibited by glucose
Vinod et al., 2020c[167]	Human	Knee	OA	DAF or differential adhesion to laminin followed by colony isolation	-	Comparison of fibronectin vs laminin adhesion assay for ACPC isolation	Higher population doublings in laminin-selected ACPCs; No difference in expression of CD105, CD73, CD90, CD34, CD45, HLA-DR, CD146, CD166, CD49e, and CD29; increased expression of COL2A1 in laminin-selected ACPCs; Increased osteogenic and adipogenic differentiation
Wang, Y et al., 2020[126]	Human	Knee (tibial plateau)	OA	Collagenase treatment followed by outgrowth	-	Differentiation; gene expression; migration (upon treatment with OA SF); comparison of grade 1 - 2 and 3 - 4 ACPCs	Grade 3 - 4 ACPCs showed enhanced migratory, osteogenic and adipogenic potential; decreased chondrogenic potential
Vinod et al., 2021[209]	Human	Knee	Healthy	DAF followed by colony isolation	-	Chondrogenesis under influence of a pulsed electromagnetic field	No difference between TGF-β2-treated ACPC pellets and pellets treated with a pulsed electromagnetic field
Tissue engineering studies							

Li et al., 2016[144]	Rabbit	Knee (surface zone cartilage)	Healthy	DAF	Chondrocytes; IFP-stem cells	Effect of intermittent hydrostatic pressure on ACPCs in alginate beads	Increase in migration, proliferation, GAG production, Col-II production, chondrogenic gene expression under influence of intermittent hydrostatic pressure
Schmidt et al., 2020[118]	Equine	Metacarpophalangeal joint	Healthy	DAF followed by colony isolation	BM-MSCs	3D culture in agarose in normoxic versus hypoxic conditions. Monocultures of ACPCs and MSCs, and zonal construct of ACPC/MSC	Higher production of glycosaminoglycans by ACPCs in normoxia and hypoxia. Weaker type I collagen staining in ACPC constructs, low ALP expression
Neumann et al., 2015[176]	Human	Knee (tibial plateau)	Healthy	DAF followed by colony isolation	-	BMP-2 overexpression through adenovirus; Scaffold culture loaded versus unloaded	Loading induced chondrogenesis; chondrogenesis reduced by BMP2 overexpression
Shafiee et al., 2016[137]	Human	Articular cartilage (not specified)	Unknown	DAF followed by colony isolation	Nasal septum-progenitors (NSPs); BM-MSCs; AD-MSCs	Chondrogenesis and proliferation on nanofibrous scaffolds (PCL/PLLA).	Expression of SOX9 and ACAN higher in NSPs compared to ACPCs; COL1 and COL2 lower in ACPCs compared to NSP and AD-MSC
Biofabrication studies							
Levato et al., 2017[116]	Equine	Metacarpophalangeal joint	Healthy	DAF followed by colony isolation	Chondrocytes; BM-MSCs	Cartilage formation in (layered) casted GelMA hydrogel constructs; cartilage formation in layered bioprinted cartilage construct (MSCs in middle/deep layer, ACPCs in superficial layer)	ACPCs produced higher amount and better-quality neo-cartilage matrix compared to chondrocytes, but not MSCs; Interplay of ACPCs with chondrocytes and MSCs supported neo-cartilage synthesis in layered co-cultures
Lim et al., 2018[192]	Equine	Metacarpophalangeal joint	Healthy	DAF followed by colony isolation	-	Chondrogenic differentiation in DLP-printed bio-resin constructs	DLP-printed bio-resin supported chondrogenic differentiation of ACPCs
Mouser et al., 2018[187]	Equine	Metacarpophalangeal joint	Healthy	DAF followed by colony isolation	-	Encapsulation in GelMA/gellan/HAMA hydrogels and 3D (zonal) bioprinting	Successful chondrogenic differentiation in hydrogel

Bernal et al., 2019[193]	Equine	Metacarpophalangeal joint	Healthy	DAF followed by colony isolation	-	Fibrocartilage formation in volumetric bioprinted meniscus-shaped constructs	GAG, type I and II collagen production; increased compressive modulus after chondrogenic culture
Diloksumpan et al., 2020[188]	Equine	Metacarpophalangeal joint	Healthy	DAF followed by colony isolation	-	Encapsulation in GelMA in a biofabricated osteochondral plug	ACPCs produce cartilage matrix and differentiation of ACPCs was not hampered by the presence of a bone scaffold
Mancini et al., 2020[189]	Equine	Metacarpophalangeal joint	Healthy	DAF followed by colony isolation	BM-MSCs	Encapsulation in hyaluronic acid/poly(glycidol) hybrid hydrogel in a layered biofabricated osteochondral plug in an equine model	No difference in histological scoring. Repair tissue was stiffer in ACPC/MSC zonal constructs compared to constructs containing MSCs only
Peiffer et al., 2020[190]	Equine	Metacarpophalangeal joint	Healthy	DAF followed by colony isolation	-	Encapsulation of ACPCs in hydrogel reinforced with a melt electrowritten scaffold printed on curvature	Cartilage-like tissue formation throughout the construct with high shape fidelity
Piluso et al., 2020[191]	Equine	Metacarpophalangeal joint	Healthy	DAF followed by colony isolation	BM-MSCs; DPSCs	Cytocompatibility of riboflavin and sodium persulfate; cytocompatibility in silk fibroin hydrogel	Riboflavin did not affect viability, sodium persulfate decreased viability after three hours in high concentration. ACPCs in hydrogel maintained viability over 28 days of culture
In vitro and in vivo studies							
Tao et al., 2018[120]	Murine	Knee	Unknown	DAF followed by colony isolation	Chondrocytes	Effect of FN on proliferation, migration, and chondrogenesis. Effect of FN in early *in vivo* OA model	Increased proliferation, migration, and Col-II and Aggrecan expression by FN. Inhibited by integrin-$\alpha5\beta1$ inhibitor. FN promoted cartilage repair *in vivo* and increased $CD105^+$ and $CD166^+$ cells
Wang, R et al., 2020[210]	Murine	Joint (not further specified)	Unknown	DAF followed by colony isolation	-	EVs from MRL/MpJ super-healer mice-ACPCs were used for intra-articular injection in an OA model	Super-healer mice ACPC-EVs could ameliorate OA severity in vivo and improve chondrocyte function *in vitro*

						and for chondrocyte migration and proliferation	
Tong et al., 2015[132]	Rat	Hip and knee	Unknown	DAF	Chondrocytes; BM-MSCs	Chondrogenesis under influence of IL1B and NF-κB pathway inhibitor	NF-κB pathway inhibitor was successful in rescuing ACPC chondrogenesis
Cai et al., 2020[143]	Rat	Knee	OA (ACLT-induced)	DAF	-	Chondrogenesis and migration under influence of magnoflorine	Chondrogenesis and migration were stimulated by magnoflorine
Liu et al., 2020[184]	Rat	Knee	Unknown	-	-	Effect of kartogenin on ACPCs	Kartogenin promoted proliferation; increased percentage of G2-M stage cells, increased gene expression of IL-6 and Gp130; phosphorylation of Stat3 enhanced. *In vivo* destabilization of the medial meniscus: increased cartilage thickness after kartogenin injection; upregulation of Stat3 phosphorylation; enhanced distribution of $CD44^+/CD105^+$ cells
Williams et al., 2010[90]	Caprine	Knee	Healthy	DAF followed by colony isolation	Full-depth chondrocytes	Caprine *in vivo* cartilage defect filling with cell-seeded type I/III collagen membrane	Good integration with surrounding cartilage. No difference between full-depth chondrocytes and ACPCs.
Tallheden et al., 2003[153]	Human	Knee	Healthy	-	BM-MSCs	*In vivo* osteochondrogenic assay in SCID mice	Cartilage matrix formation in the chondrocyte group compared to bone matrix formation in the MSC group
Carluccio et al., 2020[95]	Human	Hip	OA	Outgrowth from cartilage tissue using platelet lysate	Chondrocytes	*In vivo* ectopic chondrogenesis and osteogenesis (pellet and biomaterials)	ACPCs (PL expanded) provided a better option than chondrocytes for stable cartilage regeneration
In vivo studies							
Marcus et al., 2014[136]	Bovine	Metacarpophalangeal joint	Healthy	DAF followed by colony isolation	-	Intramuscular injection in SCID mice	ACPCs were able to survive, but failed to produce cartilage matrix (while chondrocytes did)

Frisbie et al., 2015[194]	Equine	Trochlear ridge of femur (superficial zone)	Healthy	DAF followed by colony isolation	-	*In vivo* chondral defect filling in autologous fibrin, comparison of autologous and allogeneic cells	Autologous cells provide a benefit in outcomes in terms of pain, synovial effusion, range of motion, radiographs, and histology. No apparent benefit of allogeneic cells
In human studies							
Jiang et al., 2016[93]	Human	Knee (femoral condyle)	OA	-	-	MACT procedure using ACPCs	Significant clinical improvement based on IKDC and Lysholm scores; full coverage of defect site after one year; hyaline-like cartilage architecture

ACLT anterior cruciate ligament transection, *AD* adipose tissue-derived, *ALP* alkaline phosphatase, *CFE* colony-forming efficiency, *DAF* differential adhesion to fibronectin, *DLP* digital light processing, *EV* extracellular vesicle, *FBS* fetal bovine serum, *FN* fibronectin, *GAG* glycosaminoglycan, *IFP* infrapatellar fat pad, *IKDC* International Knee Documentation Committee, *LLP* Link protein N-terminal peptide, *MACT* matrix-assisted autologous chondrocyte transplantation, *NGF* nerve growth factor, *NSP* nasal septum progenitor, *OA* osteoarthritis, *PCL* polycaprolactone, *PL* platelet lysate, *PLLA* polycaprolactone/polylactic acid, *PRP* platelet-rich plasma, *SCID* severe combined immunodeficient mice

Chapter 3

Progenitor cells in healthy and osteoarthritic human cartilage have extensive culture expansion capacity while retaining chondrogenic properties

Margot Rikkers
Jasmijn V. Korpershoek
Riccardo Levato
Jos Malda
Lucienne A. Vonk

CARTILAGE (2021)

ABSTRACT

Objective

Articular cartilage-derived progenitor cells (ACPCs) are a potential new cell source for cartilage repair. This study aims to characterize endogenous ACPCs from healthy and osteoarthritic (OA) cartilage, evaluate their potential for cartilage regeneration, and compare this to cartilage formation by chondrocytes.

Design

ACPCs were isolated from full-thickness healthy and OA human cartilage and separated from the total cell population by clonal growth after differential adhesion to fibronectin. ACPCs were characterized by growth kinetics, multilineage differentiation, and surface marker expression. Chondrogenic redifferentiation of ACPCs was compared to chondrocytes in pellet cultures. Pellets were assessed for cartilage-like matrix production by (immuno)histochemistry, quantitative analyses for glycosaminoglycans and DNA content, and expression of chondrogenic and hypertrophic genes.

Results

Healthy and OA ACPCs were successfully differentiated towards the adipogenic and chondrogenic lineage, but failed to produce calcified matrix when exposed to osteogenic induction media. Both ACPC populations met the criteria for cell surface marker expression of MSCs. Healthy ACPCs cultured in pellets deposited extracellular matrix containing proteoglycans and type II collagen, devoid of type I collagen. Gene expression of hypertrophic marker type X collagen was lower in healthy ACPC pellets compared to OA pellets.

Conclusion

This study provides further insight into the ACPC population in healthy and OA human articular cartilage. ACPCs show similarities to MSCs, yet do not produce calcified matrix under well-established osteogenic culture conditions. Due to extensive proliferative potential and chondrogenic capacity, ACPCs show potential for cartilage regeneration and possibly for clinical application, as a promising alternative to MSCs or chondrocytes.

INTRODUCTION

Cartilage defects larger than 2 cm^2 are currently treated by transplantation of autologous culture-expanded chondrocytes[41,211]. As chondrocytes are the resident cell type in cartilage, this cell type is the prime candidate for cartilage repair. Although long term results are promising with good patient reported outcomes and radiographic signs of cartilage formation[211,212], drawbacks of the treatment remain. Extensive culture of chondrocytes for autologous administration induces dedifferentiation and loss of phenotype[213]. Additionally, graft hypertrophy can lead to continued ailments and may necessitate further revision surgery[46]. These drawbacks can potentially be resolved by other cell sources. Mesenchymal stromal cells (MSCs) are frequently used[113] due to the relatively non-invasive methods for isolation, extensive culture-expansion potential[214,215], and efficient *in vitro* differentiation into chondrocytes producing cartilaginous tissue[216,217]. However, the associated risk of MSCs differentiating into hypertrophic chondrocytes and subsequent endochondral ossification poses a challenge[218]. While chondrocytes and MSCs are impacting the way cartilage defects are treated, different cell sources overcoming potential limitations may further advance the quality of repair tissue, and hence possibly clinical outcomes, leaving a gap for improvement in cell-based cartilage tissue engineering.

Initially, a small portion of isolated articular chondrocytes was described to grow clonally and differentiate into several lineages[111]. Next, a distinct progenitor cell with stem cell-like characteristics was identified in the superficial zone, first in bovine[15] and later also in human cartilage[90]. This endogenous progenitor population is referred to as cartilage stem cells, mesenchymal or chondrogenic progenitor cells, or articular cartilage-derived progenitor cells (ACPCs).

Besides extensive culture-expansion[219], ACPCs are successful at producing neo-cartilage *in vitro*[95,118] and *in vivo*[90,93]. Several reports indicate that ACPCs have no tendency to differentiate into hypertrophic chondrocytes, unlike MSCs[92,116]. These combined features give ACPCs a preference over chondrocytes and MSCs for cartilage regeneration. Furthermore, similar to chondrocytes[220], pathological origin could influence ACPC performance. Indeed, OA-derived ACPCs were shown to possess chondrogenic properties, like healthy cartilage-derived ACPCs[91]. However, direct comparisons of chondrogenic potential of ACPCs from healthy and OA cartilage are limited[16,91]. Direct comparison can provide insight in the pathophysiology of OA and the potential role of ACPCs in health and disease.

The current study aims to characterize and compare fibronectin-selected ACPCs from healthy and OA human cartilage. By direct comparison of ACPC populations to full-depth cartilage cell populations derived from the same donors, their potential for cartilage regeneration is investigated.

METHODS

Tissue collection

Macroscopically healthy cartilage (n = 6, age 46 - 49) was isolated post-mortem from full-weight-bearing and non-weight-bearing locations of the knee (Department of Pathology, University Medical Center Utrecht). Osteoarthritic (OA) cartilage was obtained from redundant material from patients (n = 6, age 55 - 79) undergoing total knee arthroplasty. Anonymous collection of this tissue was performed according to medical ethics regulations of the University Medical Center Utrecht and the guideline "good use of redundant tissue for research" of the Dutch Federation of Medical Research Societies[221]. Human MSCs (n = 6, age 30 – 66) were derived from bone marrow from the iliac crest of patients receiving spondylodesis or total hip arthroplasty surgery after their informed consent and according to a protocol approved by the local medical ethical committee.

Cell isolation and expansion

Cartilage from all parts of the joint (weight-bearing and non-weight-bearing) was pooled for each donor. Cartilage pieces were digested in 0.2% (w/v) pronase (Sigma-Aldrich) in Dulbecco's modified Eagle medium (DMEM; Gibco) with 1% (v/v) penicillin/streptomycin (pen/strep; 100 U/mL, 100 µg/mL; Gibco) for two hours at 37ºC, followed by overnight digestion in 0.075% (w/v) type II collagenase (Worthington, Lakewood, NJ) in DMEM with 10% (v/v) heat-inactivated fetal bovine serum (FBS; Biowest) and 1% pen/strep under agitation. The population from here on referred to as "chondrocytes" is the total cell population isolated from cartilage, without any purification or selection[90]. Chondrocytes were expanded using chondrocyte expansion medium (DMEM, 10% FBS, 1% pen/strep). To isolate ACPCs, the digest was seeded at 500 cells/cm^2 at 37ºC on culture plastic pre-coated for one hour with fibronectin (1 µg/mL in PBS containing $MgCl_2$ and $CaCl_2$; Sigma-Aldrich) using serum-free medium (DMEM with 1% pen/strep). After 20 minutes, non-adhered cells were washed away and ACPC expansion medium was added (DMEM, 10% FBS, 1% pen/strep, 200 µM l-ascorbic acid 2-phosphate [ASAP; Sigma-Aldrich], and 5 ng/mL basic fibroblast growth factor [bFGF; PeproTech]). On day 6, colonies (>32 cells) were isolated using sterile glass cloning cylinders (Sigma-Aldrich). Collected colonies were pooled and ACPCs were further expanded on conventional tissue culture plastic with ACPC expansion medium.

The mononuclear fraction of bone marrow was separated by centrifugation using a Ficoll-Paque density gradient (GE Healthcare, The Netherlands) and plated using MSC expansion medium (Minimum Essential Media [αMEM; Gibco, The Netherlands], 10% FBS, 1% pen/strep, 200 µM ASAP, and 1 ng/mL bFGF). MSCs were expanded up to passage four before use in differentiation assays.

Flow cytometry

Cells were washed in buffer (0.5% w/v bovine serum albumin [BSA], 2mM EDTA in PBS)

and incubated with antibodies against CD49e, CD146, CD166 (Miltenyi Biotec), CD105 (Abcam), CD90, CD73, or a cocktail of markers (CD45, CD34, CD11b, CD79A, HLA-DR; all R&D Systems) according to the manufacturers' instructions. Labelled cells were analysed using a BD FACSCanto II or BD LSRFortessa (BD Biosciences, USA). Dead cells were excluded using 100 ng/mL 4′,6-diamidino-2-phenylindole (DAPI; Sigma) or 1 µg/mL 7-Aminoactinomycin D (7AAD; Molecular Probes). Results were analysed using FlowJo V10 data analysis software package (TreeStar, USA).

Colony Forming Unit Fibroblast Assay

Chondrocytes directly after isolation (passage 0) and ACPCs and chondrocytes at passages two and four were seeded at 50 and 100 cells per 6-well plate well in duplicates. Cells were cultured with corresponding expansion medium. After seven days, colonies were fixed with 10% formalin and stained for 45 minutes using 0.05% (v/v) Crystal Violet (Sigma-Aldrich) in Milli-Q water and counted.

Multilineage Differentiation

For chondrogenic and hypertrophic differentiation, 2.5 x 10^5 ACPCs (passage four) or chondrocytes (passage two) were pelleted in 15 mL Falcon tubes by centrifugation at 320 *g* for five minutes. Pellets were cultured in chondrogenic medium (DMEM with 1% pen/strep, 2% (v/v) human serum albumin [HSA; Albuman, Sanquin Blood Supply Foundation], 1% insulin-transferrin-selenium-ethanolamine [ITS-X; Gibco], 0.1 µM dexamethasone, 0.2 mM ASAP, and 10 ng/mL TGF-β1 [PeproTech]). After 21 days of chondrogenic differentiation, half of the pellets was fixed using 10% buffered formalin. The other half of the pellets was exposed to hypertrophic medium (DMEM with 1% pen/strep, 1% ITS-X, 1 nM dexamethasone, 200 µM ASAP, 10 mM β-glycerophosphate [BGP; Sigma-Aldrich], and 1 nM 3,3′,5-Triiodo-L-thyronine [Sigma-Aldrich]) for seven additional days. After a total of 28 days, the hypertrophic -treated pellets were fixed with 10% formalin and processed for histology.

For osteogenic and adipogenic differentiation, ACPCs (passage four) and chondrocytes (passage two) were seeded in 24-well plate wells using corresponding expansion media. Upon subconfluency, monolayers were treated with osteogenic medium (αMEM with 10% FBS, 1% pen/strep, 200 µM ASAP, 10 mM BGP, and 10 nM dexamethasone [Sigma-Aldrich]) or adipogenic medium (αMEM with 10% FBS, 1% pen/strep, 1 µM dexamethasone, 0.5 mM 3-Isobutyl-1-methylxanthine [IBMX; Sigma-Aldrich], 0.2 mM indomethacin [Sigma-Aldrich], and 1.72 µM insulin [Sigma-Aldrich]) for 21 days. After 21 days, monolayers were fixed with 10% formalin and stained for calcium deposits by 40 mM alizarin red S in demineralized water (pH 4.1; Sigma-Aldrich) or intracellular lipid vacuoles by 7.3 mM oil red O (Sigma-Aldrich) in 60% isopropanol. For all assays, MSCs were ran in parallel as positive controls.

Additional osteogenic differentiation was performed by expanding and differentiating ACPCs using several batches of FBS (Biowest and Gibco) and platelet lysate[222] (Sanquin Blood

Supply Foundation). Also, monolayers were treated with osteogenic medium with 100 ng/mL recombinant human Bone Morphogenetic Protein-2[223] (InductOS) and cell pellets[90] were stimulated with osteogenic medium, both for 21 days. Results are shown in Supplemental Figure S1.

Pellet redifferentiation culture

For the redifferentiation cultures, 2.5 x 10^5 cells were pelleted in ultra-low attachment 96-well plate wells by centrifugation at 320 *g* for five minutes. Pellets were cultured for 28 days in redifferentiation medium (DMEM with 1% pen/strep, 2% HSA, 2% ITS-X, and 1% ASAP). Half of the pellets was supplemented with 10 ng/mL TGF-β1. Used medium was stored at -20ºC for further analysis. Pellets were processed for biochemical analyses, gene expression, and (immuno)histochemistry.

Biochemical analysis of pellets

Pellets were digested overnight with papain (250 µg/mL papain [Sigma-Aldrich], 0.2 M NaH_2PO_4, 0.1M EDTA, 0.01M cysteine, pH 6) at 60ºC. Deposition of sulphated glycosaminoglycans (GAGs) and release into the medium was measured by a dimethylmethylene blue assay (pH 3). The 525 / 595 nm absorbance ratio was measured using chondroitin-6-sulfate (Sigma-Aldrich) as a reference. DNA was quantified using a Quant-iT™ PicoGreen assay (Invitrogen) according to the manufacturer's instructions.

Histological analysis of pellets

Pellets were processed for histology by dehydration through graded ethanol steps, clearing in xylene, and embedding in paraffin. Five µm-sections were stained for proteoglycan production with 0.125% safranin-O (Merck) counterstained with 0.4% fast green (Sigma-Aldrich) and Weigert's hematoxylin (Clin-Tech). Collagen deposition was visualized by immunohistochemistry. Sections were blocked in 0.3% (v/v) hydrogen peroxide. Antigen retrieval for type I and II collagen was performed with 1 mg/mL pronase (Sigma-Aldrich) and 10 mg/mL hyaluronidase (Sigma-Aldrich) and for type X collagen with 1 mg/mL pepsin (Sigma-Aldrich) and 10 mg/mL hyaluronidase for 30 minutes at 37ºC. Sections were blocked with 5% (w/v) BSA in PBS for one hour at room temperature and incubated with primary antibodies for type I collagen (EPR7785 [BioConnect], 1:400 in 5% PBS/BSA), type II collagen (II-II6B3 [DHSB], 1:100 in 5% PBS/BSA) and type X collagen (X53 [Quartett], 1:20 in 5% PBS/BSA) overnight at 4ºC. Appropriate IgGs were used as isotype controls. Next, type I collagen sections were incubated with BrightVision Poly-HRP-Anti Rabbit (ImmunoLogic) and type II collagen sections were incubated with goat-anti-mouse IgG HRP-conjugated (DAKO, P0447; 1:100 in 5% PBS/BSA), both for one hour at room temperature. Type X collagen sections were incubated with biotinylated sheep-anti-mouse IgG (RPN1001V [GE Healthcare]) for one hour at room temperature, then with streptavidin-HRP for one hour at room temperature (DAKO, P0397; 1:1000 in 5% PBS/BSA). Next, all stainings were developed using 3,3'-diaminobenzidine (DAB, Sigma-Aldrich). Cell nuclei were counterstained

with Mayer's hematoxylin (Klinipath).

Gene expression

Gene expression analysis was performed by real-time polymerase chain reaction (PCR). RNA was isolated from cells and pellets using TRIzol (Invitrogen) according to the manufacturer's instructions. Total RNA (200-500 ng) was reverse-transcribed using the High-Capacity cDNA Reverse Transcription Kit (Applied Biosystems). Real-time PCRs were performed using iTaq Universal SYBR Green Supermix (Bio-Rad) in the LightCycler 96 (Roche Diagnostics) according to the manufacturer's instructions. Primers (Invitrogen) are listed in Table S1. Relative gene expression was calculated using 18S as a housekeeping gene. Amplified PCR fragments extended over at least one exon border (except for 18S). The primer for detection of two splice variants of COL2A1 extended across exon 2 of the gene and results in amplification of splice variants IIa and IIb. PCR products were separated on 2% (w/v) agarose gel electrophoresis and stained with SYBR Safe (Invitrogen).

Statistical analysis

Experiments for flow cytometry, colony-forming efficiency, and multilineage differentiation were performed with cells from six healthy and six OA cartilage donors, unless stated otherwise. Pellet redifferentiation culture was performed with cells from three donors and three technical replicates per donor. All data are expressed as mean±standard deviation (SD). Data were analyzed using the GraphPad Prism 8 software package (GraphPad Software, United States). Normality was confirmed with a Shapiro-Wilk test ($p>0.05$). Groups were compared using an unpaired *t*-test, one- or two-way analysis of variance (ANOVA) with Bonferroni post-hoc test. Gene expression data was not normally distributed and therefore analysed with a Mann-Whitney or Kruskall-Wallis test with Dunn's post-hoc test. A value of $p<0.05$ was considered statistically significant.

RESULTS

Cells isolated from human cartilage have a chondrogenic profile

All samples consistently contained cells highly expressing the cartilage-specific marker cartilage link protein (HAPLN1), while having low expression of the synovial-specific marker microfibril-associated glycoprotein-2[224] (MFAP5; Figure 1A). Expression of HAPLN1 was comparable between cells directly after digestion of healthy versus OA cartilage (1.199±0.259 vs 0.687±0.678). Likewise, expression of MFAP5 was low in cells from both disease states (0.0010±0.0003 vs 0.000016±0.000001), confirming successful isolation of cartilage cells without contamination of synoviocytes from the tissues.

Expression of progenitor-specific markers in freshly isolated chondrocytes

Gene expression of freshly isolated chondrocytes revealed a significant difference in Notch receptor 1 (NOTCH1) between healthy and OA-derived cells (0.3274±0.5821 vs 0.0047±0.0016; $p=0.0022$; Figure 1B). Notably, expression of n-cadherin (CDH2) was

significantly higher in cells derived from OA cartilage compared to healthy (0.0003±0.0003 vs 0.0077±0.0053; p=0.0061; Figure 1B). Cells positive for cell surface marker CD49e (integrin-α5) were significantly decreased in OA-derived cells compared to healthy (87.3%±11.6% vs 2.6%±1.4%; p<0.0001; Figure 1C). Likewise, expression of CD166 was decreased in OA-derived cells (48.4%±43.2% vs 1.4%±0.1%; p=0.0122). Marker expression of CD105 as well as co-expression of CD105 and CD166 did not differ between the groups.

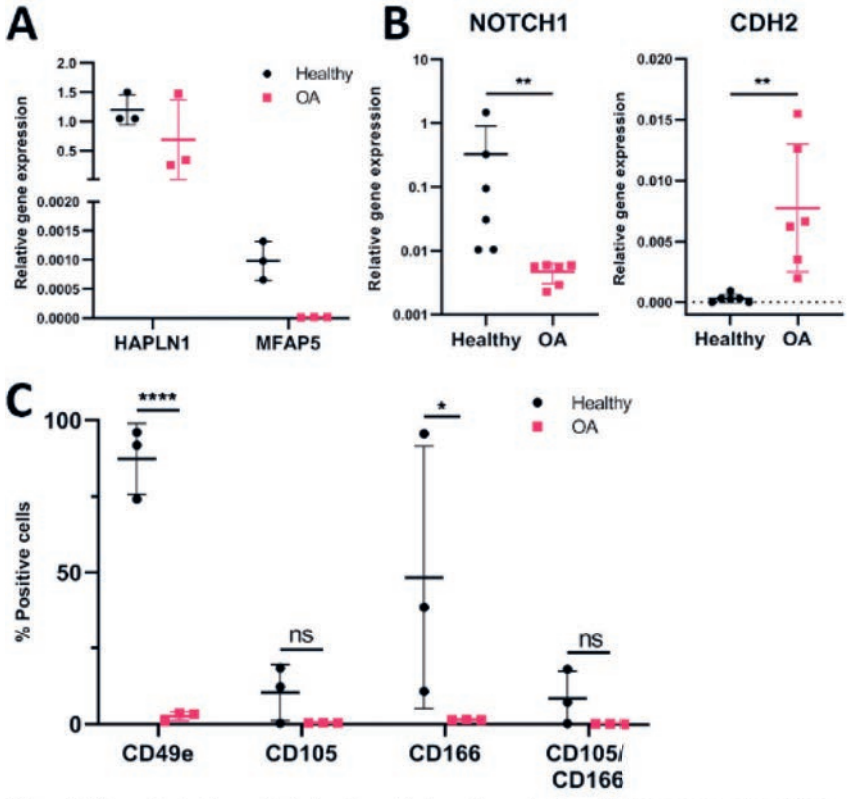

Figure 1. Characterization of full-depth cartilage cell populations (A) Expression of cartilage- and synovial-specific genes in freshly isolated chondrocytes (n = 3 for both). Gene expression of cartilage-specific gene hyaluronan and proteoglycan link protein 1 (HALPN1) is consistently high in chondrocytes isolated from healthy and osteoarthritic (OA) cartilage, while synovial-specific gene microfibril associated protein 5 (MFAP5) is low in cells from both tissues. (B) Gene expression of Notch receptor 1 (NOTCH1) was higher in healthy compared to OA cartilage. Expression of n-cadherin (CDH2) was significantly increased in OA cartilage-derived cells (n = 6 for both). (C) Surface marker expression of CD49e and CD166 were decreased in OA-derived cells compared to healthy cartilage-derived cells (n = 3 for all). *$p<0.05$ **$p<0.01$ ****$p<0.0001$. Three technical replicates per donor, each data point represents data of one donor.

Selection by adhesion to fibronectin results in a population with high clonogenicity and proliferative capacity

Colony-forming efficiency of ACPCs at passage two and four was higher than of the full population (p<0.0001 for all groups; Figure 2A). Morphology of representative Crystal Violet-stained colonies can be seen in Supplemental Figure S2. Healthy and OA ACPCs underwent 18.1±1.5 and 13.0±1.0 population doublings respectively until reaching the fourth passage after 29.3±1.0 and 28.0±3.3 days, healthy and OA chondrocytes had 6.8±0.9 and 6.4±1.0 population doublings respectively until reaching passage four after 40.7±2.1 and 41.0±3.3 days (Figure 2B). Expansion of chondrocytes and ACPCs in ACPC-expansion medium resulted in similar population doublings per passage and similar passage length (Supplemental Figure S3A and B), while expansion in chondrocyte-expansion medium resulted in a less population doublings by chondrocytes while their culture time per passage decreased (Supplemental Figure S3C and D). OA ACPCs and chondrocytes lost expression of type II collagen (COL2A1)

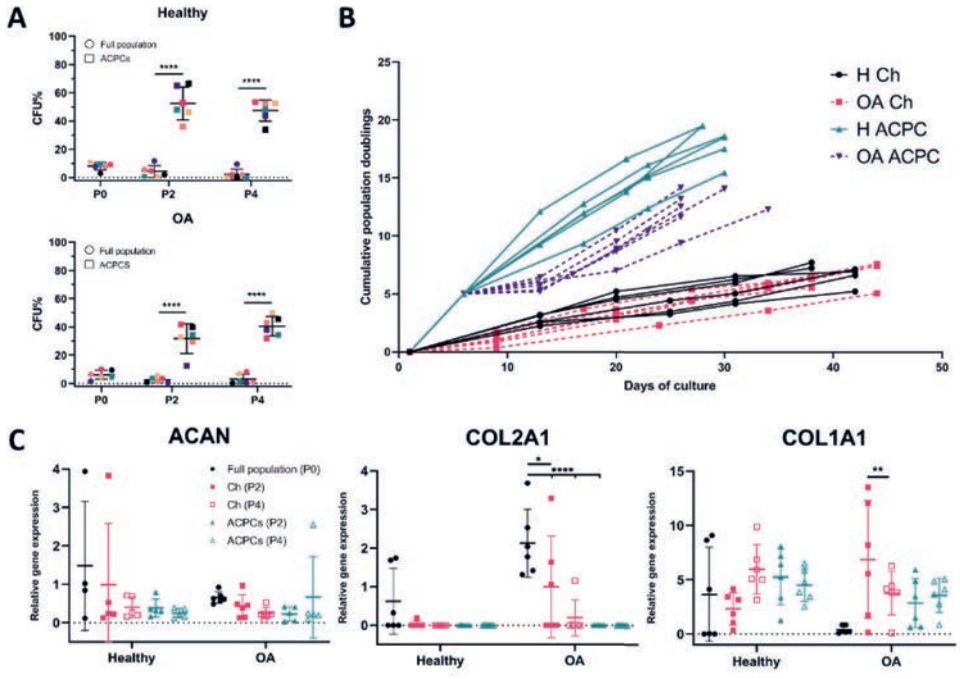

Figure 2. Culture-expansion of articular cartilage-derived progenitor cells versus non-selected chondrocytes. (A) Colony-forming units (CFU) at increasing cell passages (P0, P2, P4). Articular cartilage-derived progenitor cells (ACPCs) form significantly more colonies at passage 2 and 4, compared to chondrocytes. Colours within the graphs represent different donors (n = 6 for all). (B) Cumulative population doublings of ACPCs and chondrocytes. Healthy and osteoarthritic (OA) ACPCs underwent 18.1 ± 1.5 and 13.0 ± 1.0 population doublings respectively until reaching the fourth passage, healthy and OA chondrocytes underwent 6.8 ± 0.9 and 6.4 ± 1.0 population doublings respectively until reaching passage 4 (n = 6 for all). (C) Expression of type II collagen (collagen type I alpha 1 chain; COL2A1) decreased in OA chondrocytes and ACPCs during expansion. Expression of type I collagen (collagen type II alpha 1 chain; COL1A1) was increased in passage 2 chondrocytes (n = 6 for all). *p<0.05 **p<0.01 ****p<0.0001. Three technical replicates per donor, each data point represents data of one donor.

during expansion (Figure 2C). Expression of type II collagen splice variants IIa and IIb did not reveal any distinct differences between chondrocytes and ACPCs or between passage numbers (Supplemental Figure S4).

ACPCs fail to produce mineralized matrix upon osteogenic and hypertrophic induction

All healthy and OA ACPCs differentiated into the chondrogenic and adipogenic lineage, indicated by safranin-O and oil red O stainings (Figure 3A and 3B). Chondrocyte pellets stained less for proteoglycans than ACPC pellets (Figure 3A, left panels). Osteogenic differentiation was evident in chondrocytes (Figure 3C, left panels), while ACPCs stained negative for mineralized matrix by alizarin red (Figure 3C, right panels). Osteogenic differentiation was also unsuccessful when ACPCs were expanded with different batches of FBS and platelet lysate, and when the osteogenic differentiation medium was supplemented with 100 ng/mL BMP-2 or when ACPC pellets were stimulated with osteogenic medium (Supplemental Figure S1). All chondrocytes and ACPCs were unable to differentiate into

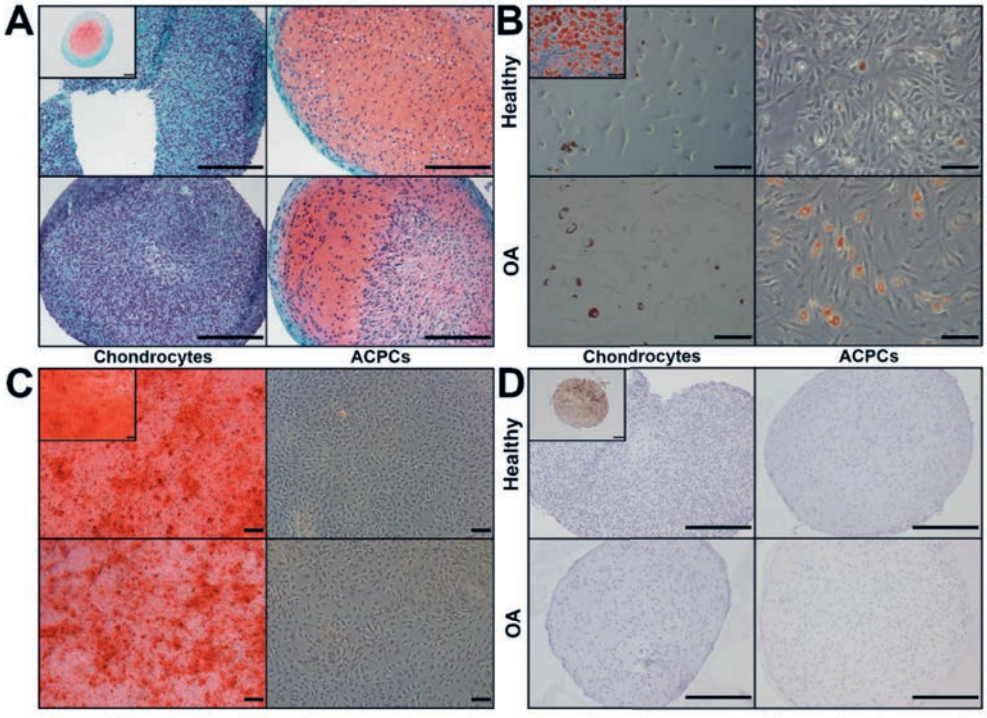

Figure 3. Differentiation of chondrocytes and articular cartilage-derived progenitor cells into four lineages. (A) Chondrogenic differentiation was more effective in articular cartilage-derived progenitor cells (ACPCs) than chondrocytes, indicated by staining of proteoglycans by safranin-O. (B) Adipogenic differentiation was achieved in chondrocytes and ACPCs, indicated by staining of lipid droplets by oil red O. (C) Osteogenic differentiation was successful in chondrocytes, but not in ACPCs, shown by staining of the mineralized matrix by alizarin red. (D) Chondrocytes and ACPCs did not differentiate into hypertrophic chondrocytes indicated by absent staining for type X collagen. Inserts show bone marrow-derived mesenchymal stromal cells (MSCs) differentiated in parallel as positive controls. N = 6 for all cell types, a representative image per cell type was selected. All scale bars = 200 µm.

hypertrophic chondrocytes, indicated by negative staining for type X collagen (Figure 3D).

Expression of bone marrow-derived MSC surface markers in culture-expanded ACPCs

Expression of cell surface markers defined for bone marrow-derived MSCs in monolayer culture[165], CD90, CD105, and CD73, was >95% in all populations. CD166-expression was >99% in all ACPC donors, but lower in OA chondrocytes (87.8%±13.6) compared to healthy ACPCs (99.7%±0.1; p=0.0322) and OA ACPCs (99.8%±0.1; p=0.0315). Expression of CD146 was higher in OA chondrocytes (39.0%±8.1) compared to healthy chondrocytes (22.2%±0.0; p=0.0322), healthy ACPCs (27.3%±15.2; p=0.0352), and OA ACPCs (20.9%±4.6; p=0.0003). Expression of several markers was tested using a cocktail containing antibodies against CD45, CD34, CD11b, CD79A, and HLA-DR. All cell types were <2% positive for this cocktail of markers (Figure 4).

ACPC pellets produce proteoglycans and type II collagen *in vitro*

Chondrocytes and ACPC pellets stained positive for proteoglycans when stimulated with 10 ng/mL TGF-β1. When the redifferentiation medium was not supplemented with TGF-β1, pellets stained negative for proteoglycans (Figure 5A). Type II collagen production was only found in healthy ACPC pellets cultured in the presence of TGF-β1. All other conditions showed no type II collagen-positive matrix (Figure 5B). Additionally, healthy ACPC pellets stimulated with TGF-β1 were the only condition negative for type I collagen (Figure 5C). All cultures were negative for X collagen (Figure 5D).

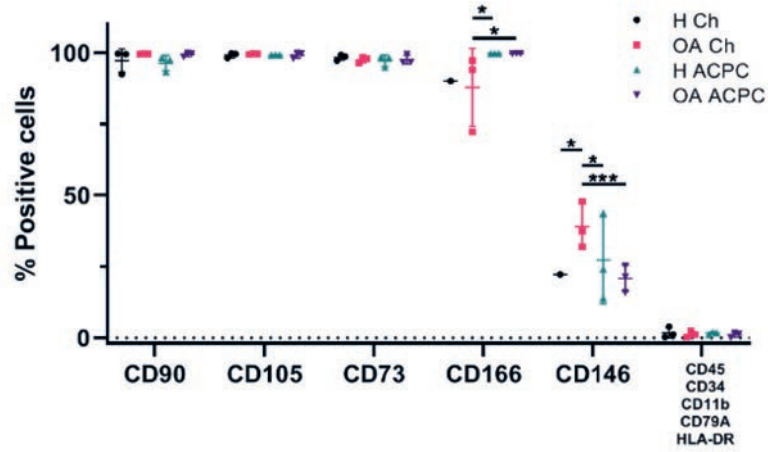

Figure 4. Cell surface marker expression by flow cytometry. Expression of CD90, CD105, CD73 was >95% in all donors (n = 3). CD166 expression was lower in osteoarthritic (OA) chondrocytes compared to healthy and OA articular cartilage-derived progenitor cells (ACPCs). CD146 expression was higher in OA chondrocytes compared to the other cell types. All cell types were <2% positive for CD45, CD34, CD11b, CD79A, and HLA-DR. **p<0.05 ***p<0.001*. Three technical replicates per donor, each data point represents data of one donor.

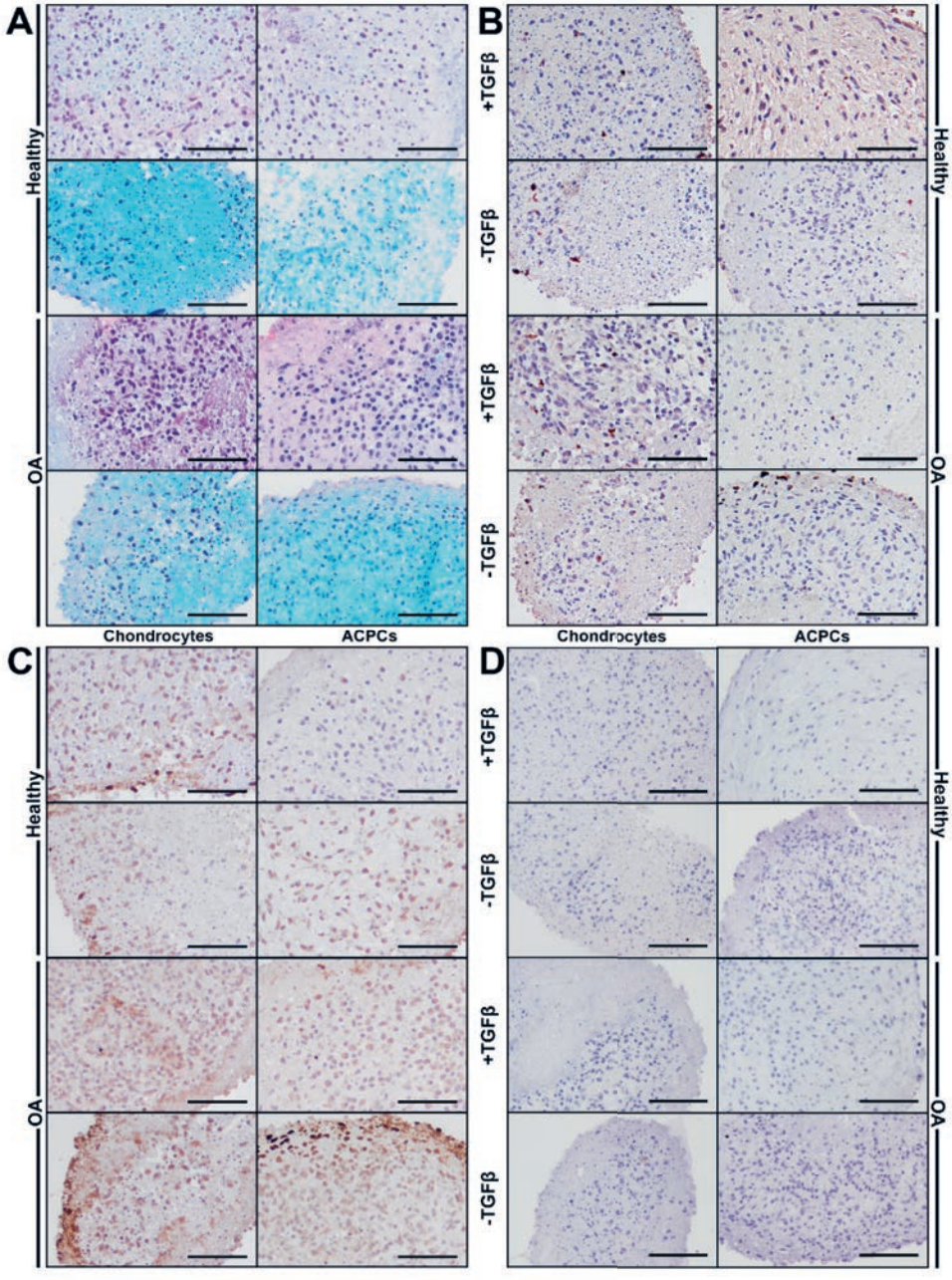

Figure 5. Histological staining of redifferentiated pellets. (A) Chondrocyte and articular cartilage-derived progenitor cells (ACPC) donor-matching pellets stained positive for proteoglycans by safranin-O when stimulated with TGF-β1 for four weeks. (B) TGF-β1-stimulated healthy ACPC pellets were positive for type II collagen and (C) negative for type I collagen. (D) None of the groups stained positive for type X collagen (D). N = 3 for all cell types, a representative image per cell type was selected. Scale bars = 100 μm.

Healthy ACPC pellets cultured with TGF-β1 contained more GAGs compared to OA chondrocyte and OA ACPC pellets (1.1±0.4 µg vs. 0.3±0.3 µg and 0.3±0.3 µg, p=0.0115 and p=0.0152, respectively; Figure 6, left panel). Similarly, DNA content was higher in healthy ACPC pellets, independent of TGF-β1 (with TGF-β1: 539.0±152.0 ng vs. 137.4±121.8 ng and 134.2±192.8 ng, p=0.0058 and p=0.0054, respectively, without TGF-β1: 389.4±151.5 ng vs. 34.0±10.7 ng and 59.7±84.5 ng, p=0.0153 and p=0.0264, respectively (Figure 6, middle panel)). Production of GAG corrected for the amount of DNA was not different between the groups (Figure 6, right panel).

Reduced expression of hypertrophic marker type X collagen

Gene expression analysis was only performed on TGF-β1-treated pellets, as insufficient amounts of RNA could be isolated from non-TGF-β1-treated pellets. No difference was found between expression of chondrogenic genes aggrecan (ACAN), type II collagen (COL2A1), and SRY-box transcription factor 9 (SOX9) between the experimental groups (Figure 7A). Noteworthy, COL2A1 expression in ACPC pellets was close to zero. Expression of the hypertrophic marker type X collagen (COL10A1) was lower in healthy ACPC pellets compared to OA ACPC pellets (0.00074±0.00071 vs. 0.01315±0.00393; p=0.0028) and compared to OA chondrocyte pellets (0.005664±0.002154; p=0.0296). Expression of type I collagen (COL1A1) and matrix metallopeptidase 13 (MMP13) was not different between the groups (Figure 7B).

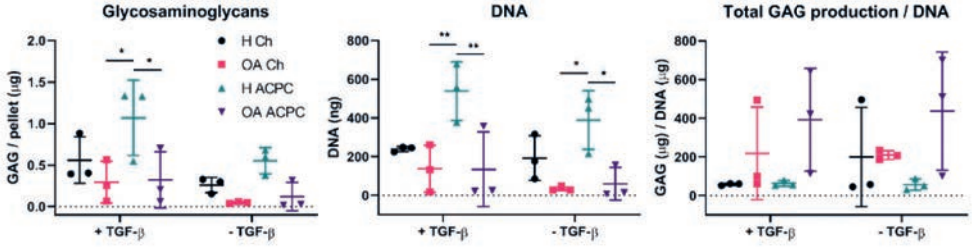

Figure 6. Glycosaminoglycan and DNA content in redifferentiated pellets after four weeks. Quantification of glycosaminoglycans (GAGs) shows significantly more GAGs produced in healthy articular cartilage-derived progenitor cells (ACPC) pellets cultured in the presence of TGF-β1 (left panel). DNA quantification shows significantly more DNA present in healthy ACPC pellets, suggesting bigger pellet sizes (middle panel). Total GAG production corrected for DNA content reveals no differences between the experimental groups (right panel). N = 3 for all cell types. *$p<0.05$ **$p<0.01$. Three technical replicates per donor, each data point represents data of one donor.

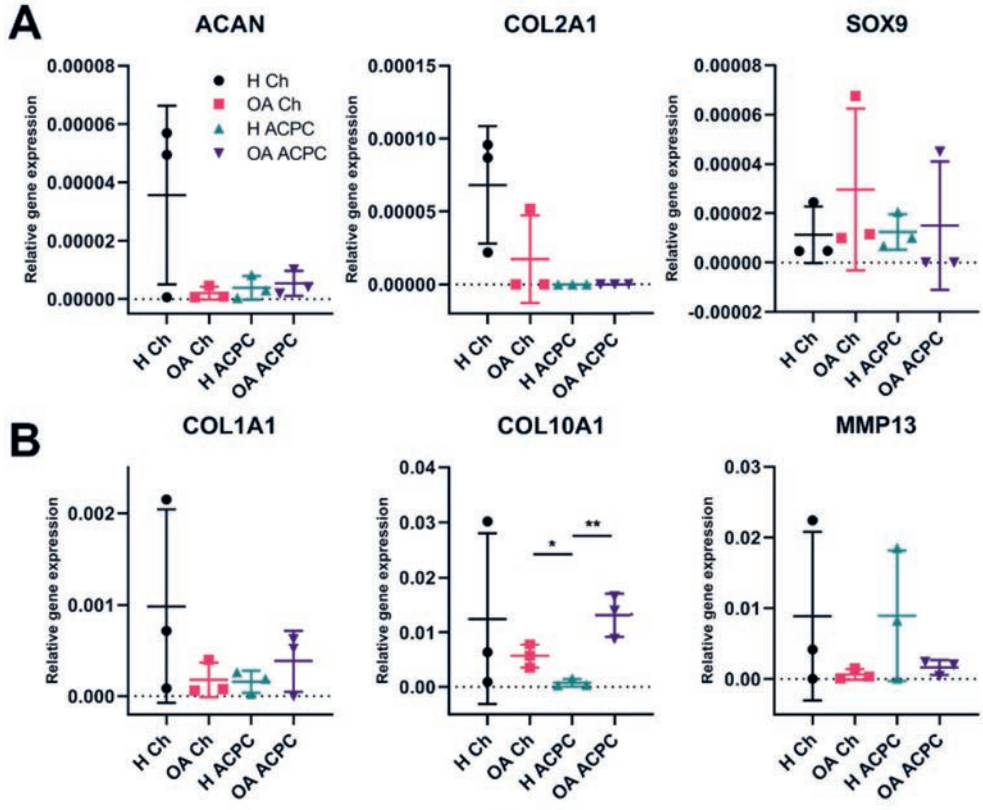

Figure 7. Gene expression of redifferentiated pellets. (A) Expression of chondrogenic genes aggrecan (ACAN), type II collagen (collagen type I alpha 1 chain; COL2A1), and SRY-box transcription factor 9 (SOX9) was not different between the groups. (B) Type X collagen expression was lower in healthy articular cartilage-derived progenitor cells (ACPC) pellets compared to osteoarthritic (OA) ACPC pellets. Expression of type I collagen (collagen type II alpha 1 chain; COL1A1) and matrix metallopeptidase 13 (MMP13) was not different between the groups. N = 3 for all cell types. *$p<0.05$ **$p<0.01$. Three technical replicates per donor, each data point represents data of one donor.

DISCUSSION

The current study aimed to characterize human ACPCs from healthy and OA cartilage and determine their potential for cartilage regeneration. While fibronectin-selected progenitor populations have been described in healthy[90] and OA human cartilage[91,141], this study is the first to directly compare chondrogenic functionality of ACPCs from healthy and OA cartilage to chondrocytes derived from matching donors. The results confirm the presence of an ACPC population in human articular cartilage[16,90,91,141]. Differential adhesion to fibronectin resulted in a cell population that was capable of clonal growth, extensive culture-expansion, multilineage differentiation, and had a limited tendency to produce mineralized matrix and terminally differentiate into hypertrophic chondrocytes. As chondrogenic potential of chondrocytes can be dependent on the disease state of cartilage[220], ACPCs derived from healthy and OA cartilage might provide as good candidates for cartilage repair. The current

side-by-side comparison of healthy- with OA-derived ACPCs and donor-matched chondrocytes provides an overview of these cells' potential for cartilage regeneration.

We investigated full-depth healthy and OA cell populations attempting to find correlations between previously reported progenitor markers and ACPC quantity. Expression of NOTCH1 was found to be higher in healthy cells compared to OA, confirming previous findings[124]. At the same time, CDH2 was significantly upregulated in OA cells. The cell-cell adhesion molecule N-cadherin is related to cellular condensation in early chondrogenesis during development and absent in differentiated cartilage[225,226]. This might be a result of chondrocyte clustering in OA[131,227] and the cells potentially obtaining a more premature chondrogenic phenotype. CDH2 in culture-expanded ACPCs was previously found to be higher in non-OA ACPCs compared to OA ACPCs[145], indicating that this difference is lost upon selection for progenitors and culture expansion. Therefore, NOTCH1 and CDH2 might be used as markers to distinguish between healthy- and OA-derived cells.

Expression of surface markers CD49e (integrin-α5, part of the key fibronectin receptor) and CD166 was lost in the total population of OA cells compared to healthy cells and no difference in CD105/CD166-double positive cells was found. These findings are in contrast to previous ones[16], where a higher percentage of double positive cells was found in OA tissue. However, others found similar amounts[122] or more CD105/CD166-double positive cells in healthy cartilage versus OA[161]. The OA cartilage in the current study was obtained from end-stage OA patients and was not scored on OA severity. Severely degraded OA cartilage has lost most of its superficial layer and would subsequently also have lost superficial zone cells, which express CD49e[15] and CD166[122]. Separation based on CD49e-expression could lead to a population with improved chondrogenic potential, like healthy cartilage-derived ACPCs.

Our results show separation based on differential adhesion to fibronectin results in a population with enriched colony-forming efficiency and increased proliferative potential. Fibronectin-selected ACPCs were previously found to maintain telomerase activity and telomere length up to at least 22 population doublings[90,135], which is more than the number of population doublings reached in our study. When using the same expansion media to expand both cell types, population doublings in chondrocytes were limited compared to ACPCs with chondrocyte-expansion medium, supporting the findings of higher cell yields of ACPCs. To add, culture time of chondrocytes decreased over passaging, indicating increasing cell size and possible dedifferentiation. On the contrary, OA-derived ACPCs lost mRNA expression of type II collagen upon culture expansion. Articular chondrocytes are known to dedifferentiate in monolayer expansion[213], but regain their phenotype when exposed to appropriate culture conditions[111,228]. Similarly, our ACPCs regained their differentiation potential and especially healthy cartilage-derived ACPCs were successful in producing type II collagen- and proteoglycan-rich matrix *in vitro*, while chondrocytes were less effective. Gene expression and protein deposition after the culture period of four weeks did not correspond, for which type II

collagen is the most evident example. While H-ACPCs pellets cultured with TGF-β1 did not express the gene corresponding for type II collagen, immunohistochemistry revealed a slightly positive staining in these pellets. While discrepancies between protein and gene expression are regularly seen[229], the chondrogenic response of ACPCs in this case might have been earlier than that of chondrocytes, resulting in differences in gene expression between the cell types at the four-week evaluation point. Evaluation of gene expression throughout the culture period would give insight into the timing of the response. Furthermore, evaluation of individual clones of ACPCs would shed more light on cell performance and would allow for selection of populations with optimal characteristics, as was investigated before[90,135]. Yet, for the purpose of the current study it would considerably delay expansion time to obtain sufficient amounts of cells for tissue engineering and limit clinical application.

Since there is a need for identification of unique markers for selecting ACPCs, we specifically looked into gene expression of type II collagen splice variants in order to investigate whether this marker could be used for discerning ACPCs and chondrocytes. Splice variant IIa is an established marker for juvenile chondrocytes or mesenchymal cells, while variant IIb is expressed by mature chondrocytes[230,231]. Although ACPCs would be chondrogenic precursors and were expected to express the immature variant of type II collagen, no differences were found here between the cell types or passage numbers, a possible result of the cells being in the expansion phase rather than in redifferentiation and are not actively producing extracellular matrix.

ACPCs are generally referred to as MSC-like as they, besides holding multilineage differentiation potential, meet the surface marker criteria to identify MSCs[165]. In addition, there are some indications that ACPCs have similar anti-inflammatory properties as MSCs[128]. More than 95% of the ACPCs described here expressed MSC-markers CD90, CD105, CD73, and CD166, and expression of a panel of negative markers is <2%. Noteworthy, ACPCs were negative for HLA-DR, making these populations potentially interesting for allogeneic applications. Culture-expanded chondrocytes exhibit a similar pattern of surface marker expression. While the expression pattern of the ACPC populations investigated here are in line with previous reports[90,95,154], caution should be taken when drawing conclusions. Evaluating expressed surface markers straight after ACPC-selection from the total pool of cells is the only way to directly compare cell populations and avoid the effect of culture expansion on the expression profile.

Both ACPC populations were unable to produce mineralized matrix upon stimulation with various osteogenic differentiation media and protocols. While osteogenesis is generally confirmed in human ACPCs[90,91,141], indications of reduced osteogenic potential exist. Interestingly, consistent results have been reported on decreased or absent expression of hypertrophic chondrocyte marker type X collagen[92,94,95,116] or early osteogenic marker alkaline phosphatase[118]. The differences in osteogenic differentiation potential between the

populations investigated here and fibronectin-isolated ACPC populations described by others are remarkable. As ACPCs originate from the cartilage, the cells might be more primed towards the chondrogenic lineage rather than to differentiate into osteoblasts or continue towards terminal hypertrophic differentiation. Since others do report on osteogenic differentiation of ACPCs, minor differences in culture media composition might explain the discrepancies. Isolation and culture protocols should be conducted side-by-side to elucidate differences between ACPC populations. Bone marrow-MSCs are associated with the risk of hypertrophic cartilage formation, when cells either differentiate or deposited matrix is remodelled into bone[92,232]. Because hypertrophy in autologous chondrocyte implantation (ACI) continues to be a challenge[46], the reduced osteogenic drift of ACPCs holds great promise for these cells.

Healthy cartilage-derived ACPCs produce cartilage ECM *in vitro* containing proteoglycans and type II collagen, and are devoid of type I collagen. In addition, these healthy ACPC pellets had low expression of type X collagen mRNA. Cartilage harvest site and tissue quality can be important for eventual cartilage production. To obtain healthy ACPCs, we combined all load-bearing and non-load-bearing cartilage from healthy knee joints, while chondrocytes isolated for ACI procedures are generally from non-load-bearing areas. However, chondrocytes from macroscopically healthy, full-weight bearing cartilage were shown to produce more proteoglycans and type II collagen *in vitro*[220]. Separating sub-groups of ACPC populations based on the degree of weight-bearing might provide further insights into the physiological role of progenitors in cartilage homeostasis. While we have not investigated it in the current study, several studies report on an increased number of ACPCs in OA cartilage[16,91,123,126] and numbers of ACPCs increasing after mechanical stimulation[130,133].

ACPCs were used in a caprine model and had good lateral integration with the native cartilage[90], showing potential for use in a two-step cartilage repair procedure. Furthermore, a pilot study with 15 patients employing matrix-assisted autologous chondrocyte transplantation reported satisfactory histological and pain scoring one year after surgery[93]. ACPCs were expanded for a maximum of three weeks, substantially shorter than the expansion time needed for chondrocytes, which is generally four to eight weeks[233–235], depending on growth speed and defect size. In spite of these promising early clinical results, direct comparisons between chondrocytes and ACPCs are necessary to identify advantages in length of culture expansion and quality of the repair tissue.

To conclude, ACPCs isolated here show potential for cartilage regeneration, possibly in an autologous approach replacing chondrocytes. The limited potential of these ACPC populations to produce mineralized matrix and absence of type X collagen protein and mRNA expression in healthy cartilage-derived ACPCs is promising. These observations combined with extensive *in* vitro expansion potential of ACPCs can have major implications for future cartilage repair treatments.

SUPPLEMENTAL TABLE

Table S1. Primer sequences for quantitative real-time PCR Forward (Fw) and reverse (Rv) primers. ACAN, *aggrecan*; CDH2, *cadherin 2*; COL10A1, *collagen type X alpha 1 chain*; COL1A1, *collagen type I alpha 1 chain*; COL2A1, *collagen type II alpha 1 chain*; HAPLN1, *hyaluronan and proteoglycan link protein 1*; MFAP5, *microfibril associated protein 5; MMP13, matrix metallopeptidase 13*; NOTCH1, *Notch receptor 1*; SOX9, *SRY-box transcription factor 9*.

Gene name	Oligonucleotide sequence (5' to 3')	Annealing temperature (°C)	Product size (bp)
18S	Fw: GTAACCCGTTGAACCCCATT Rv: CCATCCAATCGGTAGTAGCG	57	151
ACAN	Fw: CAACTACCCGGCCATCC Rv: GATGGCTCTGTAATGGAACAC	56	160
CDH2	Fw: GCGTCTGTAGAGGCTTCTGG Rv: GCCACTTGCCACTTTTCCTG	60	293
COL10A1	Fw: CACTACCCAACACCAAGACA Rv: CTGGTTTCCCTACAGCTGAT	56	225
COL1A1	Fw: TCCAACGAGATCGAGATCC Rv: AAGCCGAATTCCTGGTCT	57	191
COL2A1	Fw: AGGGCCAGGATGTCCGGCA Rv: GGGTCCCAGGTTCTCCATCT	57	195
COL2A1 (spanning exon 1 – 5)	Fw: CCGCGGTGAGCCATGATTCG Rv: AGGCCCAGGAGGTCCTTTGGG	54	385 (IIa) 178 (IIb)
HAPLN1	Fw: TGAAGGATTAGAAGATGATACTGTTGTG Rv: GCCCCAGTCGTGGAAAGTAA	59	80
MFAP5	Fw: CGAGGAGACGATGTGACTCAAG Rv: AGCGGGATCATTCACCAGAT	59	72
MMP13	Fw: GGAGCATGGCGACTTCTAC Rv: GAGTGCTCCAGGGTCCTT	56	208
NOTCH1	Fw: AAGCTGCATCCAGAGGCAACC Rv: TGGCATACACACTCCGAGAACAC	60	172
SOX9	Fw: CCCAACGCCATCTTCAAGG Rv: CTGCTCAGCTCGCCGATGT	60	242

SUPPLEMENTAL FIGURES

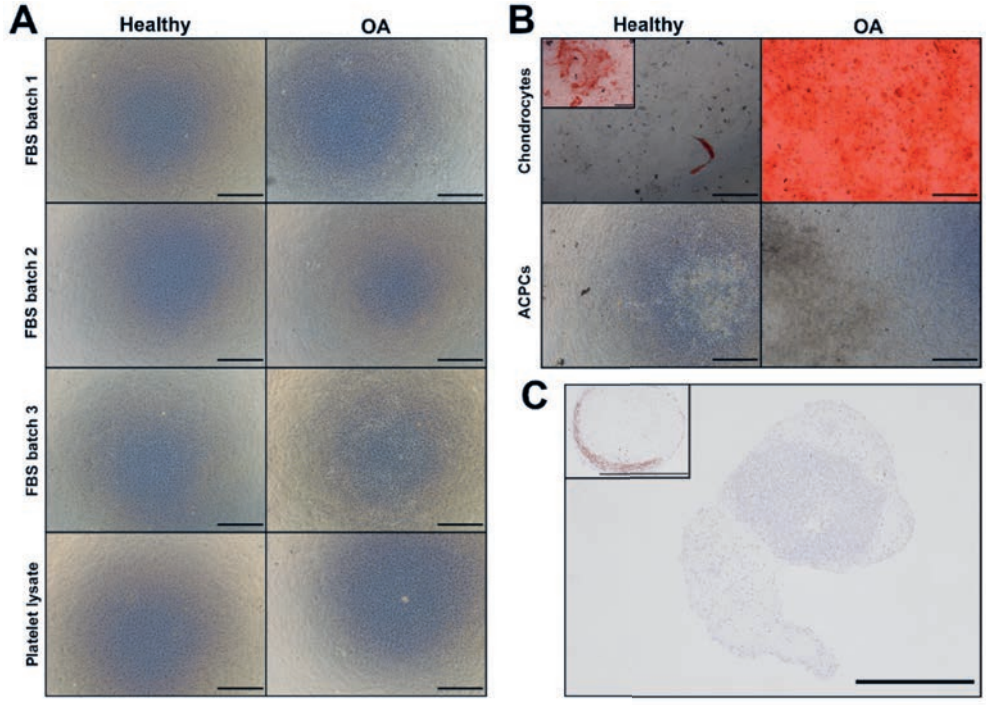

Figure S1. Osteogenic differentiation of articular cartilage-derived progenitor cells. (A) Articular cartilage-derived progenitor cells (ACPCs) were expanded and differentiated for three weeks using expansion medium and osteogenic differentiation medium supplemented with three batches of fetal bovine serum (FBS) or platelet lysate, after which the monolayers were stained with alizarin red. (B) Chondrocyte and ACPC monolayers were differentiated for three weeks using osteogenic differentiation medium supplemented with 100 ng/mL recombinant human Bone Morphogenetic Protein-2 (rhBMP-2) and stained with alizarin red. (C) A representative ACPC pellet stimulated for three weeks with osteogenic differentiation medium and stained for detection of calcium deposit by von Kossa stain. Insert shows a pellet of bone marrow-derived MSCs cultured in parallel. N = 3 for all. All scale bars = 200 µm.

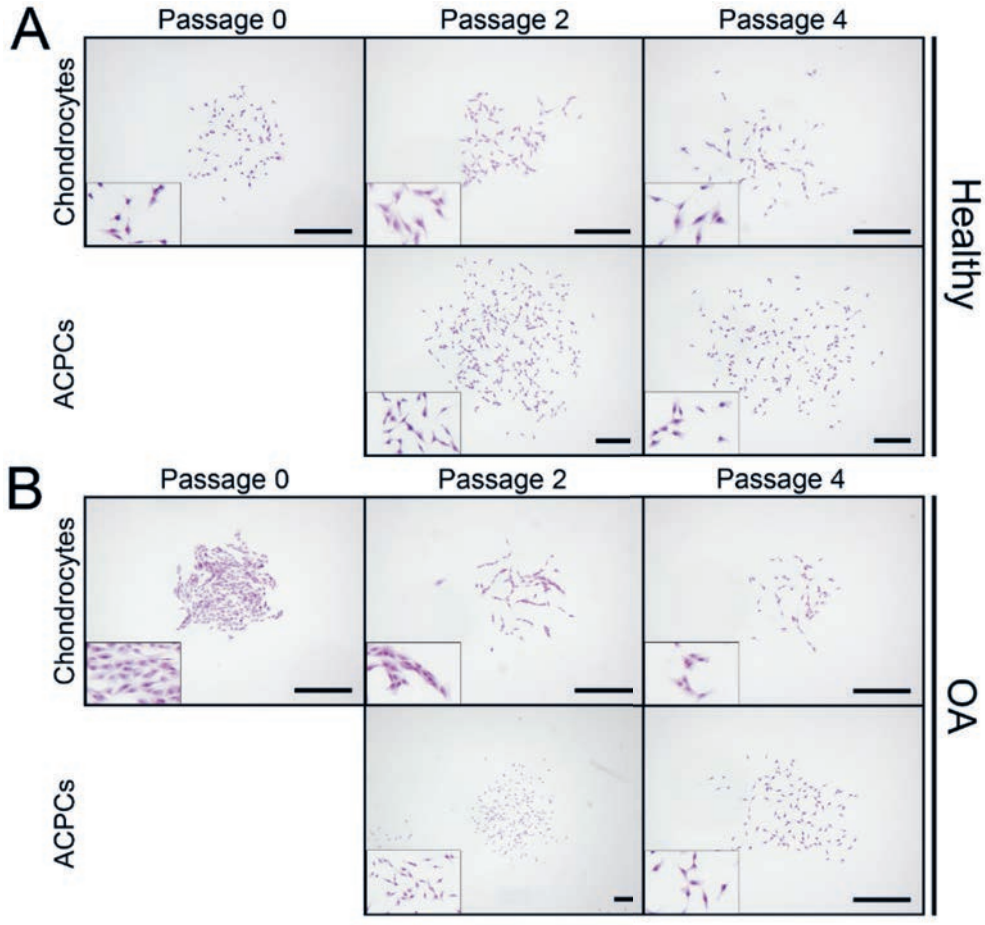

Figure S2. Morphology of colonies. Gross morphology of colonies from (A) chondrocytes and articular cartilage-derived progenitor cells (ACPCs) derived from healthy cartilage at passage 0, 2, and 4 and colonies from (B) chondrocytes and ACPCs derived from osteoarthritic (OA) cartilage stained with 0.05% Crystal Violet. The inserts show a 12X magnifications of the original image. N = 6 for all cell types. All scale bars = 200 µm. Two technical replicates per donor.

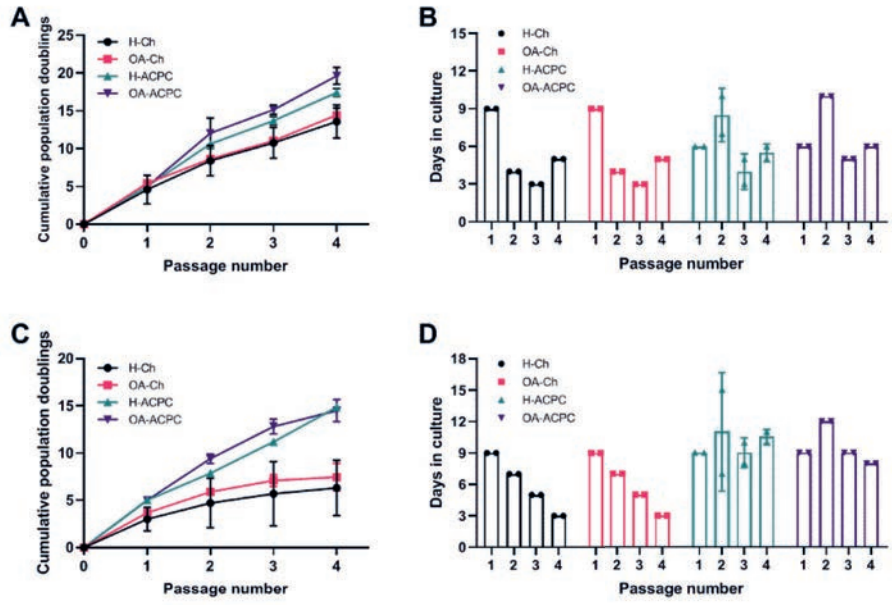

Figure S3. Expansion of articular cartilage-derived progenitor cells versus chondrocytes in two distinct media. (A) Cumulative population doublings of articular cartilage-derived progenitor cells (ACPCs) and chondrocytes in ACPC expansion medium at each consecutive passage. (B) Culture time of ACPCs and chondrocytes per passage in ACPC expansion medium. (C) Cumulative population doublings of ACPCs and chondrocytes in chondrocyte expansion medium and (D) culture time per passage in chondrocyte expansion medium. N = 2 for all experiments, ACPC and chondrocyte donors are matching.

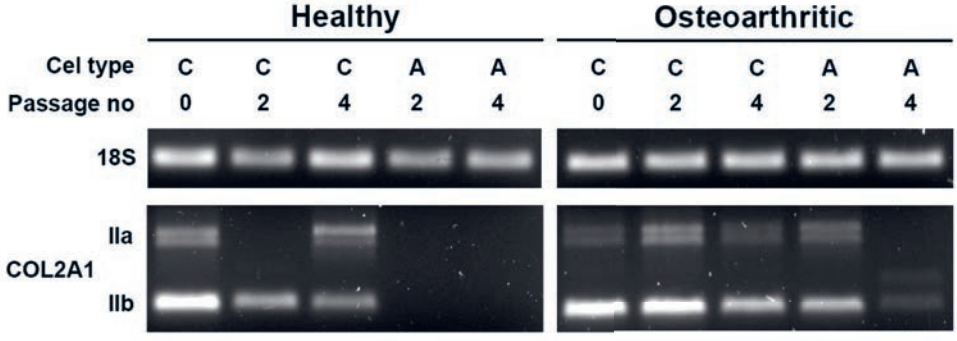

Figure S4. Gene expression of type II collagen splice variants. Polymerase chain reaction (PCR) product analysis of type II collagen splice variants IIa and IIb in chondrocytes after isolation (passage 0) and chondrocytes and articular cartilage-derived progenitor cells (ACPCs) at passage 2 and 4. Products were separated on an agarose gel and visualized with SYBR Safe. For both pathological states, 18S and COL2A1 PCR products were ran on the same gel. A, *ACPC*; C, *chondrocyte*; COL2A1, *collagen type II alpha 1 chain*; IIa, *splice variant IIa*; IIb, *splice variant IIb*.

Chapter 4

Selection of highly proliferative and multipotent progenitors from osteoarthritic meniscus through differential adhesion to fibronectin

Jasmijn V. Korpershoek
Margot Rikkers
Tommy S. de Windt
Marianna A. Tryfonidou
Daniel B.F. Saris
Lucienne A. Vonk

International Journal of Molecular Sciences (2021)

ABSTRACT

Meniscus injuries can be highly debilitating and lead to knee osteoarthritis. Progenitor cells from the meniscus could be a superior cell type for meniscus repair and tissue-engineering. The purpose of this study is to characterize meniscus progenitor cells isolated by differential adhesion to fibronectin (FN-prog). Human osteoarthritic menisci were digested and FN-prog were selected by differential adhesion to fibronectin. Multilineage differentiation, population doubling time, colony formation and MSC surface markers were assessed in the FN-prog and the total meniscus population (Men). Colony formation was compared between outer and inner zone meniscus digest. Chondrogenic pellet cultures were performed for redifferentiation. FN-prog demonstrated multipotency. The outer zone FN-prog formed more colonies than the inner zone FN-prog. FN-prog displayed more colony formation and a higher proliferation rate than Men. FN-prog redifferentiated in pellet culture and mostly adhered to the MSC surface marker profile, except for HLA-DR receptor expression. This is the first study that demonstrates differential adhesion to fibronectin for isolation of a progenitor-like population from the meniscus. The high proliferation rates and ability to form meniscus extracellular matrix upon redifferentiation together with the broad availability of osteoarthritis meniscus tissue, makes FN-prog a promising cell type for clinical translation in meniscus tissue-engineering.

INTRODUCTION

The meniscus is a fibrocartilage structure in the knee that is predominantly composed of circumferentially orientated type I collagen fibres and low amounts of glycosaminoglycans (GAGs) surrounded by water. It plays an important role in shock absorption, load transmission and stability of the knee. Meniscus injuries can lead to knee pain, locking and swelling and are highly disabling. The treatment of a meniscus injury is dependent on the location of the tissue damage, as the ability to heal differs between the inner and outer zone. The avascular inner zone is composed of chondrocyte-like cells and does not heal, while the vascularized outer zone has a fibrocartilage phenotype and some healing potential[236–238]. Therefore, meniscus tears in the outer zone of young patients can be successfully repaired, but overall 66% of meniscus tears remain irreparable[239–241]. Meniscus tears unsuitable for repair are treated using (partial) meniscectomy with a 7-fold increase in the odds of developing osteoarthritis[242,243]. Currently, approaches for (stem) cell based therapies for meniscus repair and regeneration are emerging[244,245]. These therapies often employ multipotent mesenchymal stromal cells (MSC), but hypertrophy and osteogenesis are common drawbacks of these stem-cell like or signaling cells[232,246]. Results of the first clinical trial employing MSCs after meniscectomy are suboptimal[247] and there seems to be a paradigm shift towards the use of specific progenitor cells[248]. In the last decades, the existence of a progenitor cell population in healthy as well as osteoarthritic cartilage has been suggested[15,16,90]. Cartilage progenitor cells can be isolated by employing their differential adhesion to fibronectin (DAF) based on the high affinity for the fibronectin receptor[15]. Cartilage progenitor cells have high proliferative and multipotent capacity and increased chondrogenic differentiation potential compared to bone marrow MSCs[93,111], with a lower tendency for terminal hypertrophic differentiation[92]. Recently, the presence of meniscus progenitor cells has been suggested in rabbits[246,249] and humans[86,87,250]. Meniscus progenitor cells might be a therapeutic target for meniscus preservation and a promising cell type for meniscus tissue-engineering, especially due to the high availability of osteoarthritic tissue. However, meniscus progenitor cells are not thoroughly characterized, and unlike for articular cartilage, the DAF protocol has not been explored for isolation of meniscus progenitors.

Therefore, the purpose of this study is to isolate progenitor cells from osteoarthritic menisci using DAF. To test the ability of DAF to select a progenitor population, the acquired cells (FN-prog) were compared to the total meniscus population (Men). Men and FN-prog were characterized according to the MSC guidelines by the International Society for Cellular Therapy (ISCT)[165]. Moreover, other progenitor-characteristics like clonogenicity and proliferation were assessed. Lastly, the potential of FN-prog for meniscus tissue engineering was compared to Men by assessing redifferentiation in pellet culture using gene expression, release and deposition of GAGs and deposition of collagen.

RESULTS

Selection of a clonogenic population from the meniscus inner and outer zone

Colony formation of the total meniscus, outer and inner zone digest was assessed after DAF. Of the total meniscus digest, 1.1±0.8% of cells were clonogenic with affinity for fibronectin. 0.3±0.4% of the inner zone cells formed colonies, whereas 1.5±1.1% of the outer zone cells formed colonies (Figure 1a). Fibronectin affinity of different passages of FN-prog and Men was assessed after 20 minutes adhesion to fibronectin (Figure 1b). Colony formation of FN-prog at passage 4 was higher than the formation of Men. To assess colony formation regardless of fibronectin affinity, colony formation on culture dishes was also assessed. Again, colony formation of FN-prog at passage 4 was higher than that of Men (Figure 1c). Moreover, FN-prog retained their proliferative capacities, while the proliferation rate of Men diminished after the third passage (Figure 1d). Representative pictures of the colonies are shown in Figure 1e and 1f.

Expression of MSC markers

Over 98% of FN-prog and Men expressed the surface markers CD90 and CD105. CD73 was expressed in 74±15% of Men and 85±7.0% of FN-prog. Negative markers CD45, CD34, CD79α, and CD11b were negative (<2% positive) in both FN-prog and Men. In 4 out of 5 donors 11-53% of FN-prog expressed the HLA-DR receptor and therefore did not meet the ISCT criteria[165]. In 1 out of 5 Men donors the HLA-DR receptor was expressed in 17% of the cells (Figure 2a).

Multilineage potential

All cell populations showed oil Red O staining after 3 weeks of culture indicative of adipogenic differentiation. Similarly, all populations produced mineralized matrix upon osteogenic induction confirmed by Alizarin Red staining. After 3 weeks of pellet culture in chondrogenic medium, all 5 FN-prog donors showed GAG deposition as indicated by Safranin-O staining, whereas none of the donors showed GAG deposition in the total meniscus population at passage 2. Cells of the total meniscus population at passage 4 were not able to form or maintain a firm pellet up to 4 weeks and did not show GAG deposition. None of the populations showed hypertrophic differentiation when subjected to hypertrophic media[232] as assessed by type X collagen deposition, while the positive control of bone marrow derived MSCs was positive for type X collagen staining (Figure 2b).

Expression profile after monolayer expansion

Genes associated with a degenerative (Delta and Notch-like epidermal growth factor-related receptor (*DNER*)) or cartilage (Cyclin-dependent kinase 1(*CDK1*)) progenitor fate[87] were expressed relatively higher in FN-prog than Men at passage 4 (Figure 3a). CD318, a marker associated with degenerative meniscus progenitor cells, was expressed higher in FN-prog than Men (0.05±0.06 vs 6.5±4.4) (Figure 3b). A meniscus progenitor fate[87] can be assessed using the pericyte marker Melanoma Cell Adhesion Molecule (*MCAM*)[251] (also known as CD146).

Gene-expression of *MCAM* did not differ significantly between FN-prog at passage 4 and Men at passage 2 (Figure 3a). Expression of *MCAM* in Men passage 4 was below the limit for quantification using qPCR. Surface marker expression of MCAM as assessed by flow cytometry did not differ significantly between Men and FN-prog (7.5±9.0 vs 2.5±1.5 % positive cells) (Figure 3b). Expression of extracellular matrix genes collagen type I α1 chain (*COL1A1*) and aggrecan (*ACAN*) were lower in FN-prog than in Men (Figure 3c). Expression of collagen type II α1 chain (*COL2A1*) was detectable but not quantifiable.

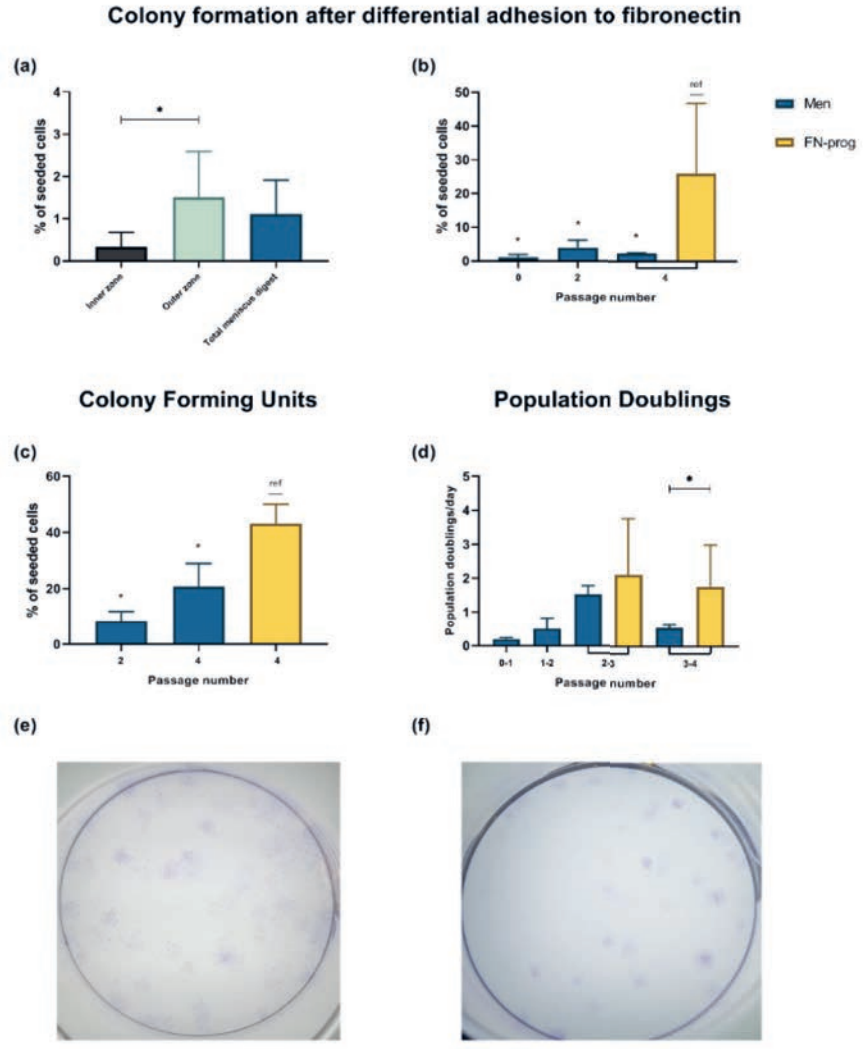

Figure 1. Colony formation after fibronectin selection of (a) inner zone, outer zone and total meniscus digest at passage 0 and (b) different passages of the total meniscus population (Men) and fibronectin selected cells (FN-prog), comparison between different passage numbers of the total meniscus population (Men) and fibronectin selected cells (FN-prog) in (c) colony forming units on culture dishes without fibronectin coating and (d) population doublings per day. Representative pictures of colonies formed after seeding (e) Men at 11 cells/cm^2 or (f) FN-prog at 6 cells/cm^2 both at passage 4, stained with crystal violet blue. *$p<0.05$; ref, reference category.

Chondropermissive/Redifferentiation culture

After culturing both cell populations in pellets in chondropermissive medium for 28 days, gene expression of meniscus matrix genes, GAG production and collagen and GAG stainings were analysed. *COL1A1*, *COL2A1* and *ACAN* expression of FN-prog did not differ from Men. Upon addition of TGF-β1 to the chondropermissive medium, only *COL2A1* expression was higher in FN-prog compared to Men (Figure 4a). DNA content did not differ between groups. Similarly, total production of GAGs (deposition and release) was comparable. Collagen deposition in FN-prog seemed higher than Men but this did not reach statistical significance (p=0.16) (Figure 4b). In absence of TGF-β1, safranin-O staining indicative of glycosaminoglycan deposition was absent in all pellets. The deposition of type I collagen was more pronounced by pellets of Men cells compared to FN-prog. In the Men pellets, type I

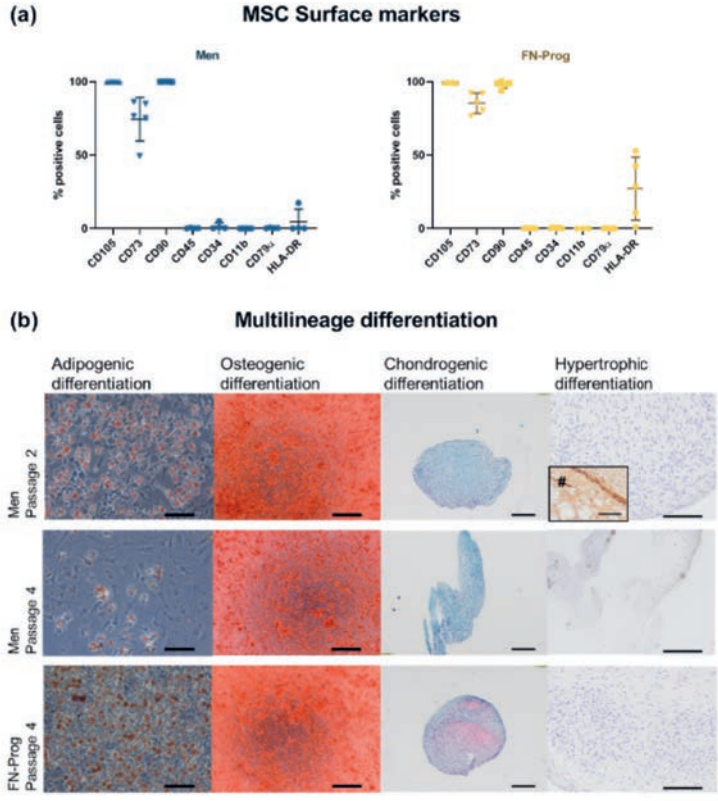

Figure 2. Characterization according to the MSC guidelines of the International Society for Cell & Gene Therapy[165] for (a) surface marker expression and (b) adipogenic (oil Red O staining), osteogenic (Alizarin Red staining), chondrogenic (Safranin-O/ Fast Green staining), hypertrophic (type X collagen immunohistochemistry) differentiation. N=5 donors per group per condition. Donor-matched samples were used to culture the total meniscus population (Men) and fibronectin selected cells (FN-prog). #, bone marrow mesenchymal stromal cells passage 4 that were hypertrophically differentiated were used as positive control for type X collagen immunohistochemistry. Scale bars represent 100μm.

collagen was mainly found in the inner regions of the pellets, while for FN- prog it was distributed throughout the pellets, but in lower amounts. In the pellets that were cultured in presence of TGF-β1, safranin-O staining was positive in one donor of Men and all donors of the FN-prog. There was a low deposition of type I collagen by Men in some areas of the pellet, while FN-prog had deposited more type I collagen, that was located mostly towards the outer regions of the pellet. Type II collagen staining was absent or low in all groups (Figure 5).

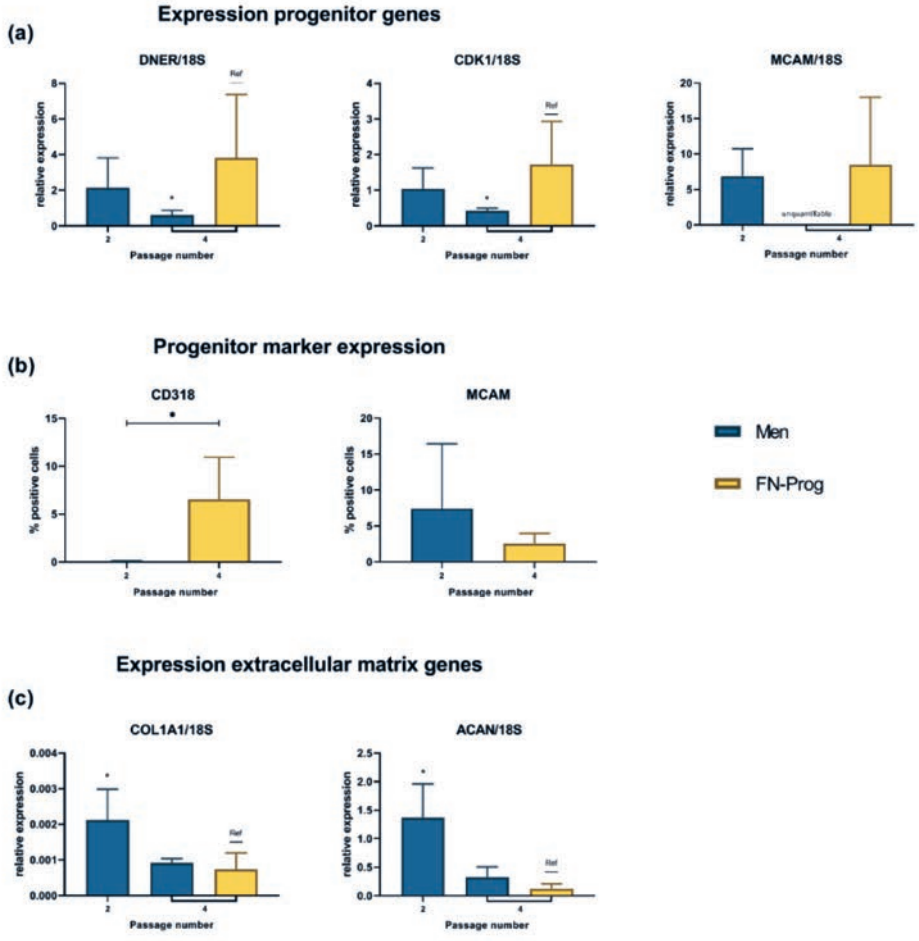

Figure 3. Expression of (a) genes associated with meniscus extracellular matrix production and (b) meniscus progenitor phenotype as measured by quantitative real-time PCR and (c) progenitor marker expression measured using flow-cytometry after monolayer expansion. N=5 donors per group per condition. *ACAN*, aggrecan; *COL1A1*, collagen type I alpha 1 chain; *CDK1*, Cyclin-dependent kinase 1; *DNER*, Delta and Notch-like epidermal growth factor-related receptor; FN-prog, fibronectin selected cells; *MCAM*, Melanoma cell adhesion molecule; Men, total meniscus population *, $p<0.05$; ref, reference category.

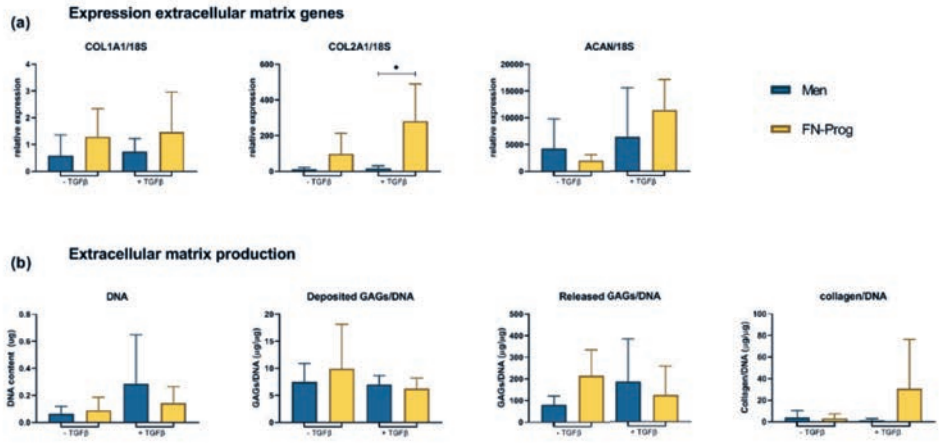

Figure 4. A) Expression of genes associated with meniscus extracellular matrix production, and B) DNA content, glycosaminoglycan deposition and release normalized for DNA content and collagen deposition measured by hydroxyproline assay, normalized for DNA content after 28 days of pellet culture in chondropermissive medium in absence or presence of TGF-β1. N=5 donors per group per condition. *ACAN*, aggrecan; *COL1A1*, collagen type I α1 chain; *COL2A1*, collagen type II α1 chain; GAG, glycosaminoglycan; TGFβ, transforming growth factor beta 1; **, p<0.05.*

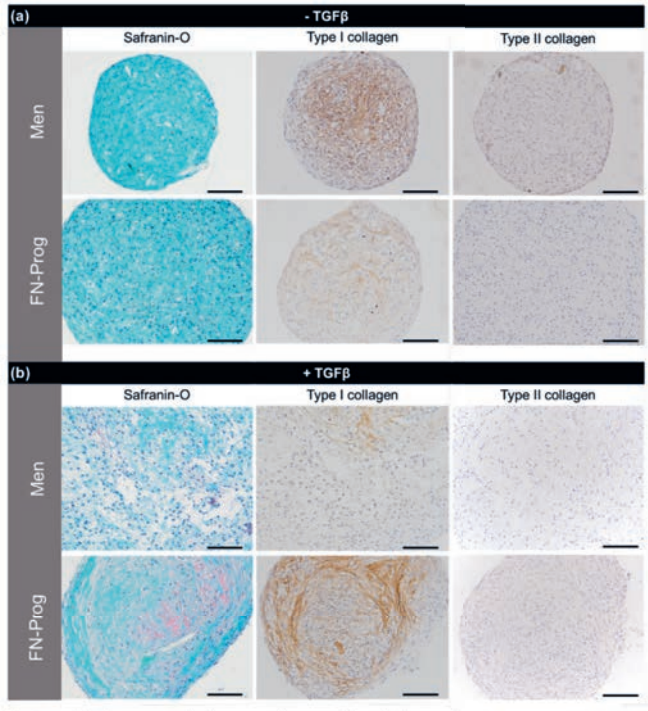

Figure 5. Representative sections of pellets cultured for 28 days in differentiation medium in (a) absence of TGF-β1 or (b) presence of TGF-β1. N=5 donors per group per condition. Scale bars represent 100 µm.

DISCUSSION

This is the first study to isolate meniscus progenitor cells through DAF and to characterize the obtained cell population according to the MSC criteria of the ISCT. We confirmed selection of a distinctive cell population which differs from the total meniscus population in terms of colony formation, proliferation, chondrogenic differentiation, and gene-expression. The advantages of this population in terms of expansion and redifferentiation potential make this a promising cell type for meniscus tissue engineering.

DAF has been used for isolation of progenitor cells from cartilage for almost two decades[15], but was never used for isolation of meniscus progenitors. Here, isolated FN-Prog showed affinity for fibronectin up to at least passage 4. Interestingly, FN-prog from both inner and outer zone meniscus digest formed colonies. The inner zone of the meniscus is regarded as unable to regenerate, but the presence of progenitor-like cells in inner zone meniscus has been suggested previously to contain CD146+ cells[252], clonogenic cells[249], and migrating cells[86,253] with progenitor-like properties. The reason for aberrant regeneration in the inner zone in presence of progenitor cells is unclear, but the lack of contact with blood-derived stimulating factors might prevent the progenitor cells to respond to injury. In agreement with our findings, the number of progenitor-like cells in the inner zone was lower compared to the outer zone in these studies. Therefore, FN-prog from the outer zone are presumably overrepresented in the FN-prog population. Nevertheless, the entire meniscus could be used as a cell source to obtain FN-prog. This facilitates easy isolation and increases the amount of available tissue. Moreover, the presence of FN-prog or progenitor-like cells in the inner meniscus creates potential for repair or regeneration in the inner zone, for example by enhancing the activity or density of FN-prog. This could change the current dogma of the inability of inner zone meniscus to regenerate.

The ability to grow clonally is one of the characteristics of progenitor cells. In the current study, FN-prog formed more colonies and proliferated faster than Men. Likewise, a larger colony number and size were previously reported in progenitor-like cells compared to meniscus cells[249,253]. The possibilities for fast and extensive culture expansion creates potential for the use of FN-prog for clinical tissue engineering purposes. The prolonged and fast proliferation might indicate a more progenitor-like state/stemness of this population.

Another indicator of the progenitor-like phenotype of FN-prog is the multilineage potential. Multilineage potential of meniscus progenitor cells was previously reported in progenitor populations selected based on colony formation[249,254,255], or migration from the meniscus[86,253,256]. Here, FN-prog differentiated towards the adipogenic, osteogenic, and chondrogenic lineage, contrary to meniscus cells that did not display chondrogenic differentiation. Here, in contrast to bone-marrow derived MSCs, and similar to results shown for cartilage progenitor cells[92], a lack of hypertrophic differentiation was demonstrated in FN-prog. Again, these characteristics support the use of FN-prog over MSCs for meniscus tissue

engineering[232,257].

COL1A1 and *ACAN* expression of FN-prog were low during expansion and normalized upon redifferentiation, a phenomenon also seen in culture expanded chondrocytes[111,153]. Notably, upon addition of TGF-β to the chondropermissive medium, the *COL2A1* expression was higher in FN-prog than in Men upon culture, although the expression was too low to translate into an abundant deposition of type II collagen on histology. Together with the GAG deposition, this indicates a progenitor-like state with chondrogenic tendency and makes FN-prog a feasible cell type for cartilage tissue engineering. However, only a limited amount of GAGs is found in the healthy native meniscus[258]. Therefore, GAG deposition might be a suboptimal outcome to assess meniscus extracellular matrix formation, and type I collagen deposition could be used instead. Both FN-prog and Men showed type I collagen deposition.

The surface marker profile of FN-prog corresponded largely to the profile for MSC marker expression as defined by the ISCT. High expression of CD90 and CD105 are also found in populations of both progenitor cells and fibrochondrocytes as shown by single cell RNA sequencing at passage 0[87]. However, apart from the differences in CD73 expression, the markers do not discriminate between Men and FN-prog. Additionally, MSC marker expression increases after culture expansion[250]. The inability to discriminate between cell populations based on immunophenotype is a known drawback in MSC research[259]. To verify the existence of a true and pure meniscus progenitor population, specific markers are currently lacking. More specific markers might increase the purity of this population or demonstrate the physiological or pathological role in the meniscus.

Furthermore, HLA-DR expression was positive in 4 out of 5 FN-prog donors. Although MSCs are explicitly defined by negativity for HLA-DR[165], HLA-DR expression is found even in clinical batches of bone marrow MSCs from 2 different Good Manufacturing Practice facilities and should not be used as a strict criterion for release of MSC[260,261]. HLA-DR expression of bone marrow MSCs is upregulated in an inflammatory environment, e.g. by contact with interferon γ[260,262]. Similarly, the HLA-DR expression in meniscus progenitors might be upregulated due to the osteoarthritic inflammatory environment. However, HLA-DR positive and negative MSCs do not differ in morphological, differentiation and immunomodulatory characteristics, thus HLA-DR expression might not be relevant for the MSC function or even improve the anti-inflammatory properties of MSCs[260,262]. Furthermore, expression might be decreased by expansion beyond confluence[263], which might be applied to FN-prog for allogeneic use to decrease the risk of immune reactions. The effect of HLA-DR expression on FN-prog behaviour and the effect of increasing culture time on HLA-DR expression of FN-prog remain to be investigated.

Finally, the progenitor cells were selected by differential adhesion to fibronectin, which has been extensively used for the selection of progenitor cells from articular cartilage[15,90,127,144]. At

passage 4, the FN-prog still had more affinity for fibronectin compared to Men. This does imply that expansion of the total meniscus population does not selectively increase the population of FN-adherent cells and that the FN-prog is a distinctive population. For articular cartilage progenitors, the fibronectin receptor CD49e is responsible for the increased fibronectin adhesion capacity[90]. For these cells it was shown that expression of CD49e did not change between passage 0 and 10[139], but the expression of the fibronectin receptor is dynamic as it increased in culture[164]. In the meniscus, fibronectin is located in the cell membrane of fibrochondrocytes and in the territorial matrix throughout the meniscus[264]. To our knowledge, it is unknown how osteoarthritis influences this distribution. In our current study, fibronectin is only used for the initial selection directly after isolation of the cells from the meniscus. Subsequently, the cells are transferred and passaged on tissue culture plastic without fibronectin coating. Therefore, it is unlikely that the fibronectin adhesion has an influence on the differentiation of the selected cells at passage 4.

Limitations

The cell populations compared in this study are both isolated from OA meniscus, which draws into question the applicability of these cell types for tissue engineering of healthy meniscus. The inflammatory environment of an OA joint might activate degenerative pathways, like the interleukin 1β induced activation of degenerated meniscus progenitor cells[87]. The use of healthy meniscus cells is not a practical alternative, due to the limited availability. Moreover, the degenerative state of meniscus progenitors might be reversible as a shift from degenerative meniscus progenitors to meniscus progenitors was seen upon TGF-β treatment[87]. This identifies TGF-β as a possible treatment target. The use of meniscus fragments obtained during meniscectomy of traumatic meniscus injury might hold potential over the use of osteoarthritic injury. Indeed, in chondrocytes from cartilage defect rims performed better than chondrocytes from healthy (non-weight bearing) regions[265]. However, caution should be exercised until a comparison with populations from healthy meniscus has been made.

Implications

The currently isolated progenitor population is an attractive option for tissue engineering purposes. The availability of FN-prog is almost unlimited as the entire OA meniscus can be used for isolation which is often discarded as redundant material after total knee replacement. Fast expansion and continued *in vitro* redifferentiation as indicated by type I deposition and proteoglycan production enables large scale (off the shelf) usage. Further research should elucidate the role of FN-prog in healthy and osteoarthritic tissue in order to employ these cells as therapeutic target or increase the defective endogenous regeneration and at clinical translation of this cell population.

MATERIALS AND METHODS

Cell Isolation and Culture

Collection of meniscus tissue was performed according to the Medical Ethics regulations of the University Medical Center Utrecht and the guideline "Human Tissue and Medical Research: Code of Conduct for responsible use" of the Dutch Federation of Medical Research Societies[221,266]. Meniscus tissue was obtained from patients with Kellgren and Lawrence grade III and IV osteoarthritis undergoing total knee arthroplasty (n = 11, age 52–84). Both female and male donors were used and both donor genders were balanced within experiments. No individual grading was performed on the tissue. Lateral and medial menisci were pooled and cut into cubical pieces of approximately 2 mm^3 and digested for 2 h in Dulbecco's modified Eagle medium (DMEM, Gibco, Life Technologies Europe B.V., Bleiswijk, The Netherlands) with 100 U/mL penicillin (Gibco) and 100 µg/mL streptomycin (Gibco) (1% p/s) and 0.2% pronase (Roche Diagnostics GmbH, Mannheim, Germany) under continuous movement (20 rpm) at 37°C, followed by digestion in DMEM with 1% p/s, 5% heat-inactivated Fetal Bovine Serum (FBS; Biowest, Nuaillé, France) and 0.075% collagenase II (Wortington Biochemical Corporation, Lakewood, NJ, USA). For the total meniscus population (men), the digest was plated on culture flasks and cultured in meniscus expansion medium (DMEM with 10% FBS and 1% p/s) up to passage 2. For the isolation of FN-prog, culture flasks were coated with 10 ng/mL fibronectin (Sigma-Aldrich, Saint Louis, MO, USA) in PBS at 37°C for 2 h. A total of 500 cells/cm^2 were plated on the coated flasks and non-adherent cells were removed after 20 min (Figure 6). FN-prog were cultured up to passage 4 in progenitor expansion medium (αMEM (minimal essential medium, Gibco) with 10% FBS, 20 mM l-ascorbic acid-2-phospate (1% ASAP; Sigma-Aldrich) and 5 ng/mL basic fibroblast growth factor (bFGF; Peprotech, London, UK) at 37°C and 5% CO_2. For comparison between Men and FN-prog, Men cells were switched to progenitor expansion medium after the first passage and cultured up to passage 4 in progenitor expansion medium. Cells were passaged upon reaching 90% confluency. Population doublings per day were calculated by dividing the number of harvested cells by the number of seeded cells and the number of days. For comparison between inner and outer zones, the outer third and inner third of 5 menisci were digested separately and colony formation was assessed as described below.

Colony Formation

To assess colony formation and affinity for fibronectin, cells were seeded on fibronectin coated wells in a density of 500 cells/cm^2 (passage 0), 222 cells/cm^2 (Men passage 2), 111 cells/cm^2 (Men passage 4), or 22 cells/cm^2 (FN-prog passage 4). After 20 min, non-adherent cells were removed, and progenitor expansion medium was added. After 3 days, medium was renewed, and after 7 days the cells were fixed and colonies visualized using 0.05% Crystal Violet (Sigma-Aldrich) in Milli-Q water. To assess colony formation in absence of a prior fibronectin adhesion step, 11 cells/cm^2 (Men passage 2, FN-prog passage 4) and 6 cells/cm^2 (FN-prog passage 4).

Multilineage Differentiation

For osteogenic differentiation, cells were cultured in monolayer until 50–70% confluent and differentiated for 3 weeks in osteogenic medium (αMEM with 10% FBS, 1% ASAP, 1% p/s, 10 mM β-glycerolphosphate, and 10 nM dexamethasone). For adipogenic differentiation, cells were cultured until confluent and differentiated for 3 weeks in adipogenic medium (αMEM with 10% FBS, 1% p/s, 1μM dexamethasone (Sigma-Aldrich), 0.5 mM isobutylmethylxanthine (Sigma-Aldrich), 0.2 mM indomethacin (Sigma-Aldrich), and 1.72 μM insulin (Sigma-Aldrich)). For chondrogenic differentiation, 250,000 cells were pelleted and cultured for 3 weeks in chondrogenic medium (DMEM, 1% ASAP, 1% p/s, 1% Insulin-Transferrin-Selenium+ Premix (Corning, Corning, NY, USA), 0.1 μM dexamethasone, and 10 ng/mL TGF-β1 (Peprotech)). For hypertrophic differentiation, pellets were cultured for chondrogenic differentiation followed by a 1-week culture in hypertrophic medium (DMEM, 1% ASAP, 1% p/s, 0.2 mM dexamethasone, 10 mM β-glycerolphosphate, and 1 nM triiodothyronine (Sigma-Aldrich)). Following osteogenic differentiation, cells were fixed in 70% ethanol and stained with 40 mM Alizarin Red S (pH 4.1; Sigma-Aldrich) for 5 min. Following adipogenic differentiation, cells were fixed in 4% buffered formaldehyde solution and stained with 0.3% Oil Red O (Sigma-Aldrich) in isopropanol for 30 min. Following chondrogenic and hypertrophic differentiation, pellets were fixated in a 4% buffered formaldehyde solution and further processed as described in 'histology and immunohistochemistry'.

Expression of MSC Markers

Cells were labeled with antibodies against CD105, CD73 (R&D Systems, Minneapolis, USA), CD90, CD34, CD79A, HLA-DR (Miltenyi Biotec Bergisch Gladbach, Germany), CD11b, and CD45 (Biolegend, San Diego, CA, USA) according to the manufacturer's instructions. Cells were mixed with the antibodies in FACS buffer (0.5% bovine serum albumin, 2 mM EDTA in PBS) and incubated in the dark at room temperature for 30 min. Samples were analyzed on a FACSCantoII and LSR Fortessa X20 (BD Biosciences, Allschwil, Switzerland). Stainings with single antibodies and fluorescence minus one were used as controls.

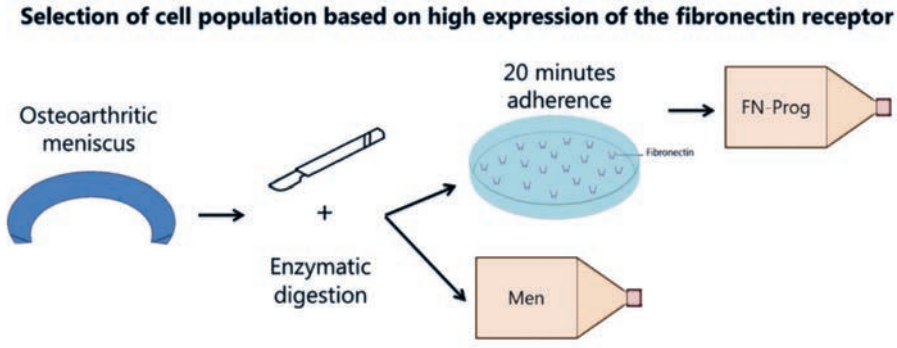

Figure 6. Isolation and selection of cell populations.

Chondropermissive Cultures/ Redifferentiation

For the analysis of redifferentiation after expansion, 250,000 cells were pelleted and cultured at 37 ºC and 5% CO_2 for 28 days in chondropermissive medium (DMEM, 1% ASAP, 1% p/s, 2% Albuman (Human Serum Albumin, 200 g/L; Sanquin Blood Supply Foundation, Amsterdam, the Netherlands), 2% insulin-transferrin-selenium-ethanolamine (ITS-X; Gibco)) in the absence and presence of 10 ng/mL TGF-β1. Per group, 5 donors were used. Medium was changed twice per week and collected for analysis.

Gene Expression

Gene expression was assessed at the end of the expansion phase and after 28 days of redifferentiation culture. RNA was isolated using TRIzol reagent (Invitrogen, Carlsbad, CA, USA) according to the manufacturer's recommendations. Then, 200–500 ng RNA was reverse-transcribed using the High-Capacity Reverse Transcription Kit (Applied Biosystems, Foster City, CA, USA). Real-time polymerase chain reactions (RT-PCR) were performed using an iTaq Universal SYBR Green Supermix (Bio-Rad, Hercules, CA, USA) on a LightCycler 96 (Roche Diagnostics) according to the manufacturer's recommendations. RNA levels were quantified relative to levels of housekeeping gene 18S. Primer sequences can be found in Table 1.

Release and Deposition of Glycosaminoglycans and Collagen

Pellets were harvested after 28 days and digested using a papain digestion buffer (250 µg/mL papain; Sigma-Aldrich, 0.2 M NaH_2PO_4, 0.1 M ethylenediaminetetraacetic acid [EDTA], 0.01 M cysteine, pH 6) at 60ºC overnight. GAG content in the digests (deposition) and medium (release) was assessed using a dimethylmethylene blue (DMMB; pH 3) assay to quantify sulphated GAGs. The absorbance was measured at 525 and 595 nm using a spectrophotometer and the ratio at 525/595 nm calculated. Chondroitin-6-sulfate (Sigma-Aldrich) was used as a standard.

For the analysis of collagen deposition, digests were lyophilized followed by a hydrolyzation in 4 M NaOH overnight at 108 ºC. Samples were neutralized using 1.4 M citric acid. Then, 50 mM chloramine-T (Merck, Darmstadt, Germany) in oxidation buffer was added. After 20 min incubation, dimethylaminobenzoaldehyde (Merck) in 25% (*w/ v*) perchloric acid in 2-propanol was added. Absorbance was measured at 570 nm after 20 min incubation at 60ºC. Hydroxyproline (Merck) was used a standard since 13.5% of collagen is composed of hydroxyproline [48]. DNA content of digests was measured using a Quant-iT PicoGreen dsDNA assay (Invitrogen) and was used to normalize collagen and GAG content.

Histology and Immunohistochemistry

Pellets were harvested after 28 days and fixated in a 4% buffered formaldehyde solution. After embedding in paraffin, 5 µm sections were cut. After deparaffinization, sections were stained with 0.4% Fast Green (Merck) followed by 0.125% Safranin-O (Merck) and Weigerts

hematoxylin (Clin-Tech, Surrey, UK). Immunohistochemistry for type I and II was performed as following. Antigen were retrieved with 1 mg/mL pronase (Sigma-Aldrich) for 20 min at 37 °C, followed by 10 mg/mL hyaluronidase (Sigma-Aldrich) 20 min at 37 °C. Sections were blocked with a 5% bovine serum albumin (BSA) in PBS solution for 30 min. Samples were incubated with the primary antibody (type I collagen, rabbit monoclonal 1/400 or type II collagen, mouse monoclonal 1/100 in PBS/BSA 5%) overnight at 4 °C. Sections were washed and incubated with horseradish peroxidase-conjugated anti-rabbit or mouse secondary antibody (Dako, Glostrup, Denmark) for 30 min at room temperature. For type X collagen, antigen were retrieved using 1 mg/mL pepsin (Sigma-Aldrich) in 0.5M acetic acid for 2 h at 37 °C, followed by 10 mg/mL hyaluronidase for 30 min at 37 °C. Sections were blocked with 5% BSA in PBS for 30 min. Samples were incubated with the primary antibody (type X collagen, mouse monoclonal 1/20 in PBS/BSA 5%) overnight at 4 °C. Sections were washed and incubated with biotin-conjugated anti-mouse secondary antibody (GE healthcare, Little Chalfont, UK) for 60 min at room temperature, followed by an enhancement step with streptavidin—peroxidase (Beckman Coulter, Woerden, The Netherlands) for 60 min at room temperature. Immunoreactivity was visualized using diaminobenzidine peroxidase substrate solution (DAB, Sigma-Aldrich). Mayer's hematoxylin was used as counterstaining.

Statistical Analyses

Statistical analyses were performed using GraphPad Prism 8.3 (GraphPad Software, Inc., La Jolla, CA). Data are presented as mean ± standard deviation (SD). Colony formation was compared between inner and outer zone of the same donor using a two-tailed paired t-test (Figure 1a). To test for differences in colony formation and population doubling between FN-prog and Men, a one-way ANOVA with Dunnett's multiple comparisons correction was performed (Figures 1b-d). Relative gene expression of FN-prog at passage 4 was compared to the expression Men at passages 2 and 4 using a one-way ANOVA with Dunnett's multiple comparisons correction (Figure 3a,b). To assess differences in CD318 and MCAM surface marker expression between Men and FN-prog of the same donors, a two-tailed paired t-test was used (Figure 3C). Relative gene expression and matrix formation of Men and FN-prog were compared in the presence and in absence of TGF-β1 using a one-way ANOVA with Dunnett's multiple comparisons correction (Figure 4a,b). *P* values below 0.05 were considered significant.

Table 1. Primer sequences for quantitative real-time PCR. *ACAN*, aggrecan; *bp*, base pair; *COL1A1*, collagen type I alpha 1 chain; *COL2A1*, collagen type II alpha 1 chain; *CDK1*, Cyclin-dependent kinase 1; *DNER*, Delta and Notch-like epidermal growth factor-related receptor; *Fw*, forward; *GREM1*, Gremlin-1; *MCAM*, Melanoma cell adhesion molecule; *Rv*, Reverse.

Gene name	Oligonucleotide sequence (5'to 3')	Product size (bp)
18S	Fw: GTAACCCGTTGAACCCCATT Rv: CCATCCAATCGGTAGTAGCG	151
ACAN	Fw: CAACTACCCGGCCATCC Rv: GATGGCTCTGTAATGGAACAC	160
COL2A1	Fw: AGGGCCAGGATGTCCGGCA Rv: GGGTCCCAGGTTCTCCATCT	195
COL1A1	Fw: TCCAACGAGATCGAGATCC Rv: AAGCCGAATTCCTGGTCT	191
DNER	Fw: AAGGCTATGAAGGTCCCAACT Rv: CTGAGAGCGAGGCAGGATTT	137
MCAM	Fw: AGCTCCGCGTCTACAAAGC Rv: CTACACAGGTAGCGACCTCC	102
CDK1	Fw: AAACTACAGGTCAAGTGGTAGCC Rv: TCCTGCATAAGCACATCCTGA	148

Chapter 5

Mitochondrial transport from mesenchymal stromal cells to chondrocytes increases DNA content and proteoglycan deposition

Jasmijn V. Korpershoek
Margot Rikkers
Fleur S.A. Wallis
Koen Dijkstra
Daniël B.F. Saris
Lucienne A. Vonk

Submitted

ABSTRACT

Allogeneic mesenchymal stromal cells (MSC) are used in the one-stage treatment of articular cartilage defects. Recently, a role for mitochondrial transfer in the treatment effect of MSCs has been suggested in several regenerative treatments. To investigate whether transport of mitochondria occurs between human cartilage defect chondrocytes and bone marrow-derived MSC, mitochondria were stained with MitoTracker, and CellTrace was used to distinguish between cell types. Using flow cytometry, mitochondrial transfer was demonstrated to occur within the first 4 hours until 16 hours of coculture. Fluorescence microscopy indicated that transport occurs via tunnelling nanotubes and direct cell-cell contact. Extracellular vesicles were harvested from conditioned medium and presence of mitochondria in these vesicles was demonstrated using flow cytometry. To investigate the effect of transport of MSC mitochondria to chondrocytes, mitochondria were isolated from MSCs and transferred to chondrocytes. After 28 days of pellet culture, DNA content and proteoglycan deposition were higher in chondrocyte pellets to which MSC mitochondria were transferred then the control groups. Lastly, to assess the fate of transferred mitochondria *in vivo*, DNA was isolated from biopsies of six patients taken one year after treatment with a combination of allogeneic MSCs and autologous chondrons. Using single nucleotide polymorphisms genotyping, no donor mitochondrial DNA could be detected in the biopsies. These results indicate that mitochondrial transport plays a role in the chondroinductive effect of MSCs on chondrocytes *in vitro*. However, *in vivo* transferred mitochondria cannot be traced back after one year.

INTRODUCTION

Multipotent mesenchymal stromal (stem) cells (MSCs) can be isolated from bone marrow, adipose tissue, synovial membrane, and other tissues[267]. Due to their multilineage differentiation potential[165], anti-inflammatory properties[268], and signalling through trophic factors[269], and extracellular vesicles[270], MSCs are used in a wide spectrum of regenerative treatments. One of the treatments employing MSCs is IMPACT (Instant MSC Product accompanying Autologous Chondron Transplantation). IMPACT is a new treatment for articular cartilage defects of the knee and combines 10% recycled autologous chondrons with 90% off-the-shelf available allogeneic MSCs[70,115,271]. Results of a phase I/II trial using IMPACT for treatment of articular cartilage defects show safety and feasibility of this procedure[70,115], and 5-year clinical outcomes are promising[271]. The repaired cartilage defect site does not contain autosomal DNA of the MSC donors, suggesting that the MSCs do not differentiate, but rather act as signalling cells[248,272], possibly through secretion of chondroinductive[273,274] and anti-inflammatory agents[275].

MSC-derived mitochondria enhanced phagocytic capacity of alveolar macrophages and ameliorated lung injury by improving mitochondrial function and ATP turnover in a murine model[276,277]. Furthermore, transplanted MSC mitochondria restore mitochondrial function and decrease apoptosis in rabbit cardiomyocytes postischemia[278], and intra-myocardial injection of autologous mitochondria improved ventricular function in four out of five patients after ischemic injury[279]. While the occurrence of mitochondrial transfer from equine, mice, and rat MSCs towards chondrocytes has been described[280–282], it has not been demonstrated in human cells before. Moreover, it is unclear whether transport takes place from chondrocyte to MSC as well. As shown in other tissues than cartilage, transfer of mitochondria can play a role in tissue repair, but its role in MSC-stimulated chondrogenesis is unknown. Chondrocytes need adenosine triphosphate (ATP) for production of GAGs and type II collagen[283], which is provided normally by anaerobic glycolysis[284]. However, under glucose-deprived conditions or glycolysis inhibition, chondrocytes switch to oxidative phosphorylation to maintain ATP production[285]. Thus, the presence of functional mitochondria in chondrocytes is of paramount importance for their prolonged survival. Mitochondrial dysfunction can develop after pathological mechanical loading[286], and is one of the hallmarks in the development of osteoarthritis[287]. Mitochondrial transfer could have an important role in the prevention or treatment of this mitochondrial dysfunction. Therefore, the aim of this study is to investigate whether mitochondrial transfer takes place between human chondrocytes and MSCs. We study the timing of mitochondrial transfer as well as different modes of transport *in vitro*. Additionally, we investigate the effect of inflammation and senescence on mitochondrial transfer by pre-incubating with tumor necrosis factor α (TNF-α) and mitomycin C. Using MitoCeption[288], we analyse the effect of transferring MSC-derived mitochondria to chondrocytes on DNA content and proteoglycan deposition in 3D cultures. Lastly, in order to study mitochondrial transfer *in vivo,* we isolate DNA from cartilage biopsies of six patients treated with IMPACT[70,115] and used single nucleotide polymorphisms (SNP) genotyping to

determine the presence of MSC donor mitochondrial DNA.

RESULTS

Mitochondrial transfer takes place between chondrocytes and mesenchymal stromal cells

Cells stained with CellTrace (receiving cells) gained fluorescent mitochondria from donor cells that were stained with MitoTracker (Fig. 1A, indicated by white arrows). Stained mitochondria were transferred among chondrocytes, and between chondrocytes and MSCs. Using flow cytometry, mitochondrial transfer was quantified by measuring increase in fluorescence in receiving cells. Increase in fluorescence was significant between 0 and 4 hours and 8 to 16 hours in all three coculture conditions. No further increase in fluorescence was found after 16 hours in any of the conditions (Fig. 1B).

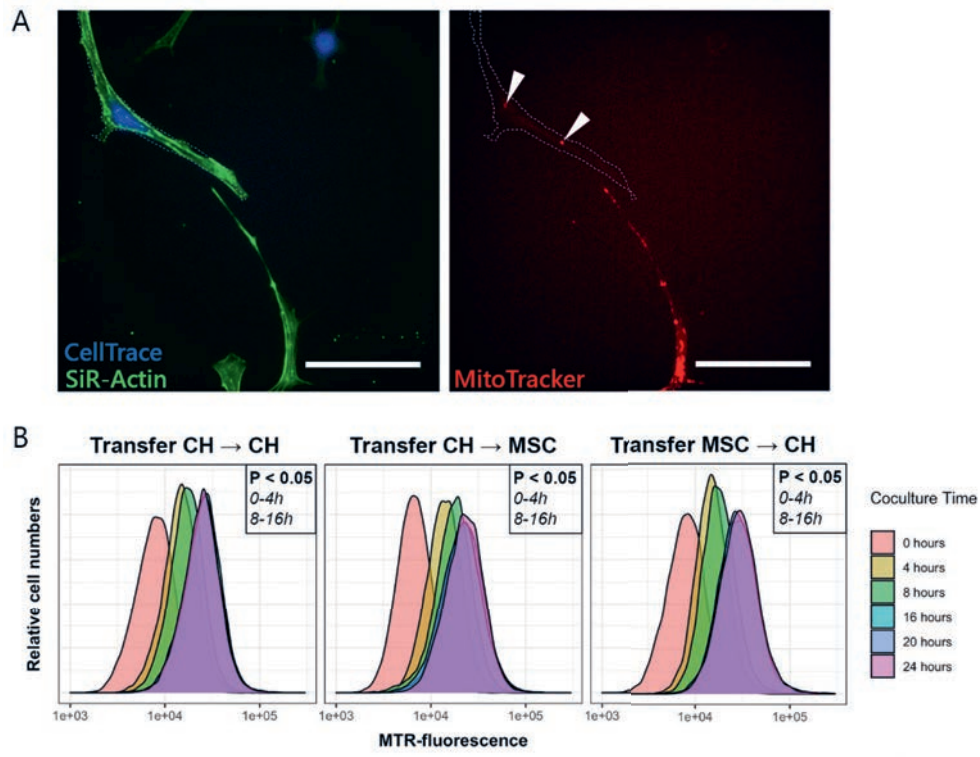

Figure 1. Transfer of mitochondria between chondrocytes and mesenchymal stromal cells. (A) Stained mitochondria (MitoTracker, in red) are transferred from a donating mesenchymal stromal cell (MSC) to a receiving chondrocyte (CH) stained with CellTrace (in blue). SiR-Actin stains F-actin in all cells (in green). Scale bar = 50 µm. (B) Quantification of transfer of mitochondria from donor to receiving cell, measured with flow cytometry. Mitochondrial transfer between all cell combinations (CH → CH, CH → MSC, and MSC → CH) occurred predominantly in the first four to eight hours after initiation of the coculture. In all cases, 20.000 events were recorded. MTR, *MitoTracker*

Mitochondrial transfer takes place through direct cell-cell contact, tunnelling nanotubes, and extracellular vesicles

Transfer of mitochondria occurred through direct cell-cell contact (Fig. 2A), as mitochondria (MitoTracker, in red) were seen in broad actin-containing (SiR-Actin, in green) cell protrusions between two cell types (indicated by white arrows). Additionally, mitochondria were detected in tunneling nanotubes (TNT) between both cell types (Fig. 2B). A mitochondrion in a TNT is indicated by the white arrow. Traces of DiD (in blue) are found in the receiving chondrocyte, suggesting transfer of the cytosolic dye from the stained MSCs. Using flow cytometry, a dual stained population (Fig. 2C, in orange) was identified as extracellular vesicles (EVs) containing mitochondria in conditioned medium of stained cells. In conditioned medium of unstained cells, this population overlapped with the population identified as background noise (in red). In conditioned medium of MSC monocultures, 35% of events were mitochondria-containing EVs, whereas in conditioned medium of CH 9% of events were mitochondria-containing EVs. In co-cultures where only MSCs were stained, 28% of events were mitochondria-containing EVs, whereas 7% of events were mitochondria-containing EV in the co-cultures where only CH were stained. In co-cultures where both CH and MSC were dual stained, 36% of the events were mitochondria-containing EVs. This indicates that MSCs are stimulated to excrete EVs containing mitochondria in presence of CH, while this is not the case for CH in presence of MSC.

Cell stress does not affect mitochondrial transfer

The effect of inflammation and senescence on mitochondrial transfer were investigated among chondrocytes and between chondrocytes and MSCs. Cells were pre-treated with TNF-α or mitomycin C to mimic cell stress. There was no significant difference in transfer between any of the groups and the control condition, although over time the fluorescence intensity increased (Fig. 3).

Uptake of MSC mitochondria increases gene expression of aggrecan and B-cell lymphoma 2 in chondrocytes

To assess the effects of MSC-derived mitochondria on chondrocytes in chondropermissive culture, mitochondria were transferred into chondrocytes by MitoCeption[288,289]. 24 hours after transfer, mitochondria (in red) were detected intracellularly in chondrocyte monolayers (Fig. 4A). The number of transferred mitochondria was dose-dependent as confirmed by flow cytometry (presented dose as equivalent to number of MSCs used for isolation). For further experiments, mitochondria of 900,000 MSCs were transferred onto 100,000 chondrocytes, in order to mimic a cell ratio of 90:10, which is optimal for chondroinduction[115,290]. When mitochondria of 900,000 MSCs were transferred on 100,000 chondrocytes, 74% ± 1.6 of the chondrocytes were positive for MitoTracker (Fig. 2B). Mitochondria derived from senescent MSCs were included to investigate whether these would exert similar effects as mitochondria from normal (proliferating) MSCs. MitoCeption of mitochondria and senescent mitochondria did not alter metabolic activity in chondrocyte monolayers at 24 and 42 hours of coculture

(Fig. 4C). At T=2h, mRNA expression of aggrecan (ACAN) was significantly up-regulated in CH that received mitochondria compared to CH controls and CH that received senescent mitochondria. Expression of type II collagen (COL2A1) at 26 hours after MitoCeption with mitochondria, seemed higher compared to the control group, but this did not reach statistical significance ($p<0.1$). ACAN and COL2A1 expression declined at 46 hours in all groups. Additionally, mRNA expression of B-cell lymphoma (BCL2), a marker for cell survival[291], was

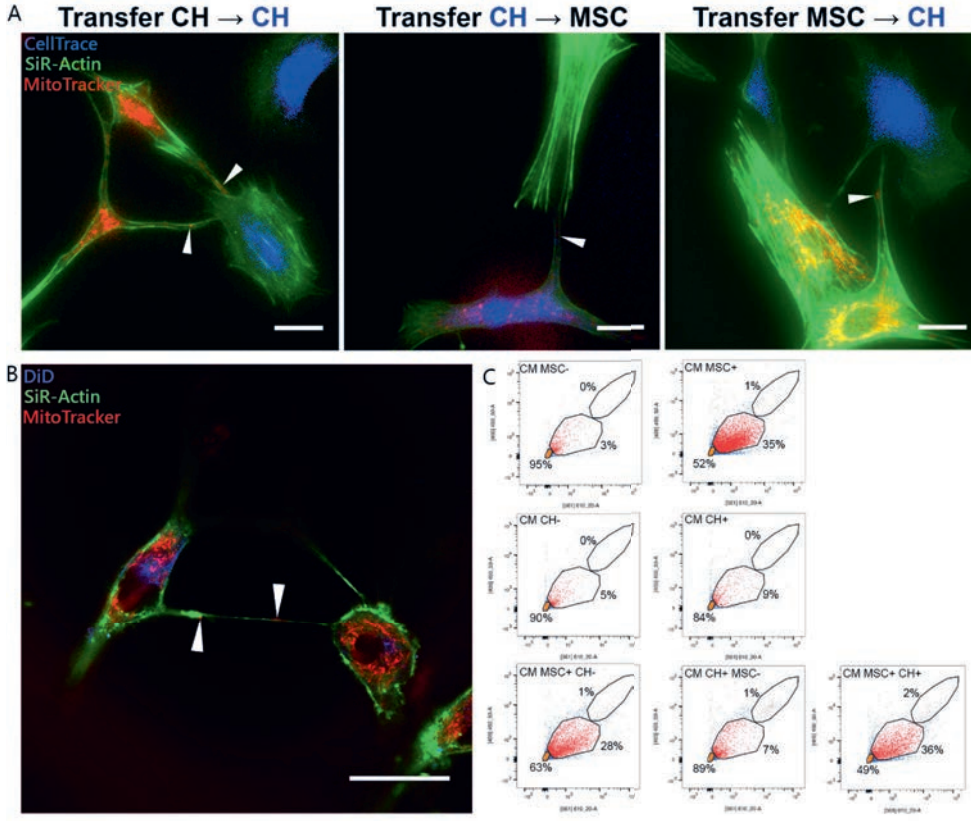

Figure 2. Mechanisms mediating transfer of mitochondria between cells. (A) Visualization of mitochondrial transfer between among chondrocytes (CH) and CH, between CH anc mesenchymal stromal cells (MSC), and vice-versa. Donating cells were stained with MitoTracker (in red), CH were stained with CellTrace (in blue), and F-actin of all cells was stained with SiR-Actin (in green). Mitochordria transported between two cell types are indicated by the white arrows. Scale bar = 25 µm. (B) Transport of mitochondria through a tunnelling nanotube between MSC and CH. Donating MSCs were stained with D D (in blue) and MitoTracker (in red). F-actin of all cells was stained with SiR-Actin (in green). Image taken after 16 hours of co-culture. Scale bar = 25 µm. (C) Flow cytometry analysis of (co)culture conditioned media (CM) for small particles including mitochondria-containing microvesicles (in orange). Noise and particles negative for both dyes are depicted in red, cells (upper gate) are depicted in grey. Intensity of MitoTracker (561/610 nm) is depicted on the x axis, intensity of CellTrace (405/450 nm) is depicted on the y axis. MSC- and CH- are unstained. MSC+ and CH+ are dual stained for MitoTracker and CellTrace. In unidirectional cocultures (lower panels, left and middle), the first cell type is dual stained while the other is unstained. In the bidirectional coculture (lower panel, right), both cell types are dual stained. In all cases, 10.000 events were recorded.

significantly higher 26 hours after MitoCeption with mitochondria, but not with senescent mitochondria (Fig. 4D).

Transferred mitochondria exert a chondrogenic effect in chondropermissive culture

To investigate the effect of transferred mitochondria on cartilage extracellular matrix production *in vitro*, isolated mitochondria from MSCs were transferred into chondrocytes using MitoCeption during formation of cell pellets at initiation of the culture. Efficiency of the MitoCeption protocol in pellets was compared to monolayers (Fig. 5A). Efficiency in pellets was comparable to monolayers in two donors, and lower in one donor (donor A, 89% ± 1.5 vs. 44% ± 4.4). Transferred mitochondria (in red) are detected in chondrocyte pellets one day after initiation of the culture (Fig. 5B). Brightness of MitoTracker was higher in one side of the pellet, where more cells were stacked on top of each other. Stained mitochondria were found throughout the entire pellet. After 28 days of chondropermissive culture, the amount of DNA was higher in pellets that received mitochondria compared to control chondrocyte pellets, as well as chondrocyte and MSC cocultures (Fig. 5C, left panel). Similarly, the amount of GAGs deposited in the pellets was higher compared to the chondrocyte and MSC coculture (Fig. 5C, middle panel). Secretion of GAGs into the culture medium was not different between the three groups (Fig. 5C, right panel). GAG deposition was insufficient to result in positive safranin-O staining in all groups. The type II collagen staining was negative in all pellets. There was a slight staining positive for type I collagen, especially in the centre of the chondrocyte with MSC mitochondria pellet (Fig. 5D).

MSC mitochondrial DNA in cartilage biopsies

Using a mitochondrial DNA SNP assay, 42 amplicons of the mitochondrial DNA were compared between MSC-donors and cartilage biopsies of six patients, taken one year after treatment with 90% allogeneic MSCs and 10% autologous chondrons. No donor mitochondrial DNA could be detected in the biopsies.

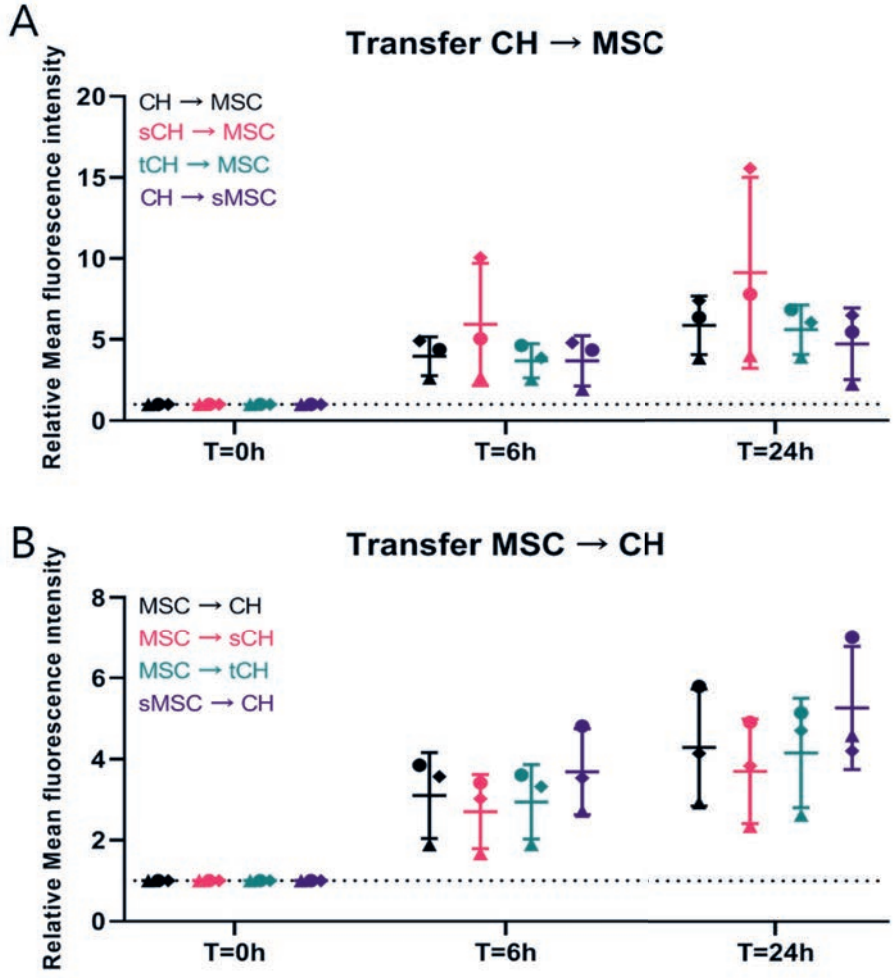

Figure 3. Effect of inflammation and senescence on mitochondrial transfer. (A) Mitochondrial transfer from chondrocytes (CH), chondrocytes pretreated with tumor necrosis factor α (TNF-α) to induce inflammation (tCH), and chondrocytes pretreated with mitomycin C to induce senescence (sCH), to mesenchymal stromal cells (MSC) and MSCs pretreated with mitomycin C to induce senescence (sMSC). tends to increase when CH are senescent (sCH). (B) Mitochondrial transfer from sMSCs and MSC to CH tends to be increased in case of sMSC and sCH. Simulating an inflammatory environment using TNF-α in CH using did not influence speed and magnitude of mitochondrial transfer. Inflammation and senescence did not significantly change mitochondrial transfer.

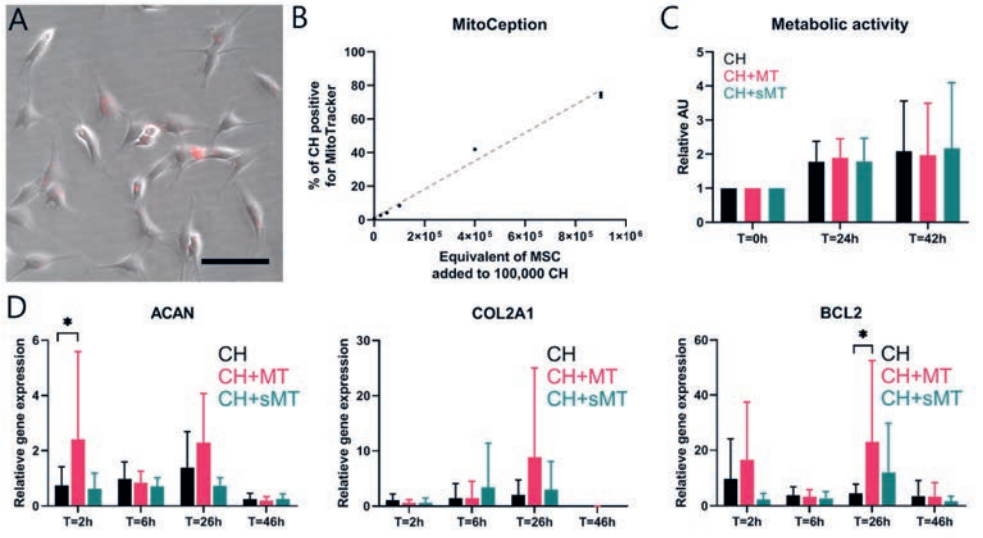

Figure 4. Direct mitochondrial transfer through MitoCeption. Mitochondria (MT) of 900,000 mesenchymal stromal cells (MSCs) were isolated and transferred into chondrocytes (CH) via MitoCeption. (A) MSC-derived mitochondria, stained with MitoTracker (in red), localized intracellularly in chondrocyte monolayers. Scale bar = 100 µm. (B) Dose dependent effect of MitoCeption using increasing concentrations of MT transferred into monolayers of 100,000 chondrocytes. Symbols depict averages of two measurements ± standard deviation and the grey line shows linear regression. (C) Metabolic activity of chondrocyte monolayers as indicated by the conversion of resazurin to resorufin (ex: 560 nm, em: 590 nm) at 24 and 42 hours after MitoCeption with MT and senescent MTs (sMT), both derived from 900,000 MSCs. N = 3 donor combinations. (D) mRNA expression of aggrecan (ACAN), type II collagen (COL2A1; both markers for chondrogenesis), and B-cell lymphoma 2 (BCL2; marker for cell survival) in chondrocyte monolayers at 2, 6, 26, and 46 hours after MitoCeption with MT and sMT derived from 900,000 MSCs. ACAN expression was increased in CH+MT compared to CH right after MitoCeption (T=2h), BCL2 was increased in CH+MT 26 hours after MitoCeption (T=26h). N = 3 donor combinations, 2 technical replicates per donor. *p<0.05

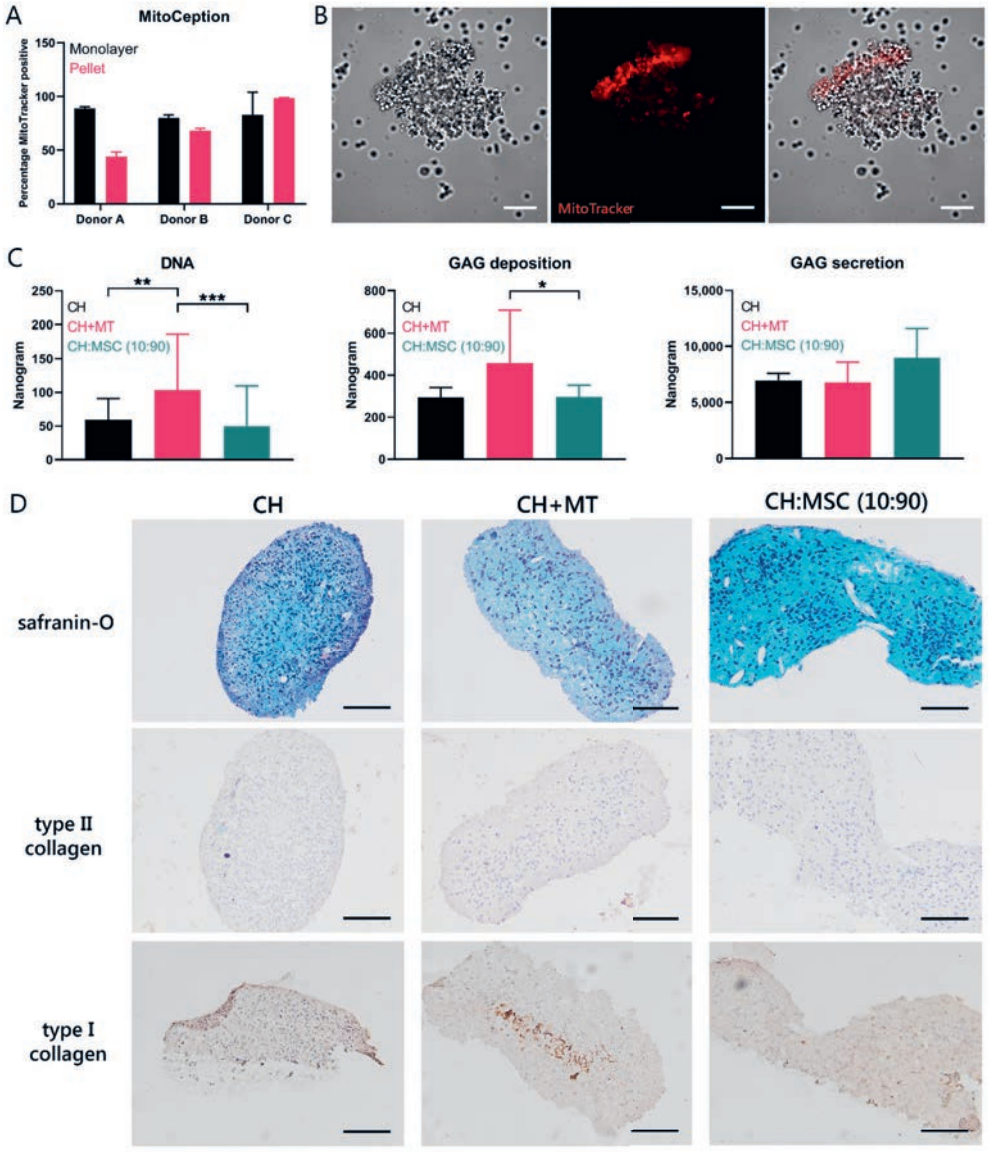

Figure 5. Chondrogenic effect of direct transfer of mitochondria. (A) Efficiency of transfer of MSC-derived mitochondria (MT) and senescent MSC-derived mitochondria (sMT) into chondrocyte (CH) pellets compared to MitoCeption on CH monolayers depicted for the three donor combinations. (B) Mitochondria stained with MitoTracker (in red) are localized in chondrocyte after simultaneous pelleting of cells and mitochondria. Scale bar = 100 µm. (C) Quantification of DNA and glycosaminoglycan (GAG) deposition and secretion of CH pellets after 28 days of chondropermissive culture in pellets. Control groups consisted of CH only and CH and MSC in coculture (CH:MSC, ratio 10:90). *p<0.05, **p<0.01, ***p<0.001. (D) Histological analysis for proteoglycans (safranin-O), type II collagen, and type I collagen. Scale bar = 100 µm.

DISCUSSION

In this study, we demonstrated bidirectional transport of mitochondria between chondrocytes and MSCs for the first time. Additionally, we identified three mechanisms responsible for mitochondrial transport, which are direct cell-cell contact, TNTs, and EVs. Finally, we showed compelling evidence of a chondrogenic effect of transferring MSC-derived mitochondria to chondrocytes through MitoCeption, indicating that mitochondrial transfer might be one of the underlying mechanisms of MSC-induced chondrogenesis.

Mitochondrial transfer could have an important role in the prevention or treatment of this mitochondrial dysfunction. Transfer of mitochondria is initiated in the first hours of coculture and reaches an equilibrium after sixteen hours. The timing of mitochondrial transfer was not explicitly researched before, but others have found indications of mitochondrial transfer at 10-12 hours from MSCs to chondrocytes[280,281] and at 4 hours between MSCs and macrophages[277]. Interestingly, the transport of mitochondria occurs not only from MSCs to chondrocytes, but chondrocytes also transfer mitochondria to MSCs. The transfer of defective mitochondria from chondrocytes towards MSCs might be a damage signal, as transfer by cardiomyocytes and endothelial cells induced the anti-apoptotic function of MSCs and secretion of cytoprotective enzymes[292]. Moreover, defective mitochondria could be excreted for degradation, a process known as transmitophagy[293]. Lastly, depolarized mitochondria might even be recycled by fusion with recipient cell mitochondria, thus increasing the metabolic state of the recipient[294]. To summarize, uptake of healthy MSC mitochondria by chondrocytes would benefit the metabolic state, while clearance of defective mitochondria could prevent the damage caused by oxidative stress.

Direct cell-cell contact, TNTs, and EVs are all mechanisms for mitochondrial transfer. The importance of direct cell-cell contact between MSCs and chondrocytes for *in vitro* chondroinduction has been shown earlier[274]. In direct cocultures, expression of gap junction protein connexin 43 was up-regulated. Although mitochondria cannot physically pass gap junctions, connexin 43 is a mediator of mitochondrial transport[295]. In fact, connexin 43 was reported to be essential in EV-mediated mitochondrial transfer between MSCs and alveolar cells[296]. MSC-derived extracellular vesicles enhance chondrogenesis of osteoarthritic chondrocytes *in vitro*[76]. Here, mitochondria containing EVs were identified, indicating that mitochondria might play a role in the chondrogenic effect of MSC-derived extracellular vesicles. Mitochondrial transport through TNT is another frequent mechanism for transport of mitochondria[297], and it has been described to occur between human MSCs and renal tubular cells[298], cardiomyocytes[299], vascular smooth muscle cells[300], and endothelial cells[301]. TNTs likely play a pivotal role in the transport between MSCs and chondrocytes, which is shown for the first-time in the current study. Next to mitochondrial transfer, TNTs allow transfer of various cellular components, including proteins, lysosomes and RNA[297], which was not studied here but could provide other explanations of the MSC-chondrocyte coculture mechanism.

Upon addition of MSC mitochondria to chondrocytes, DNA content and proteoglycan deposition increased, thus mitochondrial transfer might play an important role in the chondrogenic effect of MSCs. Gene expression showed increased ACAN and BCL2 expression, indicating a possible chondroinductive effect as well as increased survival. Similarly, a higher expression of type II collagen and proteoglycans was described[282] in osteoarthritic chondrocytes that had taken up MSC mitochondria. In the current study, an increase in type II collagen deposition could not be demonstrated with immunohistochemistry. Overall, the deposition of type I and II collagen was low, probably due to the fact that no growth factors were added in the chondropermissive culture. In the study by Wang *et al.*[282], increased chondrogenesis might be attributed to extracellular vesicles or trophic factors as well, as it was studied in co-culture. The increased chondrogenesis in chondrocytes with MSC mitochondria might be at least partially explained by promoting cell survival or proliferation in chondrocytes by restoring the energy balance[302], since matrix production per cell did not increase in chondropermissive cultures. Another effect of mitochondrial transfer might be the regulation of autophagy[303], since autophagy is activated under hypoxic stress conditions[304] and protects against mitochondrial dysfunction.

The fate of transferred mitochondria and the occurrence of mitochondrial transfer *in vivo* remain unknown, as we could not detect mitochondrial DNA of donor MSCs in cartilage biopsies taken one year after cell therapy with autologous chondrons and allogeneic MSCs. Earlier studies have shown presence of human mitochondrial DNA up to 28 days in murine macrophages[294]. Similarly, the autosomal MSC DNA decreases in 28 days of coculture[274], and no autosomal MSC DNA can be detected *in vivo* after one year[115]. The possibility that mitochondrial transfer occurs solely *in vitro* cannot be excluded, but mitochondrial transfer has been shown between MSCs and cardiac[292] or alveolar cells[296] *in vivo*. More likely, donor mitochondria are not retained in receiving chondrocytes over a prolonged period.

Limitations

In contrast to our hypothesis, mimicking cell stress conditions using induction of inflammation or senescence did not significantly alter mitochondrial transfer. Similarly, inflammation induction by IL-1β treatment did not alter total transfer during 10 hours of coculture of chondrocytes and MSCs as described by Bennett *et al.*[305]. Inflammation might not play an important role in mitochondrial transfer, or the inflammatory phenotype resulting from these treatments are not well retained *in vitro* after removing the factors. Likewise, senescence did not change mitochondrial transfer significantly. *In vivo,* senescence is induced by mechanical stress in the rim of cartilage defects[306] and drives aging and related pathologies. In osteoarthritis, senescent cells excrete catabolic factors causing cartilage degradation. Here, senescence induction by mitomycin C did not alter total mitochondrial transport. Senescence and the resulting formation of reactive oxygen species might compromise the quality and number of mitochondria, but this was not investigated here. Generally, the generalizations of this study are limited by the *in vitro* character of the experiments. However, human cartilage defect chondrocytes were used together with MSCs from our Good Manufacturing Practices

(GMP) certified cell therapy facility in order to closely mimic the clinical situation.

Implications

The presented results demonstrate the role of mitochondrial transport in the chondroinductive effect of MSCs on chondrocytes. Treatment with MSCs or mitochondria in the acute phase of cartilage injury might prevent mitochondrial dysfunction and subsequent ROS accumulation, and therefore counteract one of the first steps towards development of osteoarhritis[286]. Moreover, pre-selection of MSCs for their capacity to donate functional mitochondria or take up damaged mitochondria for degradation could enhance the effect of MSCs in cocultures. Eventually, potential of MSC-derived mitochondria as a method for cell-free therapies could be explored. Cell-free therapies have advantages including lower safety profiles, and homogenization of treatment, but limiting treatment to mitochondria neglects other functions of MSCs such as transmitophagy of defective mitochondria and reactivity to damage signals with trophic factors or extracellular vesicles. Additionally, efficient long-term storage of mitochondria should be investigated and chondroinductive actions upon thawing confirmed[307].

METHODS

Donors and cell isolation

Human MSCs were isolated from bone marrow of healthy non-HLA matched donors in the GMP-licensed Cell Therapy Facility (Department of Clinical Pharmacy, University Medical Center Utrecht) as approved by the Dutch central Committee on Research Involving Human Subjects (CCMO, Bio-banking bone marrow for MSC expansion, NL41015.041.12). The parent or legal guardian of the donor signed the informed consent approved by the CCMO (n = 5, age range = 2 – 12). In brief, the mononuclear fraction was separated, MSCs were isolated by plastic adherence, and expanded for three passages in Minimum Essential Media (αMEM, Macopharma, Utrecht, The Netherlands) with 5% (v/v) platelet lysate and 3.3 IU/mL heparin and cryopreserved. Subsequently, MSCs were culture-expanded for two or three additional passages in MSC expansion medium (αMEM (Gibco, Bleijswijk, The Netherlands), 10% (v/v) fetal bovine serum (FBS; Biowest, Nuaillé, France), 1% penicillin/streptomycin (pen/strep; 100 U/mL, 100 µg/mL; Gibco), 200 µM l-ascorbic acid 2-phosphate (ASAP; Sigma-Aldrich), and 1 ng/mL basic fibroblast growth factor (bFGF; PeproTech, London, UK)).

Cartilage was obtained after debridement of focal cartilage lesions from patients undergoing ACI procedures, and is considered medical waste or redundant material (n = 5, age range = 18 – 38). The tissue collection was performed according to the Medical Ethics regulations of the University Medical Center Utrecht and the guideline "Human Tissue and Medical Research: Code of Conduct for responsible use" of the Dutch Federation of Medical Research Societies[221,266]. Chondrocytes were isolated from the debrided cartilage by digestion in 0.2% (w/v) pronase (Sigma-Aldrich, Saint-Louis, MO, USA) in Dulbecco's Modified Eagle's medium (DMEM, 31966; Gibco) with 1% pen/strep for two hours, followed by overnight digestion in

0.075% (w/v) collagenase II (CLS-2, Worthington, Lakewood, NJ, USA) in DMEM supplemented with 10% FBS and 1% pen/strep). Isolated chondrocytes were culture-expanded to passage two in chondrocyte expansion medium (DMEM, 10% FBS, 1% pen/strep).

Quantification of monolayer mitochondrial transfer

To enable identification of the different donor and receiving cell type in culture, the donor cell type was labelled with CellTrace Violet (Invitrogen, Carlsbad, CA, USA) and MitoTracker Red CMXRos (Molecular Probes, Invitrogen) according to the manufacturer's instructions. Receiving cells were unlabelled. Cells were stained one day prior to initiation of the coculture. Additionally, cells were pre-treated with 0.02 µg/mL mitomycin C (Substipharm, Paris, France) for six days to induce senescence [308] or with 10 ng/mL tumor necrosis factor α (TNF-α, R&D Systems, Minneapolis, MN, USA) for 24 hours to mimic an *in vitro* inflammatory environment[309].

MSCs (passage 5 or 6) and chondrocytes (passage 2) were seeded in 6-well plates at a density of 100,000 cells per well in a 1:1 ratio. Dual-stained donor cells were plated 24 hours before initiation of the coculture. Unstained receiving cells were added to the pre-seeded donor cells and cocultures were maintained for 24 hours in chondrocyte expansion medium. After 0, 4, 8, 16, and 24 hours, cocultures were trypsinized, washed, and resuspended in phosphate-buffered saline (PBS) supplemented with 0.4% (v/v) human serum albumin (HSA; Albuman, Sanquin, Amsterdam, The Netherlands). Samples were analysed using a CytoFLEX S flow cytometer (Beckman Coulter, Brea, CA, USA). For each condition, 20,000 events were recorded. Flow cytometry results were extracted and analysed using RStudio (R Core Team, Vienna, Austria) and FlowJo V10 data analysis software package (Tree Star Inc, Ashland, OR, USA).

Imaging

To enable identification of the different donor and receiving cell type in culture, the donor cell mitochondria were labelled with MitoTracker Red CMXRos (Molecular Probes, Invitrogen) and the chondrocytes (or half of the cells in CH → CH) were stained with CellTrace Violet (Invitrogen) according to the manufacturer's instructions. To visualize tunneling nanotubes (TNT), the donor cell type was stained with DiD (Vybrant™ Multicolor Cell-Labeling Kit, Invitrogen) in co-cultures. Additionally, the actin skeleton of all cells in all cultures was stained using 100 nM SiR-Actin (Spirochrome AG, Tebu Bio, Heerhugowaard, The Netherlands). Monolayers were imaged using a THUNDER fluorescence microscope and LASX acquisition software (both Leica microsystems, Wetzlar, Germany). TNTs were imaged using a Leica SP8X Laser Scanning Confocal Microscope (Leica microsystems) and LASX acquisition software.

Extracellular vesicle isolation

To evaluate presence of mitochondria in extracellular vesicles (EV) and changes in EV secretion initiated by coculture, donor cells were dual stained using CellTrace Violet and

MitoTracker Red CMXRos as described in 'Quantification of monolayer mitochondrial transfer' or left unstained. Cells were cultured in monocultures or cocultures in 1:1 ratio for 24 hours in vesicle-deprived chondrocyte expansion medium, after which the conditioned medium was collected for processing. Cell debris were removed from conditioned medium by centrifugation for 5 minutes at 320 *g*, followed by 15 minutes at 1500 *g*. Subsequently, the medium was centrifuged at 16,000 *g* for 1 hour to pellet EVs[310,311]. After discarding the supernatant, EVs were washed, resuspended in buffer (PBS with 0.5% (w/v) bovine serum albumin (Roche Diagnostics GmbH, Mannheim, Germany) and 2mM ethylenediaminetetraaceticacid (EDTA)) and then analysed using a BD LSRFortessa flow cytometer (BD Biosciences, Allschwil, Switzerland) and FlowJo V10 data analysis software package (Tree Star Inc). For each condition, 10,000 events were recorded.

Delivery of MSC mitochondria to chondrocytes in monolayer

To investigate the effect of MSC-derived mitochondria on chondrocytes, mitochondria isolated from MSCs (pre-stained with MitoTracker Red CMXRos) were directly transferred into chondrocytes. MSCs were culture-expanded and half of the cells were treated with mitomycin C to induce senescence (sMSC). Mitochondria were isolated using the Mitochondria Isolation Kit for Cultured Cells (Thermo Scientific, Waltham, MA, USA) according to the manufacturer's instructions. Mitochondria were transferred into chondrocytes as previously described[288]. Briefly, mitochondria were added to monolayers of chondrocytes and subjected to two consecutive centrifugation steps with an interval of 2 hours. The moment after the first centrifugation cycle was considered T0. Efficiency of MitoCeption on pre-seeded chondrocyte monolayers was measured using increasing concentrations of mitochondria. Then, isolated mitochondria of 9 x 10^5 MSCs or senescent MSCs were used for MitoCeption on a monolayer of 1 x 10^5 pre-cultured chondrocytes (CH) to mimic a CH:MSC ratio of 10:90 as used in IMPACT[115,290]. Intra-cellular location of the mitochondria was confirmed 1 day after MitoCeption with fluorescence microscopy and effect of different dosages of mitochondria was assessed using flow cytometry.

Metabolic activity of chondrocytes after mitochondrial transfer

Metabolic activity of the MitoCepted chondrocyte monolayers was determined directly after MitoCeption (T=2h), after 26h, and 44h using the conversion of resazurin to resorufin (44 mM; Alfa Aesar, Thermo Scientific) by measuring fluorescent intensity at 560 nm excitation and 590 nm emission.

Gene expression of chondrocytes after mitochondrial transfer

Total RNA of chondrocyte monolayers was isolated at T=2h, T=6h, T=26, and T=46h after MitoCeption using TRIzol (Invitrogen) according to the manufacturer's instructions. RNA was reverse-transcribed using the High-Capacity cDNA Reverse Transcription Kit (Applied Biosystems, Foster City, CA, USA). Real-time PCRs were performed using iTaq Universal SYBR Green Supermix (Bio-Rad) in the LightCycler 96 (Roche Diagnostics GmbH) according to the manufacturer's instructions. Primers (Invitrogen) are listed in Table 1. Relative gene

expression was calculated using 18S as a housekeeping gene and normalized for gene expression of that donor before MitoCeption. Amplified PCR fragments extended over at least one exon border (except for 18S).

Delivery of MSC mitochondria to chondrocytes in 3D chondropermissive culture

To investigate whether transfer of MSC-mitochondria into chondrocytes affects chondrogenesis, isolated mitochondria were transferred into chondrocytes during the pellet formation. Mitochondria of 9 x 10^5 MSCs or sMSCs were isolated as described in 'Direct mitochondrial transfer through MitoCeption in monolayer' and added to 1 x 10^5 chondrocytes in suspension. Pellets of 1 x 10^5 chondrocytes were formed by centrifugation at 320 *g* for five minutes in 15 mL Falcon tubes. MitoCeption on monolayers was performed in parallel to compare efficiency of MitoCeption in pellets and in monolayers. Pellets were cultured for 28 days in chondropermissive medium (DMEM, 2% HSA, 2% (v/v) insulin-transferrin-selenium-ethanolamine (ITS-X; Gibco), 200 µM ASAP, and 1% pen/strep). Control pellets consisted of chondrocytes alone and CH:MSC cocultures in a 10:90 ratio (both 1 x 10^5 total). Medium was changed twice per week and collected for analysis. After one and two weeks of culture, MitoCeption was repeated on a subset of pellets. Control pellets were also subjected to centrifugation at these time points. Results are displayed in Fig. S1.

Release and deposition of glycosaminoglycans

Pellets were harvested after 28 days of culture, digested in a papain digestion buffer (250 µg/mL papain (Sigma-Aldrich), 0.2 M NaH_2PO_4, 0.1M EDTA, 0.01M cysteine, pH 6.0) at 60ºC overnight. Deposition of sulphated glycosaminoglycans (GAG) in the pellet digests and release into the culture medium was measured using a dimethylmethylene blue assay (DMMB; pH 3.0). Absorbance was measured at 525 / 595 nm using chondroitin-6-sulfate (Sigma-Aldrich) as a standard. DNA content of digests was quantified using Qubit dsDNA HS Assay Kit (Thermo Scientific) according to the manufacturer's instructions.

Histological analyses

Pellets were processed for histology by fixation in a 4% buffered formaldehyde solution, followed by dehydration through graded ethanol steps, clearing in xylene, and embedding in paraffin. Sections of 5 µm were cut, stained with 0.125% safranin-O (Merck, Darmstadt, Germany), and counterstained with 0.4% fast green (Sigma-Aldrich) and Weigert's hematoxylin (Clin-Tech, Glasgow, UK). Type I and II collagen deposition was visualized by immunohistochemistry. Sections were blocked in 0.3% (v/v) hydrogen peroxide, followed by antigen retrieval with 1 mg/mL pronase (Sigma-Aldrich) and 10 mg/mL hyaluronidase (Sigma-Aldrich), both for 30 minutes at 37ºC. Sections were blocked with 5% (w/v) BSA in PBS for one hour at room temperature and incubated with primary antibodies for type I collagen (EPR7785 (BioConnect, Huissen, The Netherlands), 1:400 in 5% PBS/BSA) and type II collagen (II-II6B3 (DHSB, Iowa City, IA, USA), 1:100 in 5% PBS/BSA) overnight at 4ºC. For type I collagen, rabbit IgG (DAKO, Glostrup, Denmark; X0903) was used as isotype control and for type II collagen, mouse IgG (DAKO X0931) was used. Next, type I collagen

sections were incubated with BrightVision Poly-HRP-Anti Rabbit (VWR, Radnor, PA, USA) and type II collagen sections were incubated with goat-anti-mouse IgG HRP-conjugated (DAKO, P0447; 1:100 in 5% PBS/BSA) for one hour at room temperature. Immunoreactivity was visualized using diaminobenzidine peroxidase substrate solution (DAB, Sigma-Aldrich). Mayer's hematoxylin (Klinipath, Olen, Belgium) was used as counterstaining.

Mitochondrial DNA

DNA was isolated from the cartilage biopsies of six patients, taken one year after treatment with IMPACT[70,115] and from corresponding MSCs. Using massive parallel sequencing, mitochondrial genome SNP analysis was performed including 42 amplicons on the mitochondrial genome. SNPs of biopsies were compared to donor MSC SNPs.

Statistical analyses

Data were analysed using GraphPad Prism version 8.3.0 (GraphPad Software, San Diego, CA, USA). Data are shown as mean ± standard deviation (SD) unless stated otherwise. P-values below 0.05 were considered statistically significant. ANOVA was used to test for significant differences in fluorescence between consecutive time-points (Fig. 1). As a follow-up, SIDAK correction for multiple comparisons was used. Two-way repeated measures ANOVA was used to test for differences between senescent and inflammatory conditions and control condition (Fig. 3), chondrocyte control and MitoCeption groups (Fig. 4), and MitoCeption groups and chondrocyte/coculture controls (Fig. 5), taking into account donor variability. Here, a Dunnet's post hoc test was performed to account for multiple comparisons.

Table 1. Primer sequences for quantitative real-time PCR. Forward (Fw) and reverse (Rv) primers. ACAN, *aggrecan*; BCL2, *B cell lymphoma 2;* COL2A1, *collagen type II alpha 1 chain*.

Gene name	Oligonucleotide sequence (5' to 3')	Annealing temperature (°C)	Product size (bp)
18S	Fw: GTAACCCGTTGAACCCCATT Rv: CCATCCAATCGGTAGTAGCG	57	151
ACAN	Fw: CAACTACCCGGCCATCC Rv: GATGGCTCTGTAATGGAACAC	56	160
BCL2	Fw: GCGTCTGTAGAGGCTTCTGG Rv: GCCACTTGCCACTTTTCCTG	60	293
COL2A1	Fw: AGGGCCAGGATGTCCGGCA Rv: GGGTCCCAGGTTCTCCATCT	57	195

SUPPLEMENTARY FIGURE

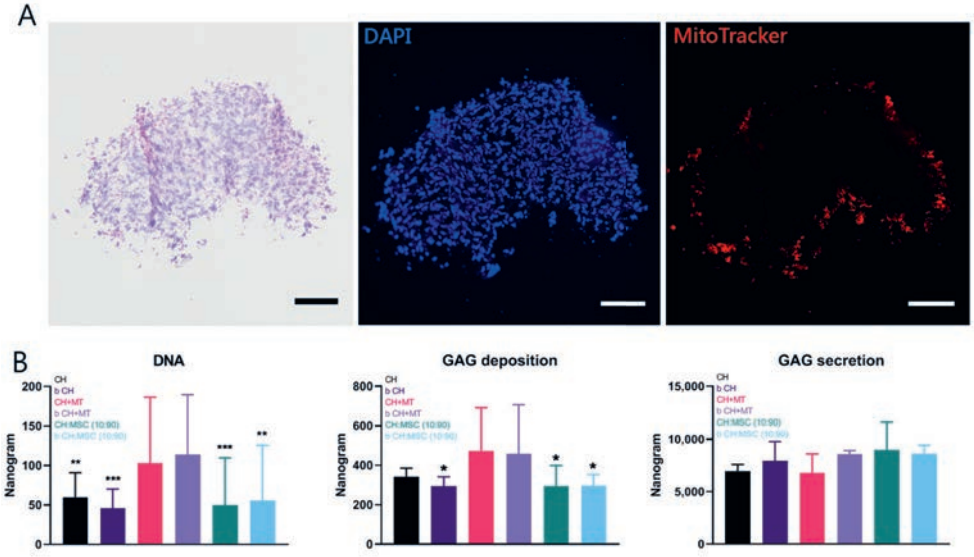

Figure S1. Chondrogenic effect of periodically repeating MitoCeption. A subset of chondrocyte (CH) pellets received additional doses of mitochondria (MT) at 7 and 14 days during chondropermissive culture. (A) Haematoxylin and eosin staining of re-MitoCepted pellet at 14 days (left panel), 4',6-diamidino-2-phenylindole (DAPI, middle panel), and MitoTracker (right panel) of the same pellet show detection of transferred mitochondria in the perimeter of the pellet. Scale bar = 100 µm. (B) Quantification of DNA and glycosaminoglycan (GAG) deposition and secretion of CH pellets after 28 days of chondropermissive culture in pellets. Group bCH+MT received additional doses of mitochondria (boost) at 7 and 14 days in culture. Additional control groups bCH and bCH:MSC (10:90) were also subjected to centrifugation at these time points. *p<0.05, **p<0.01, ***p<0.001.

Part II

Orthobiologics for cartilage repair and joint preservation

Chapter 6

Importance of timing of platelet lysate-supplementation in expanding or redifferentiating human chondrocytes for chondrogenesis

Margot Rikkers
Riccardo Levato
Jos Malda
Lucienne A. Vonk

Frontiers in Bioengeering and Biotechnology (2020)

ABSTRACT

Osteoarthritis (OA) in articular joints is a prevalent disease. With increasing life expectancy, the need for therapies other than knee replacement arises. The intrinsic repair capacity of cartilage is limited, therefore alternative strategies for cartilage regeneration are being explored. The purpose of this study is first to investigate the potential of platelet lysate (PL) as a xeno-free alternative in expansion of human OA chondrocytes for cell therapy, and second to assess the effects of PL on redifferentiation of expanded chondrocytes in 3D pellet cultures. Chondrocytes were isolated from human OA cartilage and subjected to PL in monolayer culture. Cell proliferation, morphology, and expression of chondrogenic genes were assessed. Next, PL-expanded chondrocytes were cultured in 3D cell pellets and cartilage matrix production was assessed after 28 days. In addition, the supplementation of PL to redifferentiation medium for the culture of expanded chondrocytes in 3D pellets was evaluated. Glycosaminoglycan (GAG) and collagen production were evaluated by quantitative biochemical analyses, as well as by (immuno)histochemistry. A dose-dependent effect of PL on chondrocyte proliferation was found, but expression of chondrogenic markers was decreased when compared to FBS-expanded cells. After 28 days of subsequent 3D pellet culture, GAG production was significantly higher in pellets consisting of chondrocytes expanded with PL compared to controls. However, when used to supplement redifferentiation medium for chondrocyte pellets, PL significantly decreased the production of GAGs and collagen. In conclusion, chondrocyte proliferation is stimulated by PL and cartilage production in subsequent 3D culture is maintained. Furthermore, the presences of PL during redifferentiation of 3D chondrocyte strongly inhibits GAG and collagen content. The data presented in the current study indicate that while the use of PL for expansion in cartilage cell therapies is possibly beneficial, intra-articular injection of the product in the treatment of OA might be questioned.

INTRODUCTION

Focal cartilage defects occur frequently in young and active patients and cause serious limitations on both joint function and the patient's mobility and quality of life[8]. As cartilage is an avascular tissue, spontaneous healing of the tissue is limited. In addition, with increasing life expectancy, the patient population with osteoarthritis (OA) is growing continuously[9].

A well-established surgical procedure to treat cartilage defects is autologous chondrocyte implantation (ACI). Long-term follow-up studies have demonstrated hyaline-like cartilage formation and satisfactory clinical outcome up to 20 years post-surgery[211,312]. Nevertheless, a major part of treated patients shows signs of fibrocartilage formation in the regenerated area[313]. As fibrocartilage is mechanically inferior to hyaline cartilage, it is unfit to fulfil the natural functions of hyaline cartilage and therefore more prone to degradation[314,315]. One of the causes of the fibrocartilage formation is dedifferentiation of chondrocytes during the *in vitro* expansion phase[213], which is a requirement to obtain a sufficient amount of cells for autologous cell transplantation. Maintaining chondrogenic redifferentiation capacity of chondrocytes during expansion is essential for improving the quality of the regenerated cartilage and thus potentially improves clinical outcome.

Platelet-rich plasma (PRP) is a blood product containing high growth factor levels that has been used for various applications over the past decades[316–319]. While variations in content and production methods exist, PRP consistently contains a high concentration of blood platelets. In orthopaedics, PRP and PRP-derivates like platelet lysate (PL) can be used for applications such as intra-articular injection for the treatment of knee osteoarthritis[79]. Moreover, as it is a rich source of growth factors, human PL also shows potential to be used in cell culture as a xeno-free alternative to bovine serum, possibly as a pooled off-the-shelf media supplement. In clinical cell therapy, PL is already used for the expansion of cells[70].

The effect of *in vitro* expansion in the presence of PL on the chondrogenic potential of chondrocytes remains unclear. While most studies agree that PRP and PL have a stimulatory effect on chondrocyte proliferation[80,81], contradictory results have been reported on anabolic effects of PRP-derivates on cartilage matrix formation by chondrocytes[80–82].

Therefore, the current study aims to investigate the effect of PL on the chondrogenic potential of chondrocytes. More specifically, this study looked into the effect of PL on chondrocytes during expansion and subsequent 3D culture, as well as effects on matrix production in 3D cultures while being exposed to PL.

METHOD

Experimental design and study outline

To test the hypothesis whether PL will maintain chondrogenic capacity of culture expanded

chondrocytes, chondrocyte monolayers were subjected to various concentrations of PL and compared to culture in fetal bovine serum (FBS). To subsequently assess cartilage-like matrix formation, chondrocytes were harvested and cultured in 3D cell pellets. The production of sulphated GAGs and collagens was measured biochemically, as well as histologically and by gene expression to compare between groups. In addition, the hypothesis that PL will improve redifferentiation of chondrocytes was tested using a similar 3D cell pellet culture system where PL was added fresh into the redifferentiation medium each medium change. Production of GAGs and collagens was assessed similarly as above.

Platelet lysate preparation and growth factor quantification

Platelet lysate was prepared from human blood collected in 3.2% sodium citrate-containing tubes. Blood was obtained through the Mini Donor Service, a blood donation facility for research purposes approved by the medical ethics committee of the University Medical Center Utrecht, The Netherlands. All donors have provided written informed consent, in accordance with the declaration of Helsinki. All donors were reported being healthy and free from antiplatelet drugs or non-steroid anti-inflammatory drugs. Platelet-rich plasma was prepared by centrifugation of whole blood at 130 *g* for 15 minutes, upon which pelleted erythrocytes were discarded and the plasma layer was concentrated by a second centrifugation cycle at 250 *g* for 15 minutes. Platelet count was measured using a CELL-42 DYN Emerald Hematology Analyzer (Abbott, US). Platelets were activated to release their growth factors by three freeze-thaw cycles, after which samples were centrifuged at 8000 *g* for 10 minutes and supernatant PL was stored at -20ºC until use. Pooled PL from at least three donors was used in each experiment. The concentrations of human growth factors PDGF-AB, TGF-β1, VEGF, and FGF-2 were quantitatively determined using enzyme-linked immunosorbent assays (ELISA) according to the manufacturer's instructions (DuoSet ELISA kits, R&D Systems, Minneapolis, Minnesota).

Donors and cell isolation

Osteoarthritic cartilage was obtained from redundant material from patients who had undergone total knee arthroplasty. The material is collected anonymously according to the Medical Ethics regulations of the University Medical Center Utrecht and approved by the local medical ethics committee (University Medical Center Utrecht). Cartilage was dissected from the underlying bone, rinsed in phosphate-buffered saline (PBS) and cut into 2 mm pieces. The pieces were digested in 0.2% (w/v) pronase (Sigma-Aldrich) in Dulbecco's modified Eagle's medium (DMEM, 31966; Gibco, The Netherlands) with 1% penicillin/streptomycin (100 U/mL, 100 mg/mL; Gibco) at 37ºC for two hours, followed by overnight digestion in 0.075% (w/v) collagenase type II (CLS-2, Worthington, Lakewood, NJ) in DMEM supplemented with 10% (v/v) heat-inactivated FBS (Biowest) and 1% penicillin/streptomycin under agitation. The cells were then filtered through a 70-µm cell strainer (Greiner Bio-One), washed, and counted. Chondrocytes were expanded using Expansion medium (DMEM supplemented with 1% penicillin/streptomycin and 10% FBS). Cells were cryopreserved in liquid nitrogen until

use.

Cell culture

Passage 1 chondrocytes (n = 6 donors, age 61 – 75, average 69 years) were seeded in 24-well plates at 1500 cells/cm^2 and cultured for 7 days in Expansion medium, where FBS was replaced with 0.01%, 0.1%, 1%, 2%, or 5% PL (all v/v). All media containing PL were supplemented with 3.3 U/mL heparin (Sigma-Aldrich) to prevent coagulation. Control conditions were cultured in Expansion medium with 10% FBS, with and without heparin. As a negative control, chondrocytes were expanded with serum-free medium (DMEM supplemented with 2% human serum albumin (HSA; Sanquin Blood Supply Foundation), 2% insulin-transferrin-selenium-ethanolamine (ITS-X; Gibco), 0.2 mM L-ascorbic acid 2-phosphate (ASAP; Sigma-Aldrich), and 1% penicillin/streptomycin). This did not lead to a sufficient number of chondrocytes to be used for further pellet culture and therefore this condition was not included in the following experiments. Photomicrographs can be found in Supplemental Figure S1.

For the 3D pellet culture, chondrocytes (n = 5 donors, age 55 – 75, average 65 years) were expanded in monolayers in Expansion medium with either 10% FBS, 1%, or 5% PL and heparin up to passage 2. Following expansion, pellets containing 2.5 x 10^5 cells were formed in ultra-low attachment 96-well round-bottom plate wells (Corning) by centrifugation at 300 *g* for 5 minutes. Pellets were cultured for 28 days in Redifferentiation medium (DMEM supplemented with 2% HSA, 2% ITS-X, 0.2 ASAP, and 1% penicillin/streptomycin).

For evaluating the effects of PL on chondrogenic redifferentiation, chondrocytes (n = 6 donors, age 54 – 84, average 65 years) were first expanded in Expansion medium with 10% FBS. Pellets were then cultured for 28 days in Redifferentiation medium either or not supplemented with 1% or 5% PL and heparin.

Immunofluorescent staining

Expanded monolayers were fixed after 7 days with 10% buffered formalin. Fixed monolayers were permeabilized using 0.2% Triton X-100 (Sigma-Aldrich) in PBS for 20 minutes, followed by incubation with phalloidin (TRITC-conjugated; 1/200 dilution in PBS; Sigma-Aldrich) for one hour. Nuclei were stained with 100 ng/mL 4',6-diamidino-2-phenylindole (DAPI; Sigma-Aldrich) in PBS for five minutes. Monolayers were imaged using an upright fluorescent microscope (BX51; Olympus).

Biochemical analysis of pellets

Pellets were harvested after 28 days to measure glycosaminoglycan (GAG), collagen, and DNA content. Samples were digested overnight in a papain digestion buffer (250 µg/mL papain; Sigma-Aldrich, 0.2 M NaH_2PO_4, 0.1M EDTA, 0.01M cysteine, pH 6) at 60ºC.

Sulphated GAG content was quantified using a dimethylmethylene blue (DMMB; pH 3) assay. The 525/595 nm absorbance ratio was measured using chondroitin-6-sulfate (Sigma-Aldrich) as a standard.

Total collagen content was calculated from the hydroxyproline content[320]. Papain digests were lyophilized and hydrolysed in 4 M NaOH (Sigma-Aldrich) in Milli-Q water overnight at 108ºC, after which samples were neutralized with 1.4 M citric acid (Sigma-Aldrich) in Milli-Q water. 50 mM freshly prepared Chloramin-T (Merck) in oxidation buffer was added and incubated for 20 minutes under agitation. Subsequently, 1.1 M freshly prepared dimethylaminobenzoaldehyde (Merck) in 25% (v/v) perchloric acid (Merck) in 2-propanol (Sigma-Aldrich) was added and incubated for 20 minutes at 60ºC. Samples were cooled and absorbance read at 570 nm using hydroxyproline (Merck) as a standard.

Total DNA content was quantified using a Quant-iT PicoGreen dsDNA assay (Invitrogen) according to the manufacturer's instructions. Fluorescence was measured at 485 nm excitation and 535 nm emission by a microplate fluorometer (Fluoroskan Ascent).

Histology

Pellets were processed for histology by fixation in 10% buffered formalin, dehydration through graded ethanol steps, clearing in xylene, and subsequent embedding in paraffin. 5 µm sections were cut and deparaffinised before staining. Sections were stained for GAGs with 0.125% safranin-O (Merck) counterstained with 0.4% fast green (Sigma-Aldrich) and Weigert's hematoxylin (Clin-Tech). Collagen deposition was evaluated by immunohistochemistry, with appropriate primary antibodies for type II collagen (II-II6B3; DHSB; 1:100 in PBS/BSA 5%) and type I collagen (EPR7785, BioConnect; 1:400 in PBS/BSA 5%). Samples were blocked using 0.3% H_2O_2, followed by antigen retrieval with pronase (1 mg/mL; Sigma-Aldrich) for 30 minutes at 37ºC and hyaluronidase (10 mg/mL; Sigma-Aldrich) for 30 minutes at 37ºC. Next, sections were blocked using bovine serum albumin (BSA; 5% (w/v) in PBS) for 30 minutes, followed by overnight incubation with the primary antibody at 4ºC. After washing, type II collagen sections were incubated with a goat-anti-mouse IgG HRP-conjugated (DAKO, P0447; 1:100 in PBS/BSA 5%) and type I collagen sections with Envision+ System-HRP anti-rabbit (DAKO, K4003), both for 1 hour at room temperature. Next, both stainings were developed using 3,3'-diaminobenzidine (DAB, Sigma-Aldrich). Sections were counterstained with Mayer's hematoxylin (Klinipath) and mounted in DPX mounting medium (Merck).

Real-time PCR

Total RNA was isolated from monolayers and pellets using TRIzol (Invitrogen) according to the manufacturer's instructions. Total RNA (200-500 ng) was reverse transcribed using the High-Capacity cDNA Reverse Transcription Kit (Applied Biosystems). Real-time polymerase chain reactions (PCRs) were performed using iTaq Universal SYBR Green Supermix (Bio-Rad)

in a LightCycler 96 (Roche Diagnostics) according to the manufacturer's instructions. The amplified PCR fragments extended over at least one exon border (except for 18S). Relative gene expression was calculated using 18S as a housekeeping gene. Primers (Invitrogen) used for real-time PCR are listed in Table 1.

Statistical analysis

Each experiment was performed with cells from six donors. For the monolayer expansion, three wells were used for each condition. For pellet cultures, three pellets were used for biochemical analyses, three for gene expression analysis, and two for histology. Data are expressed as mean ± standard deviation (SD). Data were statistically analysed using the GraphPad Prism 7.0 software package (GraphPad Software, USA). Normal distribution of the data was checked with a Shapiro-Wilk test ($p>0.05$) and homogeneity with a Levene's test. When the data was normally distributed and samples were homogeneous, a one-way analysis of variance (ANOVA) was performed with Dunnett's post-hoc test. When the data was non-normally distributed, a Kruskal-Wallis test was performed with Dunn's post-hoc. A value of $p<0.05$ was considered statistically significant.

Table 1. Primer sequences used for real-time PCR. Forward (Fw) and reverse (Rev) primers. COL2A1, *collagen type II alpha 1 chain*; ACAN, *aggrecan*; COL1A1, *collagen type I alpha 1 chain*; SOX9, *SRY-box transcription factor 9*; ACTA2, *actin alpha 2, smooth muscle*; NOTCH1, *notch receptor 1*; CDH2, *cadherin 2*.

Target gene	Oligonucleotide sequence (5' to 3')	Annealing temperature (°C)	Product size (bp)
18S	Fw: GTAACCCGTTGAACCCCATT Rv: CCATCCAATCGGTAGTAGCG	57	151
COL2A1	Fw: AGGGCCAGGATGTCCGGCA Rv: GGGTCCCAGGTTCTCCATCT	57	195
ACAN	Fw: CAACTACCCGGCCATCC Rv: GATGGCTCTGTAATGGAACAC	56	160
COL1A1	Fw: TCCAACGAGATCGAGATCC Rv: AAGCCGAATTCCTGGTCT	57	191
SOX9	Fw: CCCAACGCCATCTTCAAGG Rv: CTGCTCAGCTCGCCGATGT	60	242
ACTA2	Fw: ATGCCATCATGCGTCTGGAT Rv: ACGCTCAGCAGTAGTAACGA	60	101
NOTCH1	Fw: AAGCTGCATCCAGAGGCAAAC Rv: TGGCATACACACTCCGAGAACAC	60	172
CDH2	Fw: GCGTCTGTAGAGGCTTCTGG Rv: GCCACTTGCCACTTTTCCTG	60	293

RESULTS

Platelet lysate characterisation

To characterize the PL product, cell and platelet concentrations were counted and growth factor concentrations were determined in six batches of PL by ELISA (Table 2). Manually prepared PL was deprived from erythrocytes (19 ± 4 x 10^9/L) and leukocytes (0.3 ± 0.1 x 10^9/L), while platelet concentrations were maintained (458 ± 87 x 10^9/L). Furthermore, we found high concentrations of PDGF-AB (36142 ± 2518 pg/mL) and TGF-β1 (65379 ± 3889 pg/mL), while concentrations of FGF-2 (49 ± 10 pg/mL) and VEGF (150 ± 53 pg/mL) were less.

Table 2. Cell and growth factor concentrations in platelet lysate. Cell concentrations in PL were determined using a CELL-42 DYN Emerald Hematology Analyzer. Growth factor concentrations in PL were quantified by enzyme-linked immunosorbent assays (ELISA). All values are expressed as mean ± SEM (n = 6).

	Content (mean ± SEM)
Erythrocytes (10^9/L)	19 ± 4
Leukocytes (10^9/L)	0.3 ± 0.1
Platelets (10^9/L)	458 ± 87
PDGF-AB (pg/mL)	36142 ± 2518
TGF-β1 (pg/mL)	65379 ± 3889
FGF-2 (pg/mL)	49 ± 10
VEGF (pg/mL)	150 ± 53

Chondrocyte proliferation is stimulated in the presence of platelet lysate during expansion

Supplementation of Expansion medium with PL enhanced chondrocyte proliferation in a dose-dependent manner. Immunocytochemical staining of monolayers with phalloidin suggested an increase in cell amount after seven days of exposure to PL (Figure 1A). These findings were confirmed by quantification of DNA content (Figure 1C). Furthermore, changes in cellular morphology were observed. Chondrocytes cultured in the presence of PL exhibited an elongated shape opposed to a more spindle-like shape for cells in control expansion cultures (Figure 1B).

In contrast to the dose-dependent increase in DNA content, expression of chondrogenic genes coding for type II collagen (COL2A1), aggrecan (ACAN), and SRY-box transcription factor 9 (SOX9) decreased in a dose-dependent manner compared to the control group (Figure 2A-C). Expression of dedifferentiation marker type I collagen (COL1A1) was increased with increasing PL concentrations, while fibroblast marker actin alpha 2, smooth muscle (ACTA2) did not show significant changes (Figure 2E-F). Notch receptor 1 (NOTCH1) and cadherin 2 (CDH2), genes associated with stemness, were significantly increased when chondrocytes were exposed to culture medium containing 5% PL (Figure 2G-H).

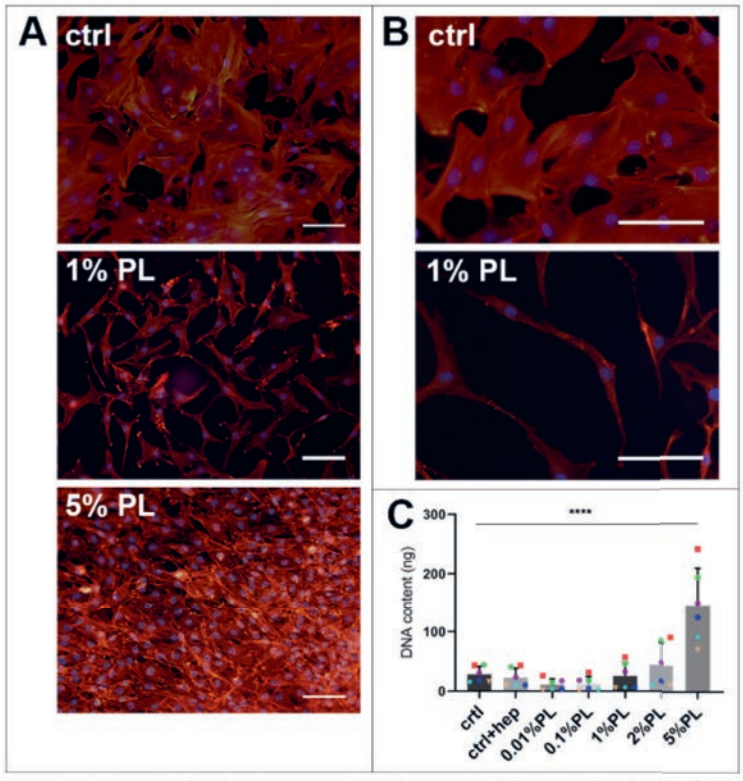

Figure 1. Effect of platelet lysate on chondrocyte proliferation. Phalloidin / DAPI staining of passage 1 chondrocytes after 7 days in monolayer culture in expansion medium supplemented with 10% FBS, 1% PL, and 5% PL (A). Higher magnification of the photomicrographs showing the morphology of chondrocytes expanded with 10% FBS and 1% PL (B). DNA content of the monolayer conditions (C). All scale bars = 100 µm. Data are presented as mean ± SD. *****p<0.0001.*

Chondrocytes expanded in the presence of platelet lysate maintain their redifferentiation potential

To compare chondrogenic potential of PL-expanded chondrocytes and chondrocytes expanded in the presence of FBS, 3D pellet cultures were performed to allow for neo-cartilage extracellular matrix (ECM) formation. Pellets consisting of PL-expanded chondrocytes were found to produce significantly more GAGs after 28 days when compared to the control conditions (Figure 3A). A slight qualitative increase in GAG production was seen across all chondrocyte donors used in this experiment (Figure 3B and Supplemental Figure S2). However, pellets consisting of 5% PL-expanded chondrocytes did not evidently show an improvement in GAG production on histology when compared to 1% PL-expanded chondrocyte pellets. Additionally, PL-expanded chondrocyte pellets did not present an increase in ACAN gene expression (Figure 3A).

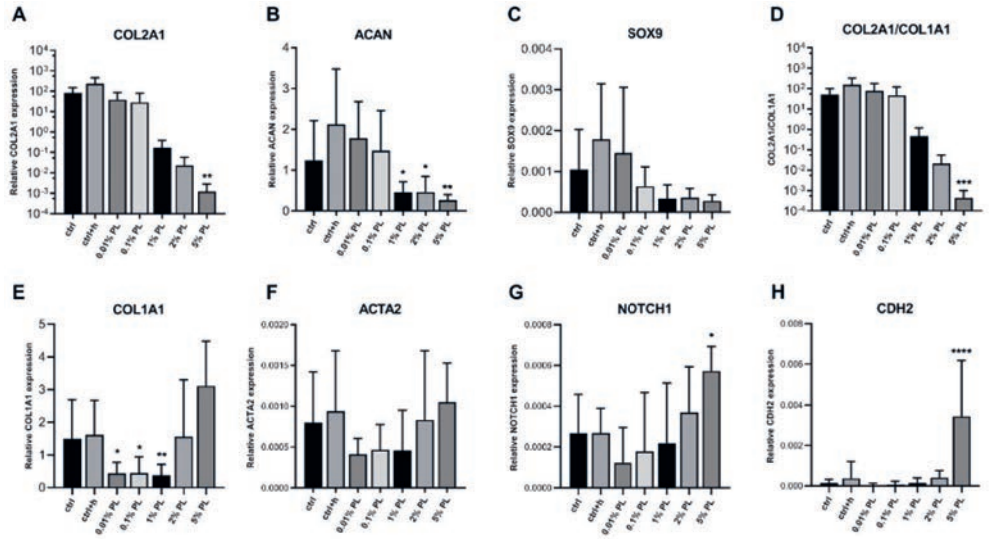

Figure 2. Gene expression of platelet lysate-expanded chondrocytes in monolayers. Gene expression type II collagen (COL2A1, A), aggrecan (ACAN, B), SRY-box transcription factor 9 (SOX9, C), ratio of type II / type I collagen (COL2A1/COL1A1, D), type I collagen (COL1A1, E), actin alpha 2, smooth muscle (ACTA2, F), notch receptor 1 (NOTCH1, G) and cadherin 2 (CDH2, H) by chondrocytes in monolayer culture in expansion medium supplemented with 10% FBS (ctrl), 10% FBS and 3.3 U/mL heparin (ctrl+h), 0.01% platelet lysate (PL), 0.1% PL, 1% PL, 2% PL, and 5% PL (all PL conditions contain heparin), normalized for the housekeeping gene 18S. Data are shown as mean ± SD. **p<0.05 **p<0.005 ***p<0.0005 ****p<0.0001*

To further investigate the chondrogenic potential of PL-expanded chondrocytes, production of collagen was determined. Quantitative biochemical analysis of total collagen content revealed an increase in 1% PL-expanded chondrocyte pellets compared to the control conditions. However, no differences were found on gene expression level of COL2A1 and COL1A1 (Figure 4A). Immunohistochemical staining revealed a slight increase in type II collagen production in two out of five donors. Overall, no evident increase of type II collagen was seen in experimental groups, in line with the mRNA data (Figure 4B and Supplemental Figure S2). Furthermore, staining for type I collagen was absent in all conditions (Figure 4B).

Taken together, these data suggest that the chondrogenic differentiation capacity is preserved in osteoarthritic chondrocytes upon expansion with PL.

Platelet lysate strongly inhibits matrix production during redifferentiation of chondrocytes

To test whether PL has a chondrogenic effect on osteoarthritic chondrocytes *in vitro*, chondrocytes were cultured in 3D pellets, after which PL was added to the Redifferentiation medium. For these experiments, all cells were expanded using conventional Expansion medium containing 10% FBS, instead of PL.

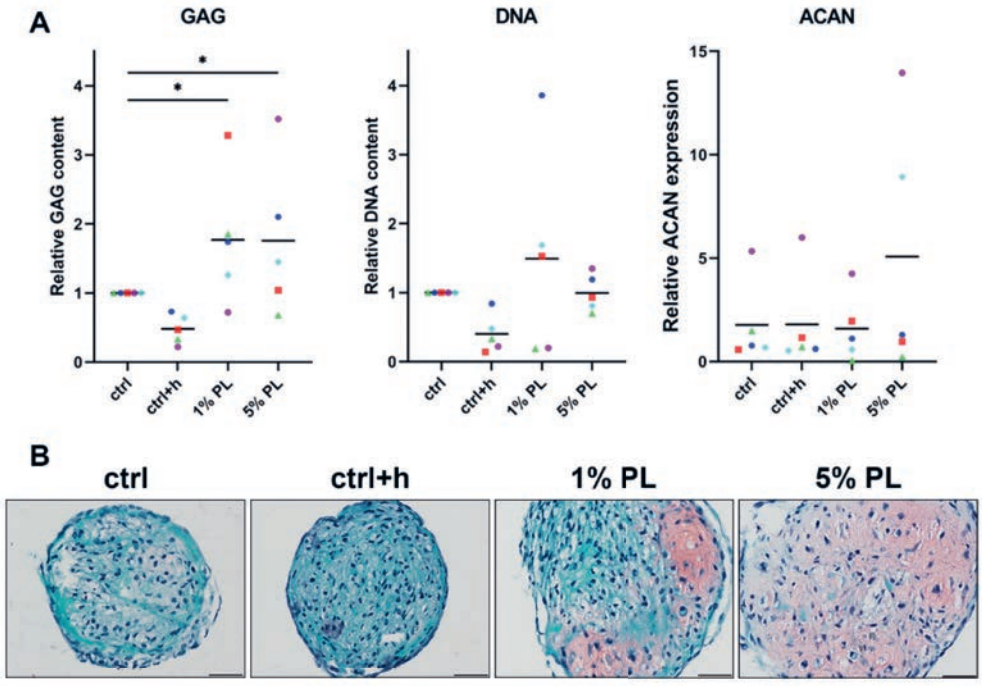

Figure 3. Glycosaminoglycan production of chondrocytes in 3D pellet cultures. Glycosaminoglycan (GAG) deposition and aggrecan (ACAN) gene expression in pellet cultures of passage 2 chondrocytes expanded in medium supplemented with 10% FBS (ctrl) with and without heparin (+h), 1- and 5% human platelet lysate (PL) cultured for 28 days in redifferentiation medium. (A) Biochemical analysis of GAGs and DNA content and relative expression of ACAN (normalized against the housekeeping gene 18S). Data are presented per donor and overall mean. *$p<0.05$. (B) Histological assessment by safranin-O. Scale bar = 100 µm.

Biochemical analyses revealed a significant decrease in GAG production in pellets differentiated in the presence of 1% or 5% PL. Further, cell numbers also decreased as confirmed by DNA quantification analysis. Quantitative analysis for total collagen did not reveal any difference between experimental and control conditions (Figure 5A). For donors with high chondrogenic capacity (Figure 5B, Donor 1) as well as donors having low chondrogenic capacity (Figure 5B, Donor 2), addition of PL during redifferentiation strongly inhibited GAG, type II and type I collagen formation. Histological stainings for GAGs and type II collagen of all donors used in this experiment are displayed in Supplemental Figure S3, confirming the uniform effect of PL on inhibition of cartilage matrix formation. Expression of chondrogenic marker COL2A1 significantly decreased in pellets cultured in the presence of 1% and 5% PL, while no difference was found in the expression of ACAN and COL1A1 (Figure 5C).

These data reveal a considerable inhibition of cartilage matrix production by PL in chondrocyte pellets, independent of chondrogenic capacity of the donor.

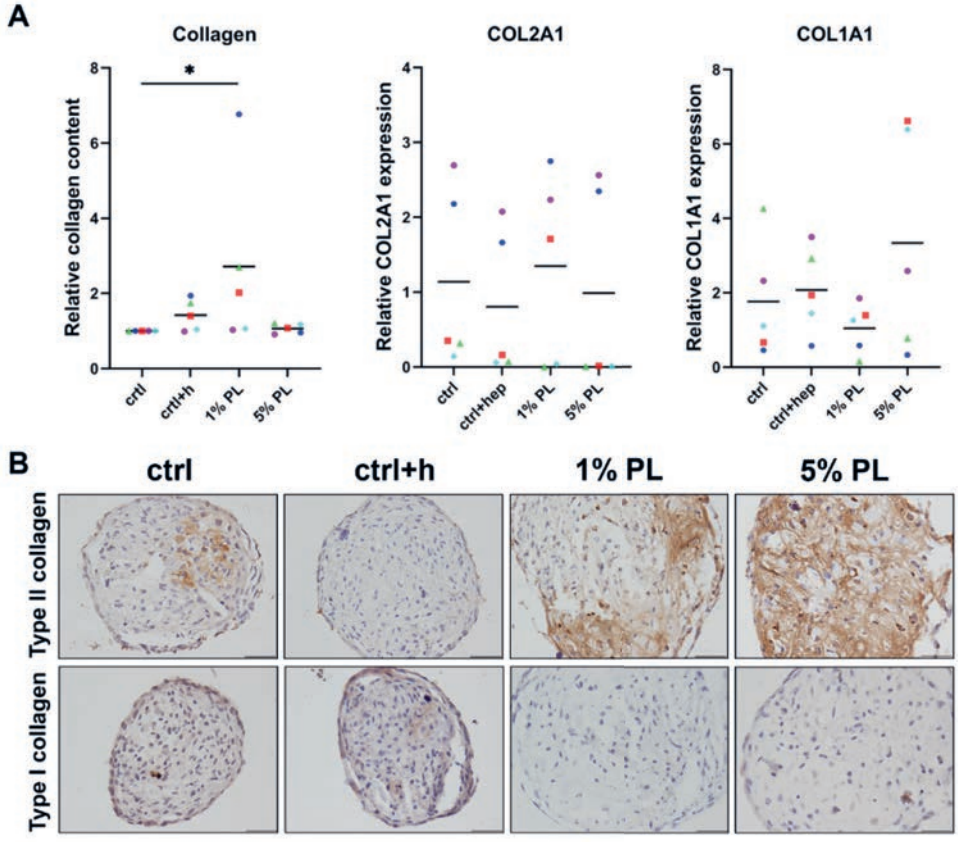

Figure 4. Collagen production of chondrocytes in 3D pellet cultures. Collagen deposition and type II (COL2A1) and I collagen (COL1A1) gene expression in pellet cultures of passage 2 chondrocytes expanded in medium supplemented with 10% FBS (ctrl) with and without heparin (+h), 1- and 5% human platelet lysate (PL) cultured for 28 days in redifferentiation medium. (A) Biochemical analysis of total collagen content and relative expression of COL2A1 and COL1A1 (normalized against the housekeeping gene 18S). Data are presented per donor and overall mean. *$p<0.05$. (B) Histological assessment by type II and I collagen immunohistochemistry. Scale bar = 100 µm.

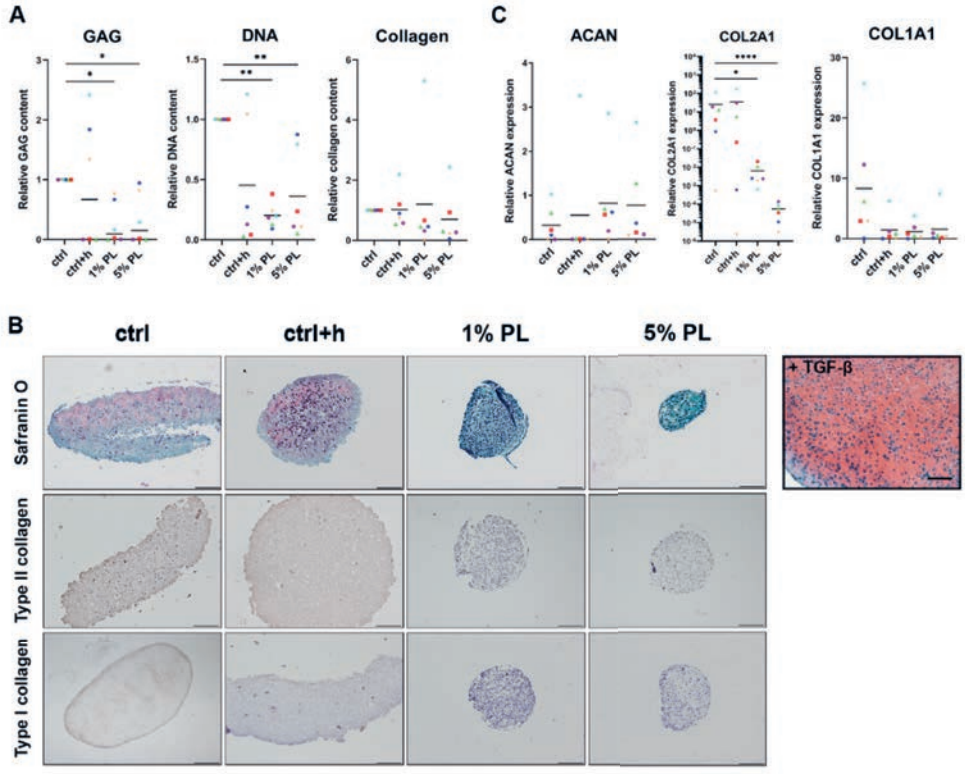

Figure 5. Matrix production and gene expression of chondrocytes in 3D pellet cultures supplemented with platelet lysate. (A) Glycosaminoglycan (GAG), collagen, and DNA content after 28 days of culture in redifferentiation medium (ctrl) with and without heparin (+h) and in the presence of 1- and 5% human platelet lysate (PL). (B) Cartilage production for one donor with high chondrogenic potential (Donor 1) and one donor with low chondrogenic potential (Donor 2) as determined by histological staining of GAGs by safranin-O, and immunohistochemical staining for type II and I collagen. Scale bar = 100 µm. (C) Relative gene expression of type II collagen (COL2A1), aggrecan (ACAN), and type I collagen (COL1A1), normalized for the housekeeping gene 18S. Data are presented per donor and overall mean. **p<0.05 **p<0.005 ****p<0.0001.*

DISCUSSION

The dedifferentiation of chondrocytes during expansion is a major challenge in the successful application of ACI as this causes the formation of fibrocartilage. PRP and PL provide a rich source of growth factors, which can provide an autologous supplement for *in vitro* cell culture. While some studies report on the stimulation of chondrocyte proliferation, chondrogenesis, and diminishing catabolic effects in the treatment of OA, consensus on this topic does not exist. Moreover, very limited work has been done on the capacity of PL to rescue cartilage matrix production in cultured OA chondrocytes.

The aim of this study was to elucidate the effects of PL on OA chondrocytes *in vitro*. We confirmed that PL exerts a stimulatory effect on the proliferation of chondrocytes. A dose-dependent effect on chondrocyte proliferation by PL was found, as determined by the quantification of DNA in the monolayer samples. This result is in line with previous studies where PL was compared to FBS-containing expansion medium[81,321–323]. In addition to the stimulation of proliferation, we found a decreased expression of chondrogenic marker genes COL2A1 and ACAN, and an increase of the dedifferentiation marker COL1A1 compared to FBS-expanded chondrocytes. Taken together, this suggests an increased dedifferentiation of chondrocytes during expansion in PL-supplemented medium. Interestingly, a recent study reports on increased expression of chondrogenic markers and decreased expression of dedifferentiation markers in MSCs and cartilage progenitor cells expanded using different concentrations of PL and the same effect was to a lesser extent visible in chondrocytes[324]. Additionally, we found that chondrocytes expanded with the highest concentration of PL exhibited an increased expression of CDH2 and NOTCH1. CDH2 has been described to be involved in embryonic limb chondrogenesis and is associated with (cartilage) stemness[225]. Specific expression of NOTCH1 has been described at the developing cartilage surface of mouse knee joints[325] and in cells with enhanced clonality at the articular surface of bovine cartilage[15]. Therefore, we suggest that the specific combination and concentration of growth factors in PL as used in the current study drives chondrocytes into a dedifferentiated state with increased chondroprogenitor-like potential.

Next, our data demonstrated that chondrocytes that were expanded with PL maintain their chondrogenic differentiation capacities when subsequently cultured in a 3D environment. The deposition of GAGs was slightly increased in PL-expanded chondrocyte pellets, while type II collagen deposition was unaltered. Moreover, type I collagen production was absent in both FBS-expanded chondrocyte pellets as well as in PL-expanded chondrocyte pellets. This supports our suggestion that chondrocytes expanded in PL do dedifferentiate but maintain progenitor-like chondrogenic potential. Several previous studies also reported on an increase[322,323] or maintenance[81] of chondrogenic potential of chondrocytes after expansion in PL, while another study observed opposite outcomes[326]. This makes it hard to draw a conclusive statement on the effects of PL on chondrogenic capacities of chondrocytes is still lacking.

The effect of intra-articular PRP injections in the treatment of OA has been evaluated in various randomized controlled trials[50,316,327–331]. Since some of these studies found a positive effect on pain and function[50,328,329], we hypothesized that PL would have a stimulatory effect on chondrogenesis in pellets consisting of OA chondrocytes that are expanded in FBS-supplemented expansion medium. Interestingly, our results showed that culture in the presence of PL remarkably inhibited GAG deposition in the pellets when compared to control conditions and complete absence of type II collagen production was observed. Furthermore, real-time PCR data revealed a strong decrease in COL2A1 expression, indicating a dedifferentiation of the chondrocyte phenotype in presence of PL, even in 3D. To the best of our knowledge, no other studies have been performed in which the direct effect of PL on OA chondrocytes in 3D pellet culture is assessed. One paper reported on the effect of PL supplementation to the differentiation medium during only the first three days of chondrocyte pellet culture. However, these chondrocytes were also expanded using PL. These pellets performed significantly worse in cartilage matrix production when compared to pellets cultured in regular differentiation medium[323]. Outcomes of studies focussing on other 3D culture models are inconsistent. When chondrocytes were cultured in alginate beads and subjected to platelet supernatant, a product similar to PL, a distinct decrease in chondrogenic genes was measured when compared to control conditions lacking platelet supernatant[321]. Others reported on induction of chondrogenesis when adding PRP or PL to a 3D culture system. When PL was incorporated in a dextran-containing hydrogel, it was able to enhance proliferation, and simultaneously, induce chondrogenesis, both for MSCs and for cocultures of MSCs and chondrocytes[332]. The different findings might be explained by differences in the growth factor concentrations and ratios between the various growth factors.

The concentrated growth factors present in PL stimulate chondrocytes to proliferate. It is known that FGF and PDGF stimulate proliferation[333,334], while TGF-β inhibits proliferation and mediates initiation of differentiation in chondrocytes[333]. Furthermore, the cocktail of growth factors in the current study seems to maintain the cells in a progenitor-like state during expansion, demonstrated by enhanced expression of NOTCH1 and CDH2. These markers are involved in pathways that have been described to be of importance in chondrocyte proliferation during development. Proliferation and regeneration of chondrocytes *in vitro* are two distinct processes that do not go hand in hand. Upon expansion, chondrocytes present a dedifferentiated phenotype, with increased type I collagen gene expression[335]. However, the cells can recover their phenotype and redifferentiate when brought back into 3D culture[336]. Further in-depth characterization of PL-treated chondrocytes will be necessary to elucidate their phenotypical change in relation to chondroprogenitor cells and MSCs.

The same cocktail of growth factors seems to be ineffective in stimulating chondrocytes to produce cartilage matrix in a 3D pellet environment. Possibly the high concentrations of FGF in PRP may interfere with the redifferentiation process by suppressing cellular senescence

and inhibition of the TGF-β pathway[337]. Human platelets are a rich source of TGF-β and PRP can contain up to 100-fold increased concentrations of TGF-β[338,339]. Accordingly, this study also found high concentrations of TGF-β in the used PL. It is known that overstimulation by TGF-β inhibits FGF- and Wnt-mediated proliferation of chondrocytes[340]. Besides that, it is likely that high concentrations of TGF-β play a role in *in vitro* fibrocartilage formation by chondrocytes[341]. Future studies looking into molecular mechanisms causing chondrocytes to dedifferentiate upon PL-exposure can shed more light on the observations in the study presented here.

The variations in outcomes between this study and previous research can partly be explained by the numerous methods available to prepare PRP. Firstly, there is a great variation in platelet and growth factor concentration that is used in PRP, caused by both donor variability, as well as by the variety of preparation methods[339,342,343]. Secondly, it remains unclear whether the concentration of growth factors in PRP is related to the concentration of platelets[338,339]. Thirdly, there is a difference between leukocyte-rich (LR-) and leukocyte-poor (LP-)PRP. It is generally assumed that leukocytes and immune modulating cytokines present in PRP contribute to a pro-inflammatory environment and is undesirable in the treatment of OA[344–346]. Nonetheless, direct comparison in a clinical study between LP- and LR-PRP injections has not given conclusive outcomes which type of PRP is most effective in the treatment of OA[347]. However, an *ex vivo* study examining the effects of different PRP preparations on cartilage and meniscal explants suggested a pro-inflammatory effect of LR-PRP preparations[348]. Clinical studies mainly use LP-PRP for injection, containing either similar numbers of leukocytes compared to whole blood[50,327], reduced amounts[328–330], or are deprived of leukocytes[331]. There is a need for additional clinical studies to make clear which type of PRP is effective in the treatment of OA, and for PRP and PL preparation methods to be aligned between different laboratories, clinics, and hospitals[349]. Objective measurements of cartilage quality after PRP treatment are not available to date. Comprehensive studies including objective analysis of cartilage quality after PRP injection are needed in addition to current analysis using mainly patient questionnaire outcomes. Furthermore, there are some limitations to *in vitro* models to consider. Laboratory models are usually limited to a single tissue or cell type, whereas PRP *in vivo* affects the whole joint environment[79]. Moreover, positive clinical outcomes may be explained by mechanisms other than a direct effect of PL on the cells in the cartilage. It has been previously shown that PRP can act anti-inflammatory both *in vitro* as well as *in vivo*[350,351]. The inflammatory mediators in PRP and PL might create an improvement in the intra-articular environment, upon which cartilage matrix production by the resident chondrocytes is stimulated. An *in vitro* model as presented in the current study is unable to take these additional factors into account. More extensive studies using multiple cell types or tissues, or animal models are necessary to answer this question. Finally, *in vitro* culture does not mimic growth factor clearance, unless a bioreactor system is used. These factors should be taken into account when comparing *in vitro* results to clinical outcomes.

Conclusion

The current study provides insights into the effects of PL on chondrogenic differentiation of human chondrocytes and its potential to be used for two different clinical applications. We propose that platelet lysate has potential to be used in the expansion of chondrocytes for application in cartilage defects. Nonetheless, PL exerts a strong inhibitory effect on chondrogenesis *in vitro*, suggesting caution for its utilization in intra-articular injections.

SUPPLEMENTAL FIGURES

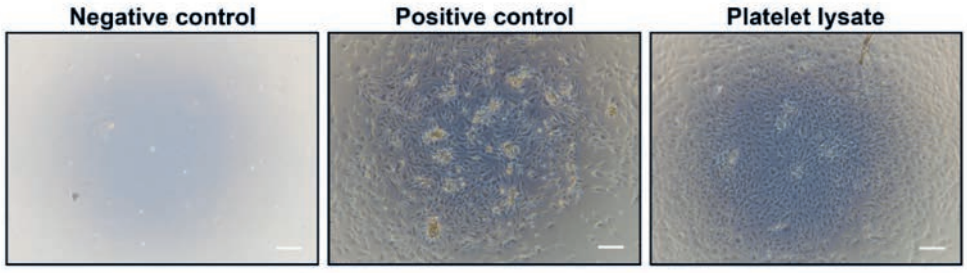

Figure S1. Photomicrographs of control conditions of chondrocyte expansion. Chondrocytes expanded for 7 days with serum-free medium (negative control), medium containing 10% FBS (positive control), and experimental medium containing 5% platelet lysate (platelet lysate). Scale bars are 200 µm.

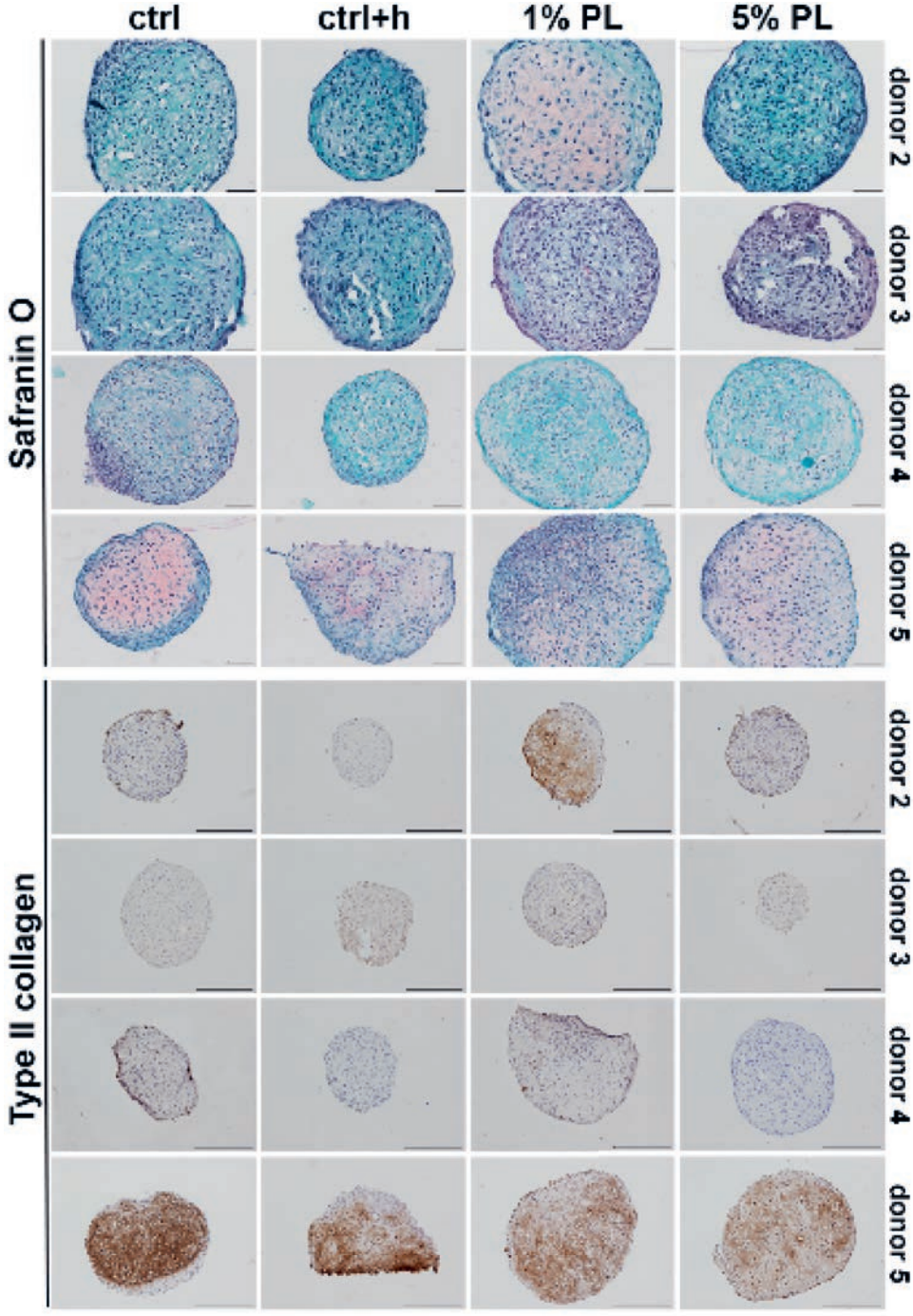

Figure S2. Histological evaluation of pellets consisting of platelet lysate-expanded chondrocytes. Safranin O staining (top panel) visualizing glycosaminoglycans (GAG) and type II collagen deposition visualized by immunohistochemistry (bottom panel) of all donors used in the experiment. Scale bars in the top panel are 100 µm. Scale bars in the bottom panel are 400 µm.

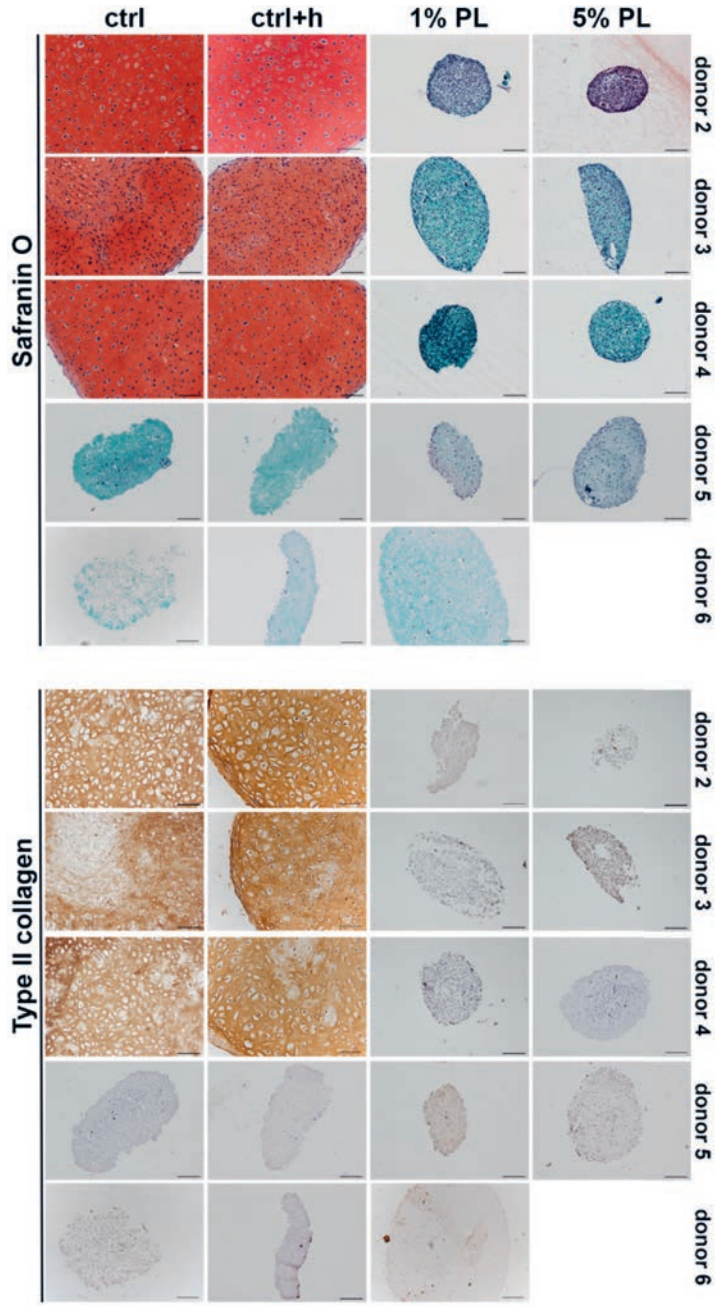

Figure S3. Histological evaluation of platelet lysate-treated pellets. Safranin O staining (top panel) visualizing glycosaminoglycans (GAG) and type II collagen deposition visualized by immunohistochemistry (bottom panel) of all donors used in the experiment. All scale bars are 100 µm.

Chapter 7

Platelet-Rich Plasma Does not Inhibit Inflammation or Promote Regeneration in Human Osteoarthritic Chondrocytes In Vitro Despite Increased Proliferation

Margot Rikkers
Koen Dijkstra
Bastiaan F. Terhaard
Jon Admiraal
Riccardo Levato
Jos Malda
Lucienne A. Vonk

CARTILAGE (2021)

ABSTRACT

Objective

The aims of the study were to assess the anti-inflammatory properties of platelet-rich plasma (PRP) and investigate its regenerative potential in osteoarthritic (OA) human chondrocytes. We hypothesised that PRP can modulate the inflammatory response and stimulate cartilage regeneration.

Design

Primary human chondrocytes from OA knees were treated with manually prepared PRP, after which cell migration and proliferation were assessed. Next, TNF-α-stimulated chondrocytes were treated with a range of concentrations of PRP. Expression of genes involved in inflammation and chondrogenesis was determined by real-time PCR. In addition, chondrocytes were cultured in PRP gels and fibrin gels consisting of increasing concentrations of PRP. The production of cartilage extracellular matrix (ECM) was assessed. Deposition and release of glycosaminoglycans (GAG) and collagen was quantitatively determined and visualized by (immuno)histochemistry. Proliferation was assessed by quantitative measurement of DNA.

Results

Both migration nor the inflammatory response were altered by PRP, while proliferation was stimulated. Expression of chondrogenic markers COL2A1 and ACAN was downregulated by PRP, independent of PRP concentration. Chondrocytes cultured in PRP gel for 28 days proliferated significantly more when compared to chondrocytes cultured in fibrin gels. This effect was dose-dependent. Significantly less GAGs and collagen was produced by chondrocytes cultured in PRP gels when compared to fibrin gels. This was qualitatively confirmed by histology.

Conclusion

Platelet-rich plasma stimulated chondrocyte proliferation, but not migration. Also, production of cartilage ECM was strongly downregulated by PRP. Furthermore, PRP did not act anti-inflammatory on chondrocytes in an *in vitro* inflammation model.

INTRODUCTION

Platelet-rich plasma (PRP) is a biological, blood-derived product. It can be produced from a patient's own blood for autologous applications. Because of the high concentration of blood platelets, PRP contains a rich cocktail of growth factors[352]. Its applications in the field of orthopaedics have been described to a large extent, both in basic and clinical research. In clinical practice, PRP is mostly administered by intra-articular injection for the treatment of osteoarthritis (OA) in various joints[331,353], tendinopathies[317], meniscal damage[318], or osteochondral lesions[319]. In general, clinical studies report on (short term) positive clinical outcomes, characterized by a decrease in pain and improvement of function[354,355]. The effects of PRP are generally attributed to the cocktail of growth factors, combined with anti-inflammatory mediators present in the PRP. Injection of PRP in OA could potentially stimulate regeneration of the cartilage by suppressing the pro-inflammatory environment in the joint and stimulate an anabolic state. Overall, clinical results are presented in a range from highly positive towards highly negative or even considering the presence of a substantial placebo effect[356–359]. In basic science, *in vitro* studies report on enhancement of chondrogenic differentiation of mesenchymal stromal cells (MSCs)[360], and matrix production by chondrocytes stimulated with PRP[81]. In addition, enhancement of proliferation by PRP has been described for a range of intra-articular cell types, such as meniscal cells[361], articular chondrocytes[362–364], tenocytes[365], and osteoblasts[366].

Moreover, PRP is ideally suited for making a gel rich in platelets by mimicking physiological blood coagulation. By activation of the fibrinogen in PRP by either centrifugation of non-anticoagulated PRP or addition of thrombin and calcium to anticoagulated PRP, a 3D platelet-rich fibrin clot can be created. This allows encapsulation of primary chondrocytes, comparable to what can be done with commercially available fibrin glue. This system has the potential to be used for tissue engineering applications, or as a biomaterial to, for example, treat focal cartilage defects in a clinical setting[115,367].

Considering the controversy around the use of PRP and variety in reported clinical results, the objective of this study was to study several potential working mechanisms of PRP with primary OA chondrocytes *in vitro* in a controlled setting. We hypothesized that PRP would have an anti-inflammatory, and migration-stimulating effect on OA chondrocytes and would be effective in stimulating matrix synthesis by OA chondrocytes in a 3D PRP gel environment.

METHODS

Platelet-Rich Plasma Preparation and Characterization

Blood was obtained from healthy donors through the Mini Donor Service of the University Medical Center Utrecht approved by the medical ethics committee. All donors provided written informed consent in accordance with the declaration of Helsinki and were healthy, and free from antiplatelet and non-steroid anti-inflammatory drugs. Blood was collected in sterile 9 mL-tubes containing 1 mL 3.2% (w/v) sodium citrate. To make PRP, the blood was

centrifuged at 130 *g* for 15 min, after which the plasma layer was transferred to a new tube. The plasma was then centrifuged at 250 *g* for 15 min and pelleted platelets were resuspended in one third of the supernatant plasma. Platelet count was measured using a CELL-DYN Emerald Hematology Analyzer (Abbott, US) (n = 9). For further experiments, platelet count was standardized at 400 x 10^9/L by dilution with phosphate buffered saline free from Ca^{2+} and Mg^{2+} (PBS0). The concentrations of TGF-β1, PDGF-AB, bFGF, and VEGF were determined using an enzyme-linked immunosorbent assay (ELISA) according to the manufacturer's instructions (all Duoset ELISA kit, R&D Systems) (n = 5).

Chondrocyte Isolation

Human osteoarthritic articular cartilage was obtained from redundant material after total knee arthroplasty surgery. The anonymous collection of this material is approved by the local medical ethic committee (University Medical Center Utrecht)[221,266]. Cartilage was separated from the bone, washed with PBS0, and cut into 2mm pieces using a scalpel. To minimize intra- and inter-donor variability, all cartilage was pooled per donor for cell isolation. Chondrocytes were extracted by exposing the cartilage pieces to 0.15% (w/v) collagenase II (CLS-2, Worthington, Lakewood, NJ) in Dulbecco's Modified Eagle Medium (DMEM, Gibco, Life Technologies) supplemented with 10% (v/v) fetal bovine serum (FBS, Biowest), and penicillin and streptomycin (100 U/mL and 100 µg/mL; 1%) overnight at 37ºC on a moving platform. Isolated cells were expanded at 37ºC and 5% CO_2 using chondrocyte expansion medium, consisting of DMEM supplemented with 10% FBS and 1% penicillin/streptomycin. Chondrocytes were used at passage 2, cells from different donors were kept separate throughout the experiments.

Proliferation and Migration Assay

Proliferation and migration of chondrocytes upon addition of PRP into the culture medium was assessed using a micro-wound assay[368–370]. Chondrocytes (n = 2, age range 48 - 64) were seeded in monolayers in 24-well plates using expansion medium. Upon confluence, a micro-wound was created across each well using a sterile 200 µL pipette tip. Monolayers were washed using PBS0, and treated with redifferentiation medium (DMEM supplemented with 2% [v/v] human serum albumin [HSA; Sanquin Blood Supply Foundation], 2% insulin-transferrin selenium [ITS]-X [Gibco], 0.2 mM L-ascorbic acid 2-phosphate [ASAP; Sigma-Aldrich], 100 U/mL penicillin, and 100 µg/mL streptomycin) with respectively 0-, 2-, 5-, 10-, or 20% (v/v) PRP. All PRP-containing media were supplemented with 3.3 U/mL heparin (Sigma-Aldrich). All medium was supplemented with 10µM 5-ethylnyl-2'-deoxyuridine (EdU; Click-iT™ EdU Alexa Fluor® 488 Imaging Kit; Invitrogen). After 48 hours of incubation at 37ºC and 5% CO_2, monolayers were washed with PBS0 and EdU was detected according to the manufacturer's instructions. Nuclei were counterstained with Hoechst. Photographs were taken using an inverted fluorescent microscope (IX53; Olympus). Total migrated cells and proliferated cells in the micro-wound area were quantified using ImageJ software via color thresholding and the 'analyze particles' function.

In Vitro Inflammation Assay

Chondrocytes (n = 6, age range = 48 – 74) were seeded in monolayers at 100,000 cells/cm^2 in chondrocyte expansion medium. After 24 hours of pre-incubation, monolayers were treated with 10 ng/mL recombinant human Tumor Necrosis Factor alpha (TNF-α, R&D Systems) and redifferentiation medium with respectively 0-, 2-, 5-, 10-, and 20% (v/v) PRP. Cells were incubated for 48 hours at 37ºC and 5% CO_2 before gene expression analysis.

Regeneration Assay: Gels with Variable PRP Concentration

Cells (n = 2 donors, age range = 53 – 79) were cultured in fibrin gels containing increasing concentrations of PRP. For this purpose, PRP was mixed with 1:15 in PBS0 diluted fibrinogen component (Baxter) in which cells were resuspended. The commercial fibrinogen was diluted in order to match the concentrations within the full range of conditions[371]. Gels were made by injecting 50 µL of the mixture into a 96-well plate well and adding 50 µL 1:50 in PBS0 diluted thrombin component (Baxter) and incubated for 15 minutes at 37ºC. This resulted in gels containing 0.25 x 10^6 cells per construct, with respectively 20-, 40-, 50-, 60-, and 80% PRP. Gels were cultured in 24-well plates for 28 days in redifferentiation medium. Medium was changed twice per week and saved for biochemical analysis.

Regeneration Assay: PRP vs Fibrin Gels

Chondrocytes were equally divided over the PRP and fibrin gel group. Fibrin gels were made as stated in the previous section by mixing 50 µL of each diluted component. Platelet-rich plasma gels were made by pipetting 60 µL PRP into a 96-well plate well, adding 20 µL $CaCl_2$ (500 mM in 0.9% NaCl) and 20 µL 1:50 in PBS0 diluted thrombin solution (Baxter), and incubation for 15 minutes at 37ºC. This resulted in gels containing 0.25 x 10^6 chondrocytes (n = 3 donors, age range = 56 - 79). Gels were cultured in 24-well plates for 28 days using redifferentiation medium. Medium was changed twice per week and all medium was stored for biochemical analysis. Control fibrin gels were made by combining 50 µL 1:15 diluted fibrinogen component and 50 µL 1:15 diluted thrombin component (Baxter).

Real-Time PCR

Total RNA was isolated from monolayers and gels using TRIzol (Invitrogen) according to the manufacturer's instruction. Total RNA (200-500 ng) was reverse-transcribed using the High-Capacity cDNA Reverse Transcription Kit (Applied Biosystems). Real-time polymerase chain reactions (PCRs) were performed in a LightCycler 96 (Roche Diagnostics) using iTaq Universal SYBR Green Supermix (Bio-Rad) according to the manufacturer's instructions. Quantification was performed relative to the levels of the housekeeping gene 18S. The primer sequences are listed in Table S1.

Biochemical Analysis

Gels were digested in a papain digestion buffer (250 µg/mL papain; Sigma-Aldrich, 0.2 M

NaH_2PO_4, 0.1 M EDTA, 0.01 M cysteine, pH 6) at 60ºC overnight. Glycosaminoglycan (GAG) content was measured using a dimethylmethylene blue (DMMB; pH 3) assay with chondroitin-6-sulfate (Sigma-Aldrich) as a standard. Absorbance ratio of 525/595 nm was measured using a spectrophotometer. DNA content in the digests was quantified using a Quant-iT PicoGreen dsDNA assay (Invitrogen) according to the manufacturer's instruction. Collagen content was determined by measuring the hydroxyproline content[320]. Digested samples were lyophilized and hydrolysed in 4 M NaOH (Sigma-Aldrich) in Milli-Q water at 108ºC overnight. The next day, samples were neutralized using 1.4 M citric acid (Sigma-Aldrich) in Milli-Q water, after which 50 mM freshly prepared Chloramin-T (Merck) in oxidation buffer was added. Samples were incubated under agitation for 20 minutes, after which 1.1M freshly prepared dimethylaminobenzoaldehyde (Merck) in 25% (w/v) perchloric acid (Merck) in 2-propanol (Sigma-Aldrich) was added. After incubation for 20 minutes at 60ºC, samples were cooled and absorbance at 570 nm was measured using hydroxyproline (Merck) as a standard.

Histological Analysis

Gels were fixed using 3.7% formalin, dehydrated through graded alcohol steps, immersed in xylene, and embedded in paraffin. Sections of 5 µm were cut and deparaffinised and rehydrated before staining. Proteoglycans were stained using 0.125% (w/v) safranin-O (Merck; counterstained with 0.4% fast green [Sigma-Aldrich] and Weigert's hematoxylin [Clin-Tech]). Type I and II collagen deposition was visualized by immunohistochemistry. Sections were blocked with 0.3% H_2O_2, followed by antigen retrieval with pronase (1 mg/mL; Sigma-Aldrich) for 30 minutes at 37ºC and hyaluronidase (10 mg/mL; Sigma-Aldrich) for 30 minutes at 37ºC. Sections were blocked using bovine serum albumin (BSA; 5% [w/v] in PBS) for 30 minutes, followed by overnight incubation at 4ºC with the primary antibody for either type I collagen (EPR7785, BioConnect; 1:400 in PBS/BSA 5%) or type II collagen (II-II6B3; DHSB, 1:100 in PBS/BSA 5%). Sections were washed, then incubated with an HRP-conjugated anti-rabbit or anti-mouse secondary antibody for 1 hour at room temperature, after which the staining was developed using 3,3'-diaminobenzidine (DAB, Sigma-Aldrich). Sections were counterstained using Mayer's hematoxylin (Klinipath).

Statistical Analysis

Data were analyzed using the GraphPad Prism 7.0 software package (GraphPad Software, US). Comparisons between groups were performed by paired and unpaired two-sided student's t tests and one-way analysis of variance (ANOVA) with a Tukey post-hoc test. A P-value of < 0.05 was considered statistically significant.

RESULTS

Manually Prepared Platelet-Rich Plasma Is Depleted From Leukocytes and Rich in Growth Factors

Platelet-rich plasma was prepared from citrated blood of nine donors. Cell and platelet counts were measured and revealed a significant decrease in the number of leukocytes (0.3 ± 0.1 x 10^9/L vs. 5.5 ± 1.4 x 10^9/L, p<0.001) and erythrocytes (0.02 ± 0.01 x 10^{12}/L vs. 4.0 ± 0.4 x 10^{12}/L, p<0.001) in all PRP samples compared to whole blood samples of the same donors. Platelet count was significantly increased after PRP preparation (458 ± 245 x 10^9/L vs 207 ± 74 x 10^9/L, p=0.006). Increase in platelet count varied from 1.0 to 3.0-fold (Table 1). Quantification of growth factors by ELISA revealed manually prepared PRP contains high amounts of TGFβ1 (60234 ± 23499 pg/mL) and PDGF-AB (21163 ± 6399 pg/mL) and lower concentrations of bFGF (20.4 ± 8.8 pg/mL) and VEGF (83.5 ± 44.1 pg/mL) (Figure 1).

Table 1. Cell Count in Manually Prepared Platelet-Rich Plasma. Leukocyte, erythrocyte, and platelet concentrations in whole blood and platelet-rich plasma (PRP) after the double centrifugation protocol. Data are shown as mean ± SD.

	Whole blood	PRP	P value
Leukocytes (x 10^9/L)	5.5 (± 1.4)	0.3 (± 0.1)	<0.001
Erythrocytes (x 10^{12}/L)	4.0 (± 0.4)	0.02 (± 0.01)	<0.001
Platelets (x 10^9/L)	207 (± 74)	458 (± 245)	0.006

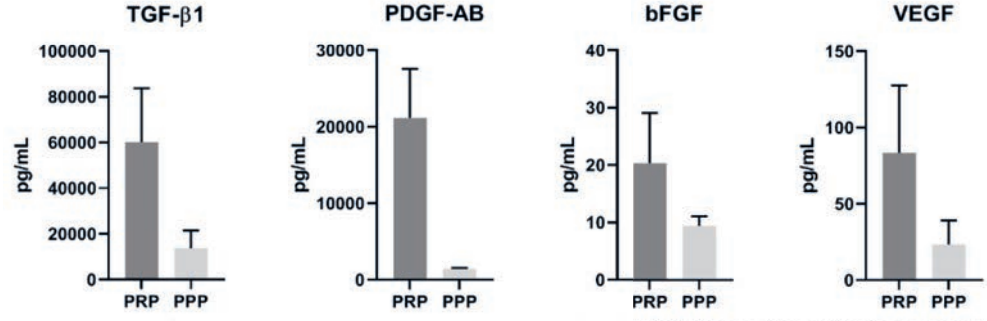

Figure 1. Growth factor Concentrations in Manually Prepared Platelet-Rich Plasma. Quantification of growth factors TGF-β1, PDGF-AB, bFGF, and VEGF in Platelet-Rich Plasma (PRP) and Platelet-Poor Plasma (PPP) of healthy human donors (n = 5), measured by enzyme-linked immunosorbent assay (ELISA).

Platelet-Rich Plasma Stimulates Chondrocyte Proliferation, but not Migration

Migration of chondrocytes into a micro-wound created in a monolayer using different concentrations of PRP was compared after 48 hours (Figure 2A-C). Quantification of cells migrated into the micro-wound area revealed no differences in groups containing PRP versus control group. On the contrary, proliferation of chondrocytes was significantly increased when micro-wounds were treated with 20% PRP (Figure 2D).

Platelet-Rich Plasma does not Inhibit an Inflammatory Response in Chondrocytes

Platelet-rich plasma was not able to inhibit the inflammatory response of chondrocytes after stimulation with TNF-α. Expression of OA-associated inflammation markers cyclooxygenase-

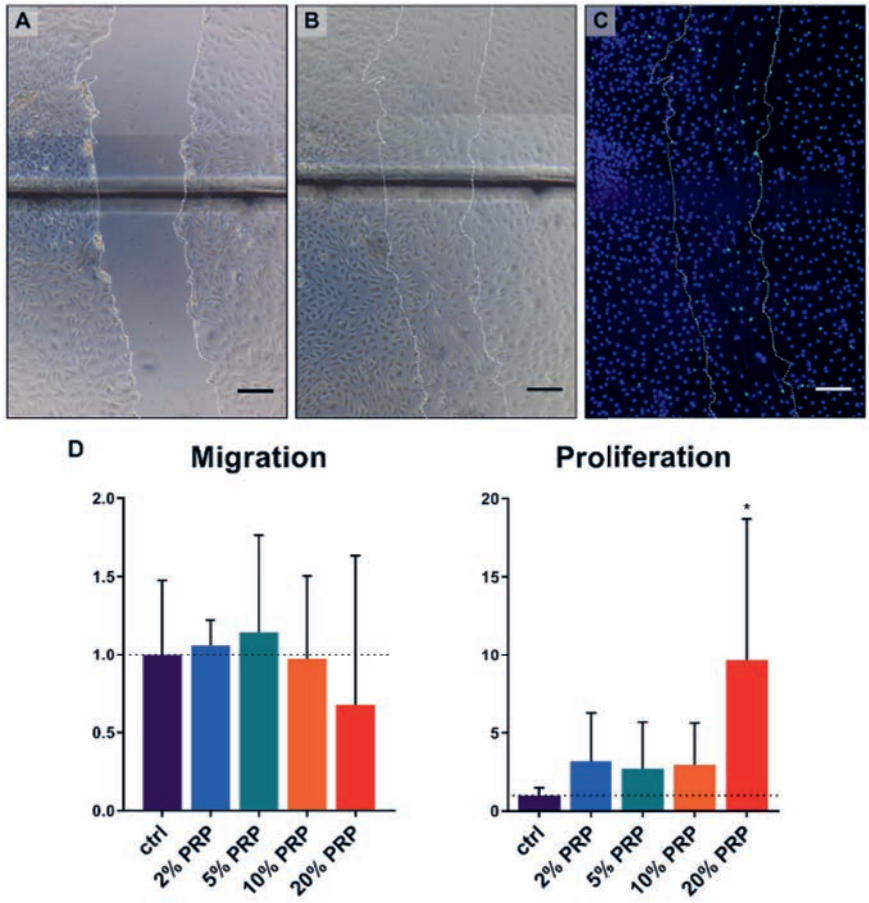

Figure 2. Migration and Proliferation of Chondrocytes into a Micro-Wound. Representative brightfield microscopy photographs of a micro-wound created in a chondrocyte monolayer at T0 (A), T48h (B), and fluorescent microscopy photograph at T48h (C). Scale bar = 200 µm. Migration and proliferation of chondrocytes into a micro-wound as quantified by amount of cells relative to the amounts in the control group (D). Migrated cells were quantified using Hoechst staining, proliferated cells by 5-ethylnyl-2'-deoxyuridine (EdU). Data are shown as mean ± SD. *$p<0.05$.

2 (COX2, also known as prostaglandin-endoperoxide synthase 2 [PTGS2]), prostaglandin E synthase (PTGES), and interleukin 17 (IL17) was significantly upregulated when chondrocytes were treated with TNF-α. Addition of PRP to the medium was ineffective to reduce gene expression of these markers. Expression of interleukin 6 (IL6) and C-C motif chemokine ligand 20 (CCL20), other important players in OA, seemed to be downregulated dose-dependently. However, this decrease was not found to be statistically significant. Expression of interleukin 1B (IL1B) was upregulated in a dose-dependent manner upon addition of PRP. Two of the most important markers for chondrogenesis, collagen type II alpha 1 chain (COL2A1) and aggrecan (ACAN), were significantly downregulated in inflamed chondrocytes. Addition of PRP to these monolayers could not recover this gene expression (Figure 3).

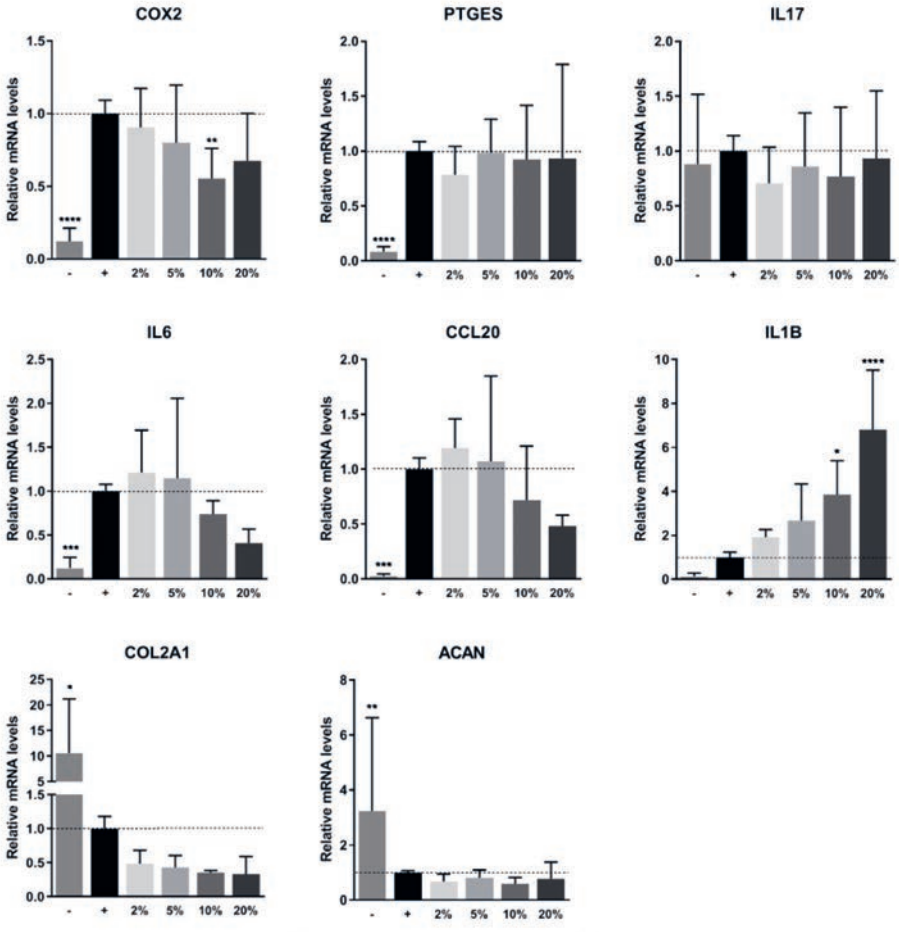

Figure 3. Gene Expression upon Inflammation. Gene expression of chondrocyte monolayers as measured by real-time PCR. Monolayers were stimulated with 10 ng/mL TNF-α and PRP for 48 hours. Gene expression was normalized for 18S. Data are presented as fold changes relative to the TNF-α stimulated control group and shown as mean ± SD. ****p<0.001, ****p<0.0001.*

No Dose-Dependent Regenerative Effect in Gels With Variable Platelet-Rich Plasma Concentration

Biochemical analysis of PRP-enriched fibrin gels revealed a stimulatory effect of PRP on the production of GAGs deposited within the gels by chondrocytes. This pattern was not found in GAG release from these gels. Similar to an increase in absolute GAG content, the amount of DNA in PRP-enriched gels was also elevated. The production of GAGs corrected for the amount of DNA in the gels was significantly decreased in PRP-containing gels (Figure 4).

Inhibition of Chondrogenic Potential of Chondrocytes in Platelet-Rich Plasma Gels vs Fibrin Gels

To assess the capacity of PRP to be used as a stand-alone biomaterial for cartilage tissue engineering, a PRP gel was made in which chondrocytes were encapsulated. Safranin-O staining revealed considerable amounts of GAGs produced by chondrocytes encapsulated in commercial fibrin gel. Morphology of chondrocytes in PRP gel was similar to that of cells cultured in fibrin gel. The chondrocytes exhibited a round morphology and seem to reside in lacunae, typical for hyaline cartilage (Figure S1). Production of GAGs in PRP-based gel was absent (Figure 5A). Biochemical quantification of the gels confirmed a significantly lower relative production of GAGs in PRP gels, as seen both in GAG content as well as in GAG release into the culture medium (Figure 5B). Quantification of the amount of DNA in the gels

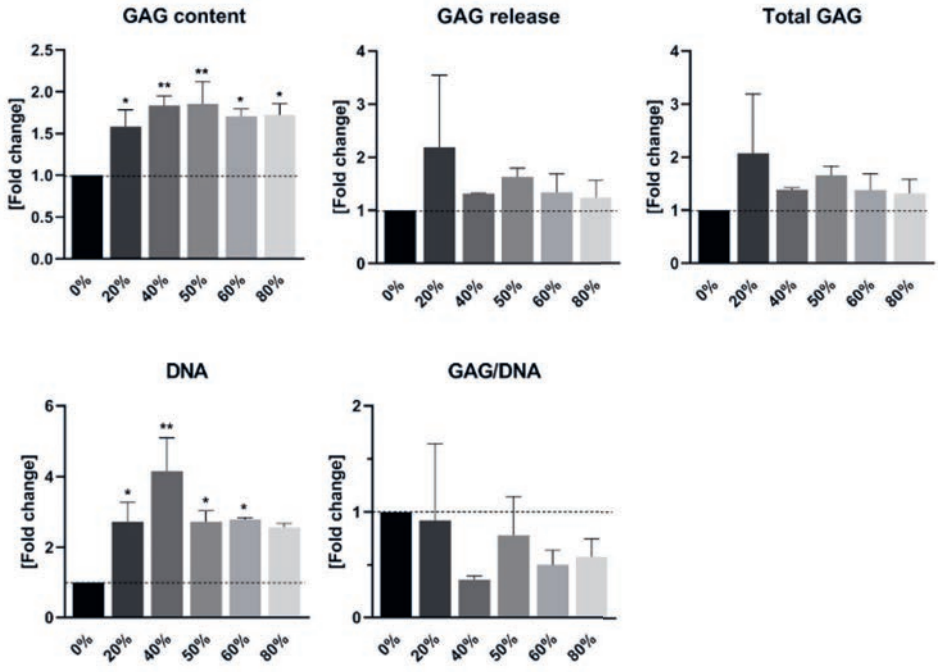

Figure 4. Cartilage Matrix Production in Fibrin Gel Enriched with Platelet-Rich Plasma. Quantification of glycosaminoglycan (GAG) and DNA contents in PRP-enriched fibrin gels by chondrocytes. Release of GAGs into the culture medium was additionally quantified. Data are presented as mean ± SD and as fold changes relative to the control group devoid of PRP. *$p<0.05$, **$p<0.01$.

revealed a significant increase in DNA in PRP gels over the culture period of 28 days when compared to fibrin gels (Figure 5C). When looking at the production of collagen in these gels, a similar pattern was seen. No positive staining for type II collagen, a major component of hyaline cartilage, could be observed in PRP gels, while this was observed in fibrin gels. No distinguishable differences were found in the production of type I collagen, an indicator for fibrocartilage (Figure 6A). In addition, total collagen content was significantly lower in PRP gels compared to fibrin gels (Figure 6B).

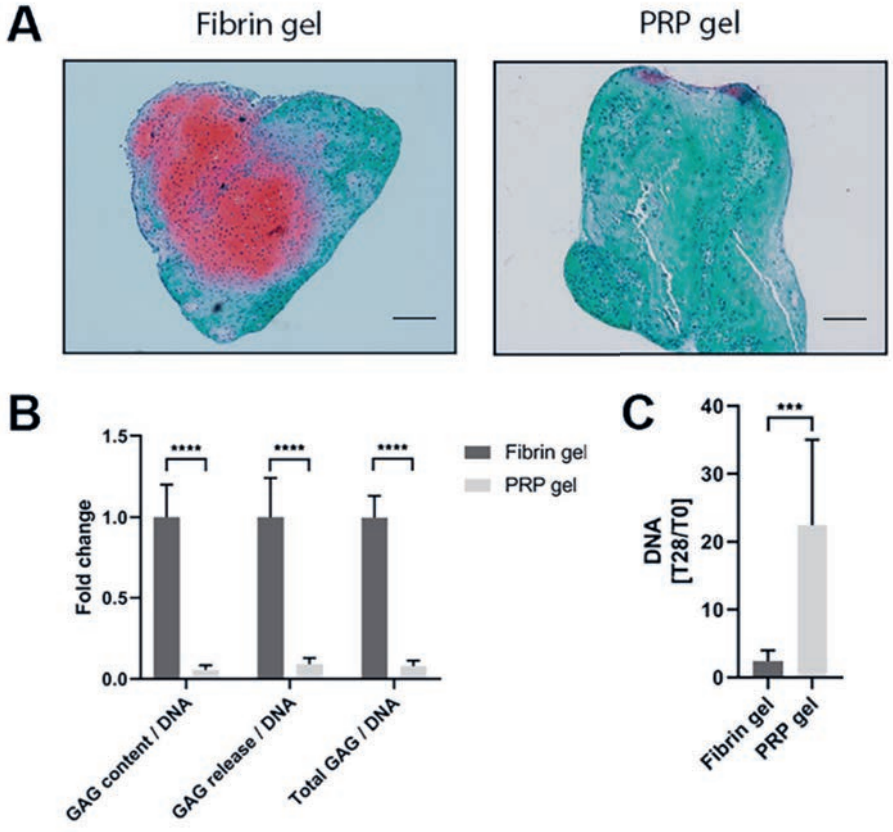

Figure 5. Proteoglycan Production and Proliferation in Platelet-Rich Plasma Gel. Proteoglycans were visualized in PRP gels as well as control fibrin gels by safranin-O staining. Scale bar = 200 µm (A). Quantification of data presented in A. Production of glycosaminoglycans (GAGs) was normalized for DNA content and presented as fold change to the fibrin gel control group. Data are shown as mean ± SD. *****p<0.0001* (B). Increase in DNA content in fibrin and PRP gels over the culture period of 28 days. Data are depicted as mean ± SD. ****p<0.001* (C).

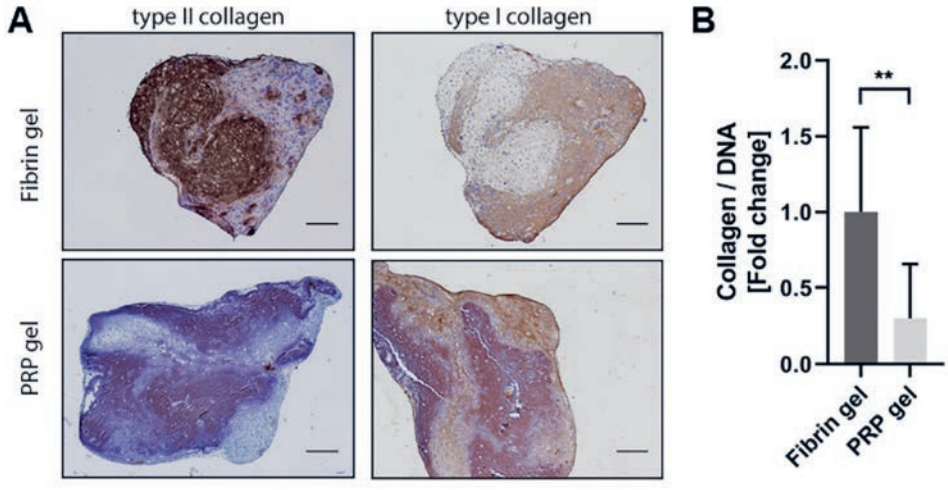

Figure 6. Collagen Production in Platelet-Rich Plasma Gel. Visualization of type II and type I collagen production in fibrin and PRP gels by immunohistochemistry. Scale bar = 200 µm (A). Total collagen was quantified and normalized for DNA content in the gels. Data are presented as fold change to the fibrin gel group and shown as mean ± SD. ***p<0.01* (B).

DISCUSSION

Platelet-rich plasma is an appealing product which is widely applied to treat orthopaedic conditions. Positive outcomes are attributed to the high concentrations of growth factors and anti-inflammatory components in PRP. Nonetheless, other studies report on negative results and consensus has not been reached. Proper understanding of the mechanism of action of PRP in the osteoarthritic joint is desired. The current study attempted to elucidate the effects of PRP specifically on chondrocytes in an *in vitro* controlled setting.

In this study, we used manually prepared, pooled human PRP which was deprived of leukocytes. It therefore can be defined as leukocyte-poor (LP-)PRP. LP-PRP generally contains a smaller amount of platelets[339,343] compared to leukocyte-rich (LR-)PRP, which results in a lower concentration of growth factors[338,339]. Substantial evidence showing lower concentrations of growth factors can negatively influence outcome in OA does not exist. For that reason, it cannot be concluded whether a certain preparation method produces qualitatively better PRP for the treatment of OA. There is a great lack of randomized controlled trials directly comparing LR- and LP-PRP. Just one study made a direct comparison in a clinical setting[347] comparing single spin and double spin PRP. Double spin PRP was shown to have a 1.4X increase in leukocyte compared to whole blood. The authors reported on initially more pain and swelling in the group that received LR-PRP, but no difference in long-term outcome. *In vitro* evidence shows a more pro-inflammatory environment when LR-PRP is used[344].

We found that our PRP stimulated proliferation of OA chondrocytes *in vitro* both in a 2D as

well as in a 3D setting. The general opinion is that PRP and PRP-derivatives like platelet lysate stimulate proliferation of a variety of cell types. Many studies looked into the effects of PRP on MSCs derived from various sources[323,372–374], where all studies report on increased proliferation when PRP was compared to conventional culture medium. Likewise, studies describing cell types derived from other tissues in the knee also report on increased proliferation[321,323,362,375,376]. It is important to highlight our study found increased proliferation only in the case where 20% PRP was added to the culture medium. Growth factor concentrations in this experimental condition are most likely much higher than when PRP is used in a clinical setting for intra-articular injections. Although stimulation of migration by PRP has been previously reported on in MSCs and other chondroprogenitor cells[323,377–379], we did not confirm this for OA chondrocytes in our micro wound setup. It was expected that the high concentrations of chemoattractants in PRP could have promoted migration similar to a report on cell outgrowth from pieces of cartilage cultured in a gel containing PRP[208].

Another key finding of the current study is that our PRP was unable to inhibit the inflammatory response in OA chondrocytes in an *in vitro* inflammation model. Some of the most important markers expressed by OA chondrocytes in OA are COX2 and PTGES. Both are involved in the synthesis of prostaglandin E, an important pro-inflammatory marker in OA[380,381]. We found that PRP had an inconsistent effect on the gene expression of COX2. The elevated expression of PTGES in inflamed chondrocytes could neither be reduced by PRP. We also showed that PRP was unable to downregulate the expression of cytokine IL6 and chemokine CCL20, both involved in the progression of OA[382,383]. Both TNF-α and PRP were unable to alter the expression of IL17. Interestingly, the increased expression of IL1B upon stimulation of the cells with TNF-α was not downregulated by PRP. On the contrary, IL1B was increasingly expressed in a dose-dependent manner upon treatment with PRP. The striking increase in gene expression of IL1B might be caused by positive feedback loops induced through production of other cytokines[382,384]. This is contradictory to previously found anti-inflammatory properties attributed to PRP[350]. The *in vitro* system presented in this study only included cartilage cells, making a translation to the clinical situation difficult. Other tissues, like the synovium, have been shown to be a very important participant in the inflammatory response in OA. The step toward animal models and clinical studies is necessary to shed light on the effects of PRP on inflammation of the whole joint environment.

In this study, we additionally investigated the potential of PRP-incorporation in a commercial fibrin gel to stimulate cartilage regeneration. We report that incorporation of PRP leads to an increase in GAG content, independent of the concentration of PRP added. At the same time, an increase in the amount of DNA was found upon addition of PRP into the gel, suggesting either an increase in proliferation or a reduction in cell death as compared to the control gels consisting of fibrin alone. Yet, the relative GAG production in PRP-supplemented gels greatly decreased, suggesting a strong inhibition of GAG formation by the cells in these gels. Our study is the first to incorporate different concentrations of PRP into a fibrin gel seeded with human OA chondrocytes. Other tissue engineering approaches where PRP is incorporated in

other types of hydrogels, like an in-situ photo-crosslinkable hydrogel[385] and an injectable PRP-containing gel[386] report on a chondrogenic effect of PRP, although both studies mentioned use MSCs.

To the best of our knowledge, our study is one of the first assessing cartilage matrix production of human OA chondrocytes in a hydrogel consisting purely of PRP. Despite a high concentration of TGF-β1 in our PRP, we found an evident inhibition of cartilage-like matrix formation, while desirable production of GAGs and type II collagen was seen in commercial fibrin gel. The biochemical data was supported by a clear absence of positive histological staining for safranin-O and type II collagen, where fibrin gels were evidently positive for both stainings. While in an unaffected joint TGF-β maintains a healthy chondrocyte phenotype[387], a high concentration of TGF-β in the OA knee joint can accelerate cartilage damage[388]. As PRP continuously releases growth factors, including TGF-β, for at least six days[389], the situation in PRP gel presented in the current study would correspond to an ongoing diseased state. *In vivo*, this can lead to progression of OA, synovial fibrosis, and development of osteophytes[390].

Again, we observed an evident increase in cell proliferation in chondrocytes cultured in the presence of high concentrations of PRP. The only study carrying out a similar approach as we did, also shows an inferior effect of PRP when compared to fibrin gel[367]. A minimal amount of studies have looked into the behaviour of cells of other species in a PRP gel[80,391]. While both studies report an increase in proliferation of the cells, their results on cartilage matrix production contradict. What specifically happens to the chondrocytes in PRP gel remains inconclusive. Although we see a similar cell morphology in fibrin and PRP gel, their capacity of forming cartilage-like matrix is evidently impaired. In addition, it should be noted that all experiments in the current study were performed with chondrocytes isolated from redundant material from OA donors. The conclusions are therefore limited to the cell origin and interpretation and extrapolation to other cell types or disease states should therefore be handled with care. Evidently, more and extensive research is needed to determine whether PRP is a suitable candidate to be used as a novel autologous scaffold for cartilage tissue engineering.

Discrepancies between studies remain a major problem in PRP research. Preparation methods vary greatly and the majority of studies fail to report on characterization of their PRP[349]. Variations in growth factor content and concentrations, as well as the presence of leukocytes may alter outcomes drastically. Also, inconsistencies remain between *in vitro* studies and clinical outcomes when PRP is used for the treatment of OA. It is crucial to consider the complexity of the articular joint and the tissues involved in the progression of OA. This illustrates the importance to move towards more complex culture systems, preferably using tissue explants in coculture to have a closer resemblance of the human joint.

In conclusion, the data presented here show absence of an anti-inflammatory effect of PRP

on OA chondrocytes. Besides, PRP fails to stimulate OA chondrocytes into producing hyaline cartilage matrix *in vitro*. In addition, a pronounced stimulation of chondrocyte proliferation was seen both in cell expansion as well as in 3D cultures.

SUPPLEMENTAL TABLE

Table S1. Primer sequences for quantitative real-time PCR. Forward (Fw) and reverse (Rv) primers for 18S, ACAN, *aggrecan*; CCL20, *C-C motif chemokine ligand 20*; COL2A1, *collagen type II alpha 1 chain*; COX2, *cytochrome c oxidase subunit II*; IL1B, *interleukin 1 beta*; IL6, *interleukin 6*; IL17, *interleukin 17*, PTGES, *prostaglandin E synthase*.

Gene name	Oligonucleotide sequence (5' to 3')	Annealing temperature (°C)	Product size (bp)
18S	Fw: GTAACCCGTTGAACCCCATT Rv: CCATCCAATCGGTAGTAGCG	57	151
ACAN	Fw: CAACTACCCGGCCATCC Rv: GATGGCTCTGTAATGGAACAC	56	160
CCL20	Fw: TCCTGGCTGCTTTGATGTCA Rv: CAAAGTTGCTTGCTGCCTTCTGA	57	70
COL2A1	Fw: AGGGCCAGGATGTCCGGCA Rv: GGGTCCCAGGTTCTCCATCT	57	195
COX2	Fw: GCCCGACTCCCTTGGGTGTC Rv: TTGGTGAAAGCTGGCCCTCG	57	190
IL1B	Fw: GCTGAGGAAGATGCTGGTTC Fv: TCCATATCCTGTCCCTGGAG	58	240
IL6	Fw: CCTTCCAAAGATGGCTGAAA Rv: CAGGGGTGGTTATTGCATC	57	230
IL17	Fw: CCGTGGGCTGCACCTGTGTC Rv: GGGAGTGTGGGCTCCCCAGA	57	71
PTGES	Fw: AAGTGAGGCTGCGGAAGAAG Rv: CCAGGAAAAGGAAGGGGTAG	57	150

SUPPLEMENTAL FIGURE

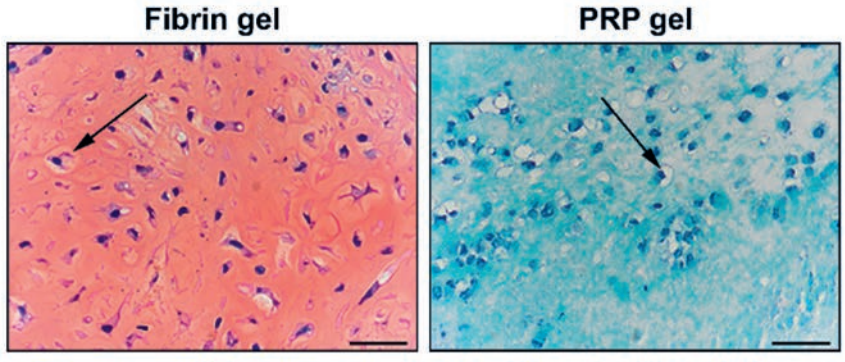

Figure S1. Chondrocyte Morphology in Gels. Chondrocytes cultured in fibrin gel as well as in PRP gel exhibit a round morphology after 28 days of culture. Cells reside in typical hyaline cartilage lacunae (black arrows). Scale bar = 50 µm.

Chapter 8

A gap-filling, regenerative implant for open-wedge osteotomy

Margot Rikkers
H. Chien Nguyen*
Nasim Golafshan*
Mylène de Ruijter
Riccardo Levato
Lucienne A. Vonk
Nienke van Egmond
Miguel Dias Castilho
Roel J.H. Custers
Jos Malda
** = These authors contributed equally*

Submitted

ABSTRACT

Purpose

Unicompartmental osteoarthritis of the knee joint can be treated with open-wedge osteotomy (OWO). However, the procedure faces several challenges like postoperative pain and bone non-union. Here, we aimed to design, fabricate, and evaluate a gap-filling implant using an osteoinductive and degradable biomaterial, that closes the space left after an OWO.

Methods

High tibial OWO procedures on three fresh frozen human cadaveric legs were planned using computed tomography (CT) scans. Based on this, a porous wedge scaffold was designed and 3D printed using a magnesium strontium phosphate-polycaprolactone (MgPSr-PCL) biomaterial ink. Wedge implants with inter-fibre spacing (IFS) of 0.7 mm, 1.0 mm, and 1.3 mm with closed outer edges were fabricated. The wedges were mechanically characterized and *in vitro* osteoinductive properties of the material were assessed using expanded human bone marrow-derived mesenchymal stromal cells (MSCs) and bone marrow concentrate (BMC) using medium with and without factors to induce osteogenesis. Next, implants were fabricated for *ex vivo* implantation during three OWOs with different heights (5 mm, 10 mm, 15 mm), and the wedges were implemented into the OWO in the human cadaveric legs.

Results

Implants with IFS-1.0 resulted in scaffolds that maintained top and bottom porosity, while exhibiting significant mechanical stability. MSCs and BMC cells attached to the MgPSr-PCL material and proliferated over 21 days in culture. Alkaline phosphatase activity, calcium, and osteocalcin production were promoted in all culture conditions, independent of osteogenic induction medium. Finally, three OWOs were performed and the fabricated wedges were implanted *ex vivo* during the OWO. A small fraction of one side of the wedges was resected to assure fit into the proximal biplanar osteotomy gap. Pre-planned wedge heights were maintained after implantation as measured by micro-CT.

Conclusion

To conclude, we have successfully designed and manufactured personalized implants to fill the gap in open-wedge osteotomies. The implants supported osteogenesis of MSCs and BMC *in vitro* and were successfully implemented into the surgical procedure, without compromising pre-planned wedge height.

INTRODUCTION

Unicompartmental knee osteoarthritis (OA) is often associated with lower limb malalignment. Especially for younger patients (age < 65 years) with unicompartimental OA and a malalignment, a correctional osteotomy can be a surgical solution, aiming to unload the affected compartment[62,392,393]. Typically, for a varus malalignment, a medial open-wedge high tibial osteotomy is performed, and for a valgus malalignment, a distal femur osteotomy is chosen. Closed-wedge osteotomies are associated with better clinical outcome[394], but when applied in the tibia require concomitant fibular osteotomy and complicate potential future total knee arthroplasties[395]. A medial high tibial OWO is associated with pain in the early postoperative stage and sometimes delayed bone union[396,397]. Postoperative pain is believed to be (at least in part) caused by bone marrow leakage from the osteotomy site, causing swelling, resulting in impairing early weight-bearing, ambulation, and rehabilitation[398].

In some cases, the opened osteotomy wedge is filled with an autologous bone graft from the iliac crest[399]. However, this procedure is aimed at accelerating union rather than completely sealing the gap and it is associated with donor site morbidity[400]. Filling the osteotomy gap with an allogeneic bone graft could be a viable solution as gap filler, as this resulted in a decrease in pain during the first 4 weeks after. This study demonstrated that almost all of the patients (99%) were able to walk > 500 meters without any support three months after surgery[397]. However, the use of allogeneic bone grafts is hampered by the limited availability of the grafts. Moreover, frozen allografts have a higher failure rate compared to living autologous grafts[401]. Likewise, synthetic bone substitutes made of hydroxyapatite and/or beta-tricalcium phosphate[396,402–404] aid in bone union without donor site morbidity, yet fall short of completely sealing the osteotomy gap to prevent bleeding and lack mechanical properties. To improve bone union, postoperative pain, and eliminate the need for an allo- or autograft in OWO procedures, a firm gap filing 3D-printed scaffold with osteoconductive properties and mechanical stability provides a solution.

Among the bioactive ceramic materials that have been used for bone tissue engineering, magnesium strontium phosphate (MgPSr) has gained particular interest due to the good solubility of magnesium phosphate phases under physiological conditions, and the presence of Sr^{2+} ions have been demonstrated to promote osteogenic differentiation of mesenchymal stromal cells (MSCs)[405–410]. However, pure ceramic scaffolds are usually brittle and prone to fracture which hampers their application in large, load bearing defects[411]. A previous study has investigated a ceramic-polymer composite of MgPSr and polycaprolactone (PCL), which is a versatile biomaterial ink that can be processed through extrusion-based 3D printing at room temperature. This biomaterial can be manufactured into different complex geometries to improve bone filling of a defect without compromising mechanical stability[412]. The porous nature of a printed osteotomy wedge scaffold allows bone marrow to populate the wedge upon implantation. Alternatively, pre-surgical seeding of the implant with a bioactive product accelerating osteogenesis, such as bone marrow concentrate (BMC), could further accelerate

bone union.

This study aimed to design and manufacture a scaffold as gap filler in OWO around the knee joint. The mechanical stability of the wedge scaffold, as well as the *in vitro* osteoinductive properties of the material on MSCs and BMC were investigated. Additionally, preservation of the pre-designed implant structure and height were assessed upon implantation into human cadaveric legs.

MATERIALS AND METHODS

Study outline

To completely fill the opening wedge gap after an OWO, 3D printed scaffolds were manufactured using patient computed tomography (CT) data and computer-aided design. The printed implants were mechanically characterized and *in vitro* potency of the MgPSr-PCL material was evaluated to induce osteogenesis when seeded with bone marrow-derived MSCs, as well as BMC. Finally, we included a proof-of-concept surgical feasibility study in a cadaver model for implementation of the implants into the current osteotomy procedure.

Computer-aided design of osteotomy wedge

To design a wedge scaffold for mechanical characterization and *in vitro* experiments, an anonymized CT scan and surgical planning for an 8 mm medial opening-wedge distal femur osteotomy was acquired from a clinical case (University Medical Center Utrecht) (Figure 1Ai). The computer-aided design (CAD) of the wedge scaffold was developed in SolidWorks software (Dassault Systèmes, Waltham, MA, USA), using the CT scan images. After assessment of the wedge scaffold, BioCAM™ software was used to define the wedge scaffold internal architecture and subsequently translate the design into a G-Code. The external wall of the osteotomy scaffold was kept closed with two outer layers, while for the internal region of the osteotomy scaffolds, three different inter-fibre spacings (IFS), 1.3 mm, 1.0 mm, and 0.7 mm (abbreviated as IFS-1.3, IFS-1.0, and IFS-0.7, respectively) were considered.

Material preparation and extrusion-based 3D-bioprinting

The biomaterial ink was prepared by combining in-house synthesized $Mg_{2.33}Sr_{0.67}(PO_4)_2$ powder and commercial medical grade poly(ε-caprolactone) (mPCL, Purasorb PC 12, Purac Biomaterials, Netherlands) in a weight ratio of 70:30 wt.% of MgPSr to PCL, according to a procedure previously described[412]. Designed scaffolds were fabricated by an extrusion-based 3D-printing system (3D Discovery, regenHU, Switzerland) using the MgPSr-PCL biomaterial ink. The ink was transferred to a 10 mL syringe (Nordson EFD, USA) and extruded though a 22G conical nozzle (inner diameter = 0.41 mm, Nordson EFD, USA) at a pressure of 0.9 bar and collected at collector speed of 6 mm/s.

Mechanical characterization of printed wedge scaffolds

Uniaxial compression tests were performed using a universal testing machine (Zwick Z010,

Germany) equipped with a 1 kN load cell. Tests were performed on cylindrical samples (d = 6 mm, h = 12 mm, n = 5) for all three groups (IFS-1.3, IFS-1.0 and IFS-0.7, without closed outer edges), at a rate of 1 mm/min (at room temperature). From the engineered stress-strain curves, the elastic modulus (defined as the slope of the linear region at the interval 0.02 - 0.05 mm/mm strain), the yield stress (defined as the point where nonlinear deformation begins), and toughness (defined as the absorbed energy by the scaffolds up to yield stress) were determined.

In vitro accelerated degradation of printed wedge scaffolds

The degradation of the materials was studied under controlled conditions which accelerated biomaterial degradation *in vitro*[412]. Wedge scaffolds were incubated in a 0.4 mg/ml lipase solution (from Pseudomonas cepacia, Sigma-Aldrich) and 1 mg/ml sodium azide (Sigma-Aldrich) at 37ºC for 15 days. At each time point (1, 5, 10, and 15 days), the enzymatic solution was refreshed and samples were monitored for weight loss, quantified as follows:

$$\text{Weight loss} = \frac{W_{D15} - D_0}{D_0} \qquad \text{Eq. 1}$$

In vitro osteogenesis of scaffolds

Donors and cell isolation

Human MSCs were derived from healthy donor bone marrow aspirates (n = 3, age range 2 – 12) as approved by the Dutch central Committee on Research Involving Human Subjects (CCMO, Bio-banking bone marrow for MSC expansion, NL41015.041.12). The parent or legal guardian of the donor signed the informed consent approved by the CCMO. In brief, the mononuclear fraction was separated using a density gradient (Lympoprep, Axis Shield). MSCs were isolated by plastic adherence and expanded for three passages in Minimum Essential Media (αMEM, Macopharma) with 5% platelet lysate and 3.3 IU/mL heparin and cryopreserved. Subsequently, MSCs were expanded for two additional passages in MSC expansion medium (αMEM [Gibco], 10% (v/v) fetal bovine serum [FBS; Biowest], 1% penicillin/streptomycin [pen/strep; 100 U/mL, 100 µg/mL], 200 µM l-ascorbic acid 2-phosphate [ASAP; Sigma-Aldrich], and 1 ng/mL basic fibroblast growth factor [bFGF; PeproTech]). BMC was obtained from donors undergoing an OWO or total knee arthroplasty surgery (n = 2, age range 39 - 49) after their informed consent (protocol approved by the local medical ethical committee). Bone marrow was concentrated to one tenth of its original volume using Ficoll paque (GE Healthcare) density separation.

In vitro culture of scaffolds

Standardized 5 mm diameter cylindrical scaffolds were printed as described before[412] and sterilized by washing in 70% ethanol and Milli-Q, followed by exposure to ultraviolet light for 1 hour. Scaffolds were cut in half with a sterile scalpel and seeded with either 15,000 MSCs / scaffold in fibrin gel (25 µL fibrinogen (1:15 in PBS) crosslinked with 25 µL thrombin (1:50 in PBS); Tisseel, Baxter) or 25 µL BMC (crosslinked with 16.6 µL thrombin and 16.6 µL $CaCl_2$ (500 mM in 0.9% NaCl)). Cell-seeded scaffolds were pre-cultured in MSC expansion medium

for two days, followed by 21 days of osteogenic induction with osteogenic differentiation medium (αMEM supplemented with 10% FBS, 1% pen/strep, 200 μM ASAP, 10 mM β-glycerophosphate (Sigma-Aldrich), and 10 nM dexamethasone (Sigma-Aldrich)). Control cell-seeded scaffolds were treated with MSC expansion medium without bFGF.

Alkaline phosphatase, calcium, and DNA quantification

Osteogenic differentiation of the cells was measured by the activity of the early osteogenic marker alkaline phosphatase (ALP) after 5, 7, and 11 days and by quantification of calcium produced after 21 days. To determine activity of ALP, cells were lysed in Tris-EDTA buffer (10 mM Tris-HCl, 1 mM EDTA, pH 8) by three freeze-thaw cycles. ALP activity was measured using the conversion of p-nitrophenyl phosphate liquid substrate (pNPP, Sigma-Aldrich). Absorbance was measured every minute for 30 minutes at 405 nm and corrected for absorbance at 655 nm. Calf intestinal ALP (Sigma-Aldrich) was used as a standard. Calcium concentration in the samples was quantified after 21 days using a colorimetric calcium assay kit (Abcam) according to the manufacturer's instructions. ALP activity and calcium levels were corrected for DNA. DNA content was determined using the Quant-iT PicoGreen dsDNA assay (Invitrogen) according to the manufacturer's instructions.

Osteocalcin immunocytochemistry

To visualise the osteogenic marker osteocalcin, scaffolds were fixed in formalin for 30 minutes for the osteocalcin immunocytochemistry after 21 days of differentiation. Samples were permeabilized with 0.2% (v/v) Triton X-100 in phosphate-buffered saline (PBS), followed by blocking with 5% (v/v) bovine serum albumin (BSA) in PBS. Next, samples were incubated overnight at 4ºC with 10 μg/mL mouse-anti-human primary antibody against osteocalcin (clone OCG4; Enzo Life Sciences). Samples were then incubated with 10 μg/mL goat-anti-mouse antibody conjugated to Alex Fluor 488 (Invitrogen) for one hour at room temperature. All samples were also stained for F-actin (1:200; phalloidin-TRITC; Sigma-Aldrich) and 4′,6-diamidino-2-phenylindole (100 ng/mL; DAPI; Sigma-Aldrich). Images were acquired with a Leica SP8X Laser Scanning Confocal Microscope and Leica LASX acquisition software.

Ex vivo surgical implantation of the printed wedges

Three fresh-frozen human cadaveric legs were obtained (all left legs, one male and two female) in accordance with the guidelines of the local medical ethical committee. CT-scans were obtained of the three included legs (Philips Healthcare, Best, The Netherlands; 100 kV and 130mAs), with 0.8 mm slice thickness. OWOs were pre-operatively planned in 3-Matic (Materialise, Leuven, Belgium), with for each leg a specific wedge height (5, 10, and 15 mm). This resulted in post-surgical 3D-models of the cadavers with left open osteotomy gaps, which functioned as surrogate for the 3D printing of the wedges. A proximal biplanar medial high tibial OWO was performed following a standard surgery protocol. During this procedure, the osteotomy gap was kept open using a lamina spreader and the 3D-printed scaffold wedge was inserted into the gap. The lower end of the wedge scaffolds was resected to fit the

osteotomy gap, without altering the outside rim of the wedge. The osteotomies were then fixated with angular stable plates (Activmotion, Newclip Technics, Nantes, France). Following implantation of the scaffold wedges, additional CT scans were obtained of the operated cadaver legs, subsequently the wedges were explanted for further analysis.

Micro-computed tomography

The pre- and post-surgical wedge scaffolds underwent micro-CT (Quantum FX-Perkin Elmer, USA) for height analyses. Scan parameters were 90 kV tube voltage, 180 μA tube current, 60 or 73 mm resolution, and 2 min scan time. Scaffold heights pre- and post-implantation were quantified using computer vision software Fiji (software version 2.1.0/1.53c, National Institutes of Health, Bethesda, USA).

Statistical analysis

Statistical analyses were performed using GraphPad Prism 8.3 (GraphPad Software, Inc., La Jolla, CA, USA). All data were presented as mean ± standard deviation (SD). To test for differences in mechanical evaluations and calcium content, a one-way analysis of variance (ANOVA) with Tukey's post hoc test was used. To test for differences in DNA and ALP quantifications, a two-way ANOVA with Tukey's post hoc was used. For scaffold wedge height, a two-tailored t-test was used. Normality was confirmed with a Shapiro-Wilk test (p>0.05). P values below 0.05 were considered significant.

RESULTS

Personalized implant design and fabrication

Wedge implants were designed for both open-wedge lateral distal femur (Figure 1A) and medial tibial osteotomies (Figure 1B) from a CT scan 3D reconstruction (Panels i). Wedges

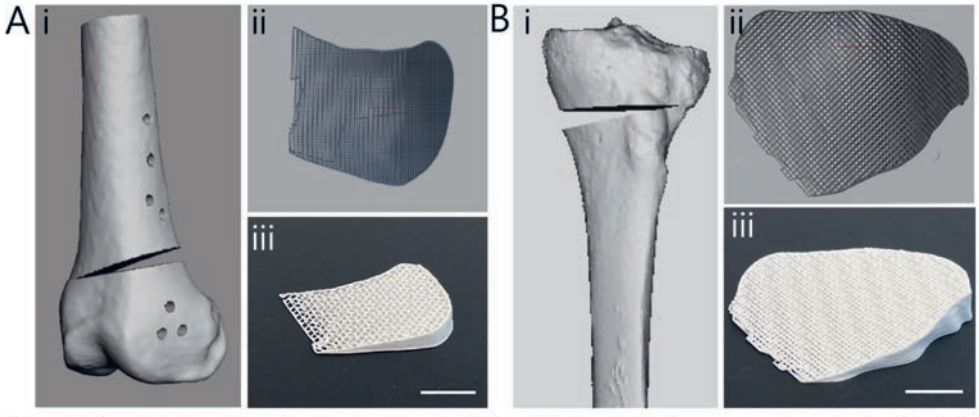

Figure 1. Surgical planning and extrusion-based printing. Wedge design for open-wedge osteotomies in (A) distal femur and (B) proximal tibia. (Panels i) Surgical planning of open-wedge osteotomies derived from computed tomography (CT) scans. (Panels ii) Top views of printing paths of computer-aided designs (CAD) of personalized wedge implants. (Panels iii) The finalized personalized wedges in magnesium strontium phosphate-polycaprolactone (MgPSr-PCL) biomaterial. Scale bar = 10 mm.

had closed outer edges, aimed at limiting leakage from the osteotomy site into the soft tissues surrounding the bone, while the interior was porous (Panels ii and iii).

Mechanical profile of printed porous material

Incorporation of the thermoplastic PCL into the ceramic MgPSr phase improved handling of the implants, overcoming downsides of brittle ceramic materials[411]. The stress-strain curves of the standardized printed discs with different IFS showed comparable profiles (Figure 2A). The decrease in IFS resulted in an increase in mechanical stability, elastic modulus increased significantly from 105.3 ± 10.26 MPa (IFS-1.3) to 151.5 ± 12.61 MPa (IFS-0.7) (Figure 2C). Yield stress, defined as the point of maximum elastic deformation, increased from 4.2 ± 1.27 MPa (IFS-1.3) to 6.0 ± 1.90 MPa and 11.4 ± 1.86 MPa for IFS-1.0 and IFS-0.7, respectively (Figure 2D). In line, strain energy increased from 0.077 ± 0.0208 J for IFS-1.3 to 0.196 ± 0.0957 J for IFS-0.7 (Figure 2E). While a disc with an IFS of 0.7 mm presented the highest elastic modulus, printing of a complete wedge scaffold with this IFS resulted in a construct that was not completely porous from top to bottom, which is essential to flow of bone marrow through the scaffold *in vivo* (Figure 2B). Scaffolds with a planned IFS of 1.0 mm resulted in completely porous wedges and only a slight difference in elastic modulus and strain energy compared to scaffolds with a planned IFS of 0.7 mm, which did not reach statistical significance. While the degradation rate of IFS-1.3 samples (as evaluated under accelerated degradation conditions) was 30% faster compared to IFS-1.0 samples (Figure 2F), the combination of tested characteristics led to the selection of IFS-1.0 for further analyses as

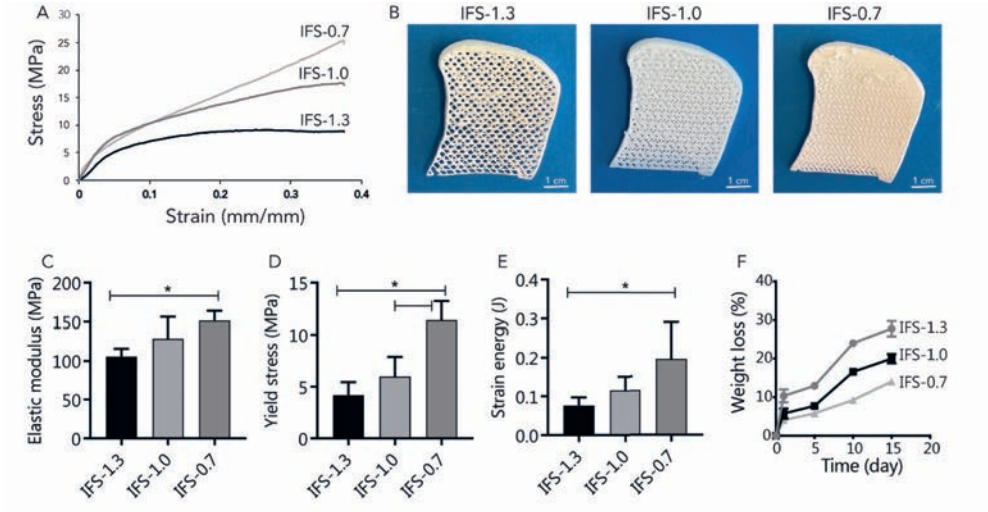

Figure 2. Evaluation of mechanical properties of the printed magnesium strontium phosphate-polycaprolactone (MgPSr-PCL) wedges. A) Longitudinal compression profile of 3D printed MgPSr-PCL wedge scaffolds for inter-fibre spacing (IFS) -1.3, IFS-1.0, and IFS-0.7. B) Corresponding photographs showed the different scaffolds after the printing. Open pores in wedges IFS-1.3 and IFS-1.0 can be appreciated, while IFS-0.7 wedges were not porous. C) Elastic modulus, D) Yield stress, and E) strain energy from compressive loading profile for IFS-1.3, IFS-1.0, and IFS-0.7. F) Weight loss of wedge scaffolds during accelerated in vitro degradation in enzymatic solution over 15 days.

the best compromise between open porosity, mechanical stability, and degradation properties.

In vitro osteogenic properties of the scaffold material

Human BM-MSCs embedded in fibrin (MSC-fibrin) were seeded in the biomaterial scaffolds to evaluate osteogenic potential. Additionally, to simulate the situation *in vivo*, a second group of scaffolds was seeded with BMC. The culture-expanded human MSCs attached to the MgPSr-PCL material and proliferated over time. Cells in BMC also proliferated on the scaffolds (Figure 4A and Supplemental Figure 1). Activity of the early osteogenic marker ALP was similar in MSC-fibrin and BMC groups when scaffolds were cultured in control medium, yet, were increased in MSC-fibrin when cultured in osteogenic medium (Figure 4B). BMC performed similar to MSC-fibrin in terms of calcium production at 21 days of culture (Figure 4C). Of note, both experimental groups had a higher ALP activity and increased calcium production compared to MSCs that were cultured in monolayers, indicating osteoconductive

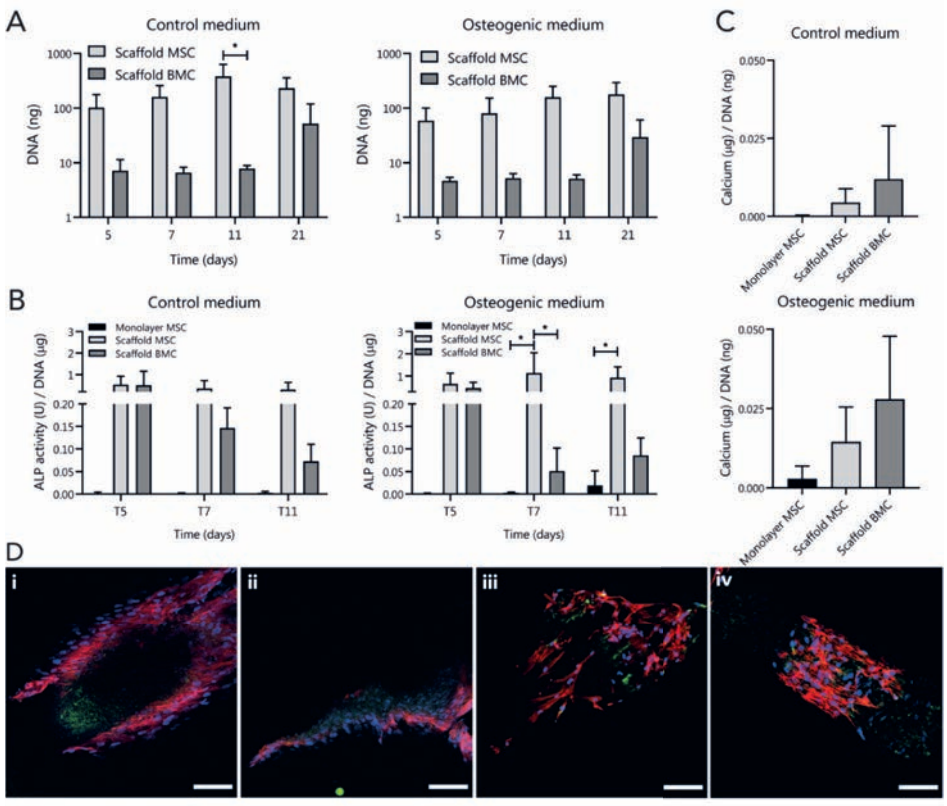

Figure 3. *In vitro* osteogenic performance of the magnesium strontium phosphate-polycaprolactone (MgPSr-PCL) biomaterial. A) Quantification of DNA in the MgPSr-PCL scaffolds at 5, 7, 11, and 21 days in culture with control (left panel) and osteogenic medium (right panel). B) Early osteogenic marker alkaline phosphatase (ALP) activity relative to the amount of DNA at 5, 7, and 11 days. C) Calcium content of the cultured constructs at day 21 in control medium (top panel) and osteogenic medium (bottom panel). E) Immunocytochemistry for osteocalcin in (i) mesenchymal stromal cells (MSC) in control medium, (ii) MSC in osteogenic medium, (iii) bone marrow concentrate (BMC) in control medium, and (iv) BMC in osteogenic medium. Nuclei are shown in blue (DAPI), osteocalcin expression in green, and F-actin in red. Scale bar = 100 µm.

effects of the scaffold material and 3D environment. Production of osteocalcin, an exclusive marker for osteoblasts, was observed in cultures under all conditions irrespective of culture medium used (Figure 3D).

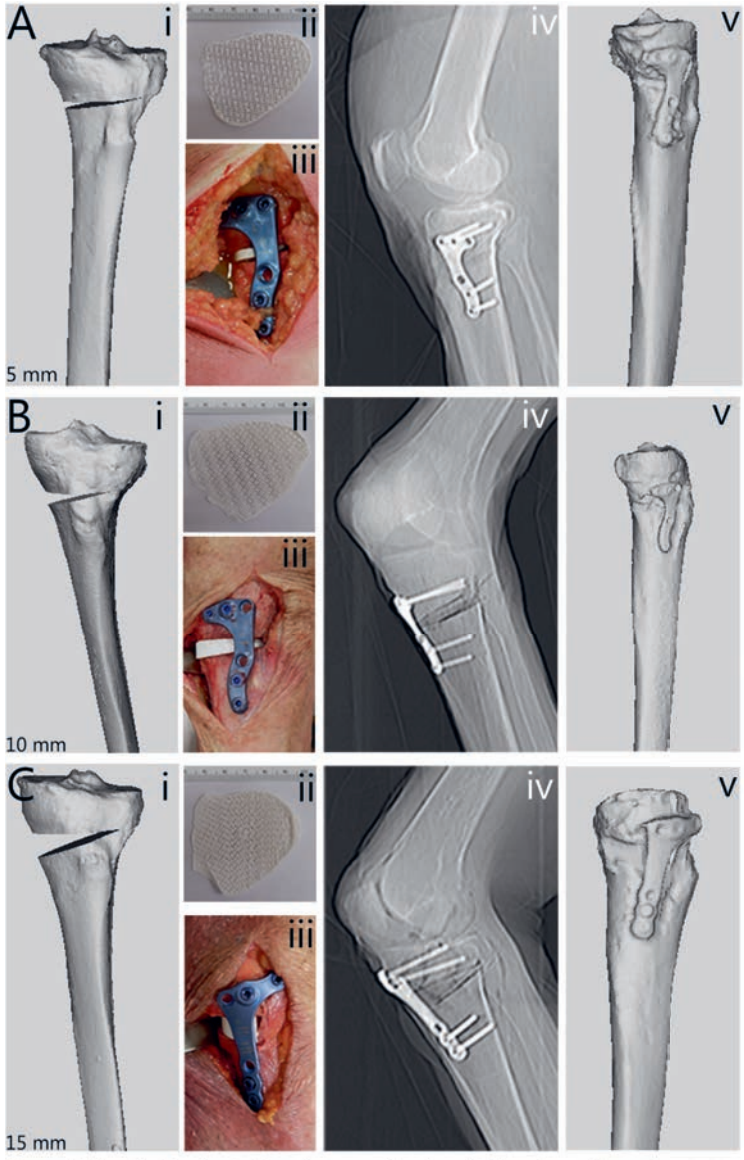

Figure 4. Surgical implantation of personalized scaffold wedges. Planned osteotomy heights of A) 5 mm, B) 10 mm, and C) 15 mm from computed tomography (CT) scans of human cadaveric legs (Panels i). (Panels ii) 3D printed wedge scaffolds in magnesium strontium phosphate-polycaprolactone (MgPSr-PCL). (Panels iii) Scaffolds implanted in the cadaveric legs. (Panels iv) X-ray of the legs after implantation. (Panels v) 3D reconstruction from CT scans after implantation of the wedge scaffolds.

Ex vivo surgical implantation

Three fresh-frozen human cadaveric legs underwent CT scanning in order to plan three OWOs with different heights; 5, 10, and 15 mm (Figure 4A, 4B, 4C). 3D models of the tibias were used to plan the osteotomy gap (Panels i) and design the personalized wedge scaffolds (Panels ii). Wedges were implanted during a standard proximal biplanar OWO procedure and fixated with an angular stable plate (Panels iii). Post-surgical X rays (Panels iv) and CT scans (Panels v) illustrate the scaffold positioning and fit. Micro-CT analyses of the wedges pre- and post-implantation indicated good analogy of the scaffolds (Figure 5A, pre-operative in red, post-operative in grey). Due to the biplanar approach of the osteotomy procedure[413], the scaffolds were adjusted at one side using an automatic saw, not altering the rest of the scaffold shape and outer rim (Figure 5B, arrows indicating trimmed side). Quantification of wedge heights from micro-CT images revealed that the wedge heights were not affected by the applied surgical procedure (Figure 5C).

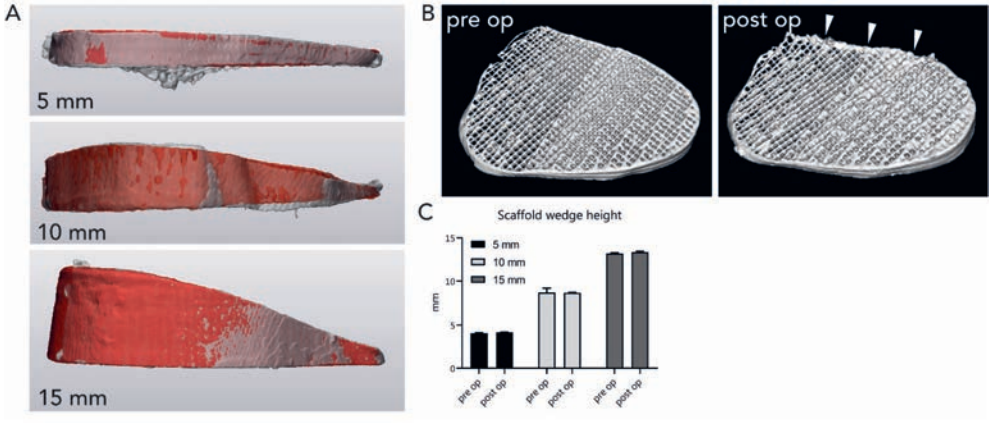

Figure 5. Micro-computed tomography (CT) analysis of printed wedge scaffolds. A) 3D reconstructions of the wedges from micro-CT images of the printed wedges pre- and post-implantation. Pre-implanted scaffolds in red, post-implanted scaffolds in grey. B) Micro-CT reconstruction of the 5 mm wedge. Note the small portion that was adjusted during the procedure (indicated by the white arrows). C) Quantification of scaffold wedge height before and after implantation into the cadaveric legs revealed no loss of scaffold height.

DISCUSSION

This study demonstrated the feasibility to manufacture implants for bone gap filling in OWOs, by 3D printing of a biodegradable and osteoinductive scaffold material. The printed material promoted osteogenesis of MSCs and BMC *in vitro* and scaffolds were implanted *ex vivo* without compromising the pre-operatively planned wedge height. We aimed to design implants that fitted the planned osteotomy gap, fabricate these and evaluate their implementation in the current osteotomy

Post-surgical pain poses a challenge in OWO care. One of the hypotheses for the cause of

pain is bleeding from the osteotomy site. Others have shown that fitting an allogeneic graft, which closes the gap completely, reduced post-operative pain and accelerated the recovery[397]. The presented methods in our study offers a possibility of personalizing the wedge implant and incorporate this into the existing 3D workflow. Yet, the manufactured implants were designed to accurately match opening-wedge height and outer shape of the bone. Adjustment of the lower scaffold end enabled proper fit into the osteotomy plane, while assuring sealing of the gap. Precisely sealing of the whole gap was proven to be challenging in the current setting. Most likely, a perfect fit can be achieved when using 3D printed patient specific instruments (PSI), with pre-operatively determined saw cuts and resulting gap morphology. In some cases of malalignment correction, PSI are preferred by orthopaedic surgeons, in the form of saw and burr guides per-operatively. This study offers the possibility of adding a personalized wedge implant into this workflow. With predetermined bone cuts and gap morphology, our wedge scaffold can be 3D printed pre-operatively to fit. However, the current study focussed on the feasibility of implanting such a 3D printed wedge scaffold, without compromising the pre-operatively planned wedge height.

While most of the load on the osteotomy gap is absorbed by the angular stable plate and screws, the implant should remain stable during the brief period before the plate is fixed. The elastic modulus of the implants presented similarities to human trabecular bone[414]. Scaffolds with a planned fibre spacing of 1.0 mm maintained open pores, through which *in vivo* bone marrow would be allowed to flow in and accelerate osteogenesis. While implant height was maintained post-implantation into the cadaveric legs, future *in vivo* and clinical studies are needed to confirm preservation of pre-planned wedge height during implantation, as well as speed of bone union.

The full-size implants degraded over time in an accelerated *in vitro* setup using an enzymatic solution. Prior research reported that degradation of the MgPSr-PCL (pore size 1 mm) in the enzymatic solution for ten days corresponds to six months *in vivo* implantation, in a non-load bearing area in an equine model[412]. Increasing inter-fibre spacing accelerated degradation by 30% in mass loss, indicating that *in vivo* mass loss might also be accelerated. However, the exact degradation and speed of bone formation of the osteotomy-specific implants in this specific anatomical location should be evaluated in a large animal model.

The printed MgPSr-PCL material facilitated osteogenesis *in vitro*, similar to previous work[412]. For large defects, pre-seeding of the scaffold with a regenerative compound, like MSCs, might be beneficial to accelerate bone healing. Seeding of the material with both culture-expanded MSCs and BMC resulted in production of osteoblast-specific markers, indicating that infiltrated bone marrow in the scaffold material after implantation may be sufficient by itself to stimulate osteogenesis. This is most likely induced by its growth factor-rich nature and the presence of progenitor cells[96]. While fabrication of personalized 3D implants from patient imaging data was demonstrated before for orthopaedic applications[415,416], this study is the

first to report on a personalized biodegradable implant for OWO.

The current study was mainly limited by the imbalance between preoperative osteotomy planning and the intra-operative surgical plane, leading to a slight mismatch between gap and scaffold. By implementing 3D printed PSI in the workflow, an optimal fit of the designed implant can be achieved. Because the purpose of this study was to design and manufacture a gap-filling wedge implant in an osteoinductive material and to evaluate this in an *ex vivo* model, achieving a perfect fit was beyond the scope of this investigation.

CONCLUSIONS

To conclude, we have designed and manufactured a gap-filling implant for open-wedge osteotomies. This implant was 3D manufactured using an osteoinductive and biodegradable material that supported cell attachment, growth, and production of early and late osteogenic markers *in vitro*. Finally, we successfully performed an *ex vivo* proof-of-concept of the surgical procedure, implementing the designed wedge scaffolds into the standard osteotomy procedure, while maintaining implant integrity and pre-planned wedge height.

SUPPLEMENTAL FIGURE

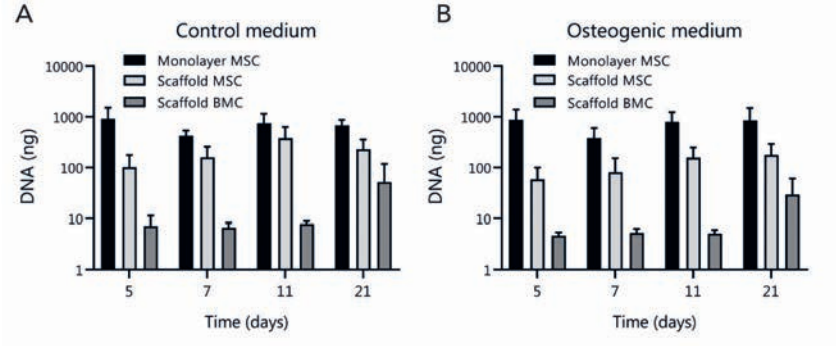

Supplemental Figure 1. DNA quantification. Quantification of DNA in scaffolds seeded with bone marrow-derived mesenchymal stromal cells (MSC) and bone marrow concentrate (BMC) compared to MSCs cultured in monolayers as controls.

Chapter 9

General discussion and future implications

Damage to articular cartilage does not only considerably increase the risk of osteoarthritis (OA) development later in life[4], symptomatic focal defects on their own have significant impact on the daily life of patients through development of pain, swelling, and limitation in function and sports activities. The incidence of OA in the adult population is around 15%, of which knee OA accounts for 80% of the cases[28]. In the Netherlands, OA is one of the three prime chronic diseases in the population and its incidence is expected to have doubled by 2040[417], emphasizing the importance of timely treatment of cartilage lesions to prevent OA development. The current treatment options for chondral defects vary from bone marrow stimulation techniques and cell-based repair through autologous chondrocyte implantation (ACI), to treatments using orthobiologics. In addition, (the progression of) early OA may be delayed by intra-articular injections with viscosupplements or corticosteroids, joint stabilization, or limb realignment, depending on the existence of any underlying pathologies. As outcomes of all interventions are variable and cartilage regeneration in humans continues to be a challenge, there is a need for improvement of therapies.

As such, within the context of the current challenges in cartilage repair, the overall aim of this thesis was to advance articular cartilage regeneration by investigating novel cell types and optimization of current treatments for patients with focal chondral defects. For this purpose, the results in this thesis were presented in two separate sections. The first section was specifically aimed at cell-based cartilage repair, by using cartilage and meniscus progenitor cells, as well as cocultures of cells and tissues. The second section of this thesis explored the potential of orthobiologics to advance cartilage repair or aid in a cartilage-preserving surgical procedure. Together, both sections share the common goal of advancing cartilage regeneration based on a biological mode of action.

CELL-BASED CARTILAGE REGENERATION

As cells construct the main building blocks for articular cartilage during fetal development[231], repair or regeneration of the damaged chondral layer in a fully developed individual through biological restoration holds significant potential. Nevertheless, cell and matrix turnover in mature normal articular cartilage is minimal[17,18]. With the use of culture-expanded chondrocytes, a treatment to repair chondral defects with good success rates is available. As the main disadvantage of this approach remains the two-step nature, which goes hand in hand with loss of chondrogenic phenotype of the cells during culture[168,169], improvements for this procedure could further enhance outcomes.

Synovial joint progenitor cells

During fetal development, chondrocytes arise from mesenchymal progenitors and actively synthesize and organize the extracellular matrix (ECM) of articular cartilage[418]. Roughly two decades ago, the first indications of the presence of a progenitor cell in human adult articular cartilage were found[15,16,90,141]. In **Chapter 3**, we have investigated this endogenous progenitor

cell for its extensive proliferative and chondrogenic potential. Articular cartilage-derived progenitor cells (ACPCs) have generated interest to replace chondrocytes in ACI-like procedures due to these characteristics.

While the employed isolation protocol and culture technicalities in **Chapter 3** were identical to previously published works[90,116,141], the cells in our study lacked the capacity to produce mineralized matrix upon osteogenic stimulation of differentiating into osteoblasts, one of the key features of ACPCs described by others. Yet, osteogenic differentiation is not as evident in all published literature. In fact, absent or limited expression of osteogenic markers in ACPCs has been reported rather consistently[92,93,116,118]. Furthermore, activation of genes associated with hypertrophic chondrocytes, upregulated in bone marrow-derived mesenchymal stromal cells (MSCs) when stimulated with chondrogenic factors, was consistently low or absent in the described ACPC populations[92,95,116,166]. The various responses by ACPC populations to osteogenic stimulation could be a result of species and donor variation. In addition, minor differences in isolation procedures and culture conditions or media compositions could have amplified these dissimilarities. Nevertheless, these limitations in osteogenic and hypertrophic chondrocyte drift of ACPCs could be beneficial for application in cartilage regeneration.

One of the important features of MSCs is that these cells are immunomodulatory, due to their capacity to ameliorate an inflammatory environment by secretion of anti-inflammatory factors and interaction with immune cells[419,420]. Increasingly, evidence arises that ACPCs possess similar (or at least mild) immunomodulatory capacities. ACPCs released a larger concentration of anti-inflammatory cytokines after injury than chondrocytes[125]. Furthermore, ACPCs inhibited proliferation of peripheral blood mononuclear cells[421] or lymphocytes[128], a measure generally used to assess immunomodulatory properties of MSCs. Although these findings need to be confirmed in *in* vivo studies, they can potentially extrapolate the therapeutic potential of ACPCs.

The discrepancies between differentiation outcomes of the study presented in **Chapter 3** and other published literature directly highlight the main limitation in ACPC research, which is characterization of isolated populations. MSCs too are a heterogeneous cell population of which characterization is a persisting challenge. Cartilaginous tissue engineered from bone marrow-derived MSCs has been shown to be substantially different from native articular cartilage[85]. Further investigation of the engineered tissues resulting from ACPC-derived (or meniscus progenitor-derived, **Chapter 4**) tissue engineered or *in vivo* implanted cartilage could provide further insight in the differences and similarities to native cartilage and provide for indications to further optimized differentiation cultures. In light of the complexity and variety of ACPC research, **Chapter 2** of this thesis provided for a systematic summary of all ACPC investigations and presents guidelines to align future studies.

Enhancing regeneration with cocultures or minimally manipulated products

Although repair of focal chondral defects using a single, autologous cell type has been proven to be effective and is used clinically, the ACI procedures still deal with several challenges, such as the two-step nature of the procedure, detachment of the graft[65], or formation of hypertrophic cartilage[46]. Combining different cell types or tissue types, so-called cocultures, circumvent several issues and practical limitations associated with autologous cell application, like processing time, costs of culture and surgical procedure[68], change of phenotype during *in vitro* culture of cells, and limitations in cell yield of the autologous product. Likewise, simplification of the procedure by using minimal manipulated products, like minced pieces or cartilage and bone marrow concentrate (BMC), are of interest for clinical application and translatability.

The culture combinations described in **Annex I**, involve cells from easily accessible tissues that underwent minimal manipulation and have the potential to move therapies towards single-stage procedures. Minced pieces of cartilage provide a product that can easily be harvested from the rim of a focal defect, a part that is discarded in regular ACI procedures. If enough cartilage can be dissected from the injured area or a non-weight bearing site of the knee joint, minced pieces of cartilage can be used as an autologous single-stage procedure. Alternatively, allogeneic particulated juvenile cartilage is currently offered as an FDA-approved treatment option with satisfactory short-term outcomes[422,423]. Such allogeneic procedures are attractive as they can be applied as a one-step and off-the-shelf approach, but hampered by limited donor availability. Although not investigated in this thesis, the size of the pieces of cartilage most likely correlates to outcomes in terms of cartilage matrix formation[424]. Likewise, cartilage paste[425] was found to relieve pain and improve function for over 15-years follow up[426], further underlining the potential of minced pieces of cartilage.

Similar to microfracture (MF) treatment for smaller focal defects, bone marrow concentrate (BMC) combines growth factors and cells from the bone marrow, which can be used as a treatment for cartilage repair[96,427]. BMC allows for control over application site, dosage, and blending with cells, bioactive cues, or materials. While BMC is presently used to treat critical limb ischemia, ligament injuries, and stimulate bone regeneration, results of the use of BMC for treatment of cartilage injury vary, although they are promising[96]. The use of BMC in **Chapter 8** and **Annex I** for both cartilage and bone regeneration, is limited to *in vitro* investigations. Although cartilage ECM formation by BMC, whether or not in coculture with chondrons or minced pieces of cartilage, was unsuccessful (**Annex I**), for bone repair it showed clear indications of mineralized matrix formation in magnesium strontium phosphate-polycaprolactone (MgPSr-PCL) scaffolds (**Chapter 8**). The application of BMC for the purpose of bone regeneration might therefore exceed their potential for chondral repair. Nevertheless, clinical use of BMC for cartilage has been shown to be safe and to some extent effective[428,429]. The joint environment most likely plays an indispensable role, making *in vivo* and bioreactor studies pivotal in further investigations.

Combined culture of MSCs and chondrons or chondrocytes has been shown to successfully generate neo-cartilage *in vitro,* as well as *in vivo*[115,430] and allogeneic MSCs can replace up to 90% of the autologous cells needed to achieve a cell density sufficient to fill a focal chondral defect[115,290]. Yet, it is uncertain how these multipotent cells contribute to enhanced cartilage regeneration. Their main mode of action is attributed to chondroinduction through cellular communication[113,274]. Despite the fact that MSCs disappear during *in vitro* coculture with chondrocytes[71,274], as well as in a clinical setting[115], communication between the two cell types, even during a relatively short time window, seems to be crucial for neo-cartilage formation[274]. One of the proposed mechanisms responsible for this stimulation was investigated in **Chapter 5**, where, for the first time, cellular communication between human chondrocytes and MSCs through exchange of mitochondria was shown. In tissues other than articular cartilage, MSCs were found to be responsible for induction of regeneration or protection of damage[288,298,431,432]. The transfer of MSC-derived mitochondria to chondrocytes seemed to be at least partly responsible for a proliferative and chondrogenic effect *in vitro*. The presented results in **Chapter 5** contribute to identifying the mechanisms of action in these cocultures and pave the road towards enhancement of MSC-therapies or off-the-shelf products. Just like MSC-derived extracellular vesicles (EVs)[76], MSC-derived mitochondria carry less risks than cells, as they cannot replicate or transform into tumorigenic cells. Replacing cells by mitochondria, EVs, or another chondropromotive compound, has potential to make a therapy safer, simpler, and more targeted at an intended effect.

ORTHOBIOLOGICS

In addition to directly improving the cellular component in ACI procedures, there is an ongoing search for improvement in other elements of the therapy, such as the replacement of animal-derived products, including the porcine collagen scaffolds used for matrix-assisted autologous chondrocyte transplantation (MACT)[43]. The current ACI treatment approved in the European Union makes use of chondrocyte spheroids, eliminating the need for an (animal-derived) scaffold or cover which was necessary in previous generations ACI[433].

Blood-derived products like platelet-rich plasma (PRP) and platelet lysate (PL) share the potential to contribute to improvement of therapies, as these can be used as autologous and minimal manipulated products. Besides direct application of both products for (early) OA, PL is broadly investigated as a cell culture additive, replacing (animal) serum and exogenous growth factors. The option to replace serum with PL for culture-expansion of chondrocytes was investigated in **Chapter 6** of this thesis, providing a large pool of growth factors stimulating chondrocyte growth and maintaining differentiation potential after expansion. As currently autologous serum is used for chondrocyte expansion in ACI procedures[434], replacing this for autologous PL is realistic and underscores its promise for clinical application.

In an effort to further investigate blood-derived products in ortho-regeneration, **Chapter 7** described that platelet-rich plasma (PRP) is inferior to fibrin glue for cartilage tissue engineering and that its anti-inflammatory properties on chondrocytes are limited. *In vitro* investigations into the use of PRP for these purposes are scarce and consensus on the chondrogenic effects of PRP is lacking[4,35]. Still, a consistent stimulation of cell proliferation by PRP is seen throughout literature[362,363], in line with our observations in **Chapter 7**, which might be correlated to clinical benefits. Even though several clinical trials report on comparable effects of intra-articular PRP injections and placebo, others do see an improvement in pain and patient mobility[79]. Upon intra-articular injection, the high concentrations of growth factors in PRP[352] might provide an initial boost in cell proliferation and repression of inflammation, after which regeneration can take place.

PERSPECTIVES IN CELL-BASED TREATMENTS FOR CARTILAGE INJURY

Putting the results of this thesis into perspectives, it can be questioned what exactly the current challenges and setbacks are in cell-based cartilage regeneration and what improvements can be made based on the presented data. Although reported patient outcomes up to several decades after an ACI procedure are reported satisfactory, several aspects of the procedure and biological features of the regenerating cartilage show room for improvement. Firstly, the two-step nature of the surgical procedure is time consuming and costly, while also resulting in additional burden for the patient. In parallel, the inevitable culture-expansion of autologous chondrocytes causes cell dedifferentiation and is lengthy. Lastly, the newly formed repair tissue can be inferior fibrous cartilage, or even hypertrophic cartilage, as opposed to regenerated hyaline cartilage. Looking at these before mentioned challenges, the results discussed in this thesis could provide improvements of each of them.

Improving cell-based treatments for cartilage injury

With regards to direct improvement of the performance of chondrocytes and prevention of dedifferentiation during culture-expansion, the approach investigated in **Chapter 6** is promising as it was shown that the cells seemed to maintain their chondrogenic memory when expanded using PL as compared to serum. Moreover, the use of ACPCs (**Chapter 3**) as an alternative autologous cell source would allow faster cell expansion, higher cell yield, and less dedifferentiation. The first in-man study using ACPCs as an alternative in MACT revealed promising histological results and patient outcomes, although ACPCs were not directly compared to chondrocytes in this study[93]. Furthermore, ACPCs might provide for an allogeneic off-the-shelf product as there are some early indications that the cells have a role in immunomodulation[125,179]. In line with this, selection for highly chondrogenic clones could be performed, providing for a stable cell source and supply. This would also allow for the use of tissue progenitors from other tissues in the synovial joint, like the meniscus-derived progenitor cells in **Chapter 4**, which also showed chondrogenic differentiation capacity. Harvesting of a cell source would be made easier as both ACPCs and meniscus progenitor

cells can be isolated from redundant material after surgeries.

A second improvement is to replace the autologous expanded chondrocytes by a well-performing coculture of different cell or tissue types to pursue a single-step approach. In **Annex I**, we have provided for initial evidence of cell and tissue combinations that have the potential to replace the currently used cell products. However, these indications are still preliminary as the options vary and the best culture combination is yet to be identified. Coculture combinations using minimal manipulated products, like BMC with minced cartilage or MSCs with minced cartilage, both provide a feasible possibility for single-stage procedures which would in turn eliminate the disadvantages of the two surgical procedures. Furthermore, in **Chapter 5**, we have established initial evidence of a mechanism that might be responsible for chondroinduction of chondrocytes by MSCs in coculture. Further in-depth research could lead to establishment of novel compounds, (a cocktail of) factors, or off-the-shelf MSC-derivatives, potentially making the MSC itself redundant.

Improving cartilage-preserving treatments and bone repair

Besides improvement of cell-based procedures for chondral regeneration, patients with unicompartmental OA can benefit from realignment of the lower limb through an open-wedge tibial or femoral osteotomy (depending on the specific nature of the malalignment). As discussed earlier in this thesis, the main limitations here are postoperative pain, most likely caused by haematoma formation from the open bone and delayed or absent union of the bone. The improvement for the osteotomy procedure presented in **Chapter 8** could resolve these issues by filling the defect and at the same time stimulating osteogenesis by the material. Moreover, donor site morbidity poses a major challenge when an autologous bone graft is needed[436]. While pain at the donor site (usually ileac crest) can be reduced by reconstructing the graft site with synthetic bone fillers[400,437], complete elimination of the need for an autograft provides an effective solution to this problem.

The findings in **Chapter 8** can be extrapolated to serve more than just one purpose. The additive manufacturing method of fabrication of the used MgPSr-PCL material provides for endless freedom and possibilities to translate into specialized and personalized purposes. Other than filling open wedges in knee or other joint osteotomies, it could also serve as a bone anchor to stabilize osteochondral implants or made into patient-specific implants in critical-size bone defects, for example after tumour resection.

MOVING TOWARDS PERSONALIZED, WHOLE-JOINT REGENERATIVE APPROACHES

In view of the regeneration of focal chondral defects, we have provided several building blocks to be translated into an osteochondral approach to treat late-stage OA. Yet, it is unlikely that the biological solutions presented in this thesis on their own are sufficient to survive the harsh mechanical environment in the synovial joint or imitate the natural structure of hyaline

cartilage. While not investigated here, a multidisciplinary approach that combines biology with mechanical stability is necessary[438]. Convergence of the proposed biological procedures with biofabrication approaches would allow for addition of mechanical stability and complex structures[105,106,190,439–441]. By doing so, personalized implants or bigger structures are within reach. One important aspect of joint regeneration which was not discussed in this thesis is the mechanical stability of an implant. In light of designing and producing a successful bigger osteochondral or (partly) joint-replacing implant, it must be able to withstand the forces that are exerted on the joint as long as the tissue is not regenerated yet. To this extent, several additive manufacturing approaches are available to combine soft matrices with thermoplastic materials, adding mechanical stability to a tissue engineered construct[440,441].

To fabricate the chondral part of an osteochondral implant, ideally an optimized cell product in the shape of PL-expanded autologous chondrocytes, (allogeneic) progenitor cells, a coculture combination, or an off-the-shelf regenerative product can be combined with a reinforced cell carrier. This could be a reinforced hydrogel[439,442] serving as a synthetic, yet biodegradable ECM that matches (or approaches) the mechanical stability of native hyaline cartilage. The chondral part can subsequently be combined with an osteal component that works as an anchor and at the same time induces osteoinduction. The setup of the osteoinductive MgPSr-PCL combined with BMC as shown in **Chapter 8** is an example of such a regenerative bone compartment. Alternatively, BMC might not be essential for regeneration as marrow flowing into the scaffold from the bone could be sufficient on its own, demonstrated in a previous *in vivo* study[412]. Mimicking native hyaline cartilage, the distinct chondral and osteal compartments should ideally be separated by a closed tidemark, serving a dual function. In the natural structure of articular cartilage, the tidemark marks the interface between the calcified and noncalcified cartilage and plays a role in inter-cellular communication and transmission of mechanical loads[443,444]. On the other hand, it should serve as a secure integration of the two compartments. Such a structure can be fabricated using additive manufacturing, ensuring a tight integration of the multimaterial structure[188]. Moving from rather basic shaped cylindrical implants towards more challenging shapes and full-joint approaches, biofabrication techniques allows for attaining challenging shapes and complex structures[105,190,445].

In the end, this could provide for a biological, regenerative replacement of a partly or total joint arthroplasty, which would be long-lasting and allow for a dynamic natural environment as opposed to a static metallic implant.

Are we moving forward towards clinical application?

Translation of the proposed solution towards a clinical application faces several hurdles. Long-term *in vivo* evaluations in large animal models relevant for chondral or osteochondral repair, like the porcine, equine, or caprine models[446], are essential to assess both implant stability and regenerative potential over time in the *in vivo* joint environment. Preceding a large animal

model with *ex vivo* models to evaluate scaffold performance provides for initial information on integration and regeneration before moving towards *in vivo* models[447,448]. More importantly, *ex vivo* models contribute to the transition to animal-free testing in advanced *in vitro* models, like bioreactors[449], organs-on-chip[450], and *in silico* models[451].

Besides evaluation of mechanical and biological performance of an implant, it is essential for clinical translation that a cell product, (bio)materials, and culture- and fabrication processes comply with Good Manufacturing Practice. In addition, the use of clinically approved materials or valorisation of materials and production methods is essential to successfully translate the current regenerative medicine techniques into clinical reality[452,453].

GENERAL CONCLUSION

With this thesis, we aimed to advance cartilage regeneration by evaluation of biological solutions to treat patients with focal chondral defects. Optimization of chondrogenic regeneration can be achieved by enhancing the performance of the currently used cell products or replacing the product by one that has the potential to be conducted in a single-step approach. Both proposed methods would contribute to improvement of long-term clinical outcome.

Not only would translation of the proposed techniques lead to an improvement of the current treatment methods for treating cartilage defects, combining the described methods in a multimaterial and multidisciplinary approach could contribute to the development of a whole-joint replacing strategy, significantly extending the clinical potential of the presented results.

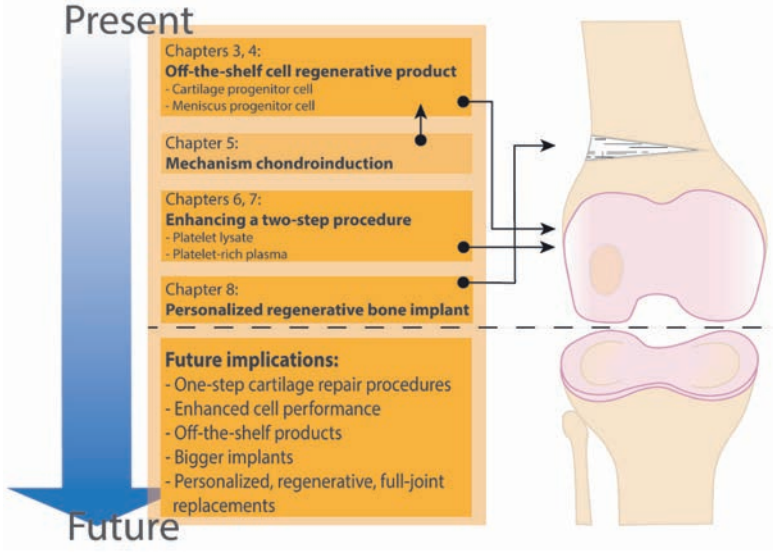

Figure 1. Chapter contributions to improve cartilage regeneration and joint preservation, as well as future implications moving towards clinical translation and whole-joint approaches.

Appendices

Annex I

Chondrogenenic performance of cocultures for use in a fibre-reinforced hydrogel system

Margot Rikkers
Iris Pennings
Riccardo Levato
Jos Malda
Lucienne A. Vonk

Preliminary data

ABSTRACT

Introduction

Treatment of focal damage in articular cartilage poses a challenge in orthopaedic research. A tissue engineered product that combines biological performance and mechanical stability might provide a promising solution. This study aimed to identify a cell product with high chondrogenic capacity and combine this in a confined swelling hydrogel in order to generate hydrostatic pressure and stimulate intrinsic neo-cartilage formation by the cell product. This chapter describes the preliminary results of this study.

Methods

Chondrocytes, chondrons, and articular cartilage-derived progenitor cells (ACPC) were isolated from human osteoarthritic (OA) and normal cartilage. Human mesenchymal stromal cells (MSC) were isolated from bone marrow aspirates. Equine cartilage was obtained for processing into minced pieces of cartilage, as well as chondron isolation. Equine bone marrow was processed into bone marrow concentrate (BMC). Coculture combinations were cultured for 28 days in fibrin and deposited proteoglycans were quantified and evaluated by safranin-O staining to assess chondrogenic potential of the cell products. Additionally, cytocompatibility of a photocrosslinkable chondroitin sulfate-hyaluronic acid (CSMA/HAMA) hydrogel was evaluated with two cell products which showed chondrogenic potential. Metabolic activity was measured by conversion of resazurin to resorufin and cell viability was visualized using Live/Dead stain during seven days.

Results

Cocultures of human chondrocytes and chondrons with MSCs showed some indications for proteoglycan deposition on histological level. In equine cells and tissue products, the coculture of chondrons and MSCs showed production of proteoglycans in one out of two donor combinations. Additionally, the coculture of minced cartilage and MSCs showed indications of proteoglycan deposition. Chondron/MSC coculture and healthy cartilage-derived ACPCs were selected for assessment of cytocompatibility in CSMA/HAMA, and were compared to fibrin. Metabolic activity, as well as cell viability in CSMA/HAMA was lower compared to fibrin during seven days in both conditions.

Conclusion and future implications

Based on the preliminary results presented in this study, a coculture of chondrons and MSCs held the highest capacity of neo-cartilage formation in fibrin *in vitro*. Additionally, CSMA/HAMA did not support cell viability and further optimization of the cell-supporting capacities of the hydrogel is needed. Future converging of a swelling hydrogel in a confining fiber-reinforced scaffold could generate hydrostatic pressure to induce endogenous growth factor production, as well as resulting in a construct with mechanical characteristics similar to articular cartilage.

INTRODUCTION

Treating acute injury of articular cartilage poses a major challenge in orthopaedic research. Due to the avascular and aneural nature of the tissue, endogenous regeneration is limited. Current therapies mainly focus on cell-based approaches, leading to satisfactory patient outcomes[454,455]. Nevertheless, repair tissue can be of lower quality than the original hyaline cartilage[46], leading to development of osteoarthritis (OA) early in life[9]. Combining biological performance and mechanical stability in a tissue engineered chondral implant can provide a promising solution.

Finding an optimal cell source, or combination of cells or tissue products, is essential to improve matrix formation. Coculturing chondrons or chondrocytes with mesenchymal stromal cells (MSCs) was shown to enhance extracellular matrix (ECM) formation both *in vitro*[71,290,456] and *in vivo*[115,290] by chondroinduction. A chondron is characterized by the presence of its pericellular matrix, mainly consisting of type VI collagen, which in the native tissue connects the cell to the territorial and interterritorial matrix[457,458]. The pericellular matrix also mediates the sensing of the surrounding ECM and plays an important role in mechanoregulation[459]. Recently, other cell sources for cartilage regeneration have been investigated. Articular cartilage-derived progenitor cells (ACPCs) are an endogenous population of multipotent cells in articular cartilage[15,16]. The extensive expansion potential and preservation of chondrogenic potential of this cell type raises interest for use in cartilage tissue engineering. Besides using isolated cells as therapeutic agents, working with minimal manipulated tissue products may help regenerative strategies while also benefitting from a more streamlined regulatory process and thus accelerating clinical translation. Among minimally manipulated products, minced pieces of cartilage[424,426] and bone marrow concentrate (BMC)[96,428] have gained attention. The ease of preparation of these products gives great advantages for autologous use in one-step procedures.

Cell differentiation and matrix production can be effectively stimulated by the addition of exogenous growth factors, like transforming growth factor beta (TGF-β). Alternatively, application of hydrostatic pressure by mechanical loading stimulates production of endogenous TGF-β, found in bone marrow-derived MSC cultures[460]. Subsequently, mechanical loading promotes chondrogenesis of both MSCs[460] and ACPCs[144]. In normal hyaline cartilage, hydrostatic pressure is a consequence of the tissue's unique combination of stiff collagen fibers and water-attracting proteoglycans[13]. Mimicking this naturally pressured environment could be an efficient way of stimulating cells to producing their necessary growth factors for cartilage ECM production.

In order to imitate the unique features of cartilage tissue, a hydrogel precisely designed to display high swelling, combined in a stiff, confined scaffold environment could stimulate cells to produce endogenous growth factors and make the addition of growth factors to the construct redundant. Furthermore, it would provide a mechanically stable implant that can withstand the forces in the joint. Incorporating a gel in a highly organized, melt-electrowritten (MEW) scaffold would not only provide the construct with increased mechanical stability[441], but also restrict the gel's swelling if the outside borders are closed. By printing thin fibers of poly(ε-caprolactone) (PCL) in columnar boxes with closed layers at both ends[461], the natural alignment of collagen fibers in articular cartilage is reproduced.

Hydrogels consisting of polysaccharides that naturally occur in the cartilage, like chondroitin sulfate (CS) and hyaluronic acid (HA) have shown their potential to encapsulate cells and support cell growth[462–464]. Due to its abundant negative charges, CS is responsible for attracting water into the cartilage,

contributing to the tissue's metabolism. HA is a non-sulfated glycosaminoglycan that is abundant in native hyaline cartilage. Addition of this viscous component improves rheological and mechanical properties of the hydrogel[465]. Furthermore, increased viscosity by addition of HA also enables possible future translation into biofabrication approaches[465]. Methacrylation of CS (CSMA) and HA (HAMA) allows the biomaterials to be crosslinked by ultraviolet (UV) or visible light into a network consisting of both molecules[463,466]. This enables covalent crosslinking under mild conditions which has been shown to be compatible with culture of encapsulated cells[465,467,468]. Confinement of the swelling of a gel would generate a build-up of hydrostatic pressure in the construct, without the need for external mechanical loading.

The aims of this study were to 1) select an optimized cell product, or coculture of cell products, to advance cartilage regeneration, 2) to evaluate cytocompatibility of a swelling hydrogel that mimics the ECM of hyaline cartilage, and 3) to combine the cell product and swelling hydrogel in a stiff scaffold in order to retain swelling and generate hydrostatic pressure taking away the need for exogenous growth factors.

METHODS

Study setup

To evaluate chondrogenic potential of different cell types, minimal manipulated products, or coculture combinations, long-term cultures in fibrin gel were performed. The production of glycosaminoglycans, one of the major ECM components of hyaline cartilage, was considered the main outcome. Cultures were performed without addition of exogenous growth factors, to examine performance of the cells alone. Secondly, the best-performing cultures were selected for culture in a swelling hydrogel consisting of methacrylated CS and HA in a pilot experiment to assess cytocompatibility.

Tissue isolation and cell expansion

Human OA cartilage was collected from either redundant tissue from patients who had undergone total knee arthroplasty (according to a protocol approved by the medical ethics committee of the University Medical Center Utrecht) or macroscopically normal cartilage from post-mortem from full-weight-bearing and non-weight-bearing locations of the knee (Department of Pathology, University Medical Center Utrecht). Chondrons were isolated overnight using dispase II (0.1% (w/v); Gibco, Netherlands) and collagenase II (0.1% (w/v); CLS-2, Worthington, Lakewood, NJ) in Dulbecco's Modified Eagle's Medium (DMEM; 31966; Gibco, Netherlands) supplemented with human serum albumin (HSA; 1%; Albuman, Sanquin Blood Supply Foundation) and penicillin/streptomycin (1% (v/v); pen/strep;100 U/mL, 100 µg/mL; Gibco, Netherlands). Chondrons were used directly after isolation. Chondrocytes were isolated overnight using collagenase II (0.15%) in supplemented DMEM. Chondrocytes were used directly after isolation, or culture-expanded to passage two in DMEM supplemented with fetal bovine serum (FBS; 10% (v/v); Biowest) and pen/strep (1%). For isolation of ACPCs, the total cell digests from cartilage were seeded at 500 cells/cm^2 on fibronectin pre-coated culture plates (1 µg/mL in phosphate-buffered saline (PBS) containing $MgCl_2$ and $CaCl_2$; Sigma-Aldrich) using DMEM with pen/strep (1%). Non-adhered cells were washed away after twenty minutes and adhered cells were culture-expanded using DMEM supplemented with FBS (10%), l-ascorbic acid 2-phosphate (ASAP; 200 µM; Sigma-Aldrich), pen/strep (1%), and basic fibroblast growth factor (bFGF; 5 ng/mL; PeproTech). After six days, colonies of >32 cells[90] were isolated, pooled, and expanded further on conventional tissue culture plastic.

Human mesenchymal stromal cells (MSCs) were isolated from iliac crest bone marrow aspirates of patients receiving spondylodesis or total hip arthroplasty surgery, after their informed consent and according to a protocol approved by the local medical ethics committee (University Medical Center Utrecht). The mononuclear fraction was separated using Ficoll paque (GE Healthcare) and MSCs were culture-isolated by plastic adherence. MSCs were expanded in Minimum Essential Media (αMEM; Gibco) supplemented with FBS (10%), ASAP (200 μM), bFGF (1 ng/mL), and pen/strep (1%) and used in passages four to six.

Macroscopically healthy equine cartilage was obtained from the metacarpophalangeal joints of two donors (donated to science by the owners) and chondrons were isolated as described above. Another portion of the cartilage was minced into pieces of ~1 mm. Equine bone marrow was obtained from the sternum of the same donors and BMC was prepared using the LAVA™ Cell Concentration device (DSM, Exton, PA) according to the manufacturer's instructions. MSCs of one additional donor were isolated and expanded as described above.

Fibrin gel cultures

Cell-laden fibrin gels were prepared by resuspension of the cells or cell products (2.5×10^6 / mL) in 15X diluted fibrinogen in PBS, crosslinked with 50X diluted thrombin in PBS (both Tisseel, Baxter). Cocultures were prepared in a ratio of 10% chondron/chondrocyte/minced cartilage (of which cell density was determined by cell isolation overnight) and 90% MSC/BMC (mononuclear cell count). Gels were incubated for fifteen minutes at 37ºC, after which they were cultured for 28 days in experimental medium consisting of DMEM supplemented with HSA (1%), ASAP (200 μM), 2% insulin-transferrin-selenium (ITS)-X (2% (v/v); Gibco), and pen/strep (1%). Medium was changed twice per week.

Glycosaminoglycan and DNA quantification

After 28 days, gels were digested overnight in a papain digestion buffer (250 μg/mL papain; Sigma-Aldrich, 0.2 M NaH_2PO_4, 0.1M EDTA, 0.01M cysteine, pH 6) at 60ºC. Glycosaminoglycans (GAGs) were quantified using a dimethyl-methylene blue (DMMB; pH 3) assay. The 525/595 nm absorbance ratio was measured using chondroitin-6-sulfate (Sigma-Aldrich) as a standard. Total DNA content was quantified using a Quant-iT PicoGreen dsDNA assay (Invitrogen) according to the manufacturer's instructions. Fluorescence was measured at 485 nm excitation and 535 nm emission.

Histology

Gels were fixed in 4% buffered formaldehyde, dehydrated through graded ethanol steps, and embedded in paraffin. Sections of 5 μm were cut using a microtome and stained for GAGs using 0.125% safranin-O (Merck) counterstained with 0.4% fast green (Sigma-Aldrich) and Weigert's hematoxylin (Clin-Tech).

Cell-laden swelling hydrogel cultures

Methacrylated CS and HA were synthesized as previously described [466]. Cell-laden gels were prepared by resuspending 2.5×10^6 / mL cells (chondron/MSC or healthy cartilage-derived ACPC) into CSMA/HAMA hydrogel precursor (CSMA:HAMA ratio 6.5 : 1, 10% (w/v) in PBS with 0.2% (w/v) lithium phenyl(2,4,6-trimethylbenzoyl)phosphinate photoinitiator (LAP, Tokyo Chemical Industry, Japan)). The gel-cell suspension was casted in Teflon cylindrical molds (diameter: 5 mm, height: 2 mm) and UV-crosslinked at 365 nm for fifteen minutes, after which the gels were transferred to experimental

medium. Cell-laded fibrin gels of identical volume were used as controls and prepared as described before.

Cell viability in swelling hydrogel

After one, three, and seven days, gels were harvested for analyses. Cell distribution and viability were analyzed using the Live/Dead Viability/Cytotoxicity Kit for mammalian cells according to the manufacturer's instructions (Thermo Fisher). Images were acquired with a Leica SP8X Laser Scanning Confocal Microscope and Leica LASX acquisition software. Metabolic activity of cells in the gels was measured by the conversion of resazurin to resorufin (44 mM; Alfa Aesar) at 560 nm excitation and 590 nm emission.

RESULTS AND DISCUSSION

Identification of a cell product with maximized neo-cartilage deposition

Human chondrocyte versus chondrocyte/MSC coculture

Comparison of OA cartilage-derived chondrocytes (n = 5 donors) in monoculture or cocultured with human MSCs revealed no detectable differences in quantified GAGs in the fibrin gels (Figure 1A, left panel). The amount of DNA in the samples was slightly lower in cocultures compared to monocultures (Figure 1B, middle panel). This trend might be explained by the fact that MSCs tend to stimulate chondrocytes in coculture to produce cartilage ECM and disappear from the culture, as opposed to chondrogenic differentiation of the MSCs themselves[115,456,469]. The production of GAGs per cell (GAG corrected for DNA content) seemed only increased in three out of five donors in coculture compared to monoculture (Figure 1A, right panel). A considerable variation between donors was found, highlighting the importance of preselection of MSC donors for chondroinduction. On histological level, higher deposition of GAGs was seen in coculture gels as compared to monoculture gels (Figure 1B). The produced GAGs were contained around the outer edges of the fibrin gels, whereas the center of the gel is to a lesser extent positive.

Direct comparison of human chondrocyte versus chondron in mono- and coculture with MSCs

Direct comparison of chondrocytes and chondrons derived from two healthy human donors revealed an increased GAG content in monocultures as compared to cocultures of both cell types with MSCs (Figure 2A, left panel). A similar trend is seen for DNA content in the fibrin gels (Figure 2A, middle panel). When GAG content was corrected for the amount of DNA, no differences were observed (Figure 2A, right panel). While donor variation is high, chondrocytes and chondrons from both healthy donors presented here produced considerably more GAGs in monoculture compared to the chondrocytes from OA donors (Figure 1). Furthermore, the amount of DNA in fibrin gels with healthy monocultures is also higher compared to gels with OA donors.

No difference was found between chondrocytes and chondrons, both in mono- and cocultures. In contrast to the biochemical quantification of GAGs, a slight difference in production was detected on histological level. A coculture of chondrons and MSCs showed slight positivity for GAGs in one donor compared to chondron monoculture as well as cultures with chondrocytes. This seems to confirm the importance of the chondrocyte's pericellular matrix and suggests a significant role in ECM formation[470,471]. However, no differences could be seen between conditions of the other cartilage donor, again emphasizing interdonor variability (Figure 2B).

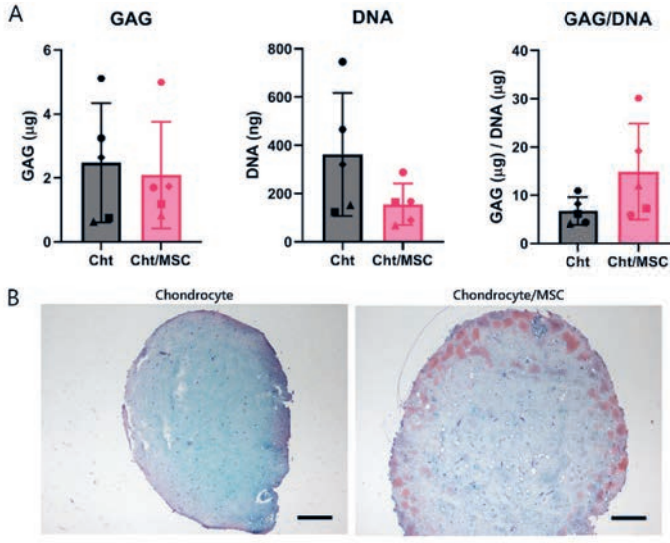

Figure 1. Chondrogenesis of human chondrocyte versus chondrocyte/mesenchymal stromal cell (MSC) coculture. (A) Quantification of glycosaminoglycans (GAG) and DNA content in the fibrin gel constructs containing osteoarthritic (OA) chondrocytes (Cht) or chondrocyte/MSC cocultures. (B) Representative donor of safranin-O histological staining for GAGs (in pink), counterstained with fast green (in blue). Scale bar = 200 µm. N = 5 chondrocyte donors, each shape represents an individual donor.

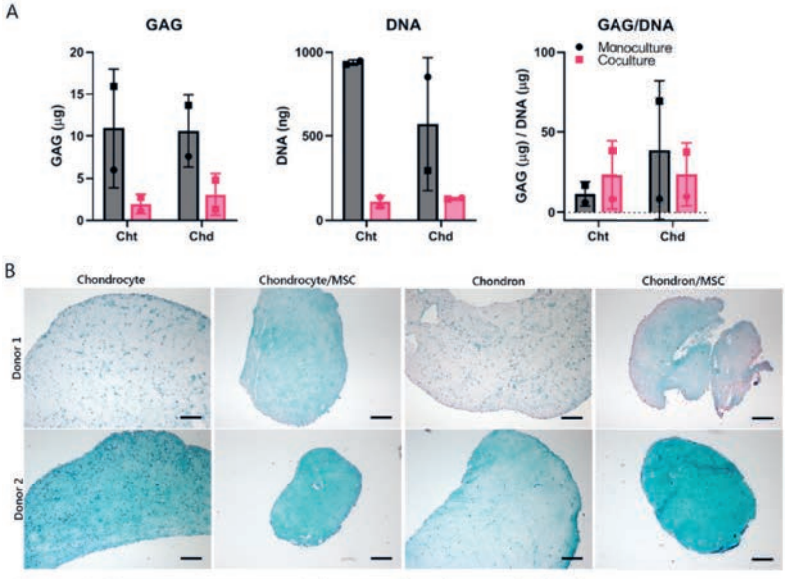

Figure 2. Direct comparison of human chondron and chondrocyte in mono- and coculture. (A) Glycosaminoglycans (GAG) and DNA content in the fibrin gel constructs containing healthy chondrons (Chd), chondrocytes (Cht), or cocultures with MSCs. (B) Microphotographs of both donors stained with safranin-O for GAGs (in pink) counterstained with fast green (in blue). Scale bar = 200 µm. N = 2 cartilage donors, each shape represents an individual donor.

Human articular cartilage-derived progenitor cells as a substitute for chondrocytes

As ACPCs proliferate considerably faster than chondrocytes and maintain their differentiation potential upon prolonged expansion[472], these cells were hypothesized to be an alternative to chondrocytes that quickly lose their differentiation potential upon expansion *in vitro*[213]. ACPCs derived from two healthy cartilage donors and one OA cartilage donor were unsuccessful in GAG production in fibrin gels (Figure 3A, left panel). However, DNA content in both cell types were comparable to that of chondrocytes and chondrons (Figure 3A, middle panel).

The overall production of GAG per cell was considerably lower in the ACPC cultures when compared to chondrocyte and chondron mono- and cocultures (Figure 3A, right panel). In addition, histological analysis shows no evidence of GAG production in ACPC-fibrin gels. The lack of cartilage ECM production by ACPCs might be due to the absence of exogenous growth factors in the current culture setup. Previous work has confirmed the necessity of adding TGF-β to enhance chondrogenesis in ACPCs[472]. Alternatively, exposing the cells to hydrostatic pressure could trigger endogenous TGF-β production to enhance differentiation and replace the necessity of adding exogenous growth factors[144].

Equine chondrons in coculture with mesenchymal stromal cells and bone marrow concentrate

The potential of BMC to substitute MSCs was evaluated for ease of use and autologous application in one-step procedures[68,428]. Furthermore, it combines growth factors, anti-inflammatory proteins, and a small portion of MSCs[96]. While variation between the two donors was significant, coculture of chondrons with autologous BMC performed worse than coculture of chondrons and allogeneic MSCs. Production of GAGs as well as DNA content were decreased in chondron/BMC cultures compared to chondron/MSC cultures (Figure 4A, left and middle panel). Production of GAG per cell was also

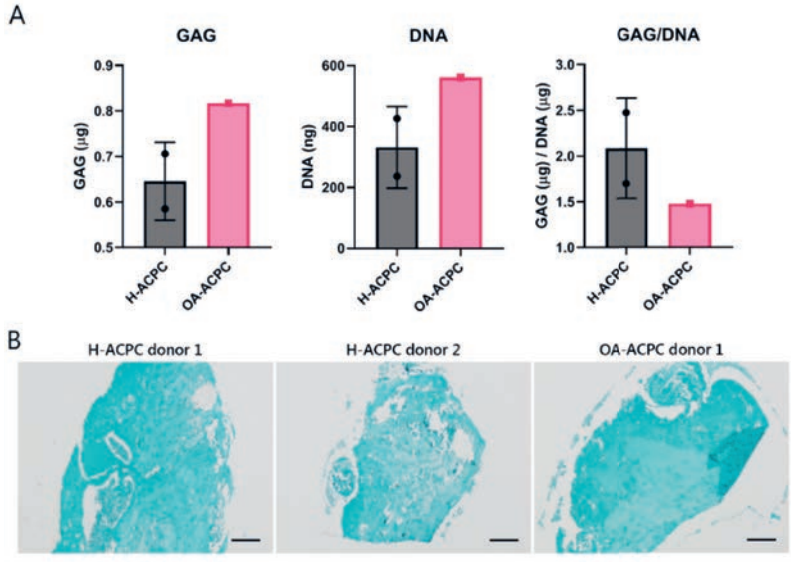

Figure 3. Articular cartilage-derived progenitor cells to replace chondrocytes or chondrons in fibrin gel. (A) Glycosaminoglycans (GAG) and DNA content in the fibrin gel constructs containing healthy articular cartilage-derived progenitor cells (H-ACPC) and osteoarthritic ACPCs (OA-ACPC). (B) Histological staining for GAGs with safranin-O counterstained with fast green (in blue) for the two healthy and one OA donor. Scale bar = 200 µm. N = 2 healthy donors and 1 OA donor.

decreased in chondron/BMC cultures (Figure 4A, right panel). Interestingly, in one equine donor (donor 2), chondron/MSC coculture produced a significant number of GAGs (Figure 4B), while the other donor (donor 1) showed no signs of GAG production. These results suggest that BMC in coculture with chondrons is insufficient in stimulating chondrogenesis in an *in vitro* setting without exogenous growth factors, whereas a coculture of chondrons and MSCs is successful in some donors.

Equine minced cartilage in coculture as a minimal manipulated product

Finally, minced cartilage was evaluated as it could substitute chondrons to facilitate ease of application. In addition, minced cartilage was cocultured with MSCs and BMC to assess the potential of combining two minimal manipulated products. Minced cartilage in fibrin did not increase in GAG and DNA content over the culture period (Figure 5A). This is most likely the result of the particulated cartilage that is included in the constructs and significantly contributes to both GAG and DNA measurements. On histological level, some GAG production in fibrin gel between the minced cartilage is seen in mince/MSC cocultures only (Figure 5B, middle panels). Minced cartilage alone or mince/BMC cocultures did not seem to stimulate any production of GAG in the fibrin gels.

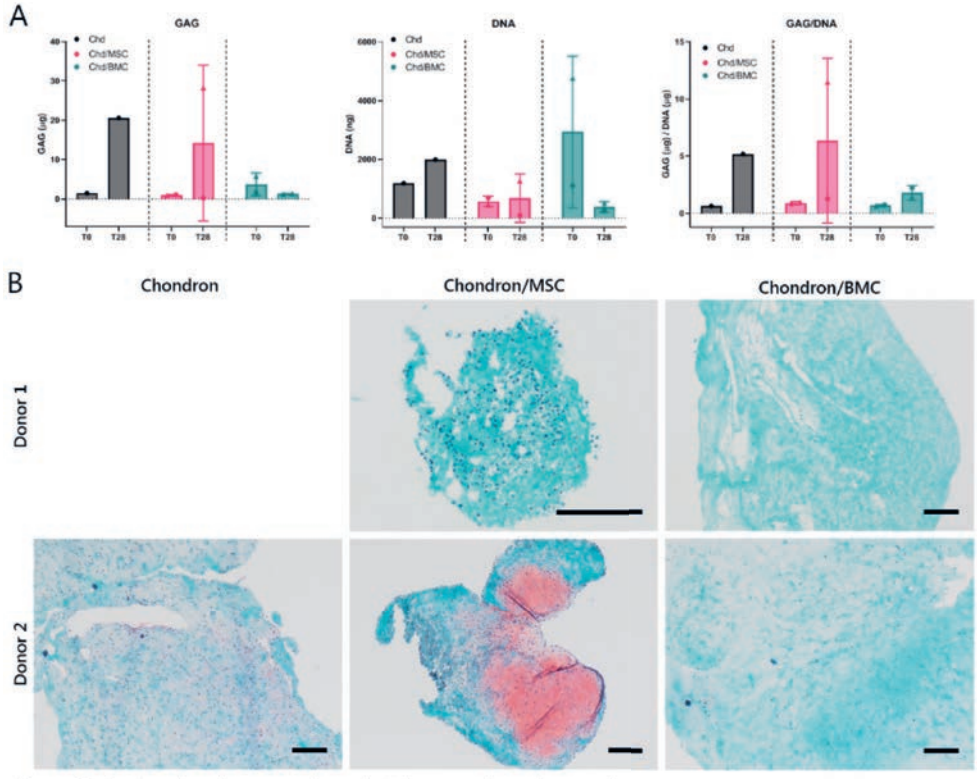

Figure 4. Equine chondrons cocultured with mesenchymal stromal cells and bone marrow concentrate. (A) Glycosaminoglycans (GAG) and DNA content in the fibrin gel constructs containing chondrons (Chd), chondrons and mesenchymal stromal cells in coculture (Chd/MSC), and chondrons and bone marrow concentrate in coculture (Chd/BMC). (B) Histological staining for GAGs with safranin-O (in pink) counterstained with fast green (in blue) for the two equine donors. All scale bars = 200 µm. N = 2 donors. Of note, the group containing a monoculture of chondrons could not be included for one donor due to insufficient number of cells.

Selection of an optimal cell combinations for chondrogenesis

Based on the presented results, two cell products were selected for evaluation in a swelling hydrogel. The coculture of chondrons and MSCs were effective in both human and equine cells, and was therefore the preferred cell product. Additionally, ACPCs derived from normal cartilage were evaluated in the gel, as these cells successfully produced GAGs and type II collagen in an earlier study when pellets were stimulated with TGF-β. While a coculture of minced cartilage and MSCs also seemed to be efficient, minced cartilage is difficult to implement, due to the envisioned culture system of a swelling hydrogel in a swelling-restricting construct to obtain hydrostatic pressure.

Cytocompatibility of hydrogel

Cytocompatiblity of the CSMA/HAMA was evaluated in a pilot study using a coculture of chondrons and MSCs, as well as H-ACPCs. Macroscopically, swelling of CSMA/HAMA was observed at one day in culture (Figure 6A). Metabolic activity of both cell products in fibrin were comparable at four and seven days, but was slightly lower at seven days. Cells in CSMA/HAMA did not actively converse resazurin into resorufin, a clear indication of no metabolic activity compared to cells in fibrin gel (Figure 6B). The

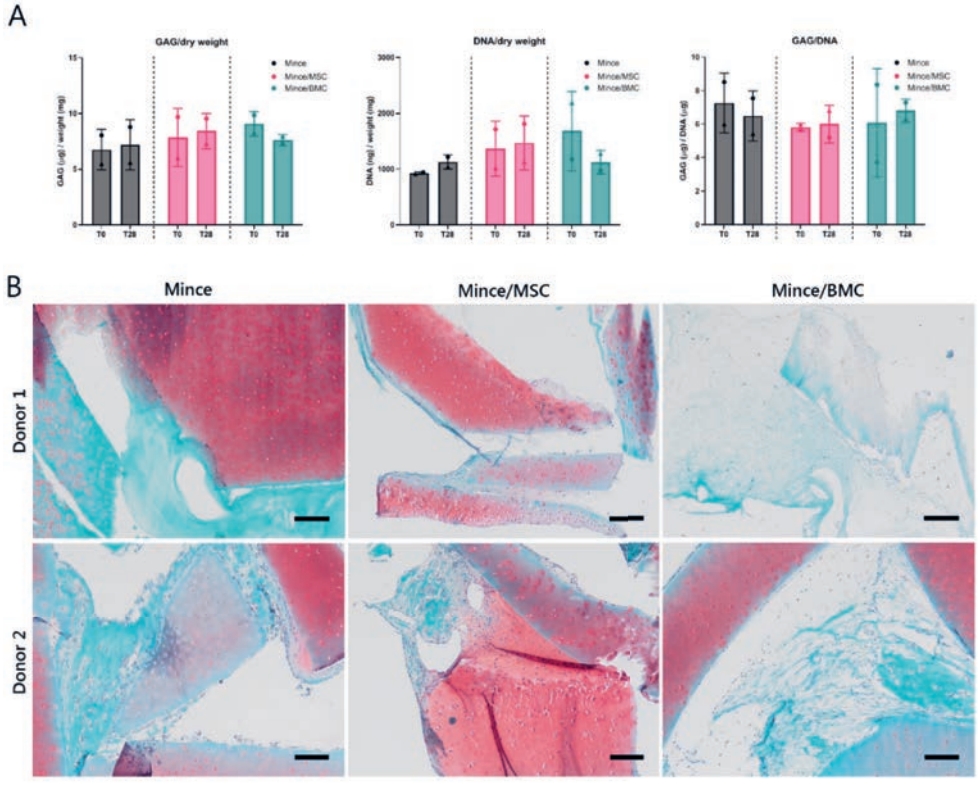

Figure 5. Equine minced cartilage and bone marrow concentrate in coculture with chondrons. (A) Glycosaminoglycans (GAG) and DNA content in the fibrin gel constructs containing minced cartilage alone, minced cartilage cocultured with mesenchymal stromal cells (Mince/MSC), and minced cartilage and bone marrow concentrate in coculture (Mince/BMC). (B) Histological staining for GAGs with safranin-O (in pink) counterstained with fast green (in blue) for the two equine donors. All scale bars = 200 µm. N = 2 donors.

metabolic activity is in line with staining for live and dead cells (Figure 6C and 6D). Coculture of chondrons and MSC in fibrin displays homogenous cell distribution, with chondrons clearly identifiable as cell clusters (Figure 6C, top images). These clusters seem to reduce over the culture period. At seven days, most of the cells have a stretched appearance, most likely due to attachment to the fibrin fibers. Coculture in CSMA/HAMA reveal a reduced number of cells visible, which exclusively display a round appearance. Furthermore, intracellular morphology shows a spotted appearance compared to homogenously stained cells in fibrin (Figure 6C, bottom images). H-ACPCs in fibrin gel have a similar morphology to coculture cells in fibrin, as the cells appear to attach to the fibrin and stretch (Figure 6D, top images). Like the coculture, H-ACPCs in CSMA/HAMA display a comparable intracellular morphology (Figure 6D, bottom images). For both cell products, no clear indication of increased cell death is seen in CSMA/HAMA.

From the presented results, it is evident that CSMA/HAMA hydrogel poses several challenges. Both cell products were not metabolically active in CSMA/HAMA and did not display a typical morphology on Live/Dead staining. The cells could be alive inside the gel, but be in a dormant state. On the other hand, it is more likely that the cells have died and were cleared from the gel, or severely damaged and in the process of dying, accounting for the observed intracellular irregularities.

Improving cytocompatibility of CSMA/HAMA hydrogel

Before chondrogenic performance of a cell product in CSMA/HAMA can be evaluated, the hydrogel system should be improved to enhance cell viability. While the gel's swelling behaviour imitates part of the native cartilage ECM (unpublished data), cells do not seem to attach to the gel and show morphological irregularities. Enhancing cell attachment to the gel might improve cell retention. Functionalization of the hydrogel with peptide sequences would provide active binding sites for cells[468,473,474]. Additionally, immobilization of bioactive compounds, like growth factors or growth factor-binding peptides, could stimulate cell growth and/or differentiation[474]. Further optimization of a cytocompatible hydrogel that supports cell growth and chondrogenesis is essential.

Chondrogenesis in a tissue engineered hydrostatic pressure system

On the condition that CSMA/HAMA (or an alternative hydrogel with considerable swelling properties) is optimized to support cell growth, the next step is to evaluate this cell-laden hydrogel in a confined setting. Previous work has confirmed the chondrogenic capacity of microfiber-reinforced gelatin–methacrylamide (gelMA) hydrogel with equine chondrocytes cultured with dynamic loading and without addition of external TGF-β[461]. It is hypothesized that the confinement of CSMA/HAMA restricts swelling and creates an increase in hydrostatic pressure in the construct, without the need for external mechanical stimulation.

Future implications

Optimization of the tissue engineered hydrostatic pressure system presented here would imitate the natural composition of hyaline cartilage. It could further enhance neo-cartilage ECM formation of a chondrogenic cell product by providing essential bioactive and/or mechanical cues, without the need for external addition of growth factors or stimulation. Furthermore, combining a cytocompatible hydrogel with fiber-reinforcement would also provide the construct with mechanical stability to survive the forces in the joint environment upon implantation. This can result in a tissue engineered product that is ready to implant into

focal chondral defects. Alternatively, a chondral component could be converged with a bone anchor[188], to adopt an osteochondral regenerative approach. This could then be developed into larger structures with challenging anatomical shapes[105,190], moving towards a tissue engineered whole joint replacement approach.

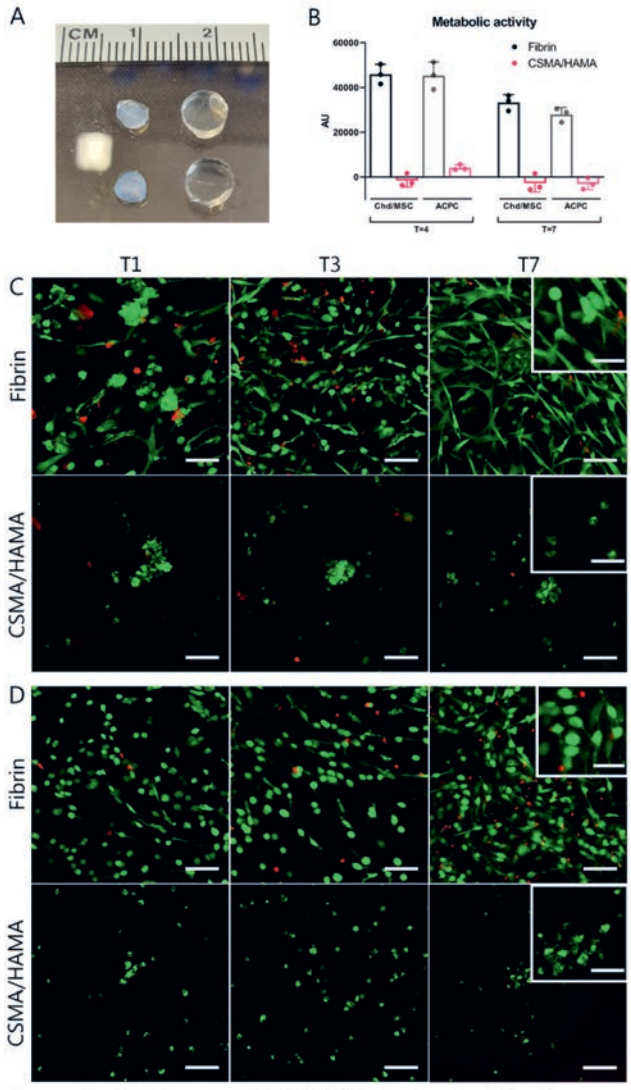

Figure 6. Viability in CSMA/HAMA hydrogel. (A) Macroscopic appearance of fibrin and methacrylated chondroitin sulfate (CSMA) / methacrylated hyaluronic acid (HAMA) gels at day one. Top row is chondron (Chd) / mesenchymal stromal cell (MSC) coculture, bottom row is healthy articular cartilage-derived progenitor cells (H-ACPC). Fibrin on the left, CSMA/HAMA on the right. (B) Metabolic activity of Chd/MSC coculture and H-ACPC in fibrin and CSMA/HAMA at four and seven days measured by conversion of resafurin to resorufin (ex: 560 nm / em: 590 nm). (C) Live/Dead images of Chd/MSC coculture and (D) H-ACPC in fibrin and CSMA/HAMA at one, three, and seven days. Scale bar = 100 µm, scale bar in inserts = 50 µm.

Annex II

Viscoelastic Chondroitin Sulfate and Hyaluronic Acid Double-Network Hydrogels with Reversible Crosslinks

Marko Mihajlovic
Margot Rikkers*
Milos Mihajlovic*
Martina Viola
Gerke H. Schuiringa
Rosalinde Masereeuw
Lucienne A. Vonk
Jos Malda
Keita Ito
Tina Vermonden
** = These authors contributed equally*

Biomacromolecules (2022)

ABSTRACT

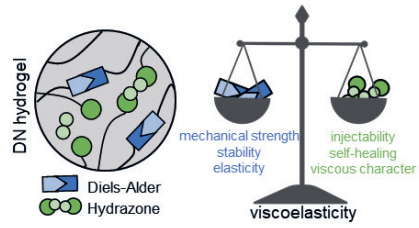

Viscoelastic hydrogels are gaining more interest as they possess necessary requirements for bioprinting and injectability. By means of reversible, dynamic covalent bonds, it is possible to achieve features that recapitulate the dynamic character of the extracellular matrix (ECM). For example, dually-crosslinked and double-network (DN) hydrogels seem to be ideal for the design of novel biomaterials and bioinks, as a wide range of properties required for mimicking advanced and complex tissues can be achieved. In this study, we investigated the fabrication of chondroitin sulfate/hyaluronic acid (CS/HA) based DN hydrogels, in which two networks are interpenetrated and crosslinked with dynamic covalent bonds of very different lifetimes. Namely, Diels-Alder adducts (between methylfuran and maleimide) and hydrazone bonds (between aldehyde and hydrazide) were chosen as crosslinks, leading to viscoelastic hydrogels. Furthermore, we showed that viscoelasticity and dynamic character of the resulting hydrogels could be tuned by changing the composition, *i.e.* the ratio between the two types of crosslinks. Also, due to a very dynamic nature and short lifetime of hydrazone crosslinks (~800 s), the DN hydrogel is easily processable (e.*g.* injectable) in the first stages of gelation, allowing the material to be used in extrusion-based 3D printing. The more long-lasting and robust Diels-Alder crosslinks are responsible for giving the network enhanced mechanical strength and structural stability. Being highly charged and hydrophilic, crosslinked CS and HA enable a high swelling capacity (maximum swelling ratio ranging from 6-12), which upon confinement results in osmotically stiffened constructs, able to mimic mechanical properties of cartilage tissue, with equilibrium moduli ranging from 0.3-0.5 MPa. The hydrogels are also cytocompatible with mesenchymal stromal cells (MSCs), as evaluated by cell viability tests. The DN hydrogels with dynamic covalent crosslinks hold great potential for the development of novel smart and tunable viscoelastic materials to be used as biomaterial inks or bioinks in bioprinting and regenerative medicine.

INTRODUCTION

Soft materials, such as hydrogels (polymeric networks imbibing large amounts of water), hold a huge potential in the design of smart biomaterials, to be used for tissue engineering and regenerative medicine applications, especially in combination with bioprinting techniques. Depending on the polymers used and the specific application, hydrogels are often found to be biocompatible and biodegradable. As such, hydrogels are good candidates to fabricate scaffolds which are highly hydrated, supporting cellular growth, differentiation and new tissue formation *in vivo*[475–478]. In recent years, hydrogel design mainly revolved around the use of natural polymers (biopolymers) in order to achieve advantageous interactions between cells and materials. Many biopolymers have been investigated, such as gelatin and different polysaccharides, as they are ubiquitously found in the extracellular matrix (ECM) of many native tissues, and are generally bioactive, cytocompatible and biodegradable. However, to efficiently mimic complex functions of ECM, hydrogels should possess dynamic (time-dependent), instructive and responsive features[479]. Therefore, hydrogel design should encompass diverse and multiple crosslinks, through which functions such as shear-thinning, self-healing, stimuli-responsiveness and tunable viscoelasticity could be attained, thus hydrogels with more sophisticated and adaptable features. Ideally, the structural design of hydrogels should encompass reversible and dynamic networks rather than covalent, static systems. The choice of a single type of network or crosslinking strategy severely limits the hydrogel in terms of the tenability of properties and functions it can possess. More recently, the use of multiple polymer networks, in addition to carefully chosen crosslinking strategies, emerged as a powerful tool to recapitulate many of the highly desired and sought-after properties. Among different design approaches of multiple-network based hydrogels, double-network (DN) hydrogels seem to be promising and an often used strategy. In DN systems, two networks are interpenetrated, with each network being separately crosslinked[480,481]. Therefore, there are no additional attachment points between the two networks. An alternative is given by dually crosslinked hydrogels, in which only one network is formed through combination of multiple crosslinking strategies. Regarding the design of DN hydrogels, the use of dynamic covalent bonds could be beneficial. Dynamic covalent bonds are rather peculiar, in a way that they are considered intermediates between traditional covalent and physical bonds. They possess higher strengths than the physical interactions, usually in the order of several 100 kJ/mol, but unlike covalent bonds, are also reversible and dynamic[482–484]. Different examples have been used in hydrogels, including Diels-Alder adducts[485], disulfide[486], acylhydrazone[485,486], oxime[487] and boronic ester bonds[487].

To generate hydrogels in this study, the chosen biopolymers were glycosaminoglycans (GAGs) chondroitin sulfate (CS) and hyaluronic acid (HA), which are linear anionic polysaccharides naturally occurring in human ECM. CS is most abundantly found in connective tissues and in the brain[488], whereas HA is most concentrated in synovial fluid and the vitreous of the eye[488]. Structurally, CS and HA are quite similar, both consisting of repeating disaccharide units, made of D-glucuronic acid (CS and HA) and *N*-acetyl-D-galactosamine (CS) or *N*-acetyl-D-glucosamine (HA). Additionally, CS carries one or more sulfate groups, whereas HA is a non-sulfated GAG[488]. Both of these polymers have been employed to fabricate hydrogels[489–493], but HA has seen far more use when compared to CS and to the best of our knowledge, CS has not been employed in hydrogel formulations based on dynamic covalent bonds and designed for bioprinting and injectability applications[494]. Besides, both CS and HA are found in cartilage tissue, with CS displaying higher water retention capacity than HA, thus potentially leading to hydrogel scaffolds with significant swelling capacity. Such feature is for instance important in mimicking load-bearing behavior of cartilage tissue, making CS a suitable biomaterial for cartilage tissue engineering

applications. Therefore, in the present work we mainly focus on CS polymer, and HA is used to a lesser extent.

Recently, Yu *et al.* developed an HA/PEG hydrogel system containing both acylhydrazone bonds and Diels-Alder adducts[485]. However, strictly speaking, such a system was a dually crosslinked network and not a DN hydrogel. This obviously has repercussions on the tunability of material's response and the formulation process. Moreover, no studies on material tunable viscoelasticity nor additive manufacturing applications were explored. Wang *et al.* on the other hand, developed a DN hydrogel based on HA, crosslinked via acylhydrazone and thiol-ene bonds[495]. The material showed interesting properties, including photostiffening and photopatterning, however it did require the use of UV light in order to induce the formation of permanent crosslinks.

In this work, we make use of dynamic covalent bonds to crosslink CS and HA into a DN hydrogel, in particular Diels-Alder adducts and acylhydrazone bonds. The Diels-Alder cycloaddition generally takes place between an electron-rich diene functional group (*e.g.,* furan) and an electron-poor dienophile (*e.g.,* maleimide), it does not require use of initiators or catalysts, forms no side products and occurs in aqueous environment[496]. The newly formed cyclohexene adduct is reversible by means of retro-Diels-Alder reaction at high temperatures. Moreover, in this study, furan was replaced with a more electron-rich methylfuran moiety, which has been shown to react faster at physiological pH with maleimide when compared to furan[497–500]. Also, a previous study suggests that the retro-Diels-Alder reaction was faster than when furan was used. With these notions in mind, we purposefully chose methylfuran, as we consider that faster transformation and inverse reaction could be beneficial for our goal of obtaining dynamic and viscoelastic hydrogels. Additionally, hydrazone bonds, deriving from reactions between carbonyls and hydrazine functionalities, are also reversible and the reaction takes place under physiological conditions, making it suitable for hydrogel fabrication[501]. Being orthogonal between each other, these two reactions make a good combination for the design of DN hydrogels. We anticipated that by combining two different types of dynamic covalent bonds, we could create a hydrogel that is strong and structurally stable, but at the same time dynamic and viscoelastic. The structural integrity and mechanical strength come from a more stable Diels-Alder adducts (long lifetime), whereas the dynamic character and processability originate from highly dynamic acylhydrazone bonds (short lifetime). Therefore, we hypothesized that properties of the DN hydrogel with crosslinks of different lifetimes, could be ultimately tuned and customized, depending on the composition. Moreover, for the stabilization of the DN, no UV or other external triggers were needed, as Diels-Alder crosslinking takes place under physiological conditions. Our main focus was the study of viscoelasticity of the DN and how the material's response could be tuned, in addition to exploring potential applications of such a DN hydrogel.

Specifically, CS was functionalized with maleimide and a separate batch of CS was oxidized to introduce aldehydes, while HA was modified with methylfuran. In addition, adipic acid dihydrazide (ADH) was used to crosslink the aldehyde containing CS. The fabricated hydrogels were investigated for their viscoelasticity and processability properties. Moreover, considering that both CS and HA are highly charged at physiological pH, we hypothesized that a hydrogel formulation (DN) based on CS and HA would result in materials with significant swelling capacity. Therefore, one of the interests was to also assess hydrogel swelling capacity and related mechanical properties, for potential cartilage-mimicking applications. Finally, cytocompatibility was evaluated. The unique assortment of features displayed by these hydrogels, alongside the possibility to tune and customize some of them by varying the

composition, make these gels suitable candidates to mimic complex soft tissues.

EXPERIMENTAL SECTION

Materials

Sodium hyaluronate was obtained from Lifecore Biomedical (82 kDa as measured with GPC, Chaska, MN). Chondroitin 4-sulfate sodium salt (bovine trachea) was purchased from Sigma-Aldrich (Zwijndrecht, The Netherlands). All other reagents were obtained from either Sigma-Aldrich (Zwijndrecht, The Netherlands) or TCI Europe N.V. and were used as received. All organic solvents were purchased from Biosolve (Valkenswaard, The Netherlands) and used without further purification.

Synthesis

Chondroitin sulfate-maleimide (CS-mal) functionalization

Chondroitin sulfate was functionalized with maleimide moieties by adapting a method previously reported for hyaluronic acid[502]. CS sodium salt was first converted in CS tetra-butyl-ammonium (TBA) salt, through resin exchange (Dowex 50 x 8w hydrogen form and tert-butyl-ammonium fluoride). CS-TBA was obtained after freeze-drying. The content of TBA ions per disaccharide unit of CS was ~1.7 Dry CS-TBA (6.0 g, 7.60 mmol disaccharide units) was then transferred in a 3-neck round bottom flask and flushed under N_2 flow. Next, 1-(2-aminoethyl) maleimide (1.035 g, 5.86 mmol) and benzotriazol-1-yloxytris(dimethylamino)phosphonium hexafluorophosphate (BOP) (3.20 g, 7.23 mmol) were combined with CS-TBA and anhydrous DMSO (300 mL) was added. The reaction mixture was stirred for 4 h at room temperature. The solution was dialyzed extensively (cutoff 14 kDa), first against NaCl (150 mM) for 4 days and then against water for 3 days. Finally, the solution was lyophilized and the product CS-mal was recovered as a white fluffy solid (yield ~90%). The degree of functionalization, defined as the number of ethyl maleimide groups per disaccharide unit (expressed as percentage), was determined by ^{1}H-NMR.

Hyaluronic acid-methylfuran (HA-MeFU) functionalization

Hyaluronic acid was functionalized with 5-methylfurfurylamine following a previously reported method[503]. Briefly, HA was weighed (3.00 g, 7.47 mmol disaccharide units), transferred in a round-bottom flask and dissolved in MES buffer (100 mM, pH 5.5) at a concentration of 1 w/v% (300 mL). Next, 4-(4,6-dimethoxy-1,3,5-triazin-2-yl)-4-methyl-morpholinium chloride (DMTMM) was added (4.15 g, 14.98 mmol), followed by a dropwise addition of 5-methylfurfurylamine (1000 µl, 8.97 mmol). The reaction mixture was stirred at room temperature for 18 h and then dialyzed against NaCl (150 mM) for 2 days, then against water for another 2 days (cutoff 14 kDa). Finally, HA-MeFU was obtained after freeze-drying as a light-yellow, cotton-like solid (yield ~80%). Degree of functionalization, defined as the number of 5-methylfuran groups per disaccharide unit (expressed as percentage), was determined by ^{1}H-NMR.

Chondroitin sulfate oxidation

Chondroitin sulfate was oxidized following a protocol previously published[504]. Briefly, CS sodium salt (7.0 g, 16.86 mmol disaccharide units) was dissolved in 275 mL of deionized water, followed by addition of sodium periodate solution (4.2 g, 19.63 mmol, in 75 mL water). The reaction was stirred at room temperature in the dark for 2h. Subsequently, the reaction was quenched by adding ethylene glycol (14.0 mL, 0.25 mol) and stirring the reaction for 1 h. Finally, dialysis against water (cutoff 14 kDa) for 4 days

and freeze drying yielded the final product, oxidized CS (CS-ox) as a white, fluffy solid (yield ~ 70%). The degree of oxidation (amount of introduced aldehyde groups) of CS-ox polysaccharide was determined using Purpald® reagent, as described previously[505–507], with a standard curve from propionaldehyde. Briefly, CS-ox sample (0.5 mg/mL) and Purpald® reagent (10 mg/mL) were dissolved in 1M NaOH solution. The two solutions were mixed in equal volumes and incubated overnight at room temperature, exposed to air. The absorption of the resulting purple colored solutions was measured with UV-Vis spectroscopy at 550 nm (SHIMADZU UV-2450).

Nuclear Magnetic Resonance (^{1}H-NMR)

^{1}H-NMR spectra were recorded on an Agilent 400-MR NMR spectrometer (Agilent Technologies, Santa Clara, U.S.A.) in D_2O. The chemical shifts were reported as δ in parts per million (ppm) and were referenced against residual solvent peak of D_2O (δ = 4.79 ppm).

Fourier-Transformed Infrared Spectroscopy (FT-IR)

FT-IR spectra were recorded on a PerkinElmer Spectrum Two spectrometer equipped with a universal attenuated total reflectance (ATR) sampling accessory. The samples were scanned in the range from 400 to 4000 cm^{-1} with an 8 scan per sample cycle and a resolution of 4 cm^{-1}.

Hydrogel fabrication

Hydrogels were fabricated by dissolving the polymers in phosphate buffered saline (PBS, 137 mM NaCl, 2.7 mM KCl, 8 mM Na_2HPO_4, and 2 mM KH_2PO_4, pH 7.4) at desired concentration (15 wt%, unless otherwise stated) and mixing them together. For SN-DA, separate solutions in PBS of CS-mal and HA-MeFU were prepared and then thoroughly mixed together. For SN-HY, a solution of CS-ox was made in PBS and then supplemented with adipic acid dihydrazide (ADH) (stock solution in PBS, 25 mg/mL). Lastly, DN hydrogel was fabricated by dissolving together CS-mal and CS-ox in PBS, while HA-MeFU was separately dissolved in PBS. Next, the two solutions were combined, mixed thoroughly and supplemented with ADH to give rise to DN hydrogel. The molar ratios between complementary functional groups, as well as mass ratios between DA and HY in DN formulations are reported in Table S1 and are also indicated throughout the manuscript. For swelling and mechanical experiments (under free swelling conditions), hydrogel disks were prepared. The combined solutions of dissolved polymers were prepared as described above, followed by injection in a Teflon mold with cylindrical wells (2 mm height, 6 mm diameter), covered with a quartz glass plate and incubated at 37°C. Incubation was set at 3 h for SN-DA and DN hydrogels and 5 min for SN-HY. For confined conditions, samples were prepared in the same way, but in addition to using the mold, the wells were fitted with a knitted spacer fabric scaffold (polyamide 6; ~2.6 mm height, 8 mm diameter and prepared by warp-knitting method, as previously reported[508], Karl Mayer Textilmaschinenfabrik GmbH, Obertshausen, Germany). This results in the formation of the hydrogel within the spacer fabric material (Figure 6A, middle sample). For achieving further confinement, such gel-filled spacer fabric was then placed inside a circular cassette (3 mm height, 8 mm diameter; R05 resin, Envisiontec), as shown in Figure 6A (sample on the right). The samples inside the cassette were used for swelling and mechanical tests.

Hydrogel swelling

Hydrogel swelling properties were assessed by a gravimetric method. The following hydrogel formulations were evaluated: SN-DA, SN-HY and DN (mass ratio between DA and HY 1:1) over time. Hydrogel disks were prepared at 15 wt% polymer concentration (see above) and placed in pre-weighed

vials. The swelling tests were carried out both under free swelling and confined conditions (as explained in the previous paragraph). The size of the hydrogel samples was 6 mm diameter, 2 mm height for free swelling samples, and 8 mm diameter, 2.6 mm height for confined samples. Initial weight (W_0) for all hydrogels was determined immediately after fabrication and the samples were incubated in 1 mL PBS (pH 7.4) at 37°C. At indicated time points, buffer was removed, hydrogel weight was measured (W_t), followed by replacement with fresh buffer. Swelling ratio SR (defined as W_t/W_0) was used to assess hydrogel swelling properties over time. All samples/conditions were measured in triplicate.

Rheology

Oscillatory shear measurements were performed using a DHR-2 rheometer (TA Instruments, Etten-Leur, The Netherlands), equipped with a plate-plate (20 mm) measuring geometry and a solvent trap to minimize water evaporation. All measurements were conducted at 37°C (unless otherwise specified), by pipetting 200 µl of polymer solution onto the measuring plate. The linear viscoelastic region (LVR) was determined using a strain sweep test at an oscillation frequency of 1 rad/s. Gelation experiments (time sweep) were performed at a frequency of 1 rad/s and a shear strain of 1%. Frequency sweep measurements were conducted at an oscillation strain of 1% (safely within LVR), in the frequency range between 0.01 and 100 rad/s. To evaluate stress relaxation properties, a step strain of 2% was applied. Dynamic amplitude tests were conducted by alternating cycles at low strain (1%, 1 min) and high strain (500%, 0.5 min), while keeping the frequency constant at 1 rad/s. To assess shear-thinning, viscosity as a function of shear rate was measured in the range between 0.1 and 25 s^{-1}.

Mechanical tests

To study the mechanical properties of the constructs, an indentation test was performed using a tensile tester (MTS Criterion, Eden Prairie, USA) equipped with a loadcell of 50 N (MTS systems corp., Eden Prairie, USA). The samples were placed in a custom-made 3D printed cassette (resin R05, Envisiontec) with a diameter of 8 mm and indented with a 5 mm diameter indenter. After a pre-load of 2.5 kPa was reached, a stress relaxation test was performed using 15% strain (strain rate of 15% strain per second). The strain was kept constant up to 180 seconds, until the equilibrium was reached. The initial modulus was calculated from the linear part of the loading curve, between 10% and 15% strain. The equilibrium modulus was determined after the sample reached equilibrium at 15% strain.

3D Printing and Imaging

The DN hydrogel (DA:HY 2:1, 15wt%) was tested for printing. CS-mal and CS-ox polymers were dissolved together in PBS, separately from HA-MeFU. The polymer solutions were then combined, thoroughly mixed and transferred in a syringe. Such solution was then supplemented with ADH crosslinker and upon formation of the hydrazone crosslinks (within minutes), the formulation was printed with a 27 G needle. Extrusion-based printing was performed using a pneumatic 3D bioprinter (Allevi 3, 3D Systems), equipped with Allevi Bioprint Online software. The GCODE file was exported from the Allevi3D website. Parameters such as layer patterns, infills, printing speeds and pressure were tuned by the software. The constructs (square mesh geometry) were printed in standard Petri dishes (Thermo Fisher Scientific). To obtain good resolution of the fibers, the constructs were printed with 2 mm infill, printing speed of 5 mm/s and a pressure of 10 psi. Before the printing process, both the collector plate and the extruder were heated up at 37°C and the temperature was kept constant throughout the experiment. The constructs were analyzed with Olympus SZ61 stereomicroscope (Yourtech) using the CellSens software.

Preparation of hydrogel degradation products (HDPs)

Degraded hydrogel products were used to assess its pro-inflammatory potential. In order to fully degrade the material, DN hydrogel was first prepared, as already described (15 wt%, DA to HY mass ratio 1:1). After the DN gel was fully crosslinked, it was placed in excess milliQ water and supplemented with hyaluronidase type II enzyme (HYAL II, from sheep testes, Sigma-Aldrich). HYAL II was used at 100 U (where one unit U is the amount of enzyme needed to free 1.0 μmol of N-acetylglucosamine from polymer backbone per minute at 37°C and at pH 4.0[509]). Samples were incubated at 37°C, under continuous agitation. Following the hydrogel's complete dissolution, the resulting solution was freeze-dried to yield a solid, white powder, corresponding to hydrogel degradation products. The formed material was used in further experiments.

Human mesenchymal stromal cells (MSCs) isolation, expansion and treatments

MSCs were derived from bone marrow aspirates from healthy donors (n = 3, age range 2 – 12) as approved by the Dutch Central Committee on Research Involving Human Subjects (CCMO, Bio-banking bone marrow for MSC expansion, NL41015.041.12). The parent or legal guardian of the donor signed the informed consent approved by the CCMO. In brief, the mononuclear fraction was separated using a density gradient (Lympoprep, Axis Shield). MSCs were isolated by plastic adherence and expanded for three passages in Minimum Essential Media (αMEM, Macopharma) with 5% (v/v) human platelet lysate and 3.3 IU/mL heparin and cryopreserved. Subsequently, MSCs were expanded for two additional passages in αMEM (Gibco), supplemented with 10% (v/v) fetal calf serum (FCS; Biowest), 100 U/mL and 100 μg/mL penicillin/streptomycin (Gibco), 200 μM L-ascorbic acid 2-phosphate (Sigma-Aldrich), and 1 ng/mL basic fibroblast growth factor (PeproTech). Subconfluent MSC monolayers were treated with individual components or crosslinker diluted into the medium for 24 h (CS-mal and HA-MeFU at 37.5 mg/mL, CS-ox at 75 mg/mL and ADH at 1.4 mg/mL). Subconfluent MSC monolayers were also treated with crosslinked double-network hydrogels in hanging cell culture inserts (pore size 0.4 μm; Merck). Analyses were performed after 1 and 7 days of culture.

THP-1 cell culture, macrophage differentiation and treatment with HDPs

Human THP-1 monocytes were grown in suspension in complete culture medium consisting of Roswell Park Memorial Institute (RPMI) 1640 medium (Lonza, Verviers, Belgium) supplemented with 10% fetal calf serum (FCS; Greiner Bio-One, Alphen aan den Rijn, The Netherlands) and 1% penicillin/streptomycin (complete culture medium), at 37°C, 5% (v/v) CO_2. Cells were subcultured twice a week in order to maintain density of approximately $0.5*10^6$ cells/ml, and were seeded at a density of $1.5*10^5$ cells/cm^2 prior to macrophage differentiation. Macrophage differentiation was achieved by exposing the cells to phorbol 12-myristate 13-acetate (PMA; 50 ng/ml; InvivoGen, The Netherlands) for 48 h (M0 macrophages), and polarization to M1 macrophages was reached after a resting phase of 48 h in complete culture medium and subsequent exposure to lipopolysaccharide (LPS from *Escherichia coli* 0127:B8 100 ng/ml) and interferon gamma (IFNγ; 20 ng/ml; InvivoGen, The Netherlands) for 72 h. Following the macrophage differentiation and polarization process, M0 and M1 macrophages were exposed for 24 h to various concentrations of hydrogel degradation products (HDPs) dissolved in complete culture medium and filter-sterilized.

Cell viability assays

THP-1

Following 24 h exposure to increasing concentrations of HDPs (0.001 – 15 mg/ml), cytotoxicity was measured using CyQUANT™ LDH Cytotoxicity Assay (Invitrogen™, Thermo Fisher Scientific) according to manufacturer's instructions. Triton X-100 1% was used as a positive control, and complete culture medium was used as a blank. The absorbance at 490 nm was measured using a GloMax Discover Microplate Reader (Promega, Madison, WI, USA). Data were corrected for the background (blank) and presented as average absorbance values at 490 nm.

MSCs

Cell viability following 1 and 24 h treatment with gel individual components, and 1 and 7 days treatment with double-network hydrogels was assessed using the Live/Dead Viability Kit for mammalian cells (ThermoFisher Scientific) according to the manufacturer's instructions. Monolayers were imaged using the Olympus IX53 fluorescent microscope and live and dead cells were quantified using ImageJ software version 1.49 (National Institutes of Health, Bethesda, MD, USA). In addition, MSCs exposed to double-network hydrogels were assessed for metabolic activity and lactate dehydrogenase (LDH) release. Metabolic activity was evaluated using a resazurin (Alfa Aesar, Germany) assay at 44 mM in the culture medium. Fluorescence of reduced resorufin was measured after 6 h of incubation at 544 nm excitation and 570 nm emission using a spectrofluorometer (Fluroskan Ascent FL; ThermoFisher) and corrected for blanks. Activity of LDH released into the culture medium was measured using the Cytotoxicity Detection KitPLUS (Roche) according to the manufacturer's instructions. Control wells were treated with 2% Trition X-100. Monolayers were lysed by three freeze-thaw cycles in Tris-EDTA buffer (10 mM Tris-HCl, 1 mM EDTA, pH 8) and DNA was quantified using the Quant-iT™ PicoGreen assay (Invitrogen) according to the manufacturer's instructions.

Enzyme-Linked Immunosorbent Assay (ELISA)

The production of interleukin 6 (IL-6), tumor necrosis factor alpha (TNF-α), interleukin 1 beta (IL-1β) and monocyte chemoattractant protein 1 (MCP-1) by macrophages was measured using an Enzyme-Linked Immunosorbent Assay (ELISA). Cell culture supernatants were collected after 24 h treatments of M0 and M1 THP-1-derived macrophages with HDPs (0.005 – 0.5 – 5 mg/ml), and centrifuged for 10 min, 240× g, 4°C, and stored at -20°C until further measurements. DuoSet® ELISA Development Systems kit (#DY201; R&D Systems, Abingdon, UK) was used to quantify the IL-1β levels in complete cell culture medium supernatants following manufacturer's instructions. Standard TMB ELISA Development kits were used to quantify remaining cytokines (IL-6 #900-T16, TNF-α #900-T25, MCP-1 #900-T31; PeproTech, London, UK) according to manufacturer's protocols. The optical density was determined using a GloMax Discover Microplate Reader (Promega, Madison, WI, USA) set to 450 nm. Each sample was measured in duplicate, and quantification was done using a four-parameter logistic (4-PL) curve-fit. Data were presented as concentration (pg/ml) normalized to DNA content quantified using Quant-iT™ PicoGreen™ assay as described above.

Statistical analysis

All data are presented as mean ± standard error of the mean (SEM). Statistical analysis was performed using one-way ANOVA followed by either Dunnett's or Tukey's multiple comparison tests. A p-value < 0.05 was considered significant. Software used for statistical analysis was GraphPad Prism (version 8.43; GraphPad software, La Jolla, CA, USA).

RESULTS AND DISCUSSION

Synthesis and characterization of HA and CS derivatives

HA furan derivative (HA-MeFU) was prepared by means of a simple, one-step reaction between HA polysaccharide and 5-methylfurfurylamine, in the presence of 4-(4,6-dimethoxy-1,3,5-triazin-2-yl)-4-methylmorpholinium chloride (DMTMM) reagent (Figure 1A)[503]. The degree of modification was determined by ^{1}H-NMR, and it was found to be ~30% (around 30 in 100 disaccharide repeating units are functionalized with furan) and all signals are in line with the proposed structure (Figure S1). Moreover, successful modification with furan was confirmed by FT-IR measurements (Figure S2A). In fact, upon conjugation of 5-methylfurfurylamine to the carboxylate groups of HA, the signal corresponding to carbonyl stretch was shifted from 1617 to 1652 cm^{-1}, confirming the formation of amide bonds. A new signal at 795 cm^{-1}, corresponding to alkene bending, also indicates the presence of furan[503].

For the formation of Diels-Alder crosslinks, the 5-methylfuran moiety is coupled with a maleimide group. Therefore, maleimide was introduced on CS polymer following a two-step approach. First, CS sodium salt was converted in a more lipophilic salt (CS-TBA) through a resin exchange step to enable dissolution of CS in a DMSO. The next step was the coupling reaction between 1-(2-aminoethyl) maleimide and carboxylate of CS, in the presence of BOP as coupling reagent (Figure 1A). The successful formation of CS-mal was confirmed with ^{1}H-

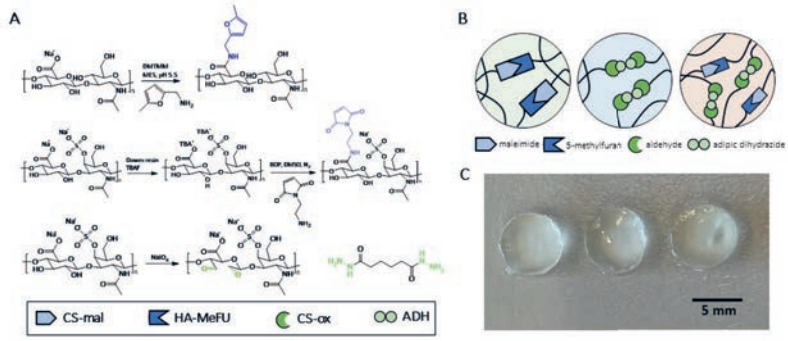

Figure 1. Modification of CS and HA polymers and hydrogel formulations. A) Synthesis routes for the preparation of HA-MeFU, CS-mal and CS-ox, including the structure of adipic acid dihydrazide (ADH). B) Schematic representation of the polymer networks of the hydrogels; SN-DA (single-network Diels-Alder) through coupling between maleimide and methylfuran functionalities; SN-HY (single-network hydrazone) formed in a reaction between aldehydes of CS-ox and hydrazides of ADH; DN (double-network) hydrogel formed when all components are present, containing both Diels-Alder and hydrazone crosslinks. C) Hydrogels upon in situ crosslinking at 37 0C, from left to right SN-DA (15 wt%, methylfuran to maleimide ratio 5:1), SN-HY (15 wt%, aldehyde to hydrazide molar ratio of 1:1) and DN (15 wt%, SN-DA to SN-HY mass ratio of 1:1, methylfuran to maleimide 5:1, aldehyde to hydrazide 1:1), prepared in a Teflon mold (6 mm diameter, 2 mm height).

NMR (signals in line with the proposed structure) and FT-IR. Degree of modification was measured to be ~8% (Figure S1). FT-IR showed a signal at 1704 cm^{-1} for the carbonyl stretch, and at 695 cm^{-1} the presence of alkene bending (indicative of maleimide) was observed[503]. Although maleimide functionalized HA has been reported before, to the best of our knowledge this is the first time a method for direct coupling of maleimide groups to CS is described[502].

For the formation of the second type of crosslinks, hydrazone bonds were employed. Consequently, aldehyde groups were introduced on CS following a previously reported method[504], using $NaIO_4$, which led to ring opening of the glucuronic acid and introduction of dialdehyde functionalities (Figure 1A). Aldehyde formation was confirmed by FT-IR, where a shoulder peak at 1731 cm^{-1} was observed (corresponding to aldehyde carbonyl stretch)[510,511] (Figure S3). Quantification of the aldehyde groups was carried out by Purpald® method, confirming an oxidation degree of ~10% (10% of disaccharide units contain aldehyde moieties). This value is in line with previously reported results for oxidation of CS and HA polymers when using 1.2:1 molar ratio of $NaIO_4$ to disaccharide unit[504,510]. In order to form a hydrogel with CS-ox, hydrazone crosslinks are formed between aldehydes and hydrazide functionalities. In the present work, a bifunctional hydrazide, adipic acid dihydrazide (ADH), was used in combination with CS-ox (Figure 1A). Overall, ^{1}H-NMR and FT-IR confirmed successful modification of the HA and

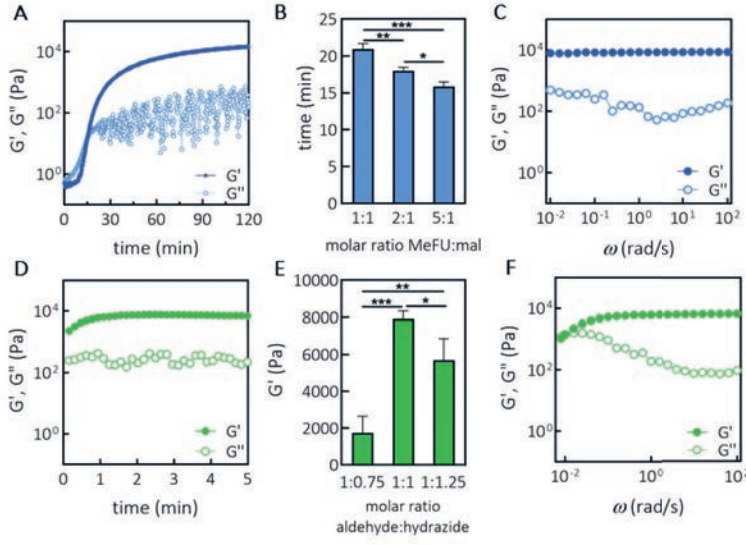

Figure 2. Formation of single-network hydrogels and rheological characterization. A) Time sweep (ω = 1 rad/s, γ = 1%) of SN-DA at 15 wt% (methylfuran to maleimide ratio of 5:1). B) Relation between gelation time (crossover point) and molar ratio between methylfuran and maleimide, as determined from the time sweep measurements, n = 3. C) Frequency sweep (ω = 0.01-100 rad/s, γ = 1%) of SN-DA at 15 wt% (methylfuran to maleimide ratio of 5:1). D) Time sweep (ω = 1 rad/s, γ = 1%) of SN-HY at 15 wt% (aldehyde to hydrazide molar ratio of 1:1). E) Storage modulus G'(ω) of SN-HY as a function of molar ratio between aldehyde and hydrazide moieties, as determined from the time sweep measurements, n = 3. F) Frequency sweep (ω = 0.01-100 rad/s, γ = 1%) of SN-HY at 15 wt% (aldehyde to hydrazide molar ratio of 1:1). * $p < 0.05$, ** $p < 0.01$, *** $p < 0.001$ (One-way ANOVA, Tukey's multiple comparison test).

CS polysaccharides.

The following nomenclature was used in this work to distinguish the hydrogel samples by their composition: SN-DA for the single-network hydrogel containing only Diels-Alder crosslinks (between methylfuran and maleimide groups of HA-MeFU and CS-mal respectively), SN-HY for the single-network hydrogel crosslinked only by hydrazone bonds (between aldehyde and hydrazide functionalities of CS-ox and ADH), and finally DN for the double-network hydrogel containing both types of crosslinks (Diels-Alder and hydrazones), meaning DN is a 4-component system. A schematic representation of hydrogel-constituting networks, made by different types of crosslinks, is given in Figure 1B.

Single-network hydrogel formation and rheological characterization.

Using shear oscillatory rheometry, gelation of single-network based hydrogels was investigated. Specifically, SN-DA hydrogel prepared at 15 wt% polymer content (5:1 molar ratio of methylfuran to maleimide) displayed a crossover point between G'(ω) and G"(ω) at ~15 minutes, indicating the progress of the crosslinking process and formation of the Diels-Alder adduct between methylfuran and maleimide. The storage modulus reached a plateau value of ~15 kPa after 120 minutes (Figure 2A). The effect of the ratio between methylfuran and maleimide functionalities on the kinetics of gelation (gelation time, here defined as the time needed to reach the crossover point (G'>G")) was further evaluated. By increasing the ratio of methylfuran to maleimide from 1:1 to 2:1 and 5:1, a decrease in gelation time was observed. Specifically, the ratio of 1:1 requires ~21 minutes to start gelling, whereas for 2:1 and 5:1 ratios, the gelling time was ~18 and 15 minutes respectively (Figure 2B). This suggests that an excess of methlyfuran moiety leads to a faster gelation process, as the maleimides groups are more rapidly consumed and thus the Diels-Alder crosslinks formed. Using the ratios with excess maleimide to furan would have most likely led to the similar trends in gelation, however in the current study these were not investigated as the excess of maleimide could lead to unwanted side reactions with biological components. Unlike maleimide, the excess of furan moieties is not expected to have a negative impact on the application of the material.

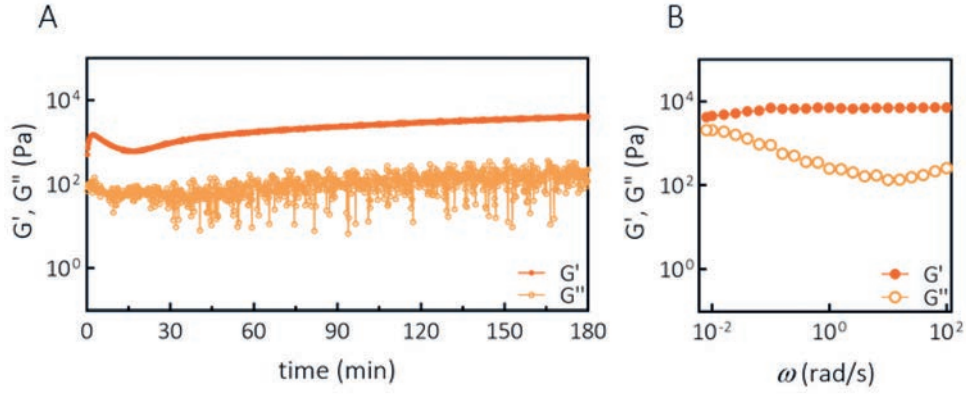

Figure 3. Formation of double-network hydrogel and rheological characterization. A) Gelation (ω = 1 rad/s, γ = 1%) of DN at 15 wt% (SN-DA to SN-HY mass ratio of 1:1, methylfuran to maleimide molar ratio of 5:1, aldehyde to hydrazide molar ratio of 1:1). B) Frequency sweep (ω = 0.01-100 rad/s, γ = 1%) of DN at 15 wt% (SN-DA to SN-HY mass ratio of 1:1, methylfuran to maleimide molar ratio of 5:1, aldehyde to hydrazide molar ratio of 1:1).

Moreover, the gelation of the SN-HY hydrogel was also assessed. Interestingly, it was observed that upon addition of ADH crosslinker to the solution of CS-ox (1:1 aldehyde to hydrazide, 15 wt% CS-ox), a hydrogel was instantly formed (Figure 2D). This is in line with what was seen by Hafeez *et al*., where oxidized alginate took ~45 minutes to form hydrazone crosslinks, at the polymer concentration of 2 % (*w/v*)[512]. Further, by changing the ratio between aldehyde and hydrazide functionalities to 1:0.75 and 1:1.25 hydrogels were also instantly formed, however they resulted in a lower storage modulus (Figure 2E). Deviating further in either direction from this range of ratios, the gelling was not observed. Specifically, we found that the optimal ratio of aldehyde to hydrazide was 1:1, leading to the stiffest gels (~8000 Pa, at 15 wt%) (Figure 2E). Figure 1C shows a representative picture of the SN-DA and SN-HY hydrogels formed *in situ* at 37 ^{0}C.

The general viscoelastic behavior of the hydrogels was examined by performing a frequency sweep measurement on the SN-DA and SN-HY hydrogels. For the SN-DA it is quite apparent that in the frequency range examined (ω = 0.01-100 rad/s), there was frequency independence of the G'(ω), whereas G" (ω) showed a very weak dependence in the same frequency range, displaying a mild upturn at lower frequencies (Figure 2C). Such a pattern is very typical of and often observed for chemically crosslinked hydrogels, which is expected considering that Diels-Alder reaction leads to covalent bond formation[513]. A similar behavior was observed with other hydrogels based on Diels-Alder crosslinking[514]. Differently, SN-HY shows a completely different behavior. Namely, in the same frequency range, SN-HY exhibited quite a significant variation of moduli (Figure 2F). At lower frequencies, G"(ω) showed a significant upturn, while G'(ω) started decreasing, indicating structural relaxation processes in the network, eventually leading to a crossover point between G'(ω) and G"(ω). This is an indication of a dynamic and nonpermanent nature of the SN-HY network, which is in line with the reversible character of the hydrazone bonds[501]. The crossover point is observed at ω = 8.4 x 10^{-3} rad/s, and from this a characteristic relaxation time for the hydrazone network τ = 750 s is derived ($\tau = 1/f$, f is frequency).

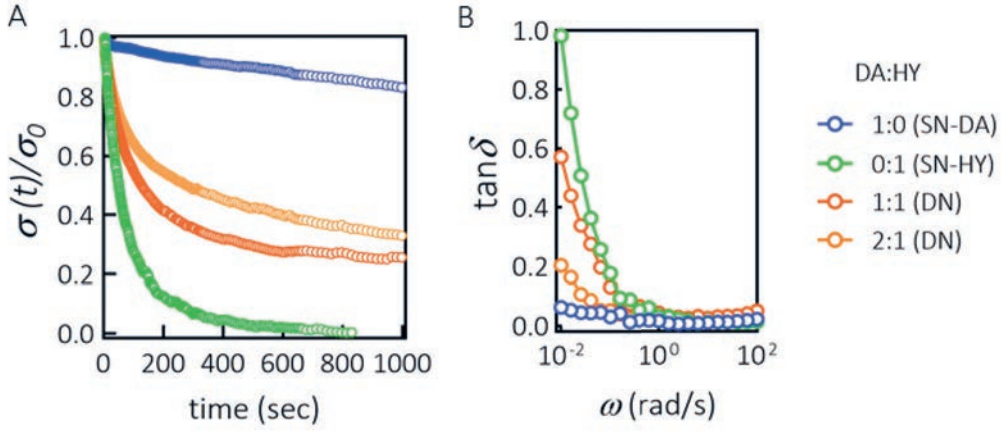

Figure 4. Tunable viscoelastic properties of DN hydrogels. A) Stress relaxation of different hydrogel formulations after a step strain of γ = 2%. All hydrogel formulations were prepared at 15 wt% polymer concentration (mass ratio between DA and HY was varied as indicated, whereas molar ratios of methylfuran to maleimide and aldehyde to hydrazide were kept at 5:1 and 1:1 respectively). B) Loss factor tan δ, defined as the ratio G"(ω)/G'(ω), as a function of angular frequency (calculated from the corresponding frequency sweep measurements).

Strain sweep measurements (γ = 0.01-1000%) were carried out for both SN-DA (methylfuran to maleimide 5:1, 15 wt%) and SN-HY (aldehyde to hydrazide 1:1, 15 wt%) hydrogels to determine the extension of the linear viscoelastic region for these materials (Figure S4). The results showed that yielding strains of ~50 and ~80% were observed for SN-DA and SN-HY respectively, confirming that all oscillatory shear experiments were performed at strain values safely within linear viscoelastic region.

To further test the reversible character of hydrazone crosslinks, the SN-HY hydrogel was subjected to a dynamic amplitude test (Figure S5). In alternating fashion, low (γ = 1%) and high (γ = 500%) shearing were applied and the moduli were monitored in time. Initially, at low strain the hydrogel exhibited gel-like structure, with G'(ω) and G"(ω) both being stable in time. Next, by applying strain values well outside the linear viscoelastic region, G"(ω) was higher than G'(ω), suggesting a lack of gel structure, due to the breaking of hydrazone crosslinks under shear. Finally, by restoring the strain back to linear region, there was an immediate recovery of the G'(ω) and the gel structure, indicating that hydrazone bonds were reformed. Therefore, the SN-HY hydrogel exhibits yield behavior that is reversible, making the gel also self-healing[515]. Therefore, based on these results, 5:1 methylfuran to malemide and 1:1 aldehyde to hydrazide ratios were chosen for further formulation of the DN hydrogels.

DN hydrogel formation and rheological characterization

Following the optimization of gelation of the single-network hydrogel formulations (SN-DA and SN-HY), DN hydrogels were prepared and characterized. A mass ratio between the two networks was set at 1:1 at 15 wt% polymer content (keeping the molar ratio between functional groups as previously optimized; methylfuran to maleimide 5:1 and aldehyde to hydrazide 1:1) and the gelation was monitored in time. Figure 3A shows the gelation profile for the DN hydrogel. It is evident that immediately after the start of the measurement, SN-HY was being formed, as G'(ω) was higher than G" (ω). Following the formation of hydrazone crosslinks, network started relaxing due to a very fast exchange of hydrazone bonds between bound and unbound states. Such decrease in moduli could be related to a slow hydrolysis of the polysaccharide and thus depletion of available aldehydes. It has been reported that ring-opened structure of polysaccharides (such as di-aldehyde structures obtained by periodate oxidation) are susceptible to hydrolysis[510,516,517]. Figure S6A shows the gelation of SN-HY (7.5 wt%, aldehyde to hydrazide 1:1 ratio) with noticeable decrease of moduli following quick gelation. Next, after ~15 minutes the moduli started increasing further, suggesting that the Diels-Alder crosslinks were formed in sufficient amount to affect material's stiffness as seen with SN-DA (Figure 2A). The gelation followed a slower kinetics compared to SN-DA, which is most likely related to a lower fraction of HAMeFU and CS-mal polymers (thus methylfuran and maleimide functionalities) in the present formulation. After 2-3 h the DN seemed to be fully crosslinked and equilibrated, showing a final modulus of ~6 kPa. The G'(ω) is directly related to the crosslinking density of the network, therefore a lower modulus found for DN compared to SN-DA can be attributed to the lower density of Diels-Alder crosslinks in DN (as the concentration of the reactive groups was halved compared to SN-DA formulation). After 3 h, the hydrazone crosslinks, being characterized by short relaxation times, were not expected to contribute significantly to the overall crosslinking density and stiffness of the DN. The results in Figure S6B show the extension of the LVR for the DN hydrogel, with yielding strain of ~60%. Figure 1C shows a representative picture of the DN hydrogel formed *in situ* at 37°C.

Furthermore, being very dynamic, hydrazone bonds could be used to allow for material's processing before the dynamic covalent crosslinking of the DA. In order to test whether the final hydrogel properties and gelation process are affected by shearing of the first-formed HY crosslinks, a gelation experiment

with a short initial shearing was performed. This simulates the gelation process of DN in case the initially formed SN-HY is destroyed before the Diels-Alder reaction is complete.

Figure S6C shows the gelation of the DN with initial shearing applied. This resulted in the temporary destruction of the hydrazone crosslinks (G"(ω) > G'(ω)), but as soon as the shear was removed, the HY crosslinks reformed, recovering the gel's stiffness (Figure S6D). It can be noticed that the gelation kinetics were not affected and the final properties of the DN were not different compared to the gelation without shearing (Figure 3A). This implies that the hydrogel in its initial gelling stages could be processed, *e.g.* extruded and still maintain its gelation capacity. A potential benefit of initial processability of the DN could be employed during the 3D printing processes of hydrogel formulation. This aspect is further described in the following sections.

Furthermore, the viscoelastic response as a function of frequency of the DN was assessed (Figure 3B). In the frequency range investigated (ω = 0.01-100 rad/s), it can be noted that the loss modulus G"(ω) displayed a significant upturn at lower frequencies, indicating a viscous character. This is due to the presence of highly dynamic hydrazone crosslinks in the network. On the other hand, storage modulus G'(ω) showed a weak dependency in the frequency range investigated, indicating a more elastic and more permanent nature of the gel, similarly as observed with SN-DA. Even at the lowest frequency measured (0.01 rad/s), G'(ω) was larger than G" (ω), in contrast to SN-HY system. This suggests that the general viscoelastic behavior of the DN is in between those corresponding to the single networks consisting purely of DA or HY crosslinked hydrogels. Clearly, the DN gel exhibits quite significant viscous properties (due to hydrazone crosslinks), while it still maintains an elastic character as well, resulting in a stable structure in time (due to Diels-Alder crosslinks).

Tunable stress relaxation and viscoelastic properties

Assessment of the tunability of the viscoelastic behavior of the present hydrogel systems was further studied by means of stress relaxation, a measure of the dissipated energy when a fixed deformation is applied. This is an important feature of viscoelastic materials to investigate as they display time-dependent mechanical response. Figure 4A shows the stress relaxation response of the SN and 2 formulations of DN hydrogels (DA:HY ratios of 1:1 and 2:1), measured at 37^{0}C following a step strain of 2%. Each hydrogel formulation showed a different overall response. In SN-DA hydrogel, being covalently crosslinked, the stress was dissipated very slowly. Over 16 minutes, the amount of stress dissipated was ~17%. For the chemically crosslinked hydrogels, the stress relaxation is likely due to the changes in the conformation of chains in the network. If the hydrogel is perfectly and irreversibly crosslinked, it should result in no stress dissipation and infinite relaxation time[518,519]. However, in case of SN-DA there was a slow and continuous relaxation observed, which indicates that the network could contain some imperfections that do not support stress (loops or un-crosslinked chains). Although DA crosslinks are not permanent, their reversibility (slow process) was not observed in this experiment.

In contrast to SN-DA, both SN-HY and DN hydrogels showed a two-stage response. At short times, there was a quick stress relaxation, which is related to the conformational changes of chains, but in addition to that, there was also a structural reorganization of the network due to the reversible nature of the hydrazone crosslinks. Dissociation of the hydrazone crosslinks in the network led to efficient and fast dissipation of elastic energy, resulting in 50% of stress released after only ~45 s for SN-HY, whereas for DN 1:1 and DN 2:1 it took ~115 and 250 s respectively (Figure 4A). At longer times, the DA network in the system, lead to a slower energy dissipation. The overall trend suggests that it is

possible to tune stress relaxation behavior of the hydrogels depending on the composition, more specifically on the ratio between DA and HY crosslinks. The more DA crosslinks are present, the slower the energy dissipation is expected to be. Interestingly, for SN-HY the complete relaxation of the network was achieved after ~810 s, which is in accordance with the previously discussed characteristic relaxation time from the frequency sweep data (Figure 2F).

Furthermore, tunable viscoelastic response of hydrogels was evaluated by plotting the loss tangent (tan δ) against frequency (Figure 4B). In this way, an indication of the viscous contribution of each material could be evaluated. The observed trend was consistent with the data obtained from the stress relaxation measurements. The upturn of tan δ at low frequencies indicates an increase of viscous contribution to the hydrogel's response. This feature is observed for SN-HY and DN formulations, confirming that those gels display a significant viscous character. Specifically, at the lowest frequencies probed, tan δ was 1 for SN-HY (crossover point), whereas for DN gels it varied between ~0.2 and 0.6, depending on the ratio between DA and HY crosslinks. In contrast, for SN-DA, the response was predominantly elastic and less frequency-sensitive, with tan δ varying from ~0.01 to 0.06. These finite values measured here could be indicative of hydrogel imperfections, as observed with stress relaxation experiments.

Therefore, the lifetime of the DA crosslinks is longer than the slowest timescales probed in our experiments, whereas the lifetime of HY crosslinks could be determined by oscillatory shear experiments in this study. SN-DA was not effective to dissipate elastic energy quickly, whereas SN-HY displayed complete and fast relaxation, resulting in hydrogels that are not stable in time (showed further in the manuscript). However, DN hydrogels were effective in energy dissipation, while still preserving structural stability.

Injectability and 3D printing

After evaluating the viscoelastic behavior of the SN and DN hydrogels and dynamic nature of the HY crosslinks, we further investigated the extrusion-based processability of hydrogels and consequently the material's feasibility for 3D printing applications. Generally, for a material to be injectable, the stress applied should be sufficient to induce yielding of the material and consequently its transition from a solid-like to a liquid-like state. Additionally, once the material under stress becomes liquid-like, its viscosity should be low enough to allow for the material to flow when a reasonable force is applied to the piston. Since in the DN hydrogel DA crosslinks are not very dynamic under testing conditions and at experimental timescales, injectability and flow behavior of the DN formulation were assessed during the time frame when HY crosslinks were formed, but the majority of the DA crosslinks were not yet formed. Therefore, we hypothesized that the DN hydrogel could be processed in the first 10-15 min upon mixing of the polymers, before the Diels-Alder reaction between methylfuran and maleimide starts contributing significantly to the material's stiffness. Therefore, injectability and flow behavior were evaluated first for the SN-HY hydrogel. As observed from the strain sweep experiment for SN-HY (Figure S4B), the hydrogel displayed yielding behavior, and thus non-linear response at strain values above ~80% with decreasing $G'(\omega)$ and $G''(\omega)$. However, the actual transition from solid-like to liquid-like form takes place at higher strain values, when $G''(\omega) > G'(\omega)$, which for SN-HY was observed at ~200% strain (at 1 rad/s). As the material becomes fluidic under shear, its capacity to flow was assessed by measuring the viscosity as a function of the shear rate. As shown in Figure 5A, the viscosity dramatically decreased upon increasing the shear rate from 0.1 to 25 s^{-1}. From the rate-dependent viscosity measurements, there was a reduction in viscosity of ~2 orders of magnitude, indicating shear-thinning behavior. This observation is in agreement with previously reported hydrazone-crosslinked

systems[495,520]. A consecutive run with decreasing shear rate was also performed, showing that the original viscosity was recovered at low shear rates[521].

Additionally, we tested whether SN-HY could be injected through a 27 G needle (Figure 5B). In fact, by applying a gentle force, the hydrogel could be injected. Immediately after leaving the needle, the material appeared solid-like, indicating that the hydrogel structure was recovered (due to the reformation of the HY bonds). Therefore, both the yielding and shear-thinning properties of the SN-HY enabled injectability.

The schematic representation shown in Figure 5C explains in more detail what happens at a molecular

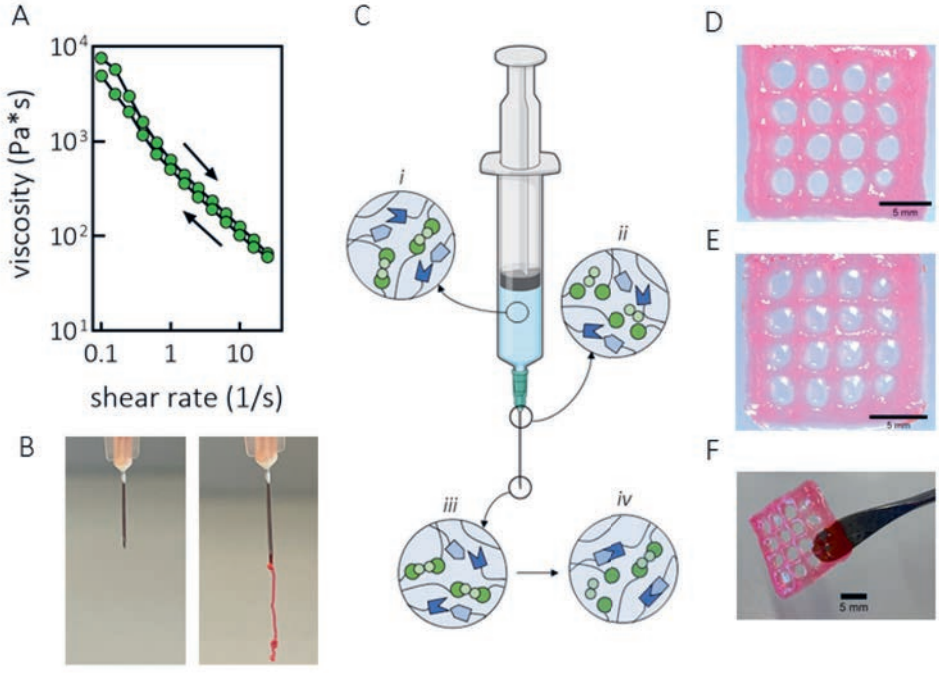

Figure 5. Injectability, flow behavior and extrusion-based 3D printing. A) Viscosity as a function of shear rate for SN-HY hydrogel (15 wt%, aldehyde to hydrazide molar ratio of 1:1). Consecutive runs of increasing (0.1-25 1/s) and decreasing shear rates (25-0.1 1/s) were performed. B) Extrusion of SN-HY hydrogel formulation (10 wt%, aldehyde to hydrazide molar ratio 1:1) through a 27G needle and syringe, confirming the hydrogel's injectability. Rhodamine dye was added for visualization. C) Schematic representation of the network structure of DN formulation during extrusion process; i) prior to extrusion, in the syringe HY bonds are formed quickly after addition of ADH crosslinker to the formulation, while DA is hardly contribution to the network in this stage; ii) during extrusion through a needle, there is transition from a solid-like to liquid-like state, supported by dissociation of HY crosslinks under shear; iii) immediately after extrusion, HY crosslinks are reformed, going back to the original, solid-like state; iv) over time, more DA adducts are being formed, leading to a continuous fixation of the hydrogel structure. D) Image of 3D printed lattice construct of DN hydrogel (15 wt%, DA to HY mass ratio of 2:1, methylfuran to maleimide and aldehyde to hydrazide molar ratios of 5:1 and 1:1 respectively), taken ~30 min after printing (following DA crosslinking). E) Image of the same 3D printed lattice structure of DN taken the following day, after being kept in a humid container overnight and then immersed in PBS for ~30 min. F) Self-supporting 3D printed construct of DN hydrogel displaying structural integrity and stability. Rhodamine dye was added for visualization.

level as the DN hydrogel formulation is being processed (*e.g.,* injected). At first instant, after transferring the solution of solubilized polymers (CS-mal, HA-MeFU and CS-ox), ADH crosslinker is added. This results in immediate formation of HY crosslinks and SN-HY formation, while the CS-mal and HA-MeFU are reacting much slower and the majority of these bonds are not formed yet. At this point, the force is applied and the material can be extruded through a needle. Under shear, the HY crosslinks disassemble, and the hydrogel undergoes transition from solid to liquid state. Immediately upon exiting the needle, the material recovers its original, gel-like state due to HY bond reformation. This enables the formulation to maintain its gel-like structure until the DA crosslinks are formed. After few minutes, DA covalent crosslinking leads to the fixation of the structure. This approach has been employed before for similar systems based on HA polymer, but photopolymerization was required to induce stabilization of the network[495]. In addition, Rodell *et al.* developed HA-based physical hydrogel based on guest-host interactions, which was further covalently crosslinked via methacrylate-mediated photopolymerization, thus needing UV light[522]. In the present work, thanks to the spontaneous Diels-Alder reaction, such fixation and stabilization of the double-crosslinked hydrogel takes place in situ, under physiological conditions. SN-HY could also be processed in this way, but the stability over time of ejected hydrogel was compromised, due to fast exchange kinetics of HY bonds and lack of stability offered by DA crosslinks (data not shown).

For initial printing experiments, we used the DN formulation at 15 wt% polymer content, DA to HY mass ratio of 2:1. Upon solubilization of polymers, the solution was transferred in the syringe and ADH crosslinker was added, resulting in SN-HY formation within few minutes. At this point, the hydrogel formulation was extruded through a 27 G needle, into a 4-layer lattice construct with 2 mm spacing between the filaments. Due to dynamic nature of HY crosslinks and their re-association, the hydrogel maintained its shape and integrity upon ejection (Figure 5D). Next, formation of DA crosslinks followed, leading to stabilization of the structure. The printed construct was then kept in a humid container overnight, to allow for DA crosslinking to complete. During that time the filaments remained stable and did not deform. Subsequently, the hydrogel construct was placed for ~30 minutes in PBS. As expected, the hydrogel remained stable due to DA covalent crosslinks, although it did seem to swell a little bit (Figure 5E). Overall, the DN formulation was confirmed to be injectable and processable in its initial stages, whereas upon Diels-Alder reaction between CS-mal and HA-MeFU the structure was rendered robust. The printed construct was shown to maintain shape fidelity, as well as structural integrity and it was able to support its own weight (Figure 5F).

Swelling behavior, stability and mechanical properties of hydrogels

After preparing different hydrogel formulations and characterizing them rheologically, we assessed their swelling behavior and mechanical properties. Mechanical performance of hydrogels is an important aspect to investigate as various biomedical applications require the material to be robust and stable. Water-retention capacity and swelling behavior are related to changes in mechanical properties over time. Because of the polymer's hydrophilic nature and the presence of negative charges, it is expected that upon the crosslinking between polymer chains, the resulting material is able to absorb and retain water. Prepared hydrogel disks were fabricated either as free or confined gels before testing (Figure 6A). First, SN-DA, SN-HY and DN were evaluated for their swelling potential. Swelling capacity was calculated as the ratio between the weight of the swollen gel and its initial weight and was defined as swelling ratio (SR). Figure 6B shows the swelling ratio of SN-DA and DN hydrogels in time. Under free swelling in PBS and at 37°C, both hydrogels steadily absorbed water in time, as observed from the increase of corresponding swelling ratios. In detail, SN-DA hydrogel exhibited a maximum SR of ~12 at

day 43 and it was fully degraded after 51 days. Degradation of SN-DA was due to the reversible character of the Diels-Alder adduct. The retro Diels-Alder reaction usually requires temperatures above 60°C to occur, but it was reported taking place under physiological conditions as well, although very slowly[523,524]. Moreover, there is another mechanism that could play a role in the degradation of the swelling hydrogel. The retro-Diels Alder reaction is characterized by a relatively low activation energy (~25 kcal/mol)[525], making the DA adduct mechanically labile, when compared to other covalent bonds in polymer networks. Indeed, mechanically induced retro-Diels-Alder reactions have been reported before[526–528]. In this case, we hypothesize that the physical expansion of the hydrogel sample was sufficient to put strain on the polymer chains (and crosslinks), therefore driving the retro-Diels- Alder reaction. In either case, the reformed maleimide is susceptible to hydrolysis leading to ring opening. As this hydrolysis is non-reversible, it causes elimination of this functional group from the Diels-Alder/retro-Diels-Alder equilibrium and therefore permanent cleavage of the DA crosslinks[524].

Unlike SN-DA, DN swelled less extensively, reaching a maximum SR of ~6.5 after 40 days (Figure 6B). The dissolution phase took until day 45, after which the gel was completely degraded. The shorter stability of the gel, compared to SN-DA, could be explained by the presence of less DA crosslinks. On the other hand, SN-HY hydrogel displayed a very short stability in time (Figure 6C). In fact, the hydrogel reached a maximum SR of ~1.7 after only 10 minutes and disintegrated completely within half an hour. This comes as no surprise, taking into account extremely dynamic character of hydrazine bonds. These results are in agreement with previously described viscoelastic and stress relaxation properties of HY crosslinks.

Considering the high swelling capacity of the present hydrogels (SN-DA and DN), we hypothesized that restraining their swelling could lead to osmotically-based pressure buildup and improvement in material elastic modulus and stiffness. This osmotically-induced stiffening could be useful for mimicking properties of load-bearing tissues, such as cartilage. Therefore, we further investigated their swelling profile under confined swelling conditions. Hydrogels were prepared in a spacer fabric material (PA6) and inserted into a cassette, with the aim to physically restrain the hydrogel from swelling. Figure 6D shows the swelling profile for SN-DA and DN hydrogels when they were confined and immersed in PBS at 37°C. The swelling ratio was not increasing in time and displayed a relatively constant profile over 80 days. After 10 days, the SR reached a maximum, ~2.3 and 1.9 for SN-DA and DN respectively, after which it was stable and equilibrated at ~1.7 until the experiment was stopped (day 80). The swelling profile was quite discordant with that obtained from the free swelling experiment, suggesting that physical confinement of the gel, and the impossibility to physically expand in response to water absorption and swelling, leads to improved stability in time. This observation indeed suggests that the predominant mechanism of the hydrogel swelling and degradation is likely the mechanically-induced retro-Diels-Alder reaction of the DA adducts, as no significant physical expansion of the material could be achieved, and thus mechanical strain on the polymer chains.

Related to the observed swelling behavior of these hydrogels, assessment of their mechanical properties upon confinement was performed. Previously, it has been reported that swelling hydrogels under

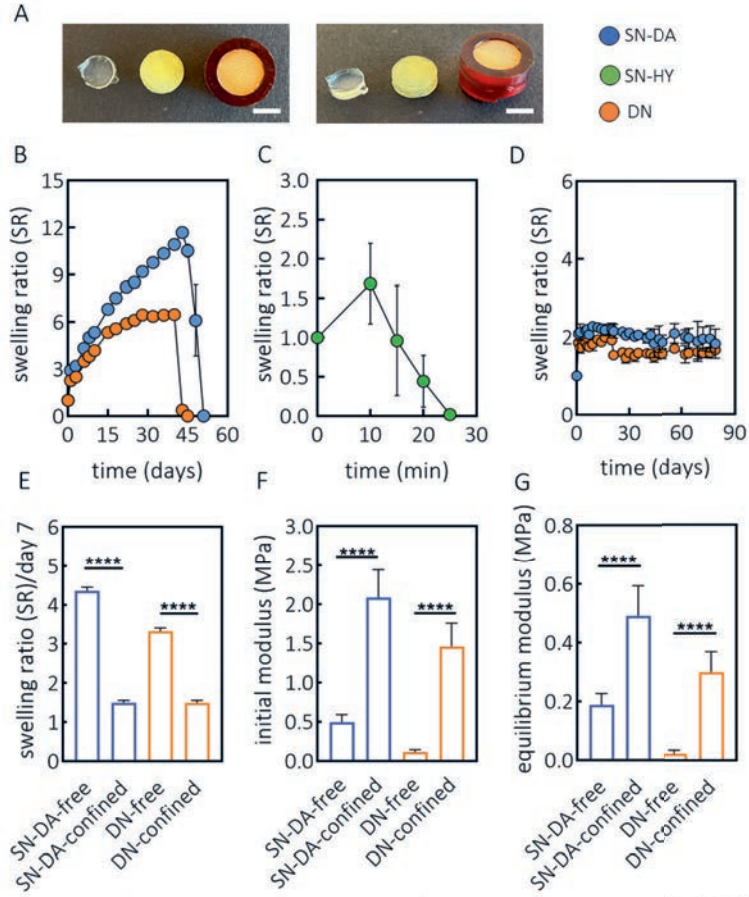

Figure 6. Swelling and mechanical properties. A) Representative pictures of hydrogels prepared for free swelling and confined tests (example given by SN-DA). From left to right: free swelling hydrogel, semi-confined (formed within spacer fabric scaffold PA6) and confined hydrogel (spacer fabric filled with hydrogel and inserted into a cassette). Swelling and mechanical tests were performed with free swelling and confined samples. Scale bar 5 mm. B) Swelling behavior of SN-DA (15 wt%, methylfuran to maleimide 5:1) and DN (15 wt%, DA to HY mass ratio 1:1, methylfuran to maleimide 5:1 and aldehyde to hydrazone 1:1) under free swelling conditions (PBS, 37°C). C) Swelling profile of SN-HY (15 wt%, aldehyde to hydrazide molar ratio 1:1) under free swelling conditions (PBS, 37°C). D) Swelling properties of SN-DA and DN (same composition as free swelling), under confined conditions (PBS, 37°C), indicating superior stability and reduced swelling of both formulations. E) Swelling ratio of SN-DA and DN hydrogel formulations, under free and confined swelling conditions, measured at day 7. F) Initial modulus for SN-DA and DN (free swelling and confined) determined after compression of 15%. G) Equilibrium modulus of free swelling and confined SN-DA and DN formulations following 15% compression. **** $p < 0.0001$ (One-way ANOVA, Tukey's multiple comparison test). Measurements were performed in triplicate (B-D) or sextuplicate (E-G).

confined conditions led to osmotic pressure buildup and therefore osmotically-induced stiffening of the construct[529]. SN-DA and DN hydrogels were first prepared and allowed to swell for 7 days under both free swelling and confined conditions (Figure 6E). The SR of SN-DA was ~4.3 for the free swelling sample, whereas for the confined one it was found to be ~1.5, with an achieved confinement of ~65%.

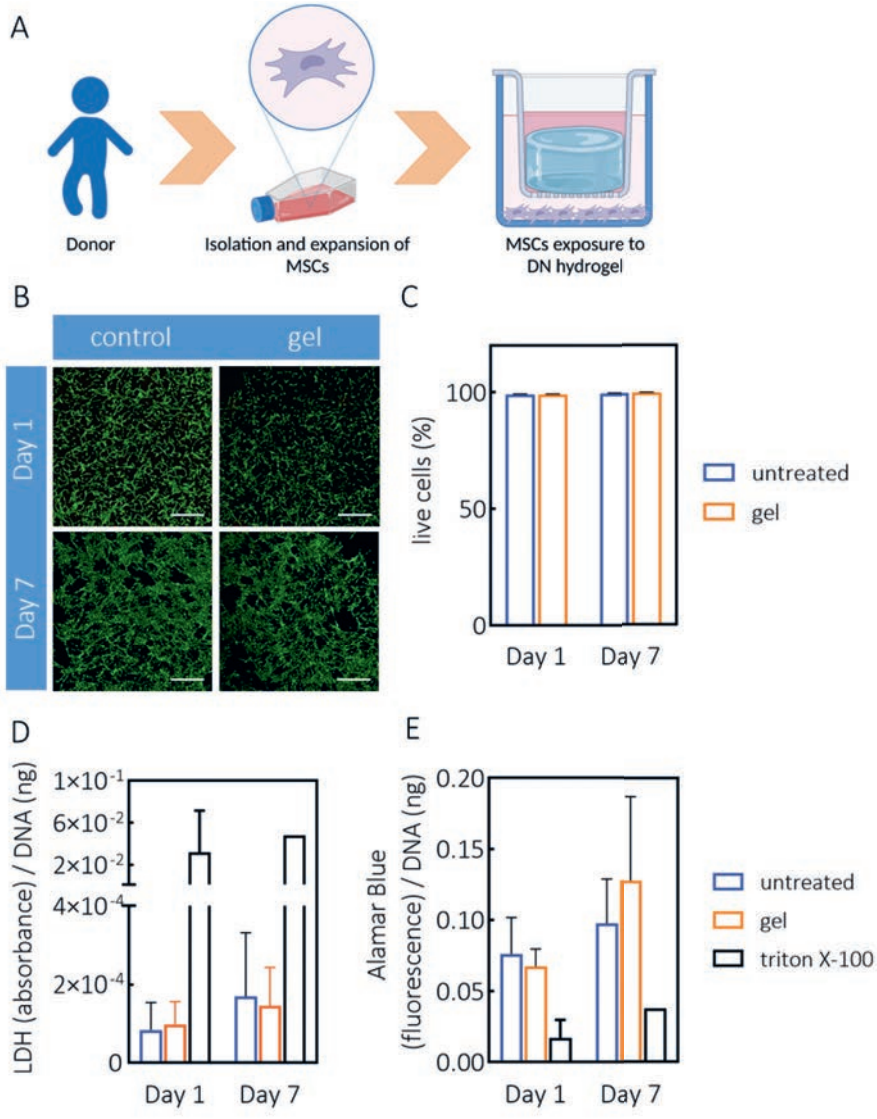

Figure 7. Cytocompatibility of DN hydrogel. A) Experimental set-up of mesenchymal stromal cells viability in the presence of DN hydrogel. B) Representative images showing live cells (in green) upon treatment with DN hydrogel (15 wt%, DA to HY mass ratio 1:1, methylfuran to maleimide 5:1 and aldehyde to hydrazone 1:1), after 1 and 7 days. Scale bar 1000 µm. C) Quantification of live cells following Live/Dead assay, using ImageJ. D) LDH release from cells measured after 1 and 7 days of treatment with DN gels and normalized against DNA content. Triton X-100 was used as a positive control. E) Cell metabolic activity measured after 1 and 7 days of treatment with DN gels and normalized against DNA content. Triton X-100 was used as a negative control.

For DN, a total confinement of ~55% was achieved, with SR going from ~3.3 for the free-swelling sample to ~1.5 for the confined sample. An ideal confinement would ensure a SR of 1, however in this case, the final construct (cassette and the spacer fabric) had a partially open structure, therefore still allowing some swelling. These samples were subsequently used for mechanical testing. Specifically, the time-dependent response was evaluated by means of an indentation test up to 15% deformation, followed by a hold at constant deformation (15%) until an equilibrium was reached. From the quick step deformation, an initial modulus was derived, as shown in Figure 6F. Free swollen SN-DA displayed a modulus of ~0.5 MPa, while the confined counterpart was found to have ~2 MPa (4-fold increase). Similarly, DN had a modulus of ~0.1 MPa after 7 days under free swelling, which upon confinement reached values of ~1.5 MPa. These results suggest that by confining the gels that exhibit swelling tendencies, it was possible to induce pressurization in the system leading to a significant increase in mechanical properties. However, considering that these materials are not purely elastic, but display viscoelastic properties (already discussed), it would be more accurate to talk in terms of time-dependent behavior. The corresponding load relaxation profiles (at 15% deformation) were analyzed and an equilibrium modulus was derived, taking into account material's relaxation properties. As shown in Figure 6G, SN-DA possessed an equilibrium compressive modulus of ~0.2 MPa when allowed to swell freely, which increased by a factor of 2.5 to ~0.5 MPa under confined conditions. DN however, showed an increase from ~0.02 to ~0.3 MPa, going from free to confined swelling. Such a remarkable increase in both initial and equilibrium moduli upon hydrogel confinement is in agreement with the previously reported swelling hydrogels[529]. The difference in both moduli observed between SN-DA and DN hydrogels is most likely due to the inherent difference in swelling capacity between the free gels. The overall mechanical performance is determined by both the crosslinking density and restricted swelling-induced pressurization.

This feature is particularly interesting and useful in the development of cartilage-mimicking scaffolds. Cartilage tissue, due to its unique composition and structural organization between hydrated polyelectrolyte matrix and collagen fibers, is characterized by increased osmotic swelling pressure, which leads to unique mechanical properties of cartilage. The confined hydrogel materials in this study are able to reproduce this aspect of cartilage tissue. The found values for equilibrium compressive modulus of the present SN-DA and DN confined hydrogels are in proximity of the range expected for articular cartilage (0.36-1.11 MPa)[530]. These observations indicate that especially SN-DA hydrogel has potential to fabricate scaffolds for cartilage tissue engineering. Overall, swelling properties and improvement of both stability and mechanical performance of the hydrogels following their physical confinement, opens a new window of possibilities and potential applications, specifically related to cartilage tissue engineering.

Cytocompatibility of hydrogels

Following detailed material characterization, the next step was to assess the cytocompatibility of the hydrogel. MSCs were used for cell viability studies (live-dead, LDH release and metabolic activity) in the presence of crosslinked DN hydrogels (15 wt%), using hanging cell culture inserts and cytotoxicity was evaluated after 1 and 7 days (Figure 7A). Live-Dead images for 1 and 7 days are shown in Figure 7B, with majority of cells found to be alive when exposed to DN hydrogel. The percentage of live cells was not different between treated and control conditions (Figure 7C). To confirm the high viability observed with Live/Dead assay, additional tests were performed, aimed at assessing the release of LDH, as well as the metabolic activity of the cells when exposed to DN hydrogels for up to 7 days. In fact, gel-treated MSCs did not release an increased amount of LDH, a measure of cellular damage and cytotoxicity (Figure

7D). The metabolic activity also showed high cell viability, confirming the results seen with the Live/Dead assay (Figure 7E). Concluding, the human MSCs exposed to fully crosslinked DN hydrogels were not affected and maintained high viability after 7 days.

Additionally, we also investigated the effect of each individual component of the DN hydrogel, at concentrations relevant for fabricating DN hydrogels at 15 wt% and it was found that after 1 h none of the components caused cytotoxicity (Figure S7). Overall, these preliminary cytocompatibility results indicate the suitability of the DN hydrogels for use in regenerative medicine applications. The high

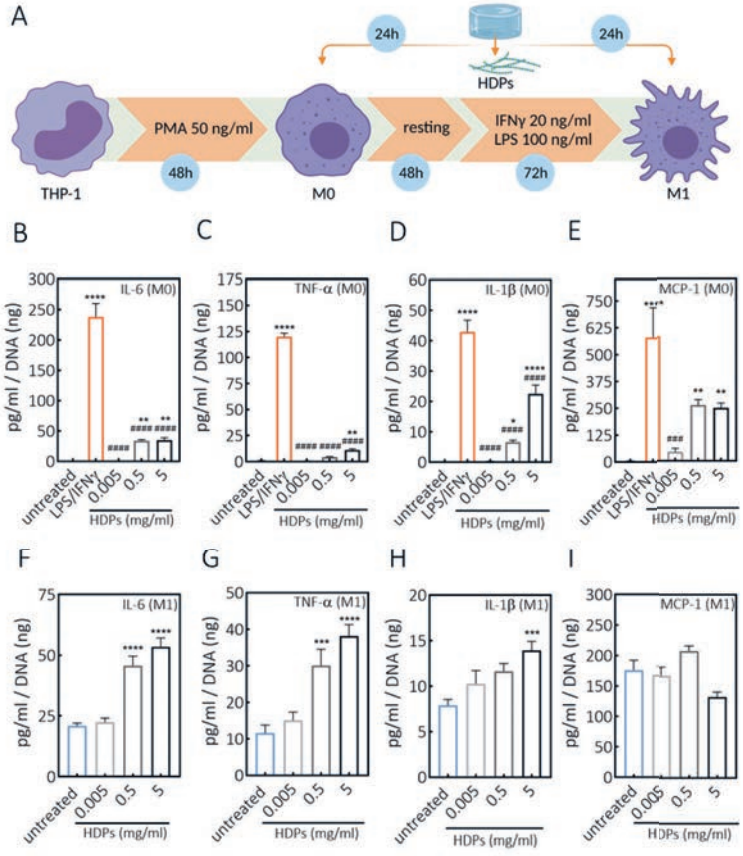

Figure 8. Effect of DN hydrogel degradation products on the cytokine production by THP-1 derived macrophages. A) Schematic representation of human THP-1 differentiation to macrophages, polarization to M1 macrophages and exposure to HDPs. B-E) Release of IL-6, TNF-α, IL-1β and MCP-1 cytokines by M0 macrophages, F-I) Release of IL-6, TNF-α, IL-1β and MCP-1 cytokines by M1 macrophages, as indicated in the figure plots and following 24h treatments with increasing concentrations of HDPs, deriving from DN hydrogel (15 wt%, DA to HY mass ratio 1:1, methylfuran to maleimide 5:1 and aldehyde to hydrazone 1:1). * $p < 0.05$, ** $p < 0.01$, *** $p < 0.001$, **** $p < 0.0001$, ### $p < 0.001$, #### $p < 0.0001$; * compared to untreated control, # compared to LPS/IFNγ treatment (One-way ANOVA, Tukey's multiple comparison test). Measurements were performed in triplicate. PMA: phorbol 12-myristate 13-acetate.

viability of MSCs after 7 days of exposure to DN gels supports future use for cell encapsulation studies and bioprinting applications.

DN hydrogel effects on human macrophages

Next, we studied the safety aspects regarding a potential inflammatory response to the biomaterials used in this study, in particular the effect of biomaterials on the macrophages. These cells are key players in the host body reactions and, as such, are able to affect overall material's biocompatibility[531,532]. In relation to the potential application of DN gels for cartilage replacement therapies, as previously mentioned, it is even more important to check foreign body response features, as it is known that in inflammatory diseases of the joints macrophages play a crucial role in disease progression by releasing proinflammatory mediators[533]. To study the effect of DN hydrogels on macrophages, DN hydrogel was incubated with HYAL II enzyme until full material degradation. Recovered material, corresponding to the degraded hydrogel, is referred to as hydrogel degradation products (HDPs). The THP-1 human monocyte cell line was used for differentiation towards M0 (non-activated) and M1 (proinflammatory) macrophages, which were then exposed to HDPs. Both cell viability and release of proinflammatory cytokines including IL-6, TNF-α, IL-1β and MCP-1 following exposure to HDPs were assessed. In the context of cartilage scenario and inflamed synovium of the joints, we wanted to assess whether HDPs induce activation of M0 towards M1 macrophages, as well as exacerbate activity of M1. The experimental set-up is schematically depicted in Figure 8A. Exposure of M0 and M1 macrophages to increasing concentrations of HDPs did not lead to cytotoxicity when compared to positive control (Figure S8), indicating that HDPs are not cytotoxic, which is in line with the observed results with MSCs and DN hydrogel. Furthermore, both cell types were exposed to HDPs to evaluate the release of proinflammatory cytokines. Figure 8B-E shows the cytokine release by M0 macrophages. The secreted levels of all investigated cytokines showed a dose-dependent increase, thus suggesting that HDPs stimulate cytokines production. However, HDPs do not seem to be as efficient activator of M0 macrophages as LPS and IFNγ, which were used as control to mimic the maximum stimulation of M0 and polarization towards M1 phenotype. Next, the effect of HDPs was also evaluated on the activated M1 macrophages. Figure 8F-I shows the cytokine release profiles when M1 macrophages were exposed to HDPs. Also, in this case the lowest tested concentrations did not significantly influence cytokines production by M1 macrophages, thus not exacerbating their activity and proinflammatory capacity. At higher concentrations, in particular 5 mg/ml, the levels of IL-6, TNF-α and IL-1β were significantly increased, whereas the MCP-1 production by M1 was not affected at any given concentration of HDPs.

Being biopolymer remnants, HDPs could represent biologically active material capable of inducing a host reaction. In this context, macrophages are important cells, as they are the first to interact with such material *in vivo*. In this study the HDPs were observed to stimulate M0 macrophages at sufficiently high concentrations, but less efficiently than LPS and IFNγ. Furthermore, HDPs did not seem to modify inherent inflammatory activity of M1 macrophages at lower concentrations, whereas at higher concentrations it could deteriorate proinflammatory status. It has been reported that HA at low molecular weights (< 64 kDa[534,535]) is considered a DAMP (damage-associated molecular pattern) stimulus, mediating inflammatory reactions[536,537]. HDPs used in this study contain fragments of HA, at molecular weights lower than 80 kDa. Therefore, it can be expected that at increasing HDPs concentrations, the amount of HA also increases, thus leading to inflammatory events. On the other hand, CS which is also present in HDPs, has been reported to have anti-inflammatory properties, by reducing production of proinflammatory cytokines TNFα and IL-1β[538,539]. In contrast, CS has also been shown to exhibit proinflammatory properties in central nervous system disorders, through integration

of signals from the microenvironment and activation of immune cells[540]. In our study, however, HDPs are composed of mixture of CS and HA at low molecular weights, and therefore the overall response might depend on the balance between the two components and their biological activity.

In view of possible regenerative cartilage applications, the concentrations of HDPs used in this experiment were in the range of the concentrations that would be reached if DN hydrogel (diameter 1 cm, height 2 mm, 15 wt%) was fully and instantly degraded within synovium of the knee joint (~3.5 ml), without taking into consideration clearance of the synovial fluid. Therefore, it is highly unlikely that the highest investigated concentrations will be reached in an *in vivo* setting, thus arguing for a safe application of herein developed DN hydrogel. However, the safety aspects related to a possible clinical translation remain to be further investigated in appropriate animal models, from which more comprehensive and physiologically relevant conclusions could be drawn.

CONCLUSIONS

In this study, we investigated the suitability of a combination of dynamic bonds with different lifetimes, to produce CS/HA-based DN hydrogels that exhibit a wide range of useful properties, especially tunable viscoelasticity and stress relaxation, while maintaining stability and integrity. The integration of Diels-Alder and hydrazone crosslinks in a single formulation proved to be an efficient way to impart hydrogel processability and self-healing features initially (due to quickly formed dynamic hydrazone bonds), but without sacrificing long-term structural integrity (due to Diels-Alder adducts). Importantly, the DN hydrogel could be easily fabricated *in situ* (pH 7.4, 37^{0}C), without applying external stimuli (*e.g.,* UV light, temperature or changes in pH). Rheological analysis showed that hydrazone crosslinks displayed short lifetimes, in the order of ~800 s, whereas Diels-Alder crosslinks proved to be rather stable at experimental timescales. Moreover, the stress relaxation profile and viscoelasticity could be easily tuned by changing the mass ratio of Diels-Alder and hydrazone components. The results also demonstrated that DN hydrogel has the possibility to be used in extrusion-based 3D printing. Furthermore, both DN and SN-DA hydrogels showed remarkable swelling capacity and stability. The bulk degradation under physiological conditions can be predominantly ascribed to mechanically-induced retro-Diels Alder reactions. However, by physically restraining the hydrogels, stability was significantly improved, in addition to the osmotically-induced pressurization leading to stiffened constructs, which could potentially mimic cartilage mechanical properties. Finally, prepared hydrogels were non-cytotoxic to MSCs over 7 days, further demonstrating the attractive properties of the present biopolymer-based gels for biomedical applications. In the following studies, this system will be further explored as a bioink. Additionally, future studies will be directed towards cartilage regeneration applications, taking into consideration the promising swelling and mechanical properties found here.

The approach employed in this study could be easily translated to other types of crosslinking chemistries (covalent, physical or dynamic covalent bonds) in order to achieve tunable viscoelasticity of hydrogel materials without sacrificing mechanical integrity and stability. We envision that multicomponent hydrogels (*e.g.,* DN hydrogels) with different combination of dynamic crosslinks, could lead to smart, responsive and multifunctional soft materials with tunable and customizable properties[494].

Annex III

Platelet-Rich Plasma Is More Than Placebo-Rich Plasma for Early Osteoarthritis Knee Letter-to-the-Editor

Tungish Bansal
Sandeep Patel

CARTILAGE (2021)

Response to Letter-to-the-Editor

Margot Rikkers
Koen Dijkstra
Bastiaan F. Terhaard
Jon Admiraal
Riccardo Levato
Jos Malda
Lucienne A. Vonk

CARTILAGE (2021)

LETTER-TO-THE-EDITOR

Dear Editor,

We read with great interest the article titled "Platelet-Rich Plasma Does Not Inhibit Inflammation or Promote Regeneration in Human Osteoarthritic Chondrocytes In Vitro Despite Increased Proliferation" by Rikkers et al[541] in the September 2020 issue of this journal. The use of platelet-rich plasma (PRP) in knee osteoarthritis (OA) has really exploded in the last decade or so. Though enough clinical evidence exists in this regard, good-quality *in vivo* and *in vitro* studies offering information of the effects of PRP in joint milieu are few. We would like to appreciate the authors for a well-thought and well-conducted study that offers insight into the effects of PRP on human osteoarthritic chondrocytes. However, we would like clarify a few points regarding the study and offer our viewpoint on the same.

1. The donors used for chondrocytes in the study were the redundant material from total knee arthroplasty. The novelty of this study is that the authors have tried to culture the chondrocytes from osteoarthritic knee cartilage, and they have demonstrated that PRP has no effect in terms of inhibiting inflammation or promoting regeneration. This again proves the fact that PRP does not act in advanced OA stages. The best results of PRP are seen in early stages of knee OA, and multiple randomized controlled trials have established the clinical efficacy in early OA knee/ early degenerative chondropathy. In fact, the literature supports for the use of PRP in early stages and not in advanced stages.[542] Previous *in vitro* studies have used healthy cartilage as source of chondrocyte culture[543] and have demonstrated anti-inflammatory and cartilage promoting effects. If we are to analyze previous studies and the present study, the right conclusion is that PRP has anti-inflammatory effects and chondro-protective effects in early OA and not in advanced OA.
2. The knees that undergo total knee arthroplasty generally have an advanced OA in one of the compartments (mostly medial). The cartilage in the other compartments may not be affected at all. The authors have stated that they pooled all the available cartilage from each donor. How is this sample representative of human osteoarthritic chondrocytes when the normal and abnormal cartilage has been mixed together? A comparison of the effects of PRP on chondrocyte cultures from different grades of OA would have given better insights into how PRP influences chondrocytes.
3. The effectiveness of PRP in early OA knee in terms of pain relief and functional improvement is best attributed to its anti-inflammatory effects, and previous studies have focused on synovium as the primary site of action of anti-inflammatory effect.[544,545] Cartilage is usually studied for chondrogenesis and extracellular matrix production. Studies similar to the present one, if carried out on the synovium of advanced OA knees, may be a fruitful and a worthwhile experience, in order to truly demonstrate absence of anti-inflammatory effects. There are a few clinical trials that have demonstrated pain relief with PRP use in advanced stages of OA[330] and that could be due to PRP effects on synovium, which we believe to be the main site of action.
4. The details for the *in vitro* degradation profile for the fibrin and PRP gels must be highlighted. The PRP gels when activated with calcium chloride result in a burst of growth factors and they tend degrade early[546] and may not last 28 days when evaluations are carried out. So, data on degradation profiles of these gels will give more clarity on the results that were found. In such a scenario, with the dilution and early degradation of PRP gels coming into

picture, multiple applications of PRP can be an option worth considering. The superiority of multiple applications of PRP over single application has been shown in animal studies4 as well as clinical studies,[547] especially with respect to effects on the cartilage.

5. The PRP concentration used in the study is approximately 2 times the baseline. Similar studies have used platelet concentrations in the range of 4 to 6 times the baseline.[362,543] This low concentration of platelets combined with dilution at various stages in the form of low concentration of PRP used, addition of activator, and diluted fibrinogen and thrombin component may have resulted in low concentration of growth factors, which may have affected the results.

6. The title is a negative reflection of PRP for normal average readers who may misinterpret the message that PRP has no anti-inflammatory effects in knee OA (after all it is human nature to get attracted to negative papers). Recall the editorial wherein PRP was called product rich in placebo,[358] and quickly caught the attention of all readers and is widely quoted in conferences and debates by PRP antagonists. The message out of this paper is that PRP does not have anti-inflammatory effects in cartilage of advanced stages of OA. This should be read and interpreted with caution. There are a number of randomized controlled trials and meta-analysis[548–550] available today after 10 years of extensive research in this field to state that PRP is more effective than placebo and hyaluronic acid for early OA of the knee in terms of functional and pain scores. So, we conclude by saying that "PRP is more than placebo-rich plasma".

RESPONSE

We thank the authors for their interest in and point of views on our recent study "Platelet-Rich Plasma Does Not Inhibit Inflammation or Promote Regeneration in Human Osteoarthritic Chondrocytes *In Vitro* Despite Increased Proliferation"[541] published in this journal. We fully agree with their statement that the clinical use of platelet-rich plasma (PRP) for knee osteoarthritis (OA) on a large scale should be supported by qualitative *in vitro* and *in vivo* research, especially to gain more understanding of the mechanisms and effects of PRP.

1. Indeed, as the authors highlighted, our *in vitro* study was performed with chondrocytes derived from tissue that was obtained from patients that underwent total knee replacement because of end-stage OA. The authors correctly conclude that we have demonstrated that the PRP we made did not show any effect on these OA chondrocytes in terms of inhibiting inflammation or promoting regeneration *in vitro*. Subsequently, the authors conclude that this study further proves the fact that PRP does not act in advanced OA stages, but does so in early OA. We agree with the authors that there is literature suggesting PRP is effective in early OA[547] and there are recommendations PRP should be used in patients with symptomatic knee OA with Ahlback grades I to III or Kellgren-Lawrence grades I to III[542]. On the other hand, we would like to be more careful drawing a conclusion, as there are still many open questions regarding the efficacy of PRP, such as the optimal selection of the PRP and the patient. Moreover, most *in vitro* studies have been performed with chondrocytes obtained from redundant material after total joint replacement. Also, the study performed by Spreafico et al.[543], in which

promoting effects on proliferation and cartilage tissue formation were observed, was performed with chondrocytes of macroscopically normal cartilage from total hip replacement surgeries due to OA. Although our samples are a mixture of mostly macroscopically healthy cartilage and some more fibrillar tissue, it is more likely that other factors, such as the PRP composition (6 times versus 2 times platelet concentration, 126 versus 60 ng TGF-beta / mL) play a more prominent role in explaining differences between the studies. Therefore, we strongly advocate for an uniform reporting system of the characteristics of PRP used in studies[435].

2. We are aware of the fact that we used cartilage tissue from patients with advanced OA for the chondrocyte isolation, and that the degree of cartilage degradation varies between the different locations in the knee, as this is also clearly reported in the experimental methods section of our manuscript. Osteoarthritis is a whole joint disease and all joint tissues may be involved to some extent. Significant changes in chondrocyte behaviour in very early models and stages of OA have been found previously, indicating a notable effect of the OA joint on the cells[551,552]. This suggests that these chondrocytes will perform differently than cells derived from a true healthy joint and are comparable to the cells used in our study. Regarding our isolation protocol, we have to further clarify certain issues, as the authors are concerned that our cartilage is not representative for OA. In this study, we have pooled the cartilage from all parts of the joint (condyles, tibial plateaus), in order to obtain a chondrocyte population that represents the status of the cartilage in the whole OA joint. Severely degraded/fibrillated cartilage is difficult to isolate from an OA knee and was, therefore, excluded. The authors recommend a comparison of effects of PRP on chondrocyte cultures from different grades of OA. We completely agree that such an experimental design would provide excellent insight into how PRP influences chondrocytes when used in various grades of OA and could back up further studies identifying what stages of OA and maybe even which patient populations could be most effectively treated with PRP.

3. The authors emphasize that clinical effectiveness of PRP in early knee OA in terms of pain relief and functional improvement is best attributed to its anti-inflammatory effects and that previous studies have identified the synovium as the primary site of action of the anti-inflammatory effect. We believe that this is an important observation and should be addressed in further *ex vivo* and *in vivo* studies. Indeed, many pro-inflammatory events take place in the synovium and it plays a big role in pain. However, in our *in vitro* study, we focused solely on the effects of PRP on OA chondrocytes, which also produce pro-inflammatory cytokines and matrix degrading enzymes in OA[553].

4. With regard to the authors' remark about the degradation rate of the gels, we are aware of the fact that calcium activates platelets and growth factor concentrations in activated PRP or platelet lysate is increased, which we have shown in a previous study[364] as well as in the current study[541]. The aim of this particular section of the current study was to investigate the capacity of our PRP gels to be used as a biomaterial for cartilage tissue engineering purposes. In general, studies clotting PRP to create a 3D biomaterial use $CaCl_2$ to generate a hydrogel that is manageable and is able to incorporate cells[323,326,362]. The findings of this section of the manuscript do not relate to intra-articular injections of PRP and do not provide an answer whether activated or not activated PRP should be used for injection nor for effects

of single versus multiple injections. As the authors mention, there are *in vivo* and clinical studies performed that focus on these questions[545,547].

5. As per authors' remark, the platelets are indeed about two times concentrated in the PRP we used in our study compared to the whole blood. It is well known that PRP varies a lot in composition and there are also commercially available and clinically used PRPs with a two-times higher platelet concentration compared to the whole blood[328,329,554,555]. More knowledge is required on the influence of platelet concentration, as a recent *in vitro* study reported a dose- and time-dependent effect of a standardized PRP lyophilizate on chondrocytes[556]. In addition, thorough evaluation and characterization of any PRP product is extremely important, as we have clearly highlighted in the discussion of our study. As abovementioned, we highly support a uniform reporting system of the characteristics of PRP used in studies[435].

To conclude, we do not agree with the author's statement that the title of our recent study is a negative reflection on PRP. The title of our study clearly states that we have performed an *in vitro* study in OA chondrocytes. In our view, our manuscript clearly highlights the specific experimental set-ups and conditions used for *in vitro* testing, thus the data reported does not create the impression that PRP is ineffective in knee OA and this conclusion cannot be drawn from our study. The study investigated the effects of PRP on one cell type derived from a pathological tissue, with clearly reported characterisations of the PRP. Under no circumstance we want to extrapolate these results to clinical effects. Therefore, we stand with the conclusions in our *in vitro* study that PRP showed a non-favourable effect on chondrocytes derived from OA cartilage.

References

1. Lee IM, Shiroma EJ, Lobelo F, et al. Effect of physical inactivity on major non-communicable diseases worldwide: An analysis of burden of disease and life expectancy. *Lancet*. 2012;380(9838):219-229. doi:10.1016/S0140-6736(12)61031-9
2. Hjelle K, Solheim E, Strand T, Muri R, Brittberg M. Articular cartilage defects in 1,000 knee arthroscopies. *Arthroscopy*. 2002;18(7):730-734. doi:10.1053/jars.2002.32839
3. Widuchowski W, Widuchowski J, Trzaska T. Articular cartilage defects: Study of 25,124 knee arthroscopies. *Knee*. 2007;14(3):177-182. doi:10.1016/j.knee.2007.02.001
4. Madry H, Kon E, Condello V, et al. Early osteoarthritis of the knee. *Knee Surgery, Sport Traumatol Arthrosc*. 2016;24(6):1753-1762. doi:10.1007/s00167-016-4068-3
5. Brown TD, Johnston RC, Saltzman CL, Marsh JL, Buckwalter JA. Posttraumatic Osteoarthritis: A First Estimate of Incidence, Prevalence, and Burden of Disease. *J Orthop Trauma*. 2006;20(10):739-744. http://journals.lww.com/jorthotrauma.
6. Roos EM. Joint injury causes knee osteoarthritis in young adults. *Curr Opin Rheumatol*. 2005;17:195-200.
7. Lotz MK. Posttraumatic osteoarthritis: pathogenesis and pharmacological treatment options. *Arthritis Res Ther*. 2010;12(211). http://arthritis-research.com/content/12/3/211.
8. Heir S, Nerhus TK, Røtterud JH, et al. Focal cartilage defects in the knee impair quality of life as much as severe osteoarthritis: a comparison of knee injury and osteoarthritis outcome score in 4 patient categories scheduled for knee surgery. *Am J Sports Med*. 2010;38(2):231-237. doi:10.1177/0363546509352157
9. Cross M, Smith E, Hoy D, et al. The global burden of hip and knee osteoarthritis: estimates from the Global Burden of Disease 2010 study. *Ann Rheum Dis*. 2014;73(7):1323-1330. doi:10.1136/annrheumdis-2013-204763
10. Jasper LL, Jones CA, Mollins J, Pohar SL, Beaupre LA. Risk factors for revision of total knee arthroplasty: A scoping review. *BMC Musculoskelet Disord*. 2016;17(1). doi:10.1186/s12891-016-1025-8
11. Liodakis E, Bergeron SG, Zukor DJ, Huk OL, Epure LM, Antoniou J. Perioperative Complications and Length of Stay After Revision Total Hip and Knee Arthroplasties: An Analysis of the NSQIP Database. *J Arthroplasty*. 2015;30(11):1868-1871. doi:10.1016/j.arth.2015.05.029
12. Goldring MB. Chondrogenesis, chondrocyte differentiation, and articular cartilage metabolism in health and osteoarthritis. *Ther Adv Musculoskelet Dis*. 2012;4(4):269-285. doi:10.1177/1759720X12448454
13. Buckwalter JA, Mankin HJ, Grodzinsky AJ. Articular Cartilage and Osteoarthritis. *AAOS Instr Course Lect*. 2005;54:465-480.
14. Hunziker EB, Quinn TM, Häuselmann HJ. Quantitative structural organization of normal adult human articular cartilage. *Osteoarthr Cartil*. 2002;10(7):564-572. doi:10.1053/joca.2002.0814
15. Dowthwaite GP, Bishop J, Redman S, et al. The surface of articular cartilage contains a progenitor cell population. *J Cell Sci*. 2004;117(6):889-897. doi:10.1242/jcs.00912
16. Alsalameh S, Amin R, Gemba T, Lotz M. Identification of mesenchymal progenitor cells in normal and osteoarthritic human articular cartilage. *Arthritis Rheum*. 2004;50(5):1522-1532. doi:10.1002/art.20269
17. Maroudas A, Bayliss MT, Uchitel-Kaushansky N, Schneiderman R, Gilav E. Aggrecan turnover in human articular cartilage: Use of aspartic acid racemization as a marker of molecular age. *Arch Biochem Biophys*. 1998;350(1):61-71. doi:10.1006/abbi.1997.0492
18. Verzijl N, DeGroot J, Thorpe SR, et al. Effect of collagen turnover on the accumulation of advanced glycation end products. *J Biol Chem*. 2000;275(50):39027-39031. doi:10.1074/jbc.M006700200
19. Greene GW, Banquy X, Woog Lee D, Lowrey DD, Yu J, Israelachvili JN. Adaptive mechanically controlled lubrication mechanism found in articular joints. *Proc Natl Acad Sci U S A*. 2011;108(13):5255-5259. doi:10.1073/pnas.1101002108
20. Fukui N, Miyamoto Y, Nakajima M, et al. Zonal gene expression of chondrocytes in osteoarthritic cartilage. *Arthritis Rheum*. 2008;58(12):3843-3853. doi:10.1002/art.24036
21. Schuurman W, Gawlitta D, Klein TJ, et al. Zonal Chondrocyte Subpopulations Reacquire Zone-Specific Characteristics during in Vitro Redifferentiation. *Am J Sports Med*. 2009;37(1_suppl):97S-104S. doi:10.1177/0363546509350978
22. Poole CA, Flint MH, Beaumont BW. Morphological and Functional Interrelationships of Articular Cartilage Matrices. Vol 138.; 1984.
23. Guilak F, Jones WR, Ting-Beall HP, Lee GM. The deformation behavior and viscoelastic properties of

chondrocytes in articular cartilage. *Osteoarthr Cartil*. 1999;7:59-70.
24. Guilak F, Hayes AJ, Melrose J. Perlecan in pericellular mechanosensory cell-matrix communication, extracellular matrix stabilisation and mechanoregulation of load-bearing connective tissues. *Int J Mol Sci*. 2021;22(5):1-20. doi:10.3390/ijms22052716
25. Poole CA, Ayad S, Gilbert RT. Chondrons from articular cartilage. V. Immunohistochemical evaluation of type VI collagen organisation in isolated chondrons by light, confocal and electron microscopy. *J Cell Sci*. 1993;102(4):1101-1110. doi:10.1242/jcs.103.4.1101
26. Kurkijärvi JE, Nissi MJ, Rieppo J, et al. The zonal architecture of human articular cartilage described by T2 relaxation time in the presence of Gd-DTPA2-. *Magn Reson Imaging*. 2008;26(5):602-607. doi:10.1016/j.mri.2007.10.013
27. Jafarzadeh SR, Felson DT. Updated Estimates Suggest a Much Higher Prevalence of Arthritis in United States Adults Than Previous Ones. *Arthritis Rheumatol*. 2018;70(2):185-192. doi:10.1002/art.40355
28. Hunter DJ, Bierma-Zeinstra S. Osteoarthritis. *Lancet*. 2019;393:1745-1759. doi:10.1016/S0140-6736(19)30417-9
29. König F. The Classic On Loose Bodies in the Joint From the Surgery Clinic in Göttingen On loose bodies in the joint. *Clin Orthop Relat Res*. 2013;471:1107-1115. doi:10.1007/s11999
30. Krishnan Y, Grodzinsky AJ. Cartilage diseases. *Matrix Biol*. 2018;71-72:51-69. doi:10.1016/j.matbio.2018.05.005
31. Brittberg M, Peterson L. Introduction of an articular cartilage classification. *ICRS Newsl*. 1998.
32. Englund M, Roemer FW, Hayashi D, Crema MD, Guermazi A. Meniscus pathology, osteoarthritis and the treatment controversy. *Nat Rev Rheumatol*. 2012;8(7):412-419. doi:10.1038/nrrheum.2012.69
33. Lohmander LS, Englund PM, Dahl LL, Roos EM. The long-term consequence of anterior cruciate ligament and meniscus injuries: Osteoarthritis. *Am J Sports Med*. 2007;35(10):1756-1769. doi:10.1177/0363546507307396
34. Cinque ME, Dornan GJ, Chahla J, Moatshe G, LaPrade RF. High Rates of Osteoarthritis Develop After Anterior Cruciate Ligament Surgery: An Analysis of 4108 Patients. *Am J Sports Med*. 2018;46(8):2011-2019. doi:10.1177/0363546517730072
35. Neuman P, Englund M, Kostogiannis I, Fridén T, Roos H, Dahlberg LE. Prevalence of tibiofemoral osteoarthritis 15 years after nonoperative treatment of anterior cruciate ligament injury: A prospective cohort study. *Am J Sports Med*. 2008;36(9):1717-1725. doi:10.1177/0363546508316770
36. Iorio R, Healy WL. Unicompartmental arthritis of the knee. *J Bone Jt Surg - Ser A*. 2003;85(7):1351-1364. doi:10.2106/00004623-200307000-00025
37. Goldring MB. The role of the chondrocyte in osteoarthritis. *Arthritis Rheum*. 2000;43(9):1916-1926.
38. Rollín R, Marco F, Jover JA, et al. Early lymphocyte activation in the synovial microenvironment in patients with osteoarthritis: Comparison with rheumatoid arthritis patients and healthy controls. *Rheumatol Int*. 2008;28(8):757-764. doi:10.1007/s00296-008-0518-7
39. Pearle AD, Warren RF, Rodeo SA. Basic science of articular cartilage and osteoarthritis. *Clin Sports Med*. 2005;24(1):1-12. doi:10.1016/j.csm.2004.08.007
40. Buckwalter J, Mankin H. Articular cartilage repair and transplantation. *Arthritis Rheum*. 1998;41(8):1331-1342.
41. Brittberg M, Lindahl A, Nilsson A, Ohlsson C, Isaksson O, Peterson L. Treatment of deep cartilage defects in the knee with autologous chondrocyte transplantation. *New Engel J Med*. 1994;331(14):889-895. doi:10.1007/s40262-012-0001-1
42. Bartlett W, Skinner JA, Gooding CR, et al. Autologous chondrocyte implantation versus matrix-induced autologous chondrocyte implantation for osteochondral defects of the knee. A prospective, randomised study. *J Bone Jt Surg - Ser B*. 2005;87(5):640-645. doi:10.1302/0301-620X.87B5.15905
43. Steinwachs M. New Technique for Cell-Seeded Collagen Matrix-Supported Autologous Chondrocyte Transplantation. *Arthrosc - J Arthrosc Relat Surg*. 2009;25(2):208-211. doi:10.1016/j.arthro.2008.10.009
44. Siebold R, Suezer F, Schmitt B, Trattnig S, Essig M. Good clinical and MRI outcome after arthroscopic autologous chondrocyte implantation for cartilage repair in the knee. *Knee Surgery, Sport Traumatol Arthrosc*. 2018;26(3):831-839. doi:10.1007/s00167-017-4491-0

45. Fickert S, Gerwien P, Helmert B, et al. One-Year Clinical and Radiological Results of a Prospective, Investigator-Initiated Trial Examining a Novel, Purely Autologous 3-Dimensional Autologous Chondrocyte Transplantation Product in the Knee. *Cartilage*. 2012;3(1):27-42. doi:10.1177/1947603511417616
46. Niethammer TR, Pietschmann MF, Horng A, et al. Graft hypertrophy of matrix-based autologous chondrocyte implantation: A two-year follow-up study of NOVOCART 3D implantation in the knee. *Knee Surgery, Sport Traumatol Arthrosc*. 2014;22(6):1329-1336. doi:10.1007/s00167-013-2454-7
47. Steadman RJ, Rodkey WG, Rodrigo JJ. Microfracture: Surgical Technique and Rehabilitation to Treat Chondral Defects. *Clin Orthop Relat Res*. 2001;391S:S362-S369.
48. Maffulli N. Color Atlas and Text of Sports Medicine in Childhood and Adolescence. Mosby-Wolfe; 1995.
49. Hangody L, Kish G, Karpati Z, Udvarhelyi I, Szigeti I, Bely M. Mosaicplasty for the treatment of articular cartilage defects. *Orthopedics*. 1998;21:747-817. http://journals.lww.com/00003086-200110001-00030.
50. Kon E, Mandelbaum B, Buda R, et al. Platelet-rich plasma intra-articular injection versus hyaluronic acid viscosupplementation as treatments for cartilage pathology: from early degeneration to osteoarthritis. *Arthrosc J Arthrosc Relat Surg*. 2011;27(11):1490-1501.
51. Nguyen C, Lefèvre-Colau MM, Poiraudeau S, Rannou F. Evidence and recommendations for use of intra-articular injections for knee osteoarthritis. *Ann Phys Rehabil Med*. 2016;59(3):184-189. doi:10.1016/j.rehab.2016.02.008
52. Di Matteo B, Vandenbulcke F, Vitale ND, et al. Minimally Manipulated Mesenchymal Stem Cells for the Treatment of Knee Osteoarthritis: A Systematic Review of Clinical Evidence. *Stem Cells Int*. 2019;2019. doi:10.1155/2019/1735242
53. Cavallo C, Boffa A, Andriolo L, et al. Bone marrow concentrate injections for the treatment of osteoarthritis: evidence from preclinical findings to the clinical application. *Int Orthop*. 2021;45:525-538. doi:10.1007/s00264-020-04703-w/Published
54. Bolia IK, Bougioukli S, Hill WJ, et al. Clinical Efficacy of Bone Marrow Aspirate Concentrate Versus Stromal Vascular Fraction Injection in Patients With Knee Osteoarthritis: A Systematic Review and Meta-analysis. *Am J Sports Med*. 2021. doi:10.1177/03635465211014500
55. Shanmugasundaram S, Vaish A, Chavada V, Murrell WD, Vaishya R, In SC. Assessment of safety and efficacy of intra-articular injection of stromal vascular fraction for the treatment of knee osteoarthritis-a systematic review Level of evidence: Level IV, systematic review of levels II-IV studies. *Int Orthop*. 2021;45:615-625. doi:10.1007/s00264-020-04926-x/Published
56. Kim SH, Djaja YP, Park YB, Park JG, Ko YB, Ha CW. Intra-articular Injection of Culture-Expanded Mesenchymal Stem Cells Without Adjuvant Surgery in Knee Osteoarthritis: A Systematic Review and Meta-analysis. *Am J Sports Med*. 2020;48(11):2839-2849. doi:10.1177/0363546519892278
57. Carr AJ, Robertsson O, Graves S, et al. Knee replacement. *www.thelancet.com*. 2012;379. doi:10.1016/S0140
58. Robertsson O, Dunbar M, Pehrsson T, Knutson K, Lidgren L. Patient satisfaction after knee arthroplasty. *Acta Orthop Scand*. 2000;71(3):262-297.
59. Jansen MP, Boymans TAEJ, Custers RJH, et al. Knee Joint Distraction as Treatment for Osteoarthritis Results in Clinical and Structural Benefit: A Systematic Review and Meta-Analysis of the Limited Number of Studies and Patients Available. *Cartilage*. 2020. doi:10.1177/1947603520942945
60. Besselink NJ, Vincken KL, Bartels LW, et al. Cartilage Quality (dGEMRIC Index) Following Knee Joint Distraction or High Tibial Osteotomy. *Cartilage*. 2020;11(1):19-31. doi:10.1177/1947603518777578
61. Teunissen M, Miranda Bedate A, Coeleveld K, et al. Enhanced Extracellular Matrix Breakdown Characterizes the Early Distraction Phase of Canine Knee Joint Distraction. *Cartilage*. 2021. doi:10.1177/19476035211014595
62. Ekhtiari S, Haldane CE, De Sa D, Simunovic N, Musahl V, Ayeni OR. Return to work and sport following high tibial osteotomy: A systematic review. *J Bone Jt Surg - Am Vol*. 2016;98(18):1568-1577. doi:10.2106/JBJS.16.00036
63. Lobenhoffer P. The Rationale of Osteotomy around the Knee. *J Knee Surg*. 2017;30(5):386-392. doi:10.1055/s-0037-1603755
64. Malda J, Groll J, van Weeren PR. Rethinking articular cartilage regeneration based on a 250-year-old

statement. *Nat Rev Rheumatol*. 2019:2-3. doi:10.1038/s41584-019-0278-7

65. Andriolo L, Merli G, Filardo G, Marcacci M, Kon E. Failure of Autologous Chondrocyte Implantation. *Sports Med Arthrosc*. 2017;25(1):10-18. doi:10.1097/JSA.0000000000000137
66. Dell'Accio F, De Bari C, Luyten FP. Molecular markers predictive of the capacity of expanded human articular chondrocytes to form stable cartilage in vivo. *Arthritis Rheum*. 2001;44(7):1608-1619. doi:10.1002/1529-0131(200107)44:7
67. Hayes AJ, Hall A, Brown L, Tubo R, Caterson B. Macromolecular organization and in vitro growth characteristics of scaffold-free neocartilage grafts. *J Histochem Cytochem*. 2007;55(8):853-866. doi:10.1369/jhc.7A7210.2007
68. De Windt TS, Sorel JC, Vonk LA, Kip MMA, IJzerman MJ, Saris DBF. Early health economic modelling of single-stagecartilage repair. Guiding implementation of technologiesin regenerative medicine. *J Tissue Eng Regen Med*. 2016. doi:10.1002/term.2197
69. Bekkers JEJ, Creemers LB, Tsuchida AI, et al. One-stage focal cartilage defect treatment with bone marrow mononuclear cells and chondrocytes leads to better macroscopic cartilage regeneration compared to microfracture in goats. *Osteoarthr Cartil*. 2013;21(7):950-956. doi:10.1016/j.joca.2013.03.015
70. De Windt TS, Vonk LA, Slaper-Cortenbach ICM, et al. Allogeneic mesenchymal stem cells stimulate cartilage regeneration and are safe for single-stage cartilage repair in humans upon mixture with recycled autologous chondrons. *Stem Cells*. 2017;10(1):256-264. doi:10.1002/stem.2475
71. Wu L, Prins HJ, Helder MN, Van Blitterswijk CA, Karperien M. Trophic effects of mesenchymal stem cells in chondrocyte Co-Cultures are independent of culture conditions and cell sources. *Tissue Eng - Part A*. 2012;18(15-16):1542-1551. doi:10.1089/ten.tea.2011.0715
72. Hildner F, Concaro S, Peterbauer A, et al. Human Adipose-Derived Stem Cells Contribute to Chondrogenesis in Coculture with Human Articular Chondrocytes. *Tissue Eng - Part A*. 2009;15:3961-3969. www.liebertpub.com.
73. Hendriks JAA, Miclea RL, Schotel R, et al. Primary chondrocytes enhance cartilage tissue formation upon co-culture with a range of cell types. *Soft Matter*. 2010;6(20):5080-5088. doi:10.1039/c0sm00266f
74. Bigdeli N, Karlsson C, Strehl R, Concaro S, Hyllner J, Lindahl A. Coculture of human embryonic stem cells and human articular chondrocytes results in significantly altered phenotype and improved chondrogenic differentiation. *Stem Cells*. 2009;27(8):1812-1821. doi:10.1002/stem.114
75. Wei Y, Zeng W, Wan R, et al. Chondrogenic differentiation of induced pluripotent stem cells from osteoarthritic chondrocytes in alginate matrix. *Eur Cells Mater*. 2012;23:1-12. doi:10.22203/eCM.v023a01
76. Vonk LA, Dooremalen SFJ Van, Liv N, et al. Mesenchymal Stromal/stem cell-derived extracellular vesicles promote human cartilage regeneration in vitro. *Theranostics*. 2018;8(4):906-920. doi:10.7150/thno.20746
77. Gnecchi M. Paracrine Mechanisms of Mesenchymal Stem Cells in Tissue Repair. In: *Mesenchymal Stem Cells Methods and Protocols*. Vol 2. ; 2016:123-146. http://www.springer.com/series/7651.
78. Fortier LA, Barker JU, Strauss EJ, McCarrel TM, Cole BJ. The role of growth factors in cartilage repair. In: *Clinical Orthopaedics and Related Research*. Vol 469. Springer New York LLC; 2011:2706-2715. doi:10.1007/s11999-011-1857-3
79. Filardo G, Kon E, Roffi A, Di Matteo B, Merli M, Marcacci M. Platelet-rich plasma: why intra-articular? A systematic review of preclinical studies and clinical evidence on PRP for joint degeneration. *Knee Surg Sport Traumatol Arthrosc*. 2015;23(9):2459-2474. doi:10.1007/s00167-013-2743-1
80. Drengk A, Zapf A, Stürmer EK, Stürmer KM, Frosch K-H. Influence of platelet-rich plasma on chondrogenic differentiation and proliferation of chondrocytes and mesenchymal stem cells. *Cells Tissues Organs*. 2008;189(5):317-326. doi:10.1159/000151290
81. Pereira RC, Scaranari M, Benelli R, et al. Dual Effect of Platelet Lysate on Human Articular Cartilage: A Maintenance of Chondrogenic Potential and a Transient Proinflammatory Activity Followed by an Inflammation Resolution. *Tissue Eng Part A*. 2013;19(11-12):1476-1488. doi:10.1089/ten.tea.2012.0225
82. Xie X, Zhang C, Tuan RS. Biology of platelet-rich plasma and its clinical application in cartilage repair. *Arthritis Res Ther*. 2014;16(1):204. doi:10.1186/ar4493

83. Saris DBF, Vanlauwe J, Victor J, et al. Characterized chondrocyte implantation results in better structural repair when treating symptomatic cartilage defects of the knee in a randomized controlled trial versus microfracture. *Am J Sports Med*. 2008;36(2):235-246. doi:10.1177/0363546507311095
84. Bomer N, den Hollander W, Suchiman H, et al. Neo-cartilage engineered from primary chondrocytes is epigenetically similar to autologous cartilage, in contrast to using mesenchymal stem cells. *Osteoarthr Cartil*. 2016;24(8):1423-1430. doi:10.1016/j.joca.2016.03.009
85. Vail DJ, Somoza RA, Caplan AI, Khalil AM. Transcriptome dynamics of long noncoding RNAs and transcription factors demarcate human neonatal, adult, and human mesenchymal stem cell-derived engineered cartilage. *J Tissue Eng Regen Med*. 2020;14(1):29-44. doi:10.1002/term.2961
86. Muhammad H, Schminke B, Bode C, et al. Human migratory meniscus progenitor cells are controlled via the TGF-β pathway. *Stem Cell Reports*. 2014;3(5):789-803. doi:10.1016/j.stemcr.2014.08.010
87. Sun H, Wen X, Li H, et al. Single-cell RNA-seq analysis identifies meniscus progenitors and reveals the progression of meniscus degeneration. *Ann Rheum Dis*. 2019;79:408-417. doi:10.1136/annrheumdis-2019-215926
88. De Bari C, Dell'Accio F, Luyten FP. Human periosteum-derived cells maintain phenotypic stability and chondrogenic potential throughout expansion regardless of donor age. *Arthritis Rheum*. 2001;44(1):85-95. doi:10.1002/1529-0131(200101)44:1
89. Affan A, Al-Jezani N, Railton P, Powell JN, Krawetz RJ. Multiple mesenchymal progenitor cell subtypes with distinct functional potential are present within the intimal layer of the hip synovium. *BMC Musculoskelet Disord*. 2019;20(1):125. doi:10.1186/s12891-019-2495-2
90. Williams R, Khan IM, Richardson K, et al. Identification and Clonal Characterisation of a Progenitor Cell Sub-Population in Normal Human Articular Cartilage. Agarwal S, ed. *PLoS One*. 2010;5(10):e13246. doi:10.1371/journal.pone.0013246
91. Fellows CR, Williams R, Davies IR, et al. Characterisation of a divergent progenitor cell sub-populations in human osteoarthritic cartilage: the role of telomere erosion and replicative senescence. *Sci Rep*. 2017;7(1):41421. doi:10.1038/srep41421
92. McCarthy HE, Bara JJ, Brakspear K, Singhrao SK, Archer CW. The comparison of equine articular cartilage progenitor cells and bone marrow-derived stromal cells as potential cell sources for cartilage repair in the horse. *Vet J*. 2012;192(3):345-351. doi:10.1016/j.tvjl.2011.08.036
93. Jiang Y, Cai Y, Zhang W, et al. Human Cartilage-Derived Progenitor Cells From Committed Chondrocytes for Efficient Cartilage Repair and Regeneration. *Stem Cells Transl Med*. 2016;5(6):733-744. doi:10.5966/sctm.2015-0192
94. Anderson DE, Markway BD, Weekes KJ, McCarthy HE, Johnstone B. Physioxia Promotes the Articular Chondrocyte-Like Phenotype in Human Chondroprogenitor-Derived Self-Organized Tissue. *Tissue Eng - Part A*. 2018;24(3-4):264-274. doi:10.1089/ten.TEA.2016.0510
95. Carluccio S, Martinelli D, Palamà MEF, et al. Progenitor Cells Activated by Platelet Lysate in Human Articular Cartilage as a Tool for Future Cartilage Engineering and Reparative Strategies. *Cells*. 2020;9(4):1052. doi:10.3390/cells9041052
96. Fortier LA, Strauss EJ, Shepard DO, Becktell L, Kennedy JG. Biological Effects of Bone Marrow Concentrate in Knee Pathologies. *J Knee Surg*. 2019;32(1):2-8. doi:10.1055/s-0038-1676069
97. Gianakos A, Ni A, Zambrana L, Kennedy JG, Lane JM. Bone Marrow Aspirate Concentrate in Animal Long Bone Healing: An Analysis of Basic Science Evidence. *J Orthop Traumatol*. 2015;30(1):1-9. www.jorthotrauma.com.
98. Habets MGJL, Van Delden JJM, Bredenoord AL. The inherent ethical challenge of first-in-human pluripotent stem cell trials. *Regen Med*. 2014;9(1):1-3. doi:10.2217/rme.13.83
99. Tuan RS, Chen AF, Klatt BA. Cartilage regeneration. *J Am Acad Orthop Surg*. 2013;21(5):303-311. doi:10.5435/JAAOS-21-05-303
100. Rodríguez Ruiz A, Dicks A, Tuerlings M, et al. Cartilage from human-induced pluripotent stem cells: comparison with neo-cartilage from chondrocytes and bone marrow mesenchymal stromal cells. *Cell Tissue Res*. 2021. doi:10.1007/s00441-021-03498-5
101. Takei Y, Morioka M, Yamashita A, Kobayashi T, Shima N, Tsumaki N. Quality assessment tests for tumorigenicity of human iPS cell-derived cartilage. *Sci Rep*. 2020;10(1). doi:10.1038/s41598-020-

69641-4
102. Yamashita A, Tamamura Y, Morioka M, Karagiannis P, Shima N, Tsumaki N. Considerations in hiPSC-derived cartilage for articular cartilage repair. *Inflamm Regen*. 2018;38(1). doi:10.1186/s41232-018-0075-8
103. Yamashita A, Tsumaki N. Recent progress of animal transplantation studies for treating articular cartilage damage using pluripotent stem cells. *Dev Growth Differ*. 2020;63:72-81.
104. Pot MW, Gonzales VK, Buma P, et al. Improved cartilage regeneration by implantation of acellular biomaterials after bone marrow stimulation: A systematic review and meta-analysis of animal studies. *PeerJ*. 2016;2016(9). doi:10.7717/peerj.2243
105. Visser J, Peters B, Burger TJ, et al. Biofabrication of multi-material anatomically shaped tissue constructs. *Biofabrication*. 2013;5(3). doi:10.1088/1758-5082/5/3/035007
106. Levato R, Jungst T, Scheuring RG, Blunk T, Groll J, Malda J. From Shape to Function: The Next Step in Bioprinting. *Adv Mater*. 2020;32(12). doi:10.1002/adma.201906423
107. Hutmacher DW. Sca!Olds in Tissue Engineering Bone and Cartilage. Vol 21.; 2000.
108. Klein TJ, Rizzi SC, Reichert JC, et al. Strategies for zonal cartilage repair using hydrogels. *Macromol Biosci*. 2009;9(11):1049-1058. doi:10.1002/mabi.200900176
109. Guettler JH, Demetropoulos CK, Yang KH, Jurist KA. Osteochondral defects in the human knee: Influence of defect size on cartilage rim stress and load redistribution to surrounding cartilage. *Am J Sports Med*. 2004;32(6):1451-1458. doi:10.1177/0363546504263234
110. Evans C, Georgescu H. Observations on the senescence of cells derived from articular cartilage. *Mech Ageing Dev*. 1983;22:179-191.
111. Barbero A, Ploegert S, Heberer M, Martin I. Plasticity of clonal populations of dedifferentiated adult human articular chondrocytes. *Arthritis Rheum*. 2003;48(5):1315-1325. doi:10.1002/art.10950
112. von der Mark K, Gauss V, von der Mark H, Müller P. Relationship between cell shape and type of collagen synthesised as chondrocytes lose their cartilage phenotype in culture. *Nature*. 1977;267:531-532.
113. Vonk LA, De Windt TS, Slaper-Cortenbach ICM, Saris DBF. Autologous, allogeneic, induced pluripotent stem cell or a combination stem cell therapy? Where are we headed in cartilage repair and why: A concise review. *Stem Cell Res Ther*. 2015;6(1):1-11. doi:10.1186/s13287-015-0086-1
114. Mueller MB, Fischer M, Zellner J, et al. Hypertrophy in mesenchymal stem cell chondrogenesis: Effect of TGF-β isoforms and chondrogenic conditioning. *Cells Tissues Organs*. 2010;192(3):158-166. doi:10.1159/000313399
115. De Windt TS, Vonk LA, Slaper-Cortenbach ICM, Nizak R, van Rijen MHP, Saris DBF. Allogeneic MSCs and recycled autologous chondrons mixed in a one-stage cartilage cell transplantion: a first-in-man trial in 35 patients. *Stem Cells*. 2017;35(8):1984-1993. doi:10.1002/stem.2657
116. Levato R, Webb WR, Otto IA, et al. The bio in the ink: cartilage regeneration with bioprintable hydrogels and articular cartilage-derived progenitor cells. *Acta Biomater*. 2017;61:41-53. doi:10.1016/j.actbio.2017.08.005
117. Nelson L, McCarthy HE, Fairclough J, Williams R, Archer CW. Evidence of a viable pool of stem cells within human osteoarthritic cartilage. *Cartilage*. 2014;5(4):203-214. doi:10.1177/1947603514544953
118. Schmidt S, Abinzano F, Mensinga A, et al. Differential Production of Cartilage ECM in 3D Agarose Constructs by Equine Articular Cartilage Progenitor Cells and Mesenchymal Stromal Cells. *Int J Mol Sci*. 2020;21(19):7071. doi:10.3390/ijms21197071
119. Zhang K, Shi J, Li Y, et al. Chondrogenic cells respond to partial-thickness defects of articular cartilage in adult rats: an in vivo study. *J Mol Histol*. 2016;47(3):249-258. doi:10.1007/s10735-016-9668-1
120. Tao T, Li Y, Gui C, et al. Fibronectin Enhances Cartilage Repair by Activating Progenitor Cells Through Integrin alpha5beta1 Receptor. *Tissue Eng Part A*. 2018;24(13-14):1112-1124. doi:10.1089/ten.TEA.2017.0322
121. Walsh SK, Schneider SE, Amundson LA, Neu CP, Henak CR. Maturity-dependent cartilage cell plasticity and sensitivity to external perturbation. *J Mech Behav Biomed Mater*. 2020;106:103732. doi:10.1016/j.jmbbm.2020.103732
122. Pretzel D, Linss S, Rochler S, et al. Relative percentage and zonal distribution of mesenchymal progenitor cells in human osteoarthritic and normal cartilage. *Arthritis Res Ther*. 2011;13(2):R64.

doi:10.1186/ar3320
123. Su X, Zuo W, Wu Z, et al. CD146 as a new marker for an increased chondroprogenitor cell sub-population in the later stages of osteoarthritis. *J Orthop Res*. 2015;33(1):84-91. doi:10.1002/jor.22731
124. Grogan SP, Miyaki S, Asahara H, D'Lima DD, Lotz MK. Mesenchymal progenitor cell markers in human articular cartilage: normal distribution and changes in osteoarthritis. *Arthritis Res Ther*. 2009;11(3):R85. doi:10.1186/ar2719
125. Riegger J, Palm H, Brenner R. The functional role of chondrogenic stem/progenitor cells: novel evidence for immunomodulatory properties and regenerative potential after cartilage injury. *Eur Cells Mater*. 2018;36:110-127. doi:10.22203/eCM.v036a09
126. Wang Y-X, Zhao Z-D, Wang Q, et al. Biological potential alterations of migratory chondrogenic progenitor cells during knee osteoarthritic progression. *Arthritis Res Ther*. 2020;22(1):62. doi:10.1186/s13075-020-2144-z
127. Ustunel I, Ozenci AM, Sahin Z, et al. The immunohistochemical localization of notch receptors and ligands in human articular cartilage, chondroprogenitor culture and ultrastructural characteristics of these progenitor cells. *Acta Histochem*. 2008;110(5):397-407. doi:10.1016/j.acthis.2007.12.005
128. De Luca P, Kouroupis D, Viganò M, et al. Human Diseased Articular Cartilage Contains a Mesenchymal Stem Cell-Like Population of Chondroprogenitors with Strong Immunomodulatory Responses. *J Clin Med*. 2019;8(4):423. doi:10.3390/jcm8040423
129. Schminke B, Frese J, Bode C, Goldring MB, Miosge N. Laminins and Nidogens in the Pericellular Matrix of Chondrocytes: Their Role in Osteoarthritis and Chondrogenic Differentiation. *Am J Pathol*. 2016;186(2):410-418. doi:10.1016/j.ajpath.2015.10.014
130. Seol D, McCabe DJ, Choe H, et al. Chondrogenic progenitor cells respond to cartilage injury. *Arthritis Rheum*. 2012;64(11):3626-3637. doi:10.1002/art.34613
131. Hoshiyama Y, Otsuki S, Oda S, et al. Chondrocyte clusters adjacent to sites of cartilage degeneration have characteristics of progenitor cells. *J Orthop Res*. 2015;33(4):548-555. doi:10.1002/jor.22782
132. Tong W, Geng Y, Huang Y, et al. In Vivo Identification and Induction of Articular Cartilage Stem Cells by Inhibiting NF-κB Signaling in Osteoarthritis. *Stem Cells*. 2015;33(10):3125-3137. doi:10.1002/stem.2124
133. Jang KW, Ding L, Seol D, Lim TH, Buckwalter JA, Martin JA. Low-Intensity pulsed ultrasound promotes chondrogenic progenitor cell migration via focal adhesion kinase pathway. *Ultrasound Med Biol*. 2014;40(6):1177-1186. doi:10.1016/j.ultrasmedbio.2013.12.007
134. Jones PH, Watt FM. Separation of human epidermal stem cells from transit amplifying cells on the basis of differences in integrin function and expression. *Cell*. 1993;73(4):713-724. doi:10.1016/0092-8674(93)90251-K
135. Khan IM, Bishop JC, Gilbert S, Archer CW. Clonal chondroprogenitors maintain telomerase activity and Sox9 expression during extended monolayer culture and retain chondrogenic potential. *Osteoarthr Cartil*. 2009;17(4):518-528. doi:10.1016/j.joca.2008.08.002
136. Marcus P, De Bari C, Dell'Accio F, Archer CW. Articular Chondroprogenitor Cells Maintain Chondrogenic Potential but Fail to Form a Functional Matrix When Implanted Into Muscles of SCID Mice. *Cartilage*. 2014;5(4):231-240. doi:10.1177/1947603514541274
137. Shafiee A, Kabiri M, Langroudi L, Soleimani M, Ai J. Evaluation and comparison of the in vitro characteristics and chondrogenic capacity of four adult stem/progenitor cells for cartilage cell-based repair. *J Biomed Mater Res Part A*. 2016;104(3):600-610. doi:10.1002/jbm.a.35603
138. Vinod E, Kachroo U, Ozbey O, Sathishkumar S, Boopalan P. Comparison of human articular chondrocyte and chondroprogenitor cocultures and monocultures: To assess chondrogenic potential and markers of hypertrophy. *Tissue Cell*. 2019;57:42-48. doi:10.1016/j.tice.2019.01.007
139. Vinod E, Kachroo U, Rebekah G, Yadav BK, Ramasamy B. Characterization of human articular chondrocytes and chondroprogenitors derived from non-diseased and osteoarthritic knee joints to assess superiority for cell-based therapy. *Acta Histochem*. 2020;122(6):151588. doi:10.1016/j.acthis.2020.151588
140. Vinod E, Ramasamy B, Kachroo U. Comparison of immunogenic markers of human chondrocytes and chondroprogenitors derived from non-diseased and osteoarthritic articular cartilage. *J Orthop Trauma Rehabil*. 2020;27(1):63-67. doi:10.1177/2210491720915927

141. Nelson L, McCarthy HE, Fairclough J, Williams R, Archer CW. Evidence of a Viable Pool of Stem Cells within Human Osteoarthritic Cartilage. *Cartilage*. 2014;5(4):203-214. doi:10.1177/1947603514544953
142. He R, Wang B, Cui M, et al. Link Protein N-Terminal Peptide as a Potential Stimulating Factor for Stem Cell-Based Cartilage Regeneration. *Stem Cells Int*. 2018;2018:1-11. doi:10.1155/2018/3217895
143. Cai Z, Hong M, Xu L, et al. Prevent action of magnoflorine with hyaluronic acid gel from cartilage degeneration in anterior cruciate ligament transection induced osteoarthritis. *Biomed Pharmacother*. 2020;126. doi:10.1016/j.biopha.2019.109733
144. Li Y, Zhou J, Yang X, Jiang Y, Gui J. Intermittent hydrostatic pressure maintains and enhances the chondrogenic differentiation of cartilage progenitor cells cultivated in alginate beads. *Dev Growth Differ*. 2016;58(2):180-193. doi:10.1111/dgd.12261
145. Zhang S, An Q, Hu P, et al. Core regulatory RNA molecules identified in articular cartilage stem/progenitor cells during osteoarthritis progression. *Epigenomics*. 2019;11(6):669-684. doi:10.2217/epi-2018-0212
146. Kachroo U, Vinod E. Comparative analysis of gene expression between articular cartilage-derived cells to assess suitability of fibronectin adhesion assay to enrich chondroprogenitors. *Knee*. 2020;27(3):755-759. doi:10.1016/j.knee.2020.04.015
147. Majumdar MK, Thiede MA, Mosca JD, Moorman M, Gerson SL. Phenotypic and functional comparison of cultures of marrow-derived mesenchymal stem cells (MSCs) and stromal cells. *J Cell Physiol*. 1998;176(1):57-66. doi:10.1002/(SICI)1097-4652(199807)176:1<57::AID-JCP7>3.0.CO;2-7
148. Fickert S, Fiedler J, Brenner RE. Identification of subpopulations with characteristics of mesenchymal progenitor cells from human osteoarthritic cartilage using triple staining for cell surface markers. *Arthritis Res Ther*. 2004;6(5):422-432. doi:10.1186/ar1210
149. Joos H, Wildner A, Hogrefe C, Reichel H, Brenner RE. Interleukin-1 beta and tumor necrosis factor alpha inhibit migration activity of chondrogenic progenitor cells from non-fibrillated osteoarthritic cartilage. *Arthritis Res Ther*. 2013;15(5):R119. doi:10.1186/ar4299
150. Jiang Y, Hu C, Yu S, et al. Cartilage stem/progenitor cells are activated in osteoarthritis via interleukin-1β/nerve growth factor signaling. *Arthritis Res Ther*. 2015;17(1):327. doi:10.1186/s13075-015-0840-x
151. Zhou C, Zheng H, Seol D, Yu Y, Martin JA. Gene expression profiles reveal that chondrogenic progenitor cells and synovial cells are closely related. *J Orthop Res*. 2014;32(8):981-988. doi:10.1002/jor.22641
152. Koelling S, Kruegel J, Irmer M, et al. Migratory Chondrogenic Progenitor Cells from Repair Tissue during the Later Stages of Human Osteoarthritis. *Cell Stem Cell*. 2009;4(4):324-335. doi:10.1016/j.stem.2009.01.015
153. Tallheden T, Denis J, Lennon D, Sjogren-Jansson E, Caplan A, Lindahl A. Phenotypic Plasticity of Human Articular Chondrocytes. *J Bone Jt Surgery-American Vol*. 2003;85(Suppl 2):93-99. doi:10.2106/00004623-200300002-00012
154. Bernstein P, Sperling I, Corbeil D, Hempel U, Fickert S. Progenitor cells from cartilage-No osteoarthritis-grade-specific differences in stem cell marker expression. *Biotechnol Prog*. 2013;29(1):206-212. doi:10.1002/btpr.1668
155. Mantripragada VP, Bova WA, Boehm C, et al. Progenitor cells from different zones of human cartilage and their correlation with histopathological osteoarthritis progression. *J Orthop Res*. 2018;36(6):1728-1738. doi:10.1002/jor.23829
156. Mantripragada VP, Bova WA, Boehm C, et al. Primary Cells Isolated from Human Knee Cartilage Reveal Decreased Prevalence of Progenitor Cells but Comparable Biological Potential During Osteoarthritic Disease Progression. *J Bone Jt Surg*. 2018;100(20):1771-1780. doi:10.2106/JBJS.18.00005
157. Mantripragada VP, Bova WA, Piuzzi NS, et al. Native-Osteoarthritic Joint Resident Stem and Progenitor Cells for Cartilage Cell-Based Therapies: A Quantitative Comparison With Respect to Concentration and Biological Performance. *Am J Sports Med*. 2019;47(14):3521-3530. doi:10.1177/0363546519880905
158. Mantripragada VP, Kaplevatsky R, Bova WA, et al. Influence of Glucose Concentration on Colony-Forming Efficiency and Biological Performance of Primary Human Tissue–Derived Progenitor Cells. *Cartilage*. February 2020:194760352090660. doi:10.1177/1947603520906605
159. Salamon A, Jonitz-Heincke A, Adam S, et al. Articular cartilage-derived cells hold a strong osteogenic differentiation potential in comparison to mesenchymal stem cells in vitro. *Exp Cell Res*. 2013;319(18):2856-2865. doi:10.1016/j.yexcr.2013.09.008

160. Peng X, Yang L, Chang H, et al. Wnt/β-Catenin Signaling Regulates the Proliferation and Differentiation of Mesenchymal Progenitor Cells through the p53 Pathway. Samant R, ed. *PLoS One*. 2014;9(5):e97283. doi:10.1371/journal.pone.0097283
161. Xia Z, Ma P, Wu N, et al. Altered function in cartilage derived mesenchymal stem cell leads to OA-related cartilage erosion. *Am J Transl Res*. 2016;8(2):433-446. http://www.ncbi.nlm.nih.gov/pubmed/27158337.
162. Thornemo M, Tallheden T, Sjögren Jansson E, et al. Clonal Populations of Chondrocytes with Progenitor Properties Identified within Human Articular Cartilage. *Cells Tissues Organs*. 2005;180(3):141-150. doi:10.1159/000088242
163. Karlsson C, Stenhamre H, Sandstedt J, Lindahl A. Neither Notch1 Expression nor Cellular Size Correlate with Mesenchymal Stem Cell Properties of Adult Articular Chondrocytes. *Cells Tissues Organs*. 2008;187(4):275-285. doi:10.1159/000113409
164. Kachroo U, Ramasamy B, Vinod E. Evaluation of CD49e as a distinguishing marker for human articular cartilage derived chondroprogenitors. *Knee*. 2020;27(3):833-837. doi:10.1016/j.knee.2020.04.002
165. Dominici M, Blanc K Le, Mueller I, et al. Minimal criteria for defining multipotent mesenchymal stromal cells. The International Society for Cellular Therapy position statement. *Cytotherapy*. 2006;8(4):315-317. doi:10.1080/14653240600855905
166. Anderson DE, Markway BD, Bond D, McCarthy HE, Johnstone B. Responses to altered oxygen tension are distinct between human stem cells of high and low chondrogenic capacity. *Stem Cell Res Ther*. 2016;7(1):154. doi:10.1186/s13287-016-0419-8
167. Vinod E, Parameswaran R, Manickam Amirtham S, Livingston A, Ramasamy B, Kachroo U. Comparison of the efficiency of laminin versus fibronectin as a differential adhesion assay for isolation of human articular cartilage derived chondroprogenitors. *Connect Tissue Res*. May 2020:1-9. doi:10.1080/03008207.2020.1761344
168. Mayne R, Vail MS, Mayne PM, Miller EJ. Changes in type of collagen synthesized as clones of chick chondrocytes grow and eventually lose division capacity. *Proc Natl Acad Sci*. 1976;73(5):1674-1678. doi:10.1073/pnas.73.5.1674
169. Diaz-Romero J, Gaillard JP, Grogan SP, Nesic D, Trub T, Mainil-Varlet P. Immunophenotypic analysis of human articular chondrocytes: Changes in surface markers associated with cell expansion in monolayer culture. *J Cell Physiol*. 2005;202(3):731-742. doi:10.1002/jcp.20164
170. Yu Y, Zheng H, Buckwalter JA, Martin JA. Single cell sorting identifies progenitor cell population from full thickness bovine articular cartilage. *Osteoarthr Cartil*. 2014;22(9):1318-1326. doi:10.1016/j.joca.2014.07.002
171. Jiang Y, Tuan RS. Origin and function of cartilage stem/progenitor cells in osteoarthritis. *Nat Rev Rheumatol*. 2015;11(4):206-212. doi:10.1016/j.physbeh.2017.03.040
172. Melero Martin JM, Smith M, Al-Rubeai M. Cryopreservation and in Vitro Expansion of Chondroprogenitor Cells Isolated from the Superficial Zone of Articular Cartilage. *Biotechnol Prog*. 2005;21(1):168-177. doi:10.1021/bp049821o
173. Melero-Martin JM, Dowling M-A, Smith M, Al-Rubeai M. Expansion of chondroprogenitor cells on macroporous microcarriers as an alternative to conventional monolayer systems. *Biomaterials*. 2006;27(15):2970-2979. doi:10.1016/j.biomaterials.2006.01.023
174. Melero-Martin JM, Dowling M-A, Smith M, Al-Rubeai M. Optimal in-vitro expansion of chondroprogenitor cells in monolayer culture. *Biotechnol Bioeng*. 2006;93(3):519-533. doi:10.1002/bit.20735
175. Kachroo U, Zachariah SM, Thambaiah A, et al. Comparison of Human Platelet Lysate versus Fetal Bovine Serum for Expansion of Human Articular Cartilage–Derived Chondroprogenitors. *Cartilage*. May 2020:194760352091863. doi:10.1177/1947603520918635
176. Neumann AJ, Gardner OFW, Williams R, Alini M, Archer CW, Stoddart MJ. Human Articular Cartilage Progenitor Cells Are Responsive to Mechanical Stimulation and Adenoviral-Mediated Overexpression of Bone-Morphogenetic Protein 2. Garcia Aznar JM, ed. *PLoS One*. 2015;10(8):e0136229. doi:10.1371/journal.pone.0136229
177. Nevo Z, Beit-Or A, Eilam Y. Slowing down aging of cultured chick chondrocytes by maintenance under lowered O2 tension. *Mechanis*. 1988;45:157-165.
178. Foldager CB, Nielsen AB, Munir S, et al. Combined 3D and hypoxic culture improves cartilage-specific gene

expression in human chondrocytes. *Acta Orthop*. 2011;82(2):234-240. doi:10.3109/17453674.2011.566135

179. Zhou C, Zheng H, Buckwalter JA, Martin JA. Enhanced phagocytic capacity endows chondrogenic progenitor cells with a novel scavenger function within injured cartilage. *Osteoarthr Cartil*. 2016;24(9):1648-1655. doi:10.1016/j.joca.2016.04.016
180. Roman-Blas JA, Jimenez SA. NF-κB as a potential therapeutic target in osteoarthritis and rheumatoid arthritis. *Osteoarthr Cartil*. 2006;14(9):839-848. doi:10.1016/j.joca.2006.04.008
181. Zhu M, Tang D, Wu Q, et al. Activation of β-catenin signaling in articular chondrocytes leads to osteoarthritis-like phenotype in adult β-catenin conditional activation mice. *J Bone Miner Res*. 2009;24(1):12-21. doi:10.1359/jbmr.080901
182. Iannone F, De Bari C, Dell'Accio F, et al. Increased expression of nerve growth factor (NGF) and high affinity NGF receptor (p140 TrkA) in human osteoarthritic chondrocytes. *Rheumatology*. 2002;41(12):1413-1418. doi:10.1093/rheumatology/41.12.1413
183. Morgan BJ, Bauza-Mayol G, Gardner OFWW, et al. Bone Morphogenetic Protein-9 Is a Potent Chondrogenic and Morphogenic Factor for Articular Cartilage Chondroprogenitors. *Stem Cells Dev*. 2020;29(14):scd.2019.0209. doi:10.1089/scd.2019.0209
184. Liu T, Li X, Wang T, et al. Kartogenin mediates cartilage regeneration by stimulating the IL-6/Stat3-dependent proliferation of cartilage stem/progenitor cells. *Biochem Biophys Res Commun*. 2020;532(3):385-392. doi:10.1016/j.bbrc.2020.08.059
185. Koelling S, Miosge N. Sex differences of chondrogenic progenitor cells in late stages of osteoarthritis. *Arthritis Rheum*. 2010;62(4):1077-1087. doi:10.1002/art.27311
186. Mouser VHM, Levato R, Bonassar LJ, et al. Three-Dimensional Bioprinting and Its Potential in the Field of Articular Cartilage Regeneration. *Cartilage*. 2017;8(4):327-340. doi:10.1177/1947603516665445
187. Mouser VHM, Levato R, Mensinga A, Dhert WJA, Gawlitta D, Malda J. Bio-ink development for three-dimensional bioprinting of hetero-cellular cartilage constructs. *Connect Tissue Res*. 2018;61(2):137-151. doi:10.1080/03008207.2018.1553960
188. Diloksumpan P, de Ruijter M, Castilho M, et al. Combining multi-scale 3D printing technologies to engineer reinforced hydrogel-ceramic interfaces. *Biofabrication*. 2020;12(2):025014. doi:10.1088/1758-5090/ab69d9
189. Mancini IAD, Schmidt S, Brommer H, et al. A composite hydrogel-3D printed thermoplast osteochondral anchor as example for a zonal approach to cartilage repair: in vivo performance in a long-term equine model. *Biofabrication*. 2020;12(3):035028. doi:10.1088/1758-5090/ab94ce
190. Peiffer QC, de Ruijter M, van Duijn J, et al. Melt electrowriting onto anatomically relevant biodegradable substrates: Resurfacing a diarthrodial joint. *Mater Des*. 2020;195:109025. doi:10.1016/j.matdes.2020.109025
191. Piluso S, Flores Gomez D, Dokter I, et al. Rapid and cytocompatible cell-laden silk hydrogel formation via riboflavin-mediated crosslinking. *J Mater Chem B*. 2020;8(41):9566-9575. doi:10.1039/D0TB01731K
192. Lim KS, Levato R, Costa PF, et al. Bio-resin for high resolution lithography-based biofabrication of complex cell-laden constructs. *Biofabrication*. 2018;10(3). doi:10.1088/1758-5090/aac00c
193. Bernal PN, Delrot P, Loterie D, et al. Volumetric Bioprinting of Complex Living-Tissue Constructs within Seconds. *Adv Mater*. 2019;31(42). doi:10.1002/adma.201904209
194. Frisbie DD, McCarthy HE, Archer CW, Barrett MF, McIlwraith CW. Evaluation of Articular Cartilage Progenitor Cells for the Repair of Articular Defects in an Equine Model. *J Bone Jt Surg*. 2015;97(6):484-493. doi:10.2106/JBJS.N.00404
195. Decker RS, Um H-B, Dyment NA, et al. Cell origin, volume and arrangement are drivers of articular cartilage formation, morphogenesis and response to injury in mouse limbs. *Dev Biol*. 2017;426(1):56-68. doi:10.1016/j.ydbio.2017.04.006
196. Feng C, Chan WCW, Lam Y, et al. Lgr5 and Col22a1 Mark Progenitor Cells in the Lineage toward Juvenile Articular Chondrocytes. *Stem Cell Reports*. 2019;13(4):713-729. doi:10.1016/j.stemcr.2019.08.006
197. Ji Q, Zheng Y, Zhang G, et al. Single-cell RNA-seq analysis reveals the progression of human osteoarthritis. *Ann Rheum Dis*. 2019;78(1):100-110. doi:10.1136/annrheumdis-2017-212863
198. Caplan A. Adult mesenchymal stem cells for tissue engineering versus regenerative medicine. *J Cell Physiol*.

2007;213(2):341-347. doi:10.1002/JCP.21200
199. Chan CKF, Seo EY, Chen JY, et al. Identification and specification of the mouse skeletal stem cell. *Cell*. 2015;160(1-2):285-298. doi:10.1016/j.cell.2014.12.002
200. Chan CKF, Gulati GS, Sinha R, et al. Identification of the Human Skeletal Stem Cell. *Cell*. 2018;175(1):43-56.e21. doi:10.1016/j.cell.2018.07.029
201. Mankin HJ, Dorfman H, Lippiello L, Zarins A. Biochemical and metabolic abnormalities in articular cartilage from osteo-arthritic human hips. II. Correlation of morphology with biochemical and metabolic data. *J Bone Joint Surg Am*. 1971;53(3):523-537. http://www.ncbi.nlm.nih.gov/pubmed/5580011.
202. Kean TJ, Lin P, Caplan AI, Dennis JE. MSCs: Delivery routes and engraftment , cell-targeting strategies, and immune modulation. *Stem Cells Int*. 2013;2013(?):732742.
203. Vinod E, Parameswaran R, Ramasamy B, Kachroo U. Pondering the Potential of Hyaline Cartilage–Derived Chondroprogenitors for Tissue Regeneration: A Systematic Review. *Cartilage*. August 2020:194760352095163. doi:10.1177/1947603520951631
204. Unguryte A, Bernotiene E, Bagdonas E, Garberyte S, Porvaneckas N, Jorgensen C. Human articular chondrocytes with higher aldehyde dehydrogenase activity have stronger expression of COL2A1 and SOX9. *Osteoarthr Cartil*. 2016;24(5):873-882. doi:10.1016/j.joca.2015.11.019
205. Hattori S, Oxford C, Reddi AH. Identification of superficial zone articular chondrocyte stem/progenitor cells. *Biochem Biophys Res Commun*. 2007;358(1):99-103. doi:10.1016/j.bbrc.2007.04.142
206. Nguyen VT, Cancedda R, Descalzi F. Platelet lysate activates quiescent cell proliferation and reprogramming in human articular cartilage: Involvement of hypoxia inducible factor 1. *J Tissue Eng Regen Med*. 2018;12(3):e1691-e1703. doi:10.1002/term.2595
207. Vinod E, James JV, Kachroo U, et al. Comparison of incremental concentrations of micron-sized superparamagnetic iron oxide for labelling articular cartilage derived chondroprogenitors. *Acta Histochem*. 2019;121(7):791-797. doi:10.1016/j.acthis.2019.07.004
208. Vinod E, Vinod Francis D, Manickam Amirtham S, Sathishkumar S, Boopalan PRJVC. Allogeneic platelet rich plasma serves as a scaffold for articular cartilage derived chondroprogenitors. *Tissue Cell*. 2019;56:107-113. doi:10.1016/j.tice.2018.12.006
209. Vinod E, Kachroo U, Rebekah G, Thomas S, Ramasamy B. In vitro chondrogenic differentiation of human articular cartilage derived chondroprogenitors using pulsed electromagnetic field. *J Clin Orthop Trauma*. 2021;14:22-28. doi:10.1016/j.jcot.2020.09.034
210. Wang R, Jiang W, Zhang L, et al. Intra-articular delivery of extracellular vesicles secreted by chondrogenic progenitor cells from MRL/MpJ superhealer mice enhances articular cartilage repair in a mouse injury model. *Stem Cell Res Ther*. 2020;11(1):93. doi:10.1186/s13287-020-01594-x
211. Peterson L, Vasiliadis HS, Brittberg M, Lindahl A. Autologous chondrocyte implantation: A long term follow-up. *Am J Sports Med*. 2010;38(6):1117-1124. doi:10.1177/0363546509357915
212. Andriolo L, Reale D, Di Martino A, et al. Long-term Results of Arthroscopic Matrix-Assisted Autologous Chondrocyte Transplantation: A Prospective Follow-up at 15 Years. *Am J Sports Med*. 2020;48(12):2994-3001. doi:10.1177/0363546520949849
213. Schnabel M, Marlovits S, Eckhoff G, et al. Dedifferentiation-associated changes in morphology and gene expression in primary human articular chondrocytes in cell culture. *Osteoarthr Cartil*. 2002;10(1):62-70. doi:10.1053/joca.2001.0482
214. Salerno A, Brady K, Rikkers M, et al. MMP13 and TIMP1 are functional markers for two different potential modes of action by mesenchymal stem/stromal cells when treating osteoarthritis. *Stem Cells*. July 2020. doi:10.1002/stem.3255
215. Chamberlain G, Fox J, Ashton B, Middleton J. Consise review: Mesenchymal stem cells: Their phenotype, differentiation capacity, immunological features, and potential for homing. *Stem Cells*. 2007;25:2739-2749. doi:10.1634/stemcells.2007-0197
216. Yoo JU, Barthel TS, Nishimura K, et al. The chondrogenic potential of human bone-marrow-derived mesenchymal progenitor cells. *J Bone Jt Surg - Ser A*. 1998;80(12):1745-1757. doi:10.2106/00004623-199812000-00004
217. Mackay AM, Beck SC, Murphy JM, Barry FP, Chichester CO, Pittenger MF. Chondrogenic differentiation of cultured human mesenchymal stem cells from marrow. *Tissue Eng*. 1998;4(4):415-428.

doi:10.1089/ten.1998.4.415
218. Gawlitta D, Farrell E, Malda J, Creemers LB, Alblas J, Dhert WJ. Modulating endochondral ossification of multipotent stromal cells for bone regeneration. *Tissue Eng part B*. 2010;16(4).
219. Archer C, Williams R, Nelson L, Khan I. Articular cartilage-derived stem cells: identification, characterisation and their role in spontaneous repair. *Rheumatol Curr Res*. 2012;01(S3). doi:10.4172/2161-1149.s3-005
220. Bekkers JEJ, Saris DBF, Tsuchida AI, van Rijen MHP, Dhert WJA, Creemers LB. Chondrogenic Potential of Articular Chondrocytes Depends on Their Original Location. *Tissue Eng Part A*. 2014;20(3):663-671. doi:10.1089/ten.tea.2012.0673
221. COREON. Human Tissue and Medical Research: Code of Conduct for responsible use (2011). https://www.coreon.org/wp-content/uploads/2020/04/coreon-code-of-conduct-english.pdf. Published 2011. Accessed November 15, 2021.
222. Prins H-J, Rozemuller H, Vonk-Griffioen S, et al. Bone-Forming Capacity of Mesenchymal Stromal Cells When Cultured in the Presence of Human Platelet Lysate as Substitute for Fetal Bovine Serum. *Tissue Eng Part A*. 2009;15(12):3741-3751. doi:10.1089/ten.tea.2008.0666
223. Hanada K, Dennis JE, Caplan AI. Stimulatory effects of basic fibroblast growth factor and bone morphogenetic protein-2 on osteogenic differentiation of rat bone marrow- derived mesenchymal stem cells. *J Bone Miner Res*. 1997;12(10):1606-1614. doi:10.1359/jbmr.1997.12.10.1606
224. Rapko S, Zhang M, Richards B, Hutto E, Dethlefsen S, Duguay S. Identification of the chondrocyte lineage using microfibril-associated glycoprotein-2, a novel marker that distinguishes chondrocytes from synovial cells. *Tissue Eng - Part C Methods*. 2010;16(6):1367-1375. doi:10.1089/ten.tec.2009.0772
225. Oberlender SA, Tuan RS. Expression and functional involvement of N-cadherin in embryonic limb chondrogenesis. *Development*. 1994;120(1):177-187.
226. Tuli R, Tuli S, Nandi S, et al. Transforming Growth Factor-β-mediated Chondrogenesis of Human Mesenchymal Progenitor Cells Involves N-cadherin and Mitogen-activated Protein Kinase and Wnt Signaling Cross-talk. *J Biol Chem*. 2003;278(42):41227-41236. doi:10.1074/jbc.M305312200
227. Hoshiyama Y, Otsuki S, Oda S, et al. Expression Pattern and Role of Chondrocyte Clusters in Osteoarthritic Human Knee Cartilage. *J Orthop Res*. 2015;33(4):548-555. doi:10.1002/jor.22782.Expression
228. Benya PD, Shaffer JD. Dedifferentiated chondrocytes reexpress the differentiated collagen phenotype when cultured in agarose gels. *Cell*. 1982;30(1):215-224. doi:10.1016/0092-8674(82)90027-7
229. Vogel C, Marcotte EM. Insights into the regulation of protein abundance from proteomic and transcriptomic analyses. *Nat Rev Genet*. 2012;13(4):227-232. doi:10.1038/nrg3185
230. Sandell LJ, Morris N, Robbins JR, Goldring MB. Alternatively spliced type II procollagen mRNAs define distinct populations of cells during vertebral development: Differential expression of the amino-propeptide. *J Cell Biol*. 1991;114(6):1307-1319. doi:10.1083/jcb.114.6.1307
231. Zuscik MMJ, Hilton MJM, Zhang X, Chen D, O'Keefe RJR. Regulation of chondrogenesis and chondrocyte differentiation by stress. *J Clin Invest*. 2008;118(2):429-438. doi:10.1172/JCI34174
232. Mueller MB, Tuan RS. Functional characterization of hypertrophy in chondrogenesis of human mesenchymal stem cells. *Arthritis Rheum*. 2008;58(5):1377-1388. doi:10.1002/art.23370
233. Saris D, Price A, Widuchowski W, et al. Matrix-applied characterized autologous cultured chondrocytes versus microfracture: Two-year follow-up of a prospective randomized trial. *Am J Sports Med*. 2014;42(6):1384-1394. doi:10.1177/0363546514528093
234. Ebert JR, Robertson WB, Woodhouse J, et al. Clinical and magnetic resonance imaging-based outcomes to 5 years after matrix-induced autologous chondrocyte implantation to address articular cartilage defects in the knee. *Am J Sports Med*. 2011;39(4):753-763. doi:10.1177/0363546510390476
235. Niemeyer P, Laute V, John T, et al. The Effect of Cell Dose on the Early Magnetic Resonance Morphological Outcomes of Autologous Cell Implantation for Articular Cartilage Defects in the Knee. *Am J Sports Med*. 2016;44(8):2005-2014. doi:10.1177/0363546516646092
236. McDevitt CA, Webber RJ. The ultrastructure and biochemistry of meniscal cartilage. *Clin Orthop Relat Res*. 1990;252:8-18. doi:10.1097/NCN.0b013e31823ea54e
237. Verdonk PCM, Forsyth RG, Wang J, et al. Characterisation of human knee meniscus cell phenotype. *Osteoarthr Cartil*. 2005;13(7):548-560. doi:10.1016/j.joca.2005.01.010
238. Arnoczky SP, Warren RF. Microvasculature of the human meniscus. *Am J Sports Med*. 1982;10(2):90-95.

doi:10.1177/036354658201000205
239. King D. The healing of semilunar cartilages. *Clin Orthop Relat Res*. 1990;(252):4-7.
240. Starke C, Kopf S, Petersen W, et al. Meniscal repair. *Arthroscopy*. 2009;25(9):1033-1044. doi:10.1016/j.arthro.2008.12.010
241. Espejo-Reina A, Aguilera J, Espejo-Reina MJ, Espejo-Reina MP, Espejo-Baena A. One-Third of Meniscal Tears Are Repairable: An Epidemiological Study Evaluating Meniscal Tear Patterns in Stable and Unstable Knees. *Arthrosc - J Arthrosc Relat Surg*. 2019;35(3):857-863. doi:10.1016/j.arthro.2018.08.051
242. Xu C, Zhao J. A meta-analysis comparing meniscal repair with meniscectomy in the treatment of meniscal tears: the more meniscus, the better outcome? *Knee Surgery, Sport Traumatol Arthrosc*. 2013;23:164-170. doi:10.1007/s00167-013-2528-6
243. Englund M, Roos EM, Lohmander LS. Impact of type of meniscal tear on radiographic and symptomatic knee osteoarthritis: A sixteen-year followup of meniscectomy with matched controls. *Arthritis Rheum*. 2003;48(8):2178-2187. doi:10.1002/art.11088
244. Shimomura K, Hamamoto S, Hart DA, Yoshikawa H, Nakamura N. Meniscal repair and regeneration: Current strategies and future perspectives. *J Clin Orthop Trauma*. 2018;9(3):247-253. doi:10.1016/j.jcot.2018.07.008
245. Korpershoek J V., De Windt TS, Hagmeijer MH, Vonk LA, Saris DBF. Cell-based meniscus repair and regeneration: At the brink of clinical translation?: A systematic review of preclinical studies. *Orthop J Sport Med*. 2017;5(2):1-15. doi:10.1177/2325967117690131
246. Ding Z, Huang H. Mesenchymal stem cells in rabbit meniscus and bone marrow exhibit a similar feature but a heterogeneous multi-differentiation potential: Superiority of meniscus as a cell source for meniscus repair Evolutionary developmental biology and morphology. *BMC Musculoskelet Disord*. 2015;16(1):1-14. doi:10.1186/s12891-015-0511-8
247. Vangsness CT, Farr J, Boyd J, Dellaero DT, Mills CR, LeRoux-Williams M. Adult human mesenchymal stem cells delivered via intra-articular injection to the knee following partial medial meniscectomy A Randomized, Double-Blind, Controlled Study. *J Bone Jt Surg - Ser A*. 2014;96(2):90-98. doi:10.2106/JBJS.M.00058
248. Caplan AI. Mesenchymal stem cells: Time to change the name! *Stem Cells Transl Med*. 2017;6(6):1445-1451. doi:10.1002/sctm.17-0051
249. Huang H, Wang S, Gui J, Shen H. A study to identify and characterize the stem/progenitor cell in rabbit meniscus. *Cytotechnology*. 2016;68(5):2083-2103. doi:10.1007/s10616-016-9949-2
250. Chahla J, Papalamprou A, Chan V, et al. Assessing the Resident Progenitor Cell Population and the Vascularity of the Adult Human Meniscus. *Arthrosc - J Arthrosc Relat Surg*. 2021;37(1):252-265. doi:10.1016/j.arthro.2020.09.021
251. Crisan M, Corselli M, Chen WCW, Péault B. Perivascular cells for regenerative medicine. *J Cell Mol Med*. 2012;16(12):2851-2860. doi:10.1111/j.1582-4934.2012.01617.x
252. Osawa A, Harner CD, Gharaibeh B, et al. The use of blood vessel-derived stem cells for meniscal regeneration and repair. *Med Sci Sports Exerc*. 2013;45(5):813-823. doi:10.1249/MSS.0b013e31827d1e06
253. Seol D, Zhou C, Brouillette MJ, et al. Characteristics of meniscus progenitor cells migrated from injured meniscus. *J Orthop Res*. 2017;35(9):1966-1972. doi:10.1002/jor.23472
254. Shen W, Chen J, Zhu T, et al. Intra-articular injection of human meniscus stem/progenitor cells promotes meniscus regeneration and ameliorates osteoarthritis through stromal cell-derived factor-1/CXCR4-mediated homing. *Stem Cells Transl Med*. 2014;3(3):387-394. doi:10.5966/sctm.2012-0170
255. Segawa Y, Muneta T, Makino H, et al. Mesenchymal stem cells derived from synovium, meniscus, anterior cruciate ligament, and articular chondrocytes share similar gene expression profiles. *J Orthop Res*. 2009;27(4):435-441. doi:10.1002/jor.20786
256. Gamer LW, Shi RR, Gendelman A, Mathewson D, Gamer J, Rosen V. Identification and characterization of adult mouse meniscus stem/progenitor cells. *Connect Tissue Res*. 2017;35(3-4):238-245. doi:10.1080/03008207.2016.1271797
257. Pelttari K, Winter A, Steck E, et al. Premature induction of hypertrophy during in vitro chondrogenesis of human mesenchymal stem cells correlates with calcification and vascular invasion after ectopic

transplantation in SCID mice. *Arthritis Rheum*. 2006;54(10):3254-3266. doi:10.1002/art.22136
258. Pauli C, Grogan SP, Patil S, et al. Macroscopic and histopathologic analysis of human knee menisci in aging and osteoarthritis. *Osteoarthr Cartil*. 2011;19(9):1132-1141. doi:10.1038/jid.2014.371
259. Zha K, Li X, Yang Z, et al. Heterogeneity of mesenchymal stem cells in cartilage regeneration: from characterization to application. *npj Regen Med*. 2021;6(14). doi:10.1038/s41536-021-00122-6
260. Grau-vorster M, Laitinen A, Nystedt J, Vives J. HLA-DR expression in clinical-grade bone marrow-derived multipotent mesenchymal stromal cells : a two-site study. *Stem Cells Res Ther*. 2019;9:1-8.
261. Mendicino M, Bailey AM, Wonnacott K, Puri RK, Bauer SR. MSC-based product characterization for clinical trials: An FDA perspective. *Cell Stem Cell*. 2014;14(2):141-145. doi:10.1016/j.stem.2014.01.013
262. Polchert D, Sobinsky J, Douglas GW, et al. IFN-γ activation of mesenchymal stem cells for treatment and prevention of graft versus host disease. *Eur J Immunol*. 2008;38(6):1745-1755. doi:10.1002/eji.200738129
263. Dighe PA, Viswanathan P, Mruthunjaya AK, Seetharam RN. Effect of bFGF on HLA-DR expression of human bone marrow-derived mesenchymal stem cells. *J Stem Cells*. 2013;8(1):43-57.
264. Kalnievl M, Krystev D. Immunohistochemical study of the distribution of fibronectin in some zones of the meniscus. :101-106. https://www.researchgate.net/profile/Nikolay-Dimitrov-11/publication/283121594_Normal_morphology_of_biologically_active_point_BAPST36_rat/links/562ba3de08aef25a2441ca03/Normal-morphology-of-biologically-active-point-BAP-ST36-rat.pdf#page=103. Accessed August 9, 2021.
265. Bekkers JEJ, Saris DBF, Tsuchida AI, Van Rijen MHP, Dhert WJA, Creemers LB. Chondrogenic potential of articular chondrocytes depends on their original location. *Tissue Eng - Part A*. 2014;20(3-4):663-671. doi:10.1089/ten.tea.2012.0673
266. Van Diest PJ. No consent should be needed for using leftover body material for scientific purposes. *BMJ*. 2002;325:648.
267. Viswanathan S, Shi Y, Galipeau J, et al. Mesenchymal stem versus stromal cells: International Society for Cell & Gene Therapy (ISCT®) Mesenchymal Stromal Cell committee position statement on nomenclature. *Cytotherapy*. 2019;21(10):1019-1024. doi:10.1016/j.jcyt.2019.08.002
268. Iyer SS, Rojas M. Anti-inflammatory effects of mesenchymal stem cells: Novel concept for future therapies. *Expert Opin Biol Ther*. 2008;8(5):569-581. doi:10.1517/14712598.8.5.569
269. Caplan AI, Correa D. The MSC: An injury drugstore. *Cell Stem Cell*. 2011;9(1):11-15. doi:10.1016/j.stem.2011.06.008
270. Spees JL, Lee RH, Gregory CA. Mechanisms of mesenchymal stem/stromal cell function. *Stem Cell Res Ther*. 2016;7(1):1-13. doi:10.1186/s13287-016-0363-7
271. Saris TF, De Windt TS, Kester EC, Vonk LA, Custers RJH, Saris DBF. Five-Year Outcome of 1-Stage Cell-Based Cartilage Repair Using Recycled Autologous Chondrons and Allogenic Mesenchymal Stromal Cells. *Am J Sports Med*. 2021:1-7. doi:10.1177/0363546520988069
272. De Windt TS, Vonk LA, Saris DBF. Response to: Mesenchymal Stem Cells: Time to Change the Name! *Stem Cells Transl Med*. 2017;6:1747-1748. doi:10.1002/stem.2619.
273. Wu L, Leijten JCH, Georgi N, Post JN, Van Blitterswijk CA, Karperien M. Trophic effects of mesenchymal stem cells increase chondrocyte proliferation and matrix formation. *Tissue Eng - Part A*. 2011;17(9-10):1425-1436. doi:10.1089/ten.tea.2010.0517
274. De Windt TS, Saris DBF, Slaper-Cortenbach ICM, et al. Direct cell–cell contact with chondrocytes is a key mechanism in multipotent mesenchymal stromal cell-mediated chondrogenesis. *Tissue Eng Part A*. 2015;21(19-20):2536-2547. doi:10.1089/ten.tea.2014.0673
275. Chen YC, Chang YW, Tan KP, Shen YS, Wang YH, Chang CH. Can mesenchymal stem cells and their conditioned medium assist inflammatory chondrocytes recovery? *PLoS One*. 2018;13(11):1-16. doi:10.1371/journal.pone.0205563
276. Morrison TJ, Jackson M V., Cunningham EK, et al. Mesenchymal stromal cells modulate macrophages in clinically relevant lung injury models by extracellular vesicle mitochondrial transfer. *Am J Respir Crit Care Med*. 2017;196(10):1275-1286. doi:10.1164/rccm.201701-0170OC
277. Jackson M V., Morrison TJ, Doherty DF, et al. Mitochondrial Transfer via Tunneling Nanotubes is an Important Mechanism by Which Mesenchymal Stem Cells Enhance Macrophage Phagocytosis in the In

Vitro and In Vivo Models of ARDS. *Stem Cells*. 2016;34(8):2210-2223. doi:10.1002/stem.2372
278. Masuzawa A, Black KM, Pacak CA, et al. Transplantation of autologously derived mitochondria protects the heart from ischemia-reperfusion injury. *Am J Physiol - Hear Circ Physiol*. 2013;304(7):966-982. doi:10.1152/ajpheart.00883.2012
279. Emani SM, Piekarski BL, Harrild D, del Nido PJ, McCully JD. Autologous mitochondrial transplantation for dysfunction after ischemia-reperfusion injury. *J Thorac Cardiovasc Surg*. 2017;154(1):286-289. doi:10.1016/j.jtcvs.2017.02.018
280. Bennett MP, Vivancos-Koopman I, Seewald L, Wells K, Robinette T, Delco ML. Intercellular mitochondrial transfer from mesenchymal stem cells to stressed chondrocytes. *Osteoarthr Cartil*. 2019;27(2019):S51-S52. doi:10.1016/j.joca.2019.02.074
281. Bennett MP, Vivancos-Koopman R, Seewald LA, Robinette T, Delco; ML. Development of a murine model to study mitochondrial transfer between mesenchymal stromal cells and injured chondrocytes. *Osteoarthr Cartil*. 2020;28(2020):S32-S33. doi:10.1016/j.joca.2020.02.053
282. Wang R, Maimaitijuma T, Ma YY, Jiao Y, Cao YP. Mitochondrial transfer from bone-marrow-derived mesenchymal stromal cells to chondrocytes protects against cartilage degenerative mitochondrial dysfunction in rats chondrocytes. *Chin Med J (Engl)*. 2021;134(2):212-218. doi:10.1097/CM9.0000000000001057
283. Croucher LJ, Crawford A, Hatton P V., Russell RGG, Buttle DJ. Extracellular ATP and UTP stimulate cartilage proteoglycan and collagen accumulation in bovine articular chondrocyte pellet cultures. *Biochim Biophys Acta - Mol Basis Dis*. 2000;1502(2):297-306. doi:10.1016/S0925-4439(00)00055-7
284. Lane RS, Fu Y, Matsuzaki S, Kinter M, Humphries KM, Griffin TM. Mitochondrial respiration and redox coupling in articular chondrocytes. *Arthritis Res Ther*. 2015;17(1):1-14. doi:10.1186/s13075-015-0566-9
285. Heywood HK, Knight MM, Lee DA. Both superficial and deep zone articular chondrocyte subpopulations exhibit the crabtree effect but have different basal oxygen consumption rates. *J Cell Physiol*. 2010;223(3):630-639. doi:10.1002/jcp.22061
286. Delco ML, Bonnevie ED, Bonassar LJ, Fortier LA. Mitochondrial Dysfunction Is an Acute Response of Articular Chondrocytes to Mechanical Injury. *J Orthop Res*. 2018;36(2):739-750. doi:10.1002/jor.23651.Mitochondrial
287. Coryell PR, Diekman BO, Loeser RF. Mechanisms and therapeutic implications of cellular senescence in osteoarthritis. *Nat Rev Rheumatol*. 2021;17(1):47-57. doi:10.1038/s41584-020-00533-7
288. Caicedo A, Fritz V, Brondello J-M, et al. MitoCeption as a new tool to assess the effects of mesenchymal stem/stromal cell mitochondria on cancer cell metabolism and function. *Sci Rep*. 2015;5(1):9073. doi:10.1038/srep09073
289. Kim MJ, Hwang JW, Yun CK, Lee Y, Choi YS. Delivery of exogenous mitochondria via centrifugation enhances cellular metabolic function. *Sci Rep*. 2018;8(1). doi:10.1038/s41598-018-21539-y
290. Bekkers JEJ, Tsuchida AI, van Rijen MHP, et al. Single-Stage Cell-Based Cartilage Regeneration Using a Combination of Chondrons and Mesenchymal Stromal Cells. *Am J Sports Med*. 2013;41(9):2158-2166. doi:10.1177/0363546513494181
291. Loo LSW, Soetedjo AAP, Lau HH, et al. BCL-xL/BCL2L1 is a critical anti-apoptotic protein that promotes the survival of differentiating pancreatic cells from human pluripotent stem cells. *Cell Death Dis*. 2020;11(5). doi:10.1038/s41419-020-2589-7
292. Mahrouf-Yorgov M, Augeul L, Da Silva CC, et al. Mesenchymal stem cells sense mitochondria released from damaged cells as danger signals to activate their rescue properties. *Cell Death Differ*. 2017;24(7):1224-1238. doi:10.1038/cdd.2017.51
293. Davis CHO, Kim KY, Bushong EA, et al. Transcellular degradation of axonal mitochondria. *Proc Natl Acad Sci U S A*. 2014;111(26):9633-9638. doi:10.1073/pnas.1404651111
294. Phinney DG, Di Giuseppe M, Njah J, et al. Mesenchymal stem cells use extracellular vesicles to outsource mitophagy and shuttle microRNAs. *Nat Commun*. 2015;6. doi:10.1038/ncomms9472
295. Norris RP. Transfer of mitochondria and endosomes between cells by gap junction internalization. *Traffic*. 2021;22(6):174-179. doi:10.1111/tra.12786
296. Islam MN, Das SR, Emin MT, et al. Mitochondrial transfer from bone-marrow-derived stromal cells to

pulmonary alveoli protects against acute lung injury. *Nat Med*. 2012;18(5):759-765. doi:10.1038/nm.2736

297. Vignais ML, Caicedo A, Brondello JM, Jorgensen C. Cell connections by tunneling nanotubes: Effects of mitochondrial trafficking on target cell metabolism, homeostasis, and response to therapy. *Stem Cells Int*. 2017;2017:1-14. doi:10.1155/2017/6917941
298. Plotnikov EY, Khryapenkova TG, Galkina SI, Sukhikh GT, Zorov DB. Cytoplasm and organelle transfer between mesenchymal multipotent stromal cells and renal tubular cells in co-culture. *Exp Cell Res*. 2010;316(15):2447-2455. doi:10.1016/j.yexcr.2010.06.009
299. Acquistapace A, Bru T, Ois Lesault P, et al. Human Mesenchymal Stem Cells Reprogram Adult Cardiomyocytes Toward a Progenitor-Like State Through Partial Cell Fusion and Mitochondria Transfer. *Stem Cells*. 2011;29:812-824. www.invitrogen.com.
300. Vallabhaneni KC, Haller H, Dumler I. Vascular smooth muscle cells initiate proliferation of mesenchymal stem cells by mitochondrial transfer via tunneling nanotubes. *Stem Cells Dev*. 2012;21(17):3104-3113. doi:10.1089/scd.2011.0691
301. Liu K, Ji K, Guo L, et al. Mesenchymal stem cells rescue injured endothelial cells in an in vitro ischemia-reperfusion model via tunneling nanotube like structure-mediated mitochondrial transfer. *Microvasc Res*. 2014;92:10-18. doi:10.1016/j.mvr.2014.01.008
302. Kim MJ, Hwang JW, Yun C-KK, Lee Y, Choi Y-SS. Delivery of exogenous mitochondria via centrifugation enhances cellular metabolic function. *Sci Rep*. 2018;8(3330). doi:10.1038/s41598-018-21539-y
303. Roca-Agujetas V, De Dios C, Lestón L, Marí M, Morales A, Colell A. Recent Insights into the Mitochondrial Role in Autophagy and Its Regulation by Oxidative Stress. *Oxid Med Cell Longev*. 2019;2019. doi:10.1155/2019/3809308
304. Blanco FJ, Rego-Pérez I. Mitochondria and mitophagy: biosensors for cartilage degradation and osteoarthritis. *Osteoarthr Cartil*. 2018;26(8):989-991. doi:10.1016/j.joca.2018.05.018
305. Mohammadalipour A, Dumbali SP, Wenzel PL. Mitochondrial Transfer and Regulators of Mesenchymal Stromal Cell Function and Therapeutic Efficacy. *Front Cell Dev Biol*. 2020;8(December):1-22. doi:10.3389/fcell.2020.603292
306. Gratz KR, Wong BL, Won CB, Sah RL. The Effects of Focal Articular Defects on Cartilage Contact Mechanics. *J Orthop Res*. 2009;27(5):584-592. doi:10.1002/jor.20762.The
307. Fleischer S. Long-Term Storage of Mitochondria to Preserve Energy-Linked Functions. In: *Methods in Enzymology*. Vol 55. ; 1979:28-32.
308. McKenna E, Traganos F, Zhao H, Darzynkiewicz Z. Persistent DNA damage caused by low levels of mitomycin C induces irreversible cell senescence. *Cell Cycle*. 2012;11(16):3132-3140. doi:10.4161/cc.21506
309. Goldring MB. Molecular regulation of the chondrocyte phenotype. *J Musculoskelet Neuronal Interact*. 2002;2(6):517-520.
310. Théry C, Witwer KW, Aikawa E, et al. Journal of Extracellular Vesicles Minimal information for studies of extracellular vesicles 2018 (MISEV2018): a position statement of the International Society for Extracellular Vesicles and update of the MISEV2014 guidelines. *J Extracell Vesicles*. 2018;7(1535750). https://www.tandfonline.com/loi/zjev20.
311. Carnino JM, Lee H, Jin Y. Isolation and characterization of extracellular vesicles from Broncho-Alveolar lavage fluid: A review and comparison of different methods. *Respir Res*. 2019;20(1). doi:10.1186/s12931-019-1210-z
312. Brittberg M. Autologous chondrocyte implantation-technique and long-term follow-up. *Injury*. 2008;39(S1):S40-S49. doi:10.1016/j.injury.2008.01.040
313. McCarthy HS, Mccall IW, Williams JM, et al. Magnetic Resonance Imaging Parameters at 1 Year Correlate With Clinical Outcomes Up to 17 Years After Autologous Chondrocyte Implantation. *Orthop J Sport Med*. 2018;6(8):1-10. doi:10.1177/2325967118788280
314. Knutsen G, Isaksen V, Johansen O, et al. Autologous chondrocyte implantation compared with microfracture in the knee: a randomized trial. *J Bone Jt Surg - Ser A*. 2004;86(3):455-464. doi:10.2106/00004623-200403000-00001
315. Messner K, Maletius W. The long-term prognosis for severe damage to weight-bearing cartilage in the

knee: A 14-year clinical and radiographic follow-up in 28 young athletes. *Acta Orthop Scand*. 1996;67(2):165-168. doi:10.3109/17453679608994664

316. Smith PA. Intra-articular autologous conditioned plasma injections provide safe and efficacious treatment for knee osteoarthritis. *Am J Sports Med*. 2015;44(4):884-891. doi:10.1177/0363546515624678
317. Sánchez M, Anitua E, Azofra J, Andía I, Padilla S, Mujika I. Comparison of surgically repaired achilles tendon tears using platelet-rich fibrin matrices. *Am J Sports Med*. 2007;35(2):245-251. doi:10.1177/0363546506294078
318. Zhang H, Chen S, Qiu M, Zhou A, Yan W, Zhang J. Lateral meniscus allograft transplantation with platelet-rich plasma injections: A minimum two-year follow-up study. *Knee*. 2018;25(4):568-576. doi:10.1016/j.knee.2018.03.005
319. Mei-Dan O, Carmont MR, Laver L, Mann G, Maffulli N, Nyska M. Platelet-rich plasma or hyaluronate in the management of osteochondral lesions of the talus. *Am J Sports Med*. 2012;40(3):534-541. doi:10.1177/0363546511431238
320. Neuman R, Logan M. The determination of hydroxyproline. *J Biol Chem*. 1950;184:299-306.
321. Gaissmaier C, Fritz J, Krackhardt T, Flesch I, Aicher WK, Ashammakhi N. Effect of human platelet supernatant on proliferation and matrix synthesis of human articular chondrocytes in monolayer and three-dimensional alginate cultures. *Biomaterials*. 2005;26(14):1953-1960. doi:10.1016/j.biomaterials.2004.06.031
322. Choi YC, Morris GM, Sokoloff L. Effect of platelet lysate on growth and sulfated glycosaminoglycan synthesis in articular chondrocyte cultures. *Arthritis Rheum*. 1980;23(2):220-224. doi:10.1002/art.1780230213
323. Hildner F, Eder MMJ, Hofer K, et al. Human platelet lysate successfully promotes proliferation and subsequent chondrogenic differentiation of adipose-derived stem cells: a comparison with articular chondrocytes. *J Tissue Eng Regen Med*. 2016;9:808-818. doi:10.1002/term.1649
324. Wang K, Li J, Li Z, et al. Chondrogenic progenitor cells exhibit superiority over mesenchymal stem cells and chondrocytes in platelet-rich plasma scaffold-based cartilage regeneration. *Am J Sports Med*. 2019;47(9):2200-2215. doi:10.1177/0363546519854219
325. Hayes AJ, Dowthwaite GP, Webster S, Archer CW. The distribution of Notch receptors and their ligands during articular cartilage development. *J Anat*. 2003;202(6):495-502. doi:10.1046/j.1469-7580.2003.00185.x
326. Sykes JG, Kuiper JH, Richardson JB, Roberts S, Wright KT, Kuiper NJ. Impact of human platelet lysate on the expansion and chondrogenic capacity of cultured human chondrocytes for cartilage cell therapy. *Eur Cells Mater*. 2018;35(2014):255-267. doi:10.22203/eCM.v035a18
327. Filardo G, Di Matteo B, Di Martino A, et al. Platelet-rich plasma intra-articular knee injections show no superiority versus viscosupplementation: A randomized controlled trial. *Am J Sports Med*. 2015;43(7):1575-1582. doi:10.1177/0363546515582027
328. Cerza F, Carnì S, Carcangiu A, et al. Comparison between hyaluronic acid and platelet-rich plasma, intra-articular infiltration in the treatment of gonarthrosis. *Am J Sports Med*. 2012;40(12):2822-2827. doi:10.1177/0363546512461902
329. Cole BJ, Karas V, Hussey K, Pilz K, Fortier LA. Hyaluronic acid versus platelet-rich plasma. *Am J Sports Med*. 2017;45(2):339-346. doi:10.1177/0363546516665809
330. Jubert NJ, Rodríguez L, Reverté-Vinaixa MM, et al. Platelet-rich plasma injections for advanced knee osteoarthritis: A prospective, randomized, double-blinded clinical trial. *Orthop J Sport Med*. 2017;5(2):1-11. doi:10.1177/2325967116689386
331. Patel S, Dhillon MS, Aggarwal S, Marwaha N, Jain A. Treatment with platelet-rich plasma is more effective than placebo for knee osteoarthritis: A prospective, double-blind, randomized trial. *Am J Sports Med*. 2013;41(2):356-364. doi:10.1177/0363546512471299
332. Moreira Teixeira LS, Leijten JCH, Wennink JWH, et al. The effect of platelet lysate supplementation of a dextran-based hydrogel on cartilage formation. *Biomaterials*. 2012;33(14):3651-3661. doi:10.1016/j.biomaterials.2012.01.051
333. Green JD, Tollemar V, Dougherty M, et al. Multifaceted signaling regulators of chondrogenesis: Implications in cartilage regeneration and tissue engineering. *Genes Dis*. 2015;2(4):307-327.

doi:10.3109/10641955.2015.1046604
334. Zhao GZ, Zhang LQ, Liu Y, et al. Effects of platelet-derived growth factor on chondrocyte proliferation, migration and apoptosis via regulation of GIT1 expression. *Mol Med Rep*. 2016;14(1):897-903. doi:10.3892/mmr.2016.5291
335. Darling EM, Athanasiou KA. Rapid phenotypic changes in passaged articular chondrocyte subpopulations. *J Orthop Res*. 2005;23(2):425-432. doi:10.1016/j.orthres.2004.08.008
336. Marijnissen WJCM, van Osch GJVM, Aigner J, Verwoerd-Verhoef HL, Verhaar JAN. Tissue-engineered cartilage using serially passaged articular chondrocytes. Chondrocytes in alginate, combined in vivo with a synthetic (E210) or biologic biodegradable carrier (DBM). *Biomaterials*. 2000;21(6):571-580. doi:10.1016/S0142-9612(99)00218-5
337. Ito T, Sawada R, Fujiwara Y, Seyama Y, Tsuchiya T. FGF-2 suppresses cellular senescence of human mesenchymal stem cells by down-regulation of TGF-β2. *Biochem Biophys Res Commun*. 2007;359:108-114.
338. Eppley BL, Woodell JE, Higgins J. Platelet quantification and growth factor analysis from platelet-rich plasma: Implications for wound healing. *Plast Reconstr Surg*. 2004;114(6):1502-1508. doi:10.1097/01.PRS.0000138251.07040.51
339. Sundman EA, Cole BJ, Fortier LA. Growth factor and catabolic cytokine concentrations are influenced by the cellular composition of platelet-rich plasma. *Am J Sports Med*. 2011;39(10):2135-2140. doi:10.1177/0363546511417792
340. Cleary M, van Osch G, Brama P, Hellingman C, Narcisi R. FGF, TGFβ and Wnt crosstalk: embryonic to in vitro cartilage development frommesenchymal stem cells. *J Tissue Eng Regen Med*. 2015;9:332-342. doi:10.1002/term
341. Narcisi R, Signorile L, Verhaar J, Giannoni P, van Osch G. TGFβ inhibition during expansion phase increases the chondrogenic re-differentiation capacity of human articular chondrocytes. *Osteoarthr Cartil*. 2012;20:1152-1160.
342. Dhurat R, Sukesh M. Principles and Methods of Preparation of Platelet-Rich Plasma: A Review and Author's Perspective. *J Cutan Aesthet Surg*. 2014;7(4):189-197. doi:10.4103/0974-2077.150734
343. Mazzocca AD, McCarthy MBR, Chowaniec DM, et al. Platelet-rich plasma differs according to preparation method and human variability. *J Bone Jt Surg*. 2012;94(4):308-316. doi:10.2106/JBJS.K.00430
344. Anitua E, Zalduendo M, Troya M, Padilla S, Orive G. Leukocyte inclusion within a platelet rich plasma-derived fibrin scaffold stimulates a more pro-inflammatory environment and alters fibrin properties. *PLoS One*. 2015;10(3):1-19. doi:10.1371/journal.pone.0121713
345. Riboh JC, Saltzman BM, Yanke AB, Fortier L, Cole BJ. Effect of leukocyte concentration on the efficacy of platelet-rich plasma in the treatment of knee osteoarthritis. *Am J Sports Med*. 2016;44(3):792-800. doi:10.1177/0363546515580787
346. Simental-Mendía M, Vilchez-Cavazos F, García-Garza R, et al. The matrix synthesis and anti-inflammatory effect of autologous leukocyte-poor platelet rich plasma in human cartilage explants. *Histol Histopathol*. 2018;33(6):609-618. doi:10.14670/HH-11-961
347. Filardo G, Kon E, Pereira Ruiz MT, et al. Platelet-rich plasma intra-articular injections for cartilage degeneration and osteoarthritis: Single- versus double-spinning approach. *Knee Surgery, Sport Traumatol Arthrosc*. 2012;20(10):2082-2091. doi:10.1007/s00167-011-1837-x
348. Kisiday JD, McIlwraith CW, Rodkey WG, Frisbie DD, Steadman JR. Effects of Platelet-Rich Plasma Composition on Anabolic and Catabolic Activities in Equine Cartilage and Meniscal Explants. *Cartilage*. 2012;3(3):245-254. doi:10.1177/1947603511433181
349. Fice MP, Miller JC, Christian R, et al. The Role of Platelet-Rich Plasma in Cartilage Pathology: An Updated Systematic Review of the Basic Science Evidence. *Arthrosc J Arthrosc Relat Surg*. 2019;35(3):961-976.e3. doi:10.1016/j.arthro.2018.10.125
350. Moussa M, Lajeunesse D, Hilal G, et al. Platelet rich plasma (PRP) induces chondroprotection via increasing autophagy, anti-inflammatory markers, and decreasing apoptosis in human osteoarthritic cartilage. *Exp Cell Res*. 2017;352(1):146-156. doi:10.1016/j.yexcr.2017.02.012
351. Liu J, Song W, Yuan T, Xu Z, Jia W, Zhang C. A comparison between platelet-rich plasma (PRP) and hyaluronate acid on the healing of cartilage defects. *PLoS One*. 2014;9(5).

doi:10.1371/journal.pone.0097293
352. Anitua E, Andia I, Ardanza B, Nurden P, Nurden AT. Autologous platelets as a source of proteins for healing and tissue regeneration. *Thromb Haemost*. 2004;91(1):4-15. doi:10.1160/TH03-07-0440
353. Loibl M, Lang S, Dendl LM, et al. Leukocyte-reduced platelet-rich plasma treatment of basal thumb arthritis: a pilot study. *Biomed Res Int*. 2016;2016. doi:10.1155/2016/9262909
354. Zhu Y, Yuan M, Meng HY, et al. Basic science and clinical application of platelet-rich plasma for cartilage defects and osteoarthritis: a review. *Osteoarthr Cartil*. 2013;21(11):1627-1637. doi:10.1016/j.joca.2013.07.017
355. Di Martino A, Di Matteo B, Papio T, et al. Platelet-Rich Plasma Versus Hyaluronic Acid Injections for the Treatment of Knee Osteoarthritis: Results at 5 Years of a Double-Blind, Randomized Controlled Trial. *Am J Sports Med*. 2019;47(2):347-354. doi:10.1177/0363546518814532
356. Martínez-Martínez A, Ruiz-Santiago F, García-Espinosa J. Platelet-rich plasma: myth or reality? *Radiologia*. 2018;60(6):465-475. doi:10.1016/j.rx.2018.08.006
357. Lee KS, Wilson JJ, Rabago DP, Baer GS, Jacobson JA, Borrero CG. Musculoskeletal applications of platelet-rich plasma: Fad or future? *Am J Roentgenol*. 2011;196(3):628-636. doi:10.2214/AJR.10.5975
358. Filardo G, Kon E. PRP: Product Rich in Placebo? *Knee Surgery, Sport Traumatol Arthrosc*. 2016;24(12):3702-3703. doi:10.1007/s00167-015-3778-2
359. Gato-Calvo L, Magalhaes J, Ruiz-Romero C, Blanco FJ, Burguera EF. Platelet-rich plasma in osteoarthritis treatment: Review of current evidence. *Ther Adv Chronic Dis*. 2019;10:1-18. doi:10.1177/2040622319825567
360. Mishra A, Tummala P, King A, et al. Buffered platelet-rich plasma enhances mesenchymal stem cell proliferation and chondrogenic differentiation. *Tissue Eng Part C Methods*. 2009;15(3):431-435. doi:10.1089/ten.tec.2008.0534
361. Gonzales VK, De Mulder ELW, De Boer T, et al. Platelet-rich plasma can replace fetal bovine serum in human meniscus cell cultures. *Tissue Eng - Part C Methods*. 2013;19(11):892-899. doi:10.1089/ten.tec.2013.0009
362. Akeda K, An HS, Okuma M, et al. Platelet-rich plasma stimulates porcine articular chondrocyte proliferation and matrix biosynthesis. *Osteoarthr Cartil*. 2006;14(12):1272-1280. doi:10.1016/j.joca.2006.05.008
363. Petrera M, De Croos JN, Iu J, Hurtig M, Kandel RA, Theodoropoulos JS. Supplementation with platelet-rich plasma improves the in vitro formation of tissue-engineered cartilage with enhanced mechanical properties. *Arthrosc J Arthrosc Relat Surg*. 2013;29(10):1685-1692. doi:10.1016/j.arthro.2013.07.259
364. Rikkers M, Levato R, Malda J, Vonk LA. Importance of Timing of Platelet Lysate-Supplementation in Expanding or Redifferentiating Human Chondrocytes for Chondrogenesis. *Front Bioeng Biotechnol*. 2020;8. doi:10.3389/fbioe.2020.00804
365. Anitua E, Andía I, Sanchez M, et al. Autologous preparations rich in growth factors promote proliferation and induce VEGF and HGF production by human tendon cells in culture. *J Orthop Res*. 2005;23(2):281-286. doi:10.1016/j.orthres.2004.08.015
366. Uggeri J, Belletti S, Guizzardi S, et al. Dose-dependent effects of platelet gel releasate on activities of human osteoblasts. *J Periodontol*. 2007;78(10):1985-1991. doi:10.1902/jop.2007.070116
367. Ahmed TAE, Giulivi A, Griffith M, Hincke M. Fibrin glues in combination with mesenchymal stem cells to develop a tissue-engineered cartilage substitute. *Tissue Eng Part A*. 2011;17(3-4):323-335. doi:10.1089/ten.tea.2009.0773
368. Pijuan J, Barceló C, Moreno DF, et al. In vitro Cell Migration, Invasion, and Adhesion Assays: From Cell Imaging to Data Analysis. *Front Cell Dev Biol*. 2019;7. doi:10.3389/fcell.2019.00107
369. Liang C-C, Park AY, Guan J-L. In vitro scratch assay: a convenient and inexpensive method for analysis of cell migration in vitro. *Nat Protoc*. 2007;2(2):329-333. doi:10.1038/nprot.2007.30
370. Ali Khaghani S, Denyer MCT, Youseffi M. Effect of Transforming Growth Factor-β1 in Biological Regulation of Primary Chondrocyte. *Am J Biomed Eng*. 2012;2(1):1-8. doi:10.5923/j.ajbe.20120201.01
371. Castillo TN, Pouliot MA, Hyeon Joo Kim, Dragoo JL. Comparison of growth factor and platelet concentration from commercial platelet-rich plasma separation systems. *Am J Sports Med*. 2011;39(2):266-271. doi:10.1177/0363546510387517
372. Cowper M, Frazier T, Wu X, et al. Human platelet lysate as a functional substitute for fetal bovine serum

in the culture of human adipose derived stromal/stem cells. *Cells*. 2019;8(7):724. doi:10.3390/cells8070724

373. Doucet C, Ernou I, Zhang Y, et al. Platelet lysates promote mesenchymal stem cell expansion: A safety substitute for animal serum in cell-based therapy applications. *J Cell Physiol*. 2005;205(2):228-236. doi:10.1002/jcp.20391
374. Neubauer M, Kuten O, Stotter C, et al. The effect of blood-derived products on the chondrogenic and osteogenic differentiation potential of adipose-derived mesenchymal stem cells originated from three different locations. *Stem Cells Int*. 2019;2019. doi:10.1155/2019/1358267
375. Sakata R, Mcnary SM, Miyatake K, et al. Stimulation of the superficial zone protein and lubrication in the articular cartilage by human platelet-rich plasma. *Am J Sports Med*. 2015;43(6):1467-1473. doi:10.1177/0363546515575023
376. Gilbertie JM, Long JM, Schubert AG, Berglund AK, Schaer TP, Schnabel L V. Pooled platelet-rich plasma lysate therapy increases synoviocyte proliferation and hyaluronic acid production while protecting chondrocytes from synoviocyte-derived inflammatory mediators. *Front Vet Sci*. 2018;5:150. doi:10.3389/fvets.2018.00150
377. Oprea WE, Karp JM, Hosseini MM, Davies JE. Effect of Platelet Releasate on Bone Cell Migration and Recruitment In Vitro. *J Craniofac Surg*. 2003;14(3):292-300. doi:10.1097/00001665-200305000-00006
378. Krüger JP, Hondke S, Endres M, Pruss A, Siclari A, Kaps C. Human platelet-rich plasma stimulates migration and chondrogenic differentiation of human subchondral progenitor cells. *J Orthop Res*. 2012;30(6):845-852. doi:10.1002/jor.22005
379. Kreuz PC, Krüger JP, Metzlaff S, et al. Platelet-rich plasma preparation types show impact on chondrogenic differentiation, migration, and proliferation of human subchondral mesenchymal progenitor cells. *Arthrosc J Arthrosc Relat Surg*. 2015;31(10):1951-1961. doi:10.1016/j.arthro.2015.03.033
380. Alaaeddine N, Di Battista JA, Pelletier J-P, Kiansa K, Cloutier J-M, Martel-Pelletier J. Inhibition of tumor necrosis factor ?-induced prostaglandin E2 production by the antiinflammatory cytokines interleukin-4, interleukin-10, and interleukin-13 in osteoarthritic synovial fibroblasts: Distinct targeting in the signaling pathways. *Arthritis Rheum*. 1999;42(4):710-718. doi:10.1002/1529-0131(199904)42
381. Fan HW, Liu GY, Zhao CF, Li XF, Yang XY. Differential expression of COX-2 in osteoarthritis and rheumatoid arthritis. *Genet Mol Res*. 2015;14(4):12872-12879. doi:10.4238/2015.October.21.7
382. Wojdasiewicz P, Poniatowski ŁA, Szukiewicz D. The role of inflammatory and anti-inflammatory cytokines in the pathogenesis of osteoarthritis. *Mediators Inflamm*. 2014;2014. doi:10.1155/2014/561459
383. Guan J, Li Y, Ding L Bin, et al. Relationship between serum and synovial fluid CCL20 concentrations with disease severity in primary knee osteoarthritis. *J Musculoskelet Neuronal Interact*. 2019;19(3):326-332.
384. Messerschmidt L, Fischer S, Wiedemann P, Bringmann A, Hollborn M. Osmotic induction of cyclooxygenase-2 in RPE cells: Stimulation of inflammasome activation. *Mol Vis*. 2019;25:329-344.
385. Liu X, Yang Y, Niu X, et al. An in situ photocrosslinkable platelet rich plasma – Complexed hydrogel glue with growth factor controlled release ability to promote cartilage defect repair. *Acta Biomater*. 2017;62:179-187. doi:10.1016/j.actbio.2017.05.023
386. Jooybar E, Abdekhodaie M, Alvi M, Mousavi A, Karperien M, Dijkstra P. An injectable platelet lysate-hyaluronic acid hydrogel supports cellular activities and induces chondrogenesis of encapsulated mesenchymal stem cells. *Acta Biomater*. 2019;83:233-244. doi:10.1016/j.actbio.2018.10.031
387. Yang X, Chen L, Xu X, Li C, Huang C, Deng CX. TGF-β/Smad3 signals repress chondrocyte hypertrophic differentiation and are required for maintaining articular cartilage. *J Cell Biol*. 2001;153(1):35-46. doi:10.1083/jcb.153.1.35
388. Plaas A, Velasco J, Gorski DJJ, et al. The relationship between fibrogenic TGFβ1 signaling in the joint and cartilage degradation in post-injury osteoarthritis. *Osteoarthr Cartil*. 2011;19(9):1081-1090. doi:10.1016/j.joca.2011.05.003
389. Martineau I, Lacoste E, Gagnon G. Effects of calcium and thrombin on growth factor release from platelet concentrates: Kinetics and regulation of endothelial cell proliferation. *Biomaterials*. 2004;25(18):4489-4502. doi:10.1016/j.biomaterials.2003.11.013
390. Blaney Davidson EN, Vitters EL, Van Der Kraan PM, Van Den Berg WB. Expression of transforming growth

factor-β (TGFβ) and the TGFβ signalling molecule SMAD-2P in spontaneous and instability-induced osteoarthritis: Role in cartilage degradation, chondrogenesis and osteophyte formation. *Ann Rheum Dis*. 2006;65(11):1414-1421. doi:10.1136/ard.2005.045971

391. Xie A, Nie L, Shen G, et al. The application of autologous platelet-rich plasma gel in cartilage regeneration. *Mol Med Rep*. 2014;10(3):1642-1648. doi:10.3892/mmr.2014.2358
392. Appel H, Friberg S. The Effect of High Tibial Osteotomy on Pain in Osteoarthritis of the Knee Joint. *Acta Orthop*. 1972;43(6):558-565. doi:10.3109/17453677208991278
393. Lobenhoffer P. Indication for Unicompartmental Knee Replacement versus Osteotomy around the Knee. *J Knee Surg*. 2017;30(8):769-773. doi:10.1055/s-0037-1605558
394. van Egmond N, van Grinsven S, van Loon CJM, Gaasbeek RD, van Kampen A. Better clinical results after closed- compared to open-wedge high tibial osteotomy in patients with medial knee osteoarthritis and varus leg alignment. *Knee Surgery, Sport Traumatol Arthrosc*. 2016;24(1):34-41. doi:10.1007/s00167-014-3303-z
395. Lee DC, Byun SJ. High Tibial Osteotomy. *Knee Surg Relat Res*. 2012;24(2):61-69. doi:10.5792/ksrr.2012.24.2.61
396. Han JH, Kim HJ, Song JG, et al. Is Bone Grafting Necessary in Opening Wedge High Tibial Osteotomy? A Meta-Analysis of Radiological Outcomes. *Knee Surg Relat Res*. 2015;27(4):207-220. doi:10.5792/ksrr.2015.27.4.207
397. van Genechten W, van den Bempt M, van Tilborg W, et al. Structural allograft impaction enables fast rehabilitation in opening-wedge high tibial osteotomy: a consecutive case series with one year follow-up. *Knee Surgery, Sport Traumatol Arthrosc*. 2020;28(12):3747-3757. doi:10.1007/s00167-019-05765-z
398. Cao ZW, Mai XJ, Wang J, Feng EH, Huang YM. Uni-compartmental knee arthroplasty versus high tibial osteotomy for knee osteoarthritis: a systematic review and meta-analysis. *J Arthroplasty*. 2018;33(3):952-959. doi:10.1016/j.arth.2017.10.025
399. Chae DJ, Shetty GM, Lee DB, Choi HW, Han SB, Nha KW. Tibial slope and patellar height after opening wedge high tibia osteotomy using autologous tricortical iliac bone graft. *Knee*. 2008;15(2):128-133. doi:10.1016/j.knee.2007.11.001
400. Lee JS, Park YJ, Wang L, Chang YS, Shetty GM, Nha KW. Modified Iliac Crest Reconstruction with Bone Cement for Reduction of Donor Site Pain and Morbidity after Open Wedge High Tibial Osteotomy: A Prospective Study. *Knee Surg Relat Res*. 2016;28(4):277-282. doi:10.5792/ksrr.15.046
401. Kuremsky MA, Schaller TM, Hall CC, Roehr BA, Masonis JL. Comparison of autograft vs allograft in opening-wedge high tibial osteotomy. *J Arthroplasty*. 2010;25(6):951-957. doi:10.1016/j.arth.2009.07.026
402. Lode A, Meissner K, Luo Y, et al. Fabrication of porous scaffolds by three-dimensional plotting of a pasty calcium phosphate bone cement under mild conditions. *J Tissue Eng Regen Med*. 2014;8(9):682-693. doi:10.1002/term.1563
403. Hooper NM, Schouten R, Hooper GJ. The Outcome of Bone Substitute Wedges in Medial Opening High Tibial Osteotomy. *Open Orthop J*. 2013;7(1):373-377. doi:10.2174/1874325001307010373
404. Castilho M, Moseke C, Ewald A, et al. Direct 3D powder printing of biphasic calcium phosphate scaffolds for substitution of complex bone defects. *Biofabrication*. 2014;6(1). doi:10.1088/1758-5082/6/1/015006
405. Yang X, Xie B, Wang L, Qin Y, Henneman ZJ, Nancollas GH. Influence of magnesium ions and amino acids on the nucleation and growth of hydroxyapatite. *CrystEngComm*. 2011;13(4):1153-1158. doi:10.1039/c0ce00470g
406. Yang F, Yang D, Tu J, Zheng Q, Cai L, Wang L. Strontium enhances osteogenic differentiation of mesenchymal stem cells and in vivo bone formation by activating Wnt/catenin signaling. *Stem Cells*. 2011;29(6):981-991. doi:10.1002/stem.646
407. Reitmaier S, Kovtun A, Schuelke J, et al. Strontium(II) and mechanical loading additively augment bone formation in calcium phosphate scaffolds. *J Orthop Res*. 2018;36(1):106-117. doi:10.1002/jor.23623
408. Lode A, Heiss C, Knapp G, et al. Strontium-modified premixed calcium phosphate cements for the therapy of osteoporotic bone defects. *Acta Biomater*. 2018;65:475-485. doi:10.1016/j.actbio.2017.10.036
409. Kim JA, Lim J, Naren R, Yun H suk, Park EK. Effect of the biodegradation rate controlled by pore structures

in magnesium phosphate ceramic scaffolds on bone tissue regeneration in vivo. *Acta Biomater*. 2016;44:155-167. doi:10.1016/j.actbio.2016.08.039
410. Jia J, Zhou H, Wei J, et al. Development of magnesium calcium phosphate biocement for bone regeneration. *J R Soc Interface*. 2010;7(49):1171-1180. doi:10.1098/rsif.2009.0559
411. Ostrowski N, Roy A, Kumta PN. Magnesium Phosphate Cement Systems for Hard Tissue Applications: A Review. *ACS Biomater Sci Eng*. 2016;2(7):1067-1083. doi:10.1021/acsbiomaterials.6b00056
412. Golafshan N, Vorndran E, Zaharievski S, et al. Tough magnesium phosphate-based 3D-printed implants induce bone regeneration in an equine defect model. *Biomaterials*. 2020;261(August):120302. doi:10.1016/j.biomaterials.2020.120302
413. Lobenhoffer P, Agneskirchner JD. Improvements in surgical technique of valgus high tibial osteotomy. *Knee Surgery, Sport Traumatol Arthrosc*. 2003;11(3):132-138. doi:10.1007/s00167-002-0334-7
414. Gerhardt LC, Boccaccini AR. Bioactive glass and glass-ceramic scaffolds for bone tissue engineering. *Materials (Basel)*. 2010;3(7):3867-3910. doi:10.3390/ma3073867
415. Willemsen K, Nizak R, Noordmans HJ, Castelein RM, Weinans H, Kruyt MC. Challenges in the design and regulatory approval of 3D-printed surgical implants: a two-case series. *Lancet Digit Heal*. 2019;1(4):e163-e171. doi:10.1016/S2589-7500(19)30067-6
416. Willemsen K, Tryfonidou M, Sakkers R, et al. Patient-specific 3D-printed shelf implant for the treatment of hip dysplasia: Anatomical and biomechanical outcomes in a canine model. *J Orthop Res*. 2021;(February):1-9. doi:10.1002/jor.25133
417. National Institute for Public Health and the Environment. Public Health Foresight Study 2018 (VTV-2018): diseases. https://www.vtv2018.nl/en/diseases.
418. Goldring MB, Tsuchimochi K, Ijiri K. The control of chondrogenesis. *J Cell Biochem*. 2006;97(1):33-44. doi:10.1002/jcb.20652
419. Aggarwal S, Pittenger MF. Human mesenchymal stem cells modulate allogeneic immune cell responses. *Blood*. 2005;105(4):1815-1822. doi:10.1182/blood-2004-04-1559
420. Caplan AI, Correa D. The MSC: An injury drugstore. *Cell Stem Cell*. 2011;9(1):11-15. doi:10.1016/j.stem.2011.06.008
421. Bauza G, Pasto A, Mcculloch P, et al. Improving the immunosuppressive potential of articular chondroprogenitors in a three-dimensional culture setting. *Sci Rep*. 2020;10(1). doi:10.1038/s41598-020-73188-9
422. Dawkins BJ, Shubin Stein BE, Mintz DN, et al. Patellofemoral joint cartilage restoration with particulated juvenile allograft in patients under 21 years old. *Knee*. 2021;(xxxx). doi:10.1016/j.knee.2021.07.006
423. Christensen BB, Olesen ML, Hede KTC, Bergholt NL, Foldager CB, Lind M. Particulated Cartilage for Chondral and Osteochondral Repair: A Review. *Cartilage*. 2020. doi:10.1177/1947603520904757
424. Bonasia DE, Marmotti A, Mattia S, et al. The degree of chondral fragmentation affects extracellular matrix production in cartilage autograft implantation: An in vitro study. *Arthrosc - J Arthrosc Relat Surg*. 2015;31(12):2335-2341. doi:10.1016/j.arthro.2015.06.025
425. Stone KR, Walgenbach AW, Freyer A, Turek TJ, Speer DP. Articular cartilage paste grafting to full-thickness articular cartilage knee joint lesions: A 2- to 12-year follow-up. *Arthrosc - J Arthrosc Relat Surg*. 2006;22(3):291-299. doi:10.1016/j.arthro.2005.12.051
426. Stone KR, Pelsis JR, Na K, Walgenbach AW, Turek TJ. Articular cartilage paste graft for severe osteochondral lesions of the knee: a 10- to 23-year follow-up study. *Knee Surgery, Sport Traumatol Arthrosc*. 2017;25(12):3824-3833. doi:10.1007/s00167-016-4323-7
427. Holton J, Imam M, Ward J, Snow M. The basic science of bone marrow aspirate concentrate in chondral injuries. *Orthop Rev (Pavia)*. 2016;8(3):80-84. doi:10.4081/or.2016.6659
428. Gobbi A, Karnatzikos G, Scotti C, Mahajan V, Mazzucco L, Grigolo B. One-step cartilage repair with bone marrow aspirate concentrated cells and collagen matrix in full-thickness knee cartilage lesions: Results at 2-year follow-up. *Cartilage*. 2011;2(3):286-299. doi:10.1177/1947603510392023
429. Hendrich C, Engelmaier F, Waertel G, Krebs R, Jäger M. Safety of autologous bone marrow aspiration concentrate transplantation: initial experiences in 101 patients. *Orthop Rev (Pavia)*. 2009;1(1):32. doi:10.4081/or.2009.e32
430. Zou J, Bai B, Yao Y. Progress of co-culture systems in cartilage regeneration. *Expert Opin Biol Ther*.

2018;18(11):1151-1158. doi:10.1080/14712598.2018.1533116
431. Mahrouf-Yorgov M, Augeul L, Da Silva CC, et al. Mesenchymal stem cells sense mitochondria released from damaged cells as danger signals to activate their rescue properties. *Cell Death Differ*. 2017;24(7):1224-1238. doi:10.1038/cdd.2017.51
432. Crewe C, Funcke J-B, Li S, et al. Extracellular vesicle-based interorgan transport of mitochondria from energetically stressed adipocytes. *Cell Metab*. August 2021. doi:10.1016/j.cmet.2021.08.002
433. Vonk LA, Roël G, Hernigou J, Kaps C, Hernigou P. Role of matrix-associated autologous chondrocyte implantation with spheroids in the treatment of large chondral defects in the knee: A systematic review. *Int J Mol Sci*. 2021;22(13). doi:10.3390/ijms22137149
434. Peterson L, Minas T, Brittberg M, Nilsson A, Sjögren-Jansson E, Lindahl A. Two- to 9-Year Outcome After Autologous Chondrocyte Transplantation of the Knee. *Clin Orthop Relat Res*. 2000;374:212-234. doi:10.1097/00003086-200005000-00020
435. Kon E, Di Matteo B, Delgado D, et al. Platelet-rich plasma for the treatment of knee osteoarthritis: an expert opinion and proposal for a novel classification and coding system. *Expert Opin Biol Ther*. 2020;00(00):1-14. doi:10.1080/14712598.2020.1798925
436. Heary RF, Schlenk RP, Sacchieri TA, Barone D, Brotea C. Persistent Iliac Crest Donor Site Pain: Independent Outcome Assessment. *Neurosurgery*. 2002;50(3):510-517. https://academic.oup.com/neurosurgery/article/50/3/510/2726899.
437. Resnick DK. Reconstruction of anterior iliac crest after bone graft harvest decreases pain: A randomized, controlled clinical trial. *Neurosurgery*. 2005;57(3):526-529. doi:10.1227/01.NEU.0000170558.70876.E3
438. Johnstone B, Stoddart MJ, Im G Il. Multi-Disciplinary Approaches for Cell-Based Cartilage Regeneration. *J Orthop Res*. 2020;38(3):463-472. doi:10.1002/jor.24458
439. Visser J, Melchels FPW, Jeon JE, et al. Reinforcement of hydrogels using three-dimensionally printed microfibres. *Nat Commun*. 2015;6:1-10. doi:10.1038/ncomms7933
440. Melchels FPW, Blokzijl MM, Levato R, et al. Hydrogel-based reinforcement of 3D bioprinted constructs. *Biofabrication*. 2016;8(3). doi:10.1088/1758-5090/8/3/035004
441. Bas O, De-Juan-Pardo EM, Chhaya MP, et al. Enhancing structural integrity of hydrogels by using highly organised melt electrospun fibre constructs. *Eur Polym J*. 2015;72:451-463. doi:10.1016/j.eurpolymj.2015.07.034
442. Boere KWM, Visser J, Seyednejad H, et al. Covalent attachment of a three-dimensionally printed thermoplast to a gelatin hydrogel for mechanically enhanced cartilage constructs. *Acta Biomater*. 2014;10(6):2602-2611. doi:10.1016/j.actbio.2014.02.041
443. Pouran B, Arbabi V, Bleys RL, René van Weeren P, Zadpoor AA, Weinans H. Solute transport at the interface of cartilage and subchondral bone plate: Effect of micro-architecture. *J Biomech*. 2017;52:148-154. doi:10.1016/j.jbiomech.2016.12.025
444. Redler I, Mow V, Zimny M, Mansell J. The Ultrastructure and Biomechanical Significance of the Tidemark of Articular Cartilage. *Clin Orthop Relat Res*. 1975;112:357-362.
445. Malda J, Visser J, Melchels FP, et al. 25th anniversary article: Engineering hydrogels for biofabrication. *Adv Mater*. 2013;25(36):5011-5028. doi:10.1002/adma.201302042
446. Oláh T, Cai X, Michaelis JC, Madry H. Comparative anatomy and morphology of the knee in translational models for articular cartilage disorders. Part I: Large animals. *Ann Anat*. 2021;235:151680. doi:10.1016/j.aanat.2021.151680
447. Chubinskaya S, Di Matteo B, Lovato L, Iacono F, Robinson D, Kon E. Agili-C implant promotes the regenerative capacity of articular cartilage defects in an ex vivo model. *Knee Surgery, Sport Traumatol Arthrosc*. 2019;27(6):1953-1964. doi:10.1007/s00167-018-5263-1
448. Kleuskens MWA, van Donkelaar CC, Kock LM, Janssen RPA, Ito K. An ex vivo human osteochondral culture model. *J Orthop Res*. 2021;39(4):871-879. doi:10.1002/jor.24789
449. Peroglio M, Gaspar D, Zeugolis DI, Alini M. Relevance of bioreactors and whole tissue cultures for the translation of new therapies to humans. *J Orthop Res*. 2018;36(1):10-21. doi:10.1002/jor.23655
450. Piluso S, Li Y, Abinzano F, et al. Mimicking the Articular Joint with In Vitro Models. *Trends Biotechnol*. 2019;37(10):1063-1077. doi:10.1016/j.tibtech.2019.03.003
451. Giorgi M, Verbruggen SW, Lacroix D. In silico bone mechanobiology: modeling a multifaceted biological

system. *Wiley Interdiscip Rev Syst Biol Med*. 2016;8(6):485-505. doi:10.1002/wsbm.1356
452. Jacques E, Suuronen EJ. The Progression of Regenerative Medicine and its Impact on Therapy Translation. *Clin Transl Sci*. 2020;13(3):440-450. doi:10.1111/CTS.12736
453. Shapiro SA, Smith CG, Arthurs JR, Master Z. Preparing regenerative therapies for clinical application: Proposals for responsible translation. *Regen Med*. 2019;14(2):77-84. doi:10.2217/rme-2018-0163
454. Schuette HB, Kraeutler MJ, McCarty EC. Matrix-Assisted Autologous Chondrocyte Transplantation in the Knee: A Systematic Review of Mid- to Long-Term Clinical Outcomes. *Orthop J Sport Med*. 2017;5(6):1-8. doi:10.1177/2325967117709250
455. Angele P, Docheva D, Pattappa G, Zellner J. Cell-based treatment options facilitate regeneration of cartilage, ligaments and meniscus in demanding conditions of the knee by a whole joint approach. *Knee Surgery, Sport Traumatol Arthrosc*. 2021. doi:10.1007/s00167-021-06497-9
456. De Windt TS, Hendriks JAA, Zhao X, et al. Concise Review: Unraveling Stem Cell Cocultures in Regenerative Medicine: Which Cell Interactions Steer Cartilage Regeneration and How? *Stem Cells Transl Med*. 2014;3(6):723-733. doi:10.5966/sctm.2013-0207
457. Mouser VHM, Dautzenberg NMM, Levato R, et al. Ex vivo model unravelling cell distribution effect in hydrogels for cartilage repair. *ALTEX*. 2018;35(1):65-76. doi:10.14573/altex.1704171
458. Vonk LA, Doulabi BZ, Huang C, Helder MN, Everts V, Bank RA. Preservation of the chondrocyte's pericellular matrix improves cell-induced cartilage formation. *J Cell Biochem*. 2010;110:260-271. doi:10.1002/jcb.22533
459. Wang QG, Nguyen B, Thomas CR, Zhang Z, El Haj AJ, Kuiper NJ. Molecular profiling of single cells in response to mechanical force: Comparison of chondrocytes, chondrons and encapsulated chondrocytes. *Biomaterials*. 2010;31(7):1619-1625. doi:10.1016/j.biomaterials.2009.11.021
460. Li Z, Kupcsik L, Yao SJ, Alini M, Stoddart MJ. Mechanical load modulates chondrogenesis of human mesenchymal stem cells through the TGF-β pathway. *J Cell Mol Med*. 2010;14(6 A):1338-1346. doi:10.1111/j.1582-4934.2009.00780.x
461. Castilho M, Mouser V, Chen M, Malda J, Ito K. Bi-layered micro-fibre reinforced hydrogels for articular cartilage regeneration. *Acta Biomater*. 2019;95:297-306. doi:10.1016/j.actbio.2019.06.030
462. Abbadessa A, Blokzijl MM, Mouser VHM, et al. A thermo-responsive and photo-polymerizable chondroitin sulfate-based hydrogel for 3D printing applications. *Carbohydr Polym*. 2016;149:163-174. doi:10.1016/j.carbpol.2016.04.080
463. Abbadessa A, Mouser VHM, Blokzijl MM, et al. A Synthetic Thermosensitive Hydrogel for Cartilage Bioprinting and Its Biofunctionalization with Polysaccharides. *Biomacromolecules*. 2016;17(6):2137-2147. doi:10.1021/acs.biomac.6b00366
464. Chung C, Beecham M, Mauck RL, Burdick JA. The influence of degradation characteristics of hyaluronic acid hydrogels on in vitro neocartilage formation by mesenchymal stem cells. *Biomaterials*. 2009;30(26):4287-4296. doi:10.1016/j.biomaterials.2009.04.040
465. Schuurman W, Levett PA, Pot MW, et al. Gelatin-methacrylamide hydrogels as potential biomaterials for fabrication of tissue-engineered cartilage constructs. *Macromol Biosci*. 2013;13(5):551-561. doi:10.1002/mabi.201200471
466. Schuurmans CCL, Mihajlovic M, Hiemstra C, Ito K, Hennink WE, Vermonden T. Hyaluronic acid and chondroitin sulfate (meth)acrylate-based hydrogels for tissue engineering: Synthesis, characteristics and pre-clinical evaluation. *Biomaterials*. 2021;268. doi:10.1016/j.biomaterials.2020.120602
467. Van Den Bulcke AI, Bogdanov B, De Rooze N, Schacht EH, Cornelissen M, Berghmans H. Structural and rheological properties of methacrylamide modified gelatin hydrogels. *Biomacromolecules*. 2000;1(1):31-38. doi:10.1021/bm990017d
468. Benton JA, Deforest CA, Vivekanandan V, Anseth KS. Photocrosslinking of Gelatin Macromers to Synthesize Porous Hydrogels That Promote Valvular Interstitial Cell Function. *Tissue Eng Part A*. 2009;15(11):3321-3230.
469. Pleumeekers MM, Nimeskern L, Koevoet JLM, Karperien M, Stok KS, Van Osch GJVM. Trophic effects of adipose-tissue-derived and bone-marrow-derived mesenchymal stem cells enhance cartilage generation by chondrocytes in co-culture. *PLoS One*. 2018;13(2):1-23. doi:10.1371/journal.pone.0190744
470. Larson CM, Kelley SS, Blackwood AD, Banes AJ, Lee GM. Retention of the native chondrocyte pericellular

matrix results in significantly improved matrix production. *Matrix Biol*. 2002;21(4):349-359. doi:10.1016/S0945-053X(02)00026-4

471. Graff RD, Kelley SS, Lee GM. Role of pericellular matrix in development of a mechanically functional neocartilage. *Biotechnol Bioeng*. 2003;82(4):457-464. doi:10.1002/bit.10593
472. Rikkers M, Korpershoek JV, Levato R, Malda J, Vonk LA. Progenitor Cells in Healthy and Osteoarthritic Human Cartilage Have Extensive Culture Expansion Capacity while Retaining Chondrogenic Properties. *Cartilage*. November 2021:194760352110596. doi:10.1177/19476035211059600
473. DeForest CA, Anseth KS. Advances in bioactive hydrogels to probe and direct cell fate. *Annu Rev Chem Biomol Eng*. 2012;3:421-444. doi:10.1146/annurev-chembioeng-062011-080945
474. Seliktar D. Designing Cell-Compatible Hydrogels for Biomedical Applications. *Science (80-)*. 2012;336:1124-1128. https://www.science.org.
475. Alge DL, Anseth KS. Bioactive hydrogels: Lighting the way. *Nat Mater*. 2013;12(11):950-952. doi:10.1038/nmat3794
476. Malda J, Visser J, Melchels FP, et al. 25th anniversary article: Engineering hydrogels for biofabrication. *Adv Mater*. 2013;25(36):5011-5028. doi:10.1002/adma.201302042
477. Lutolf MP, Raeber GP, Zisch AH, Tirelli N, Hubbell JA. Cell-Responsive Synthetic Hydrogels. *Adv Mater*. 2003;15(11):888-892. doi:10.1002/adma.200304621
478. Nguyen KT, West JL. Photopolymerizable hydrogels for tissue engineering applications. *Biomaterials*. 2002;23:4307-4314.
479. Chaudhuri O, Cooper-White J, Janmey PA, Mooney DJ, Shenoy VB. Effects of extracellular matrix viscoelasticity on cellular behaviour. *Nature*. 2020;584(7822):535-546. doi:10.1038/s41586-020-2612-2
480. Nakajima T, Gong JP. Double-Network Hydrogels: Soft and Tough IPN. In: *Encyclopedia of Polymeric Nanomaterials*. ; 2013:1-6. doi:10.1007/978-3-642-36199-9_67-1
481. Chen Q, Chen H, Zhu L, Zheng J. Fundamentals of double network hydrogels. *J Mater Chem B*. 2015;3(18):3654-3676. doi:10.1039/c5tb00123d
482. Rosales AM, Anseth KS. The design of reversible hydrogels to capture extracellular matrix dynamics. *Nat Rev Mater*. 2016;1. doi:10.1038/natrevmats.2015.12
483. Rowan SJ, Cantrill SJ, Cousins GRL, Sanders JKM, Stoddart JF. Dynamic Covalent Chemistry. *Angew Chem Int Ed* . 2002;41:898-952.
484. Jin Y, Yu C, Denman RJ, Zhang W. Recent advances in dynamic covalent chemistry. *Chem Soc Rev*. 2013;42(16):6634-6654. doi:10.1039/c3cs60044k
485. Yu F, Cao X, Du J, Wang G, Chen X. Multifunctional Hydrogel with Good Structure Integrity, Self-Healing, and Tissue-Adhesive Property Formed by Combining Diels-Alder Click Reaction and Acylhydrazone Bond. *ACS Appl Mater Interfaces*. 2015;7(43):24023-24031. doi:10.1021/acsami.5b06896
486. Deng G, Li F, Yu H, et al. Dynamic Hydrogels with an Environmental Adaptive Self-Healing Ability and Dual Responsive Sol–Gel Transitions. *ACS Macro Lett*. 2012;1(2):275-279. doi:10.1021/mz200195n
487. Collins J, Nadgorny M, Xiao Z, Connal LA. Doubly Dynamic Self-Healing Materials Based on Oxime Click Chemistry and Boronic Acids. *Macromol Rapid Commun*. 2017;38(6). doi:10.1002/marc.201600760
488. Lindahl U, Couchman J, Kimata K, Esko JD. Proteoglycans and Sulfated Glycosaminoglycans. In: rd, Varki A, Cummings RD, et al., eds. *Essentials of Glycobiology*. Cold Spring Harbor (NY); 2015:207-221. doi:10.1101/glycobiology.3e.017
489. Schuurmans CCL, Mihajlovic M, Hiemstra C, Ito K, Hennink WE, Vermonden T. Hyaluronic acid and chondroitin sulfate (meth)acrylate-based hydrogels for tissue engineering: Synthesis, characteristics and pre-clinical evaluation. *Biomaterials*. 2021;268:120602. doi:10.1016/j.biomaterials.2020.120602
490. Poldervaart MT, Goversen B, de Ruijter M, et al. 3D bioprinting of methacrylated hyaluronic acid (MeHA) hydrogel with intrinsic osteogenicity. *PLoS One*. 2017;12(6):e0177628. doi:10.1371/journal.pone.0177628
491. Abbadessa A, Blokzijl MM, Mouser VH, et al. A thermo-responsive and photo-polymerizable chondroitin sulfate-based hydrogel for 3D printing applications. *Carbohydr Polym*. 2016;149:163-174. doi:10.1016/j.carbpol.2016.04.080
492. Guo Y, Yuan T, Xiao Z, et al. Hydrogels of collagen/chondroitin sulfate/hyaluronan interpenetrating

polymer network for cartilage tissue engineering. *J Mater Sci Mater Med*. 2012;23(9):2267-2279. doi:10.1007/s10856-012-4684-5

493. Zhu M, Feng Q, Sun Y, Li G, Bian L. Effect of cartilaginous matrix components on the chondrogenesis and hypertrophy of mesenchymal stem cells in hyaluronic acid hydrogels. *J Biomed Mater Res B Appl Biomater*. 2017;105(8):2292-2300. doi:10.1002/jbm.b.33760
494. Aldana AA, Houben S, Moroni L, Baker MB, Pitet LM. Trends in Double Networks as Bioprintable and Injectable Hydrogel Scaffolds for Tissue Regeneration. *ACS Biomater Sci Eng*. 2021. doi:10.1021/acsbiomaterials.0c01749
495. Wang LL, Highley CB, Yeh YC, Galarraga JH, Uman S, Burdick JA. Three-dimensional extrusion bioprinting of single- and double-network hydrogels containing dynamic covalent crosslinks. *J Biomed Mater Res A*. 2018;106(4):865-875. doi:10.1002/jbm.a.36323
496. Nicolaou KC, Snyder SA, Montagnon T, Vassilikogiannakis G. The Diels-Alder reaction in total synthesis. *Angew Chem Int Ed*. 2002;41:1668-1698.
497. Smith LJ, Taimoory SM, Tam RY, et al. Diels-Alder Click-Cross-Linked Hydrogels with Increased Reactivity Enable 3D Cell Encapsulation. *Biomacromolecules*. 2018;19(3):926-935. doi:10.1021/acs.biomac.7b01715
498. Gandini A. The furan/maleimide Diels–Alder reaction: A versatile click–unclick tool in macromolecular synthesis. *Prog Polym Sci*. 2013;38(1):1-29. doi:10.1016/j.progpolymsci.2012.04.002
499. Boutelle RC, Northrop BH. Substituent effects on the reversibility of furan-maleimide cycloadditions. *J Org Chem*. 2011;76(19):7994-8002. doi:10.1021/jo201606z
500. Froidevaux V, Borne M, Laborbe E, Auvergne R, Gandini A, Boutevin B. Study of the Diels–Alder and retro-Diels–Alder reaction between furan derivatives and maleimide for the creation of new materials. *RSC Adv*. 2015;5(47):37742-37754. doi:10.1039/c5ra01185j
501. Kolmel DK, Kool ET. Oximes and Hydrazones in Bioconjugation: Mechanism and Catalysis. *Chem Rev*. 2017;117(15):10358-10376. doi:10.1021/acs.chemrev.7b00090
502. Khetan S, Guvendiren M, Legant WR, Cohen DM, Chen CS, Burdick JA. Degradation-mediated cellular traction directs stem cell fate in covalently crosslinked three-dimensional hydrogels. *Nat Mater*. 2013;12(5):458-465. doi:10.1038/nmat3586
503. Nimmo CM, Owen SC, Shoichet MS. Diels-Alder Click cross-linked hyaluronic acid hydrogels for tissue engineering. *Biomacromolecules*. 2011;12(3):824-830. doi:10.1021/bm101446k
504. Dawlee S, Sugandhi A, Balakrishnan B, Labarre D, Jayakrishnan A. Oxidized chondroitin sulfate-cross-linked gelatin matrixes: a new class of hydrogels. *Biomacromolecules*. 2005;6:2040-2048.
505. Grover GN, Braden RL, Christman KL. Oxime cross-linked injectable hydrogels for catheter delivery. *Adv Mater*. 2013;25(21):2937-2942. doi:10.1002/adma.201205234
506. Dahlmann J, Krause A, Moller L, et al. Fully defined in situ cross-linkable alginate and hyaluronic acid hydrogels for myocardial tissue engineering. *Biomaterials*. 2013;34(4):940-951. doi:10.1016/j.biomaterials.2012.10.008
507. Cournoyer JJ, Kshirsagar T, Fantauzzi PP, Figliozzi GM, Makdessian T, Yan B. Color test for the detection of resin-bound aldehyde in solid-phase combinatorial synthesis. *J Comb Chem*. 2002;4(2):120-124. doi:10.1021/cc010060g
508. Schafer B, Emonts C, Glimpel N, et al. Warp-Knitted Spacer Fabrics: A Versatile Platform to Generate Fiber-Reinforced Hydrogels for 3D Tissue Engineering. *Mater*. 2020;13(16):1-16. doi:10.3390/ma13163518
509. Dunn AL, Heavner JE, Racz G, Day M. Hyaluronidase: a review of approved formulations, indications and off-label use in chronic pain management. *Expert Opin Biol Ther*. 2010;10(1):127-131. doi:10.1517/14712590903490382
510. Weis M, Shan J, Kuhlmann M, Jungst T, Tessmar J, Groll J. Evaluation of Hydrogels Based on Oxidized Hyaluronic Acid for Bioprinting. *Gels*. 2018;4(4). doi:10.3390/gels4040082
511. Muhammad M, Willems C, Rodriguez-Fernandez J, Gallego-Ferrer G, Groth T. Synthesis and Characterization of Oxidized Polysaccharides for In Situ Forming Hydrogels. *Biomolecules*. 2020;10(8). doi:10.3390/biom10081185
512. Hafeez S, Ooi HW, Morgan FLC, et al. Viscoelastic Oxidized Alginates with Reversible Imine Type

Crosslinks: Self-Healing, Injectable, and Bioprintable Hydrogels. *Gels*. 2018;4(4). doi:10.3390/gels4040085

513. Suriano R, Griffini G, Chiari M, Levi M, Turri S. Rheological and mechanical behavior of polyacrylamide hydrogels chemically crosslinked with allyl agarose for two-dimensional gel electrophoresis. *J Mech Behav Biomed Mater*. 2014;30:339-346. doi:10.1016/j.jmbbm.2013.12.006
514. Yu F, Cao X, Li Y, et al. Diels–Alder crosslinked HA/PEG hydrogels with high elasticity and fatigue resistance for cell encapsulation and articular cartilage tissue repair. *Polym Chem*. 2014;5(17):5116-5123. doi:10.1039/c4py00473f
515. Sharma PK, Taneja S, Singh Y. Hydrazone-Linkage-Based Self-Healing and Injectable Xanthan-Poly(ethylene glycol) Hydrogels for Controlled Drug Release and 3D Cell Culture. *ACS Appl Mater Interfaces*. 2018;10(37):30936-30945. doi:10.1021/acsami.8b07310
516. Liu X, Wang L, Song X, Song H, Zhao JR, Wang S. A kinetic model for oxidative degradation of bagasse pulp fiber by sodium periodate. *Carbohydr Polym*. 2012;90(1):218-223. doi:10.1016/j.carbpol.2012.05.027
517. Hozumi T, Kageyama T, Ohta S, Fukuda J, Ito T. Injectable Hydrogel with Slow Degradability Composed of Gelatin and Hyaluronic Acid Cross-Linked by Schiff's Base Formation. *Biomacromolecules*. 2018;19(2):288-297. doi:10.1021/acs.biomac.7b01133
518. Xu J, Liu Z, Erhan SZ. Viscoelastic Properties of a Biological Hydrogel Produced from Soybean Oil. *J Am Oil Chem Soc*. 2008;85(3):285-290. doi:10.1007/s11746-008-1193-2
519. Hao J, Weiss RA. Viscoelastic and Mechanical Behavior of Hydrophobically Modified Hydrogels. *Macromolecules*. 2011;44(23):9390-9398. doi:10.1021/ma202130u
520. Wang H, Zhu D, Paul A, et al. Covalently adaptable elastin-like protein - hyaluronic acid (ELP - HA) hybrid hydrogels with secondary thermoresponsive crosslinking for injectable stem cell delivery. *Adv Funct Mater*. 2017;27(28). doi:10.1002/adfm.201605609
521. Pawar GM, Koenigs M, Fahimi Z, et al. Injectable hydrogels from segmented PEG-bisurea copolymers. *Biomacromolecules*. 2012;13(12):3966-3976. doi:10.1021/bm301242v
522. Rodell CB, Dusaj NN, Highley CB, Burdick JA. Injectable and Cytocompatible Tough Double-Network Hydrogels through Tandem Supramolecular and Covalent Crosslinking. *Adv Mater*. 2016;28(38):8419-8424. doi:10.1002/adma.201602268
523. Kirchhof S, Brandl FP, Hammer N, Goepferich AM. Investigation of the Diels-Alder reaction as a cross-linking mechanism for degradable poly(ethylene glycol) based hydrogels. *J Mater Chem B*. 2013;1(37):4855-4864. doi:10.1039/c3tb20831a
524. Kirchhof S, Strasser A, Wittmann HJ, et al. New insights into the cross-linking and degradation mechanism of Diels-Alder hydrogels. *J Mater Chem B*. 2015;3(3):449-457. doi:10.1039/c4tb01680g
525. Rulisek L, Sebek P, Havlas Z, Hrabal R, Capek P, Svatos A. An Experimental and Theoretical Study of Stereoselectivity of Furan–Maleic Anhydride and Furan–Maleimide Diels–Alder Reactions. *J Org Chem*. 2005;70(16):6295-6302.
526. Wang Z, Craig SL. Stereochemical effects on the mechanochemical scission of furan-maleimide Diels-Alder adducts. *Chem Commun*. 2019;55(81):12263-12266. doi:10.1039/c9cc06361g
527. Min Y, Huang S, Wang Y, et al. Sonochemical Transformation of Epoxy–Amine Thermoset into Soluble and Reusable Polymers. *Macromolecules*. 2015;48(2):316-322. doi:10.1021/ma501934p
528. Gostl R, Sijbesma RP. pi-extended anthracenes as sensitive probes for mechanical stress. *Chem Sci*. 2016;7(1):370-375. doi:10.1039/c5sc03297k
529. Offeddu GS, Tanase CE, Toumpaniari S, Oyen ML, Cameron RE. Stiffening by Osmotic Swelling Constraint in Cartilage-Like Cell Culture Scaffolds. *Macromol Biosci*. 2018;18(11). doi:10.1002/mabi.201800247
530. Chang C, Lauffenburger DA, Morales TI. Motile chondrocytes from newborn calf: migration properties and synthesis of collagen II. *Osteoarthr Cartil*. 2003;11(8):603-612. doi:10.1016/s1063-4584(03)00087-6
531. Chellat F, Grandjean-Laquerriere A, Le Naour R, et al. Metalloproteinase and cytokine production by THP-1 macrophages following exposure to chitosan-DNA nanoparticles. *Biomaterials*. 2005;26(9):961-970. doi:10.1016/j.biomaterials.2004.04.006
532. Anderson JM, Rodriguez A, Chang DT. Foreign body reaction to biomaterials. *Semin Immunol*. 2008;20(2):86-100. doi:10.1016/j.smim.2007.11.004

533. Kurowska-Stolarska M, Alivernini S. Synovial tissue macrophages: friend or foe? *RMD Open*. 2017;3(2):e000527. doi:10.1136/rmdopen-2017-000527
534. Baeva LF, Lyle DB, Rios M, Langone JJ, Lightfoote MM. Different molecular weight hyaluronic acid effects on human macrophage interleukin 1beta production. *J Biomed Mater Res A*. 2014;102(2):305-314. doi:10.1002/jbm.a.34704
535. Rayahin JE, Buhrman JS, Zhang Y, Koh TJ, Gemeinhart RA. High and low molecular weight hyaluronic acid differentially influence macrophage activation. *ACS Biomater Sci Eng*. 2015;1(7):481-493. doi:10.1021/acsbiomaterials.5b00181
536. Jounai N, Kobiyama K, Takeshita F, Ishii KJ. Recognition of damage-associated molecular patterns related to nucleic acids during inflammation and vaccination. *Front Cell Infect Microbiol*. 2012;2:168. doi:10.3389/fcimb.2012.00168
537. Roh JS, Sohn DH. Damage-Associated Molecular Patterns in Inflammatory Diseases. *Immune Netw*. 2018;18(4):e27. doi:10.4110/in.2018.18.e27
538. Iovu M, Dumais G, du Souich P. Anti-inflammatory activity of chondroitin sulfate. *Osteoarthr Cartil*. 2008;16 Suppl 3:S14-8. doi:10.1016/j.joca.2008.06.008
539. Stabler T V, Huang Z, Montell E, Verges J, Kraus VB. Chondroitin sulphate inhibits NF-kappaB activity induced by interaction of pathogenic and damage associated molecules. *Osteoarthr Cartil*. 2017;25(1):166-174. doi:10.1016/j.joca.2016.08.012
540. Stephenson EL, Yong VW. Pro-inflammatory roles of chondroitin sulfate proteoglycans in disorders of the central nervous system. *Matrix Biol*. 2018;71-72:432-442. doi:10.1016/j.matbio.2018.04.010
541. Rikkers M, Dijkstra K, Terhaard BF, et al. Platelet-Rich Plasma Does Not Inhibit Inflammation or Promote Regeneration in Human Osteoarthritic Chondrocytes In Vitro Despite Increased Proliferation. *Cartilage*. September 2020:194760352096116. doi:10.1177/1947603520961162
542. Meheux CJ, McCulloch PCP, Lintner DMD, et al. Efficacy of Intra-articular Platelet-Rich Plasma Injections in Knee Osteoarthritis: A Systematic Review. *Arthrosc J Arthrosc Relat Surg*. 2016;32(3):495-505. doi:10.1016/j.arthro.2015.08.005
543. Spreafico A, Chellini F, Frediani B, et al. Biochemical investigation of the effects of human platelet releasates on human articular chondrocytes. *J Cell Biochem*. 2009;108(5):1153-1165. doi:10.1002/jcb.22344
544. Liu J, Yuan T, Zhang C. [Effect of platelet-rich plasma on synovitis of rabbit knee]. *Chinese J reparative Reconstr Surg*. 2011;25(3):285-290. http://www.ncbi.nlm.nih.gov/pubmed/21500578.
545. Chouhan DK, Dhillon MS, Patel S, Bansal T, Bhatia A, Kanwat H. Multiple Platelet-Rich Plasma Injections Versus Single Platelet-Rich Plasma Injection in Early Osteoarthritis of the Knee: An Experimental Study in a Guinea Pig Model of Early Knee Osteoarthritis. *Am J Sports Med*. 2019;47(10):2300-2307. doi:10.1177/0363546519856605
546. Chevrier A, Darras V, Picard G, et al. Injectable chitosan-platelet-rich plasma implants to promote tissue regeneration: in vitro properties, in vivo residence, degradation, cell recruitment and vascularization. *J Tissue Eng Regen Med*. 2018;12(1):217-228. doi:10.1002/term.2403
547. Görmeli G, Görmeli CA, Ataoglu B, Çolak C, Aslantürk O, Ertem K. Multiple PRP injections are more effective than single injections and hyaluronic acid in knees with early osteoarthritis: a randomized, double-blind, placebo-controlled trial. *Knee Surgery, Sport Traumatol Arthrosc*. 2017;25(3):958-965. doi:10.1007/s00167-015-3705-6
548. Dai W-LL, Zhou A-GG, Zhang H, Zhang J. Efficacy of Platelet-Rich Plasma in the Treatment of Knee Osteoarthritis: A Meta-analysis of Randomized Controlled Trials. *Arthrosc J Arthrosc Relat Surg*. 2017;33(3):659-670.e1. doi:10.1016/j.arthro.2016.09.024
549. Shen L, Yuan T, Chen S, Xie X, Zhang C. The temporal effect of platelet-rich plasma on pain and physical function in the treatment of knee osteoarthritis: systematic review and meta-analysis of randomized controlled trials. *J Orthop Surg Res*. 2017;12(1):16. doi:10.1186/s13018-017-0521-3
550. Han Y, Huang H, Pan J, et al. Meta-analysis Comparing Platelet-Rich Plasma vs Hyaluronic Acid Injection in Patients with Knee Osteoarthritis. *Pain Med*. 2019;20(7):1418-1429. doi:10.1093/pm/pnz011
551. Lahm A, Dabravolski D, Spank H, Merk H, Esser J, Kasch R. Regional differences of tibial and femoral cartilage in the chondrocyte gene expression, immunhistochemistry and composite in different stages of

osteoarthritis. *Tissue Cell*. 2017;49(2):249-256. doi:10.1016/j.tice.2017.02.004

552. Lorenz H, Wenz W, Ivancic M, Steck E, Richter W. Early and stable upregulation of collagen type II, collagen type I and YKL40 expression levels in cartilage during early experimental osteoarthritis occurs independent of joint location and histological grading. *Arthritis Res Ther*. 2005;7(1). doi:10.1186/ar1471
553. Tsuchida AI, Beekhuizen M, 't Hart MC, et al. Cytokine profiles in the joint depend on pathology, but are different between synovial fluid, cartilage tissue and cultured chondrocytes. *Arthritis Res Ther*. 2014;16(1):1-15. doi:10.1186/s13075-014-0441-0
554. Oh J, Kim W, Park K, Roh Y. Comparison of the cellular composition and cytokine-release kinetics of various platelet-rich plasma preparations. *Am J Sport Med J Sport Med*. 2015;43(12):3062-3070. doi:10.1177/0363546515608481
555. Korpershoek J V, Vonk LA, De Windt TS, et al. Intra-articular injection with Autologous Conditioned Plasma does not lead to a clinically relevant improvement of knee osteoarthritis: a prospective case series of 140 patients with 1-year follow-up. *Acta Orthop*. 2020;91:1-7. doi:10.1080/17453674.2020.1795366
556. Hahn O, Kieb M, Jonitz-Heincke A, Bader R, Peters K, Tischer T. Dose-Dependent Effects of Platelet-Rich Plasma Powder on Chondrocytes In Vitro. *Am J Sports Med*. 2020;48(7):1727-1734. doi:10.1177/0363546520911035

List of Abbreviations

3D	Three-dimensional
αMEM	Minimal Essential Medium
ACI	Autologous chondrocyte implantation
ACL	Anterior cruciate ligament
ACLT	Anterior cruciate ligament transection
ACPC	Articular cartilage-derived progenitor cell
ALP	Alkaline phosphatase
ASAP	l-ascorbic acid 2-phosphate
ASC	Adipose-derived stem cell
ATP	Adenosine triphosphate
BM	Bone marrow
BMC	Bone marrow concentrate
BMP	Bone morphogenic factor
BSA	Bovine serum albumin
CaP	Calcium phosphate
CFE	Colony-forming efficiency
CH	Chondrocyte
CS	Chondroitin sulfate
CSMA	Chondroitin sulfate methacrylate
CT	Computed tomography
DAF	Differential adhesion to fibronectin
DMEM	Dulbecco's Modified Eagle Medium
DNA	Deoxyribonucleic acid
ECM	Extracellular matrix
EDTA	Ethylenediaminetetraacetic acid
EMBASE	Excerpta Medica Database
ESC	Embryonic stem cell
EV	Extracellular vesicle
FACS	Fluorescence-activated cell sorting
FBS	Fetal bovine serum
FGF	Fibroblast growth factor
FN	Fibronectin
GAG	Glycosaminoglycan
gelMA	Gelatin methacrylate
HA	Hyaluronic acid
HAMA	Hyaluronic acid methacrylate
HLA	Human leukocyte antigen
HSA	Human serum albumin
ICRS	International Cartilage Regeneration and Joint Preservation Society
IFP	Infrapatellar fat pad
IFS	Inter-fibre spacing

IGF	Insulin-like growth factor
IKDC	International Knee Documentation Committee
IMPACT	Instant MSC Product accompanying Autologous Chondrocyte Transplantation
iPSC	Induced pluripotent stem cell
ISCT	International Society for Cellular Therapy
ITS-X	Insulin-transferrin-selenium-ethanolamine
MACT	Matrix-assisted autologous chondrocyte transplantation
MEW	Melt electrowriting
MgP	Magnesium phosphate
MHC	Major histocompatibility complex
MSC	Mesenchymal stromal cell
MV	Microvesicle
NGF	Nerve growth factor
OA	Osteoarthritis
OARSI	Osteoarthritis Research Society International
OAT	Osteochondral autograft transplantation
OCD	Osteochondritis dissecans
PBS	Phosphate-buffered saline
PCL	Poly(ε-caprolactone)
PCR	Polymerase chain reaction
PDGF	Platelet-derived growth factor
PL	Platelet lysate
PRG4	Proteoglycan 4
PRISMA	Preferred Reporting Items for Systematic Reviews and Meta-Analyses
PROSPERO	International Prospective Register of Systematic Reviews
PRP	Platelet-rich plasma
PSI	Patient-specific instrument
RCT	Randomized controlled trial
RNA	Ribonucleic acid
ROS	Reactive oxygen species
SF	Synovial fluid
Sr	Strontium
SVF	Stromal vascular fraction
TE	Tissue engineering
TGF-β	Transforming growth factor beta
TKA	Total knee arthroplasty
TNF-α	Tumor necrosis factor alpha
TNT	Tunneling nanotube
VCAM	Vascular cell adhesion molecule
VEGF	Vascular endothelial growth factor

Nederlandse Samenvatting

Gewrichtskraakbeen is de witte, glanzende laag die de uiteinden van lange botten bedekt en mechanische lading en schokken absorbeert. Hierdoor beweegt het gewricht soepel en pijnloos. Schade aan het gewrichtskraakbeen is een veelvoorkomend probleem dat de patiënt beperkt in functionele activiteit en de kans op de ontwikkeling van artrose op jonge leeftijd verhoogt. Vervanging van het kniegewricht in jonge patiënten verhoogt op zijn beurt de kans op een revisie-operatie, welke over het algemeen minder succesvol is dan de eerste kunstknie.

Vanwege de afwezigheid van bloedvaten in het kraakbeen, is dit weefsel zeer gelimiteerd in zijn intrinsieke herstellend vermogen. De huidige gouden standaard voor het behandelen van kraakbeendefecten groter dan 2 cm^2 is 'autologe kraakbeen cel (chondrocyte) implantatie' (ACI). Dit is een techniek bestaande uit twee operaties, waarbij in de eerste operatie een klein stukje kraakbeen wordt geoogst, waaruit kraakbeencellen in het laboratorium worden geïsoleerd en vermenigvuldigd. In een tweede operatie worden de cellen geïmplanteerd in het kraakbeendefect, waarna ze nieuw kraakbeenweefsel vormen. Kleinere defecten in het kraakbeen kunnen worden behandeld door middel van microfractuur, waarbij kleine gaten worden gemaakt in het blootliggende bot in het kraakbeendefect. Hierdoor kan beenmerg het defect opvullen en regeneratie van het kraakbeen worden gestart. Gezien de complexiteit van artrose variëren behandelingen van deze aandoening van injecties in het gewricht tot vervanging van het complete gewricht met een implantaat. Kraakbeenbehoud kan in het geval van unilaterale (of eenzijdige) artrose onder andere worden bereikt met een standsbeencorrectie. Hiervoor wordt door middel van het doorzagen van het bot in het boven- of onderbeen (osteotomie) de as van het standbeen veranderd en de gewichtsverdeling verplaatst naar het onaangedane kniecompartiment.

Tot op heden is het zeer moeilijk gebleken om de natuurlijke structuur van kraakbeen te herstellen. Naast het feit dat patiënten twee operaties moeten ondergaan voor een ACI behandeling, verliezen kraakbeencellen buiten het lichaam deels hun vermogen tot het vormen van gewrichtskraakbeen, wat leidt tot een nieuw gevormd kraakbeen van verminderde kwaliteit. Dit proefschrift bestaat uit twee delen, waarbij het gemeenschappelijke doel van alle hoofdstukken is om de huidige behandelingen voor kraakbeenschade te verbeteren of nieuwe methodes te ontwikkelen voor het voorkomen van de ontwikkeling van artrose.

DEEL I – STAMCEL-GEBASEERDE STRATEGIEËN

Deel I van dit proefschrift is gericht op de verbetering van stamcel-gebaseerd kraakbeenherstel en communicatie tussen celtypes die dit herstel faciliteren te onderzoeken. In **hoofdstuk 2** wordt de huidige literatuur over een subtype kraakbeencellen systematisch samengevat. Onderzoek naar deze progenitor (of voorloper) cel laat zien dat deze de potentie heeft om autologe kraakbeencellen te vervangen in de ACI procedure. Daarnaast lijkt het celtype interessant om te gebruiken in *tissue engineering* benaderingen, door de uitgebreide mogelijkheid tot het vermeerderen van de cellen met behoud van kraakbeenvormend vermogen. **Hoofdstuk 3** laat met *in vitro* experimenten zien dat deze subpopulatie van

progenitor cellen uit zowel gezond als beschadigd kraakbeen geïsoleerd kan worden en sneller vermeerdert dan normale kraakbeencellen die in de ACI procedure gebruikt worden. Daarnaast zijn de progenitor cellen succesvol in het vormen van nieuw kraakbeenweefsel. In **hoofdstuk 4** wordt met een vergelijkbare methode aangetoond dat een progenitor populatie ook aanwezig is in de meniscus, een kraakbeenachtige structuur in de knie. Ook deze voorloper cel is in staat om kraakbeenweefsel te vormen en daardoor een potentiële alternatieve bron van cellen voor kraakbeenbehandelingen. In **hoofdstuk 5** is specifieker gekeken naar een combinatie van twee celtypes die gezamenlijk in één operatie in een kraakbeendefect geïmplanteerd kunnen worden. Dit hoofdstuk onderzoekt specifiek het transport van mitochondriën, celorganellen die voornamelijk verantwoordelijk zijn voor de energiehuishouding. Deze studie laat zien dat mitochondriën van mesenchymale stromale cellen (of mesenchymale stamcellen; MSCs) vervoerd worden naar kraakbeencellen, wanneer deze twee celtypes samen gekweekt worden. Ook laat dit hoofdstuk zien dat het transport van MSC-mitochondriën op zichzelf in ieder geval deels verantwoordelijk is voor een toename in kraakbeenproductie van de kraakbeencellen.

DEEL II – LICHAAMSEIGEN SUBSTANTIES VOOR GEWRICHTS-REGENERATIE (*ORTHOBIOLOGICS*)

Deel II van dit proefschrift onderzoekt mogelijkheden tot het gebruik van *orthobiologics* voor het stimuleren van kraakbeenvorming door kraakbeencellen, of voor het vertragen van progressieve schade aan het kraakbeen. **Hoofdstuk 6** laat zien dat bloedplaatjes lysaat (een lichaamseigen product dat uit bloed verworven kan worden) kan worden gebruikt om kraakbeencellen sneller te vermeerderen in het laboratorium. Hierbij behouden de cellen een verhoogde capaciteit tot het vormen van kraakbeenweefsel, in vergelijking met de gangbare manier van vermeerderen waarbij serum wordt gebruikt. In **hoofdstuk 7** wordt onderzocht wat de effecten zijn van plaatjes-rijk plasma (PRP), een product dat wordt gebruikt voor injecties in de knie bij beginnende artrose, op kraakbeencellen *in vitro*. Deze studie laat zien dat de anti-inflammatoire en kraakbeen-stimulerende effecten van PRP op kraakbeencellen alleen minimaal zijn en suggereert dus een samenspel van meerdere celtypes en weefsels in het klinische effect van het product. In **hoofdstuk 8** wordt door middel van een multidisciplinaire aanpak een oplossing geboden voor een klinisch probleem na een standsbeencorrectie. Bij een standsbeencorrectie (osteotomie) waarbij een open wig achterblijft, kan de patiënt veel pijn ervaren en vindt er soms geen heling van het bot plaats. Door middel van driedimensionaal (3D) modelleren van de wigopening vanuit CT scans, wordt een passend implantaat 3D-geprint in een biomateriaal, waarin MSCs of lichaamseigen beenmergconcentraat gezaaid kan worden. Deze studie legt de basis voor een regeneratief botimplantaat dat mogelijk postoperatieve pijn voor de patiënt vermindert en tegelijkertijd botgroei faciliteert.

CONCLUSIES EN IMPLICATIES

Het regenereren van gewrichtskraakbeen blijft tot op heden een knelpunt, zowel op klinisch gebied alsook op het gebied van *tissue engineering*. De resultaten van dit proefschrift laten zien dat verschillende (stam) cellen of cel-combinaties, maar ook *orthobiologics* ingezet kunnen worden om de vorming van gewrichtskraakbeen door kraakbeencellen te stimuleren. Ook wordt de toepassing van beenmergconcentraat geëxtrapoleerd naar een indirecte toepassing voor het behoud van gewrichtskraakbeen. Deze resultaten kunnen in de toekomst gebruikt worden om bestaande kraakbeenbehandelingen te verbeteren of nieuwe regeneratieve behandelingen te ontwikkelen. Ook biedt het de mogelijkheid om de beschreven producten te gebruiken in de ontwikkeling van regeneratieve gewichtsimplantaten, waarbij verschillende technieken en materialen gecombineerd worden om de gewrichtsarchitectuur succesvol na te bootsen.

List of Publications

THIS THESIS IS BASED ON THE FOLLOWING PUBLICATIONS

Rikkers M, Korpershoek JV, Levato R, Malda J, Vonk LA (2021). The clinical potential of articular cartilage-derived progenitor cells–a systematic review. NPJ Regen Med. doi: 10.1038/s41536-021-00203-6

Rikkers M, Korpershoek JV, Levato R, Malda J, Vonk LA (2021). Progenitor cells in healthy and osteoarthritic human cartilage have extensive culture expansion capacity while retaining chondrogenic properties. CARTILAGE. doi: 10.1177/19476035211059600

Korpershoek JV, **Rikkers M**, De Windt TS, Tryfonidou MA, Saris DB, Vonk LA (2021). Selection of highly proliferative and multipotent meniscus progenitors through differential adhesion to fibronectin: a novel approach in meniscus tissue engineering. Int J Mol Sci. doi: 10.3390/ijms22168614

Korpershoek JV, **Rikkers M**, Wallis F, Dijkstra K, Saris, DBF, Vonk LA. Transfer of mitochondria between MSCs and chondrocytes in co-culture. *Submitted*

Rikkers M, Levato R, Malda J, Vonk LA (2020). Importance of timing of platelet lysate-supplementation in expanding or redifferentiating human chondrocytes for chondrogenesis. Front. Bioeng. Biotechnol. doi: 10.3389/fbioe.2020.00804

Rikkers M, Dijkstra K, Terhaard BF, Admiraal J, Levato R, Malda J, Vonk LA (2020). Platelet-Rich Plasma Does not Inhibit Inflammation or Promote Regeneration in Human Osteoarthritic Chondrocytes In Vitro Despite Increased Proliferation. CARTILAGE. doi: 10.1177/1947603520961162

Rikkers M, Nguyen HC*, Golafshan N*, De Ruijter M, Castilho M, Van Egmond N, Vonk LA, Custers RJH, Malda J. A Patient-Specific, Regenerative Implant for Open-Wedge Osteotomy - From Scan to Surgery. *Submitted*
** = Authors contributed equally*

Mihajlovic M, **Rikkers M***, Mihajlovic M*, Viola M, Schuiringa GH, Masereeuw R, Vonk LA, Malda J, Ito K, Vermonden T (2022). Viscoelastic Choindroitin Sulfate and Hyaluronic Acid Double-Network Hydrogels with Reversible Crosslinks. Biomacromolecules. doi: 10.1021/acs.biomac.1c01583
** = Authors contributed equally*

Rikkers M, Dijkstra K, Terhaard BF, Admiraal J, Levato R, Malda J, Vonk LA (2021). Response to 'Platelet-Rich Plasma Is More Than Placebo-Rich Plasma for Early Osteoarthritis Knee'. CARTILAGE. doi:10.1177/1947603521989485

PUBLICATIONS NOT INCLUDED IN THIS THESIS

Salerno A, Brady K, **Rikkers M**, Li C, Caamaño-Gutierrez E, Falciani F, Blom AW, Whitehouse MR, Hollander AP (2020). MMP13 and TIMP1 are functional markers for two different potential modes of action by mesenchymal stem/stromal cells when treating osteoarthritis. STEM CELLS. doi:10.1002/stem.3255

Otto IA, Nuñez Bernal P, **Rikkers M**, van Rijen MHP, Mensinga A, Kon M, Breugem CC, Levato R, Malda J. Fibronectin-adhering Progenitor Cells reside in Human Adult, Pediatric and Microtia Auricular Cartilage and harbor a Potential for Regenerative Ear Reconstruction. *Submitted*

Korpershoek JV*, **Rikkers M***, Vonk LA. Isolation of Chondrons from Hyaline Cartilage. *Cartilage tissue engineering*. Book chapter.
** = Authors contributed equally*

Dankwoord

Het enige deel van dit proefschrift waarvan ik zeker weet dat iedereen het leest. Een proefschrift schrijf je niet alleen. De afgelopen jaren hebben ontzettend veel mensen mij gesteund, zowel binnen als buiten het UMC Utrecht.

Promotor en co-promotoren
Geachte **Professor dr. ir. Malda**, beste **Jos**. Al paste mijn onderzoek en interesse niet helemaal binnen jouw straatje, toch nam je mij zonder twijfel op in je steeds groter wordende groep. Ik heb hierdoor kennis mogen maken met (voor mijn gevoel) honderd verschillende manieren van bioprinten. Het was fijn om zo veel mensen met diverse achtergronden om me heen te hebben, ik heb hier enorm veel van geleerd. Volgens mij is de rek er nog lang niet uit, wordt het niet tijd voor een eigen gebouw? Bedankt voor jouw altijd kritische kijk op mijn werk, om er maar voor te zorgen dat dat het altijd een stukje beter werd. Bedankt voor je vertrouwen in me, we komen elkaar vast nog eens tegen!

Geachte **dr. Vonk**, beste **Lucienne**. Dank voor de afgelopen 6 jaar. Vanaf mijn eerste stagedag wist ik dat ik bij jou in goede handen was. Door je ongelofelijke liefde voor het vak, zowel het lab als de kliniek en vooral de connectie tussen beide, heb je mij hier ook mee aangestoken. Ik heb op beide gebieden enorm veel van je geleerd. Jij was ook degene die mij leerde dat een week maar vijf werkdagen heeft, iets wat mij met twee voeten op de grond heeft gehouden. Zelfs op afstand nam je nog alle tijd en moeite om me van hulp en advies te voorzien, wat ik als ongelofelijk waardevol heb ervaren. Je bent een bewonderenswaardige carrière aan het opbouwen waarin je altijd doet wat jou energie geeft. Ik wens je het allerbeste voor wat de toekomst jou en je gezin gaat brengen. Er gaan zeker nog meer glühwein- of karaoke-avondjes in Nederland, Duitsland of daarbuiten plaatsvinden!

Dear **dr. Levato**, dear **Riccardo**. Although your involvement started when I was already halfway through my PhD track, I am grateful for all your help in the harder second half of my PhD. Thank you for all your valuable advice, scientific input, and great conversations. I admire the big steps you are taking in your career and I wish you all the best for the future!

Reading committee
Dear **members of the reading committee**, thank you for taking the time and effort to read and assess this thesis.

Paranimfen
Lieve **Hester**, lieve zus. Over de jaren zijn we steeds een stukje verder naar elkaar toegegroeid. Ik heb altijd genoten als je 'even' deze kant op kwam om Utrecht in te gaan of gewoon voor een logeeradresje als je naar een cursus moest. Het is ook erg fijn om altijd even bij te kletsen met een kopje koffie als we weer een bliksembezoek aan de Achterhoek brengen. Onze reis naar New York samen was er eentje om gauw weer over te doen! Het geeft me een fijn gevoel dat je vandaag naast me staat tijdens zo'n belangrijk moment. Bedankt voor alles!

Geachte **dr.** (bijna dubbele dr.) **Korpershoek**, Lieve **Jasmijn**. Bedankt dat je 4 jaar PhD voor mij tot een geweldige tijd hebt gemaakt. Ondanks wat kleine tegenvallers (hoe vaak hebben we die progenitors gedifferentieerd?), heeft de Firma Rikkers & Korpershoek al die tijd op volle toeren gedraaid. We hebben memorabele bezoekjes mogen brengen aan Rome, Canada en Berlijn (Lunteren en Antwerpen tellen we voor het gemak maar even niet mee). Ik ben blij dat we nog lang niet van elkaar af zijn. Naast een geweldige collega heb ik ook een topvriendin aan je overgehouden, bedankt!

Collega's

Collega's van het RMCU-Ortholab, het is gek om na meer dan vier jaar niet meer elke dag het lab binnen te stappen. Ik wil iedereen bedanken voor de gezellige gesprekken, hulp en input bij projecten, alle taart, koekjes en chocolade, en leuke lunches inclusief tripjes naar Genmab. Thank you all!

Margo, hoe leuk was het om een bijna-naamgenoot als collega te hebben? Hoeveel repen chocolade hebben we nog tegoed (Jos, lees je mee?)? Bedankt voor alle gezelligheid in de afgelopen jaren. Heel veel succes met de laatste loodjes van jouw promotie, you can do it!

Mylène, Leidsche Rijn-buurvouw! Het was geweldig om met jou samen te werken, skilessen te nemen, te borrelen, Berlijn te ontdekken en jouw ongekende enthousiasme voor de wetenschap mee te mogen maken. De lockdown-brainstormsessie heeft tot een prachtig hoofdstuk in dit boekje geleid. Ik heb veel bewondering voor wat je aan het doen bent. Dream big, je gaat er zeker komen!

Iris, last minute RegMed collega. Jij hebt de laatste maanden van mijn promotie nóg een stukje gezelliger gemaakt. Hoewel het ons in het lab niet altijd meezat (zijn die gels überhaupt ooit goed gegaan?), vond ik het super om een sparringpartner erbij te hebben. Veel succes met jouw volgende stappen en vast tot snel!

Nasim, thank you for your contribution to the osteotomy project. Without your knowledge, printing skills and hard work, the chapter wouldn't have been as it is now.

Jasper, heb je je gehoor al terug na de rodelbaan? Wat was het leuk om samen het Orthofeest te organiseren! Ik vond het super dat je zo veel interesse had in labwerk en gaandeweg alle kneepjes van het vak onder de knie kreeg. Veel succes met het afronden van je promotie en je werk bij the X.

Koen, niet mijn stagebegeleider maar toch wel een beetje. Bedankt voor alle momenten dat ik bij je bureau langs kon komen en je meteen alles uit je handen liet vallen om te helpen. Ook bedankt voor je voorwerk voor het MitoTransfer project, het is een prachtig hoofdstuk geworden.

Mattie, naast lab-alwetende ook vast lid van de vrijdagmiddag-harde kern. Ongelofelijk veel dank voor al die keren dat je me uit de brand hebt geholpen (zelfs op zondag kwam je aanfietsen!). Ook was ik zonder jouw hulp met geen mogelijkheid die berg richting Gerlos overgekomen. Ik vond het erg leuk om samen te werken, maar nog meer om samen te skieën en borrelen, dank voor alles!

Anneloes en **Inge**, bedankt voor jullie hulp, flexibiliteit en voortdurende bereidheid om mijn werk een stukje makkelijker te maken!

Mannen (en vrouwen) van Q. Bedankt voor jullie gezelligheid, klinisch relevante en minder relevante input en natuurlijk alle limoncello (of was het meloncello?). **Chien**, bedankt voor je eindeloze inzet voor het osteotomie project! Zonder je hulp was het me nooit gelukt. Dank allemaal voor alle borrels, bitterballen, speciaalbiertjes, Oktoberfesten, Orthoski's en karaokeavonden (wanneer weer Ome Willem?).

Roel en **Nienke**, zonder jullie aanvoer van kraakbeen had ik veel van mijn labwerk niet kunnen doen, dank hiervoor. Ook bedankt voor het altijd openstellen van de OK, zodat ik weer kon zien waarvoor ik onderzoek deed. Daarnaast waardeer ik jullie input voor het osteotomie project ook ontzettend!

Laura, bedankt voor de waardevolle input die je keer op keer gaf voor mijn projecten.

Brenda, bedankt voor het altijd bereid zijn een gaatje te vinden om een meeting in te schieten. Ook bedankt voor de gezellige gesprekken!

RegMed XB collega's, dank voor de gezellige samenwerking! Helaas waren er niet zo veel congressen samen als we gewild hadden, maar er komt vast nog wel eens een mogelijkheid om te borrelen. **Keita**, thank you for the endless amount of energy you put into the RegMed team. I always valued your input!

Studenten
Sophie, **Duilia**, **Bastiaan** (ookal was je niet helemaal 'mijn' student), **Gabriel** en **Fleur**. Bedankt voor jullie hulp bij mijn projecten!

Vrienden
Lieve **Carline**, **Anouk**, **Bente** en **Sanne**, lieve Gerda's. Meiden van het eerste uur! Sinds de basisschool hebben we er al talloze gezellige uurtjes samen op zitten. Het is voor mij ongelofelijk waardevol geweest om altijd even te ontstressen als ik met jullie ben. Hoewel ik een klein beetje uit de richting ben gaan wonen, geniet ik altijd volop als we weer kunnen bijkletsen met een wijntje. Op nog heel veel jaren vriendschap en gekke avondjes!

Dear **Maya**, I'll write your part in English, for your convenience. Thank you for all the coffee

breaks in the Hubrecht and Friday beers. Thank you for being my lockdown partner-in-crime. To many more years of friendship, laughter, science (and non-science) chats, borrels on the *terras*, trips to Mallorca, *bitterballen* and Tripel Karmeliet. You have become more Dutch than I am in these last 7 years. I couldn't have wished for a better friend!

Dominik en **Inès**, **Isabelle** en **Heiko**, **Femke** en **Bob**, **Renée** en **Frans**, **Julia**, oud-huize Achtersteboven. Het eerste jaar van mijn promotie heb ik overleefd terwijl ik nog elke avond iets te lang bleef hangen. Gaan we de huisweekendjes naar Londen weer oppakken?

Lieve **Snackies**, via Jasmijn heb ik me mogen onderdompelen in jullie markante snack- en sportcultuur. Nadat ik met haar 'het ergste al had gehad', moest het met de rest van jullie wel goed komen. Bedankt voor jullie gezelligheid op en naast het volleybalveld!

Lieve **vrienden en parels uit Soest**, bedankt voor jullie gezelligheid en het warme bad waar ik in ben beland! **Irina**, heel erg bedankt voor het meedenken over de cover.

Familie

Lieve **Judith**, **Maarten** en lieve kleine **Beau**. Wat is het snel gegaan hè? Binnen twee jaar was de familie uitgebreid met drie personen. Ik ben ontzettend blij dat ik jullie heb mogen leren kennen. Bedankt voor jullie steun en interesse tijdens mijn promotietraject!

Lieve **Til** en **Hein**. Wat heb ik een geluk met jullie als schoonouders. Het is ongelofelijk fijn om te weten dat ik altijd even langs kan wippen voor een bakje koffie of het vervangen van een autolampje. Heel erg bedankt dat jullie altijd voor Michel en mij klaarstaan!

Lieve **Hester** en **Tom**. Met jullie is het altijd gezellig! Of we nu een rondje mountainbiken (vaker doen!) of een avond verplicht speciaalbier moeten drinken. Het is erg leuk om te zien hoe jullie samen je leven hebben opgebouwd. Bedankt voor jullie gezelligheid en de altijd openstaande deur in Westendorp!

Lieve **Mama** en **Papa**. Bedankt voor jullie eindeloze steun en enthousiasme voor wat ik aan het doen ben. Waar ik ook heen verhuisde, jullie stonden altijd voor me klaar (binnenkort de laatste keer verhuizen, beloofd!). Ik ben jullie enorm dankbaar voor de fijne thuisbasis waarop ik altijd terug kan vallen. Ik ben trots dat ik op jullie beiden lijk.

Lieve **Mich**. Wat ben ik blij dat ik jou heb leren kennen. Het geeft me een heerlijk gevoel om jou naast me te hebben. Bedankt voor je oneindige interesse in mijn onderzoek. Ik heb veel bewondering voor wat je aan het doen bent en ben ongelofelijk trots op je! We gaan nooit stoppen met genieten, ik hou van je.

Curriculum Vitae

Margot Rikkers was born on the 1st of February 1994 in Doetinchem, The Netherlands. After graduating high school in 2012 (Ulenhofcollege, Doetinchem), she moved to Utrecht to obtain a bachelor degree in Biomedical Sciences at Utrecht University. During her bachelor, she gained interest in the field of regenerative medicine through a research internship on liver stem cells and organoids at the veterinary department of Utrecht University, under supervision of dr. Bart Spee.

In 2015, Margot started the masters programme Regenerative Medicine and Technology (Utrecht University and Eindhoven University of Technology). During this period, her interest in the field or orthopaedics was sparked by a major research project in the group of dr. Lucienne Vonk at the University Medical Center (UMC) Utrecht. In this internship, she spent a year investigating the chondrogenic effects of cocultures of cartilage cells and mesenchymal stromal cells (MSCs). Additionally, she explored the potential of the blood-derived product platelet-rich plasma (PRP) to be used as a 3D biomaterial for cartilage tissue engineering. Margot's literature thesis was performed at the Utrecht Institute of Pharmaceutical Sciences (Utrecht University) on the clinical potential of MSCs for kidney regeneration, under supervision of Prof. Roos Masereeuw. For her minor internship, she moved to Liverpool, United Kingdom, to carry out a project at the University of Liverpool. She investigated the differentiation potential of human bone marrow-derived MSCs upon prolonged culture-expansion under supervision of Prof. Anthony Hollander and dr. Anna Salerno.

After obtaining her master's degree in 2017, Margot started her PhD in November 2017 at the department of Orthopaedics at the UMC Utrecht, under supervision of Prof. dr. in. Jos Malda, dr. Lucienne Vonk, and dr. Riccardo Levato. The project was part of the Osteoarthritis Moonshot of the Regenerative Medicine Crossing Borders (RegMed XB) virtual institute, which aims at using regenerative strategies to cure common chronic diseases.

In January 2022 Margot started working as a clinical research associate at a contract research organization, focused on medical devices. In this role, she utilizes her knowledge on preclinical and clinical research in orthopedics and various other fields.